(12) fl.

ADA026354

PAPER P-1152

WORKSHOP ON ATMOSPHERIC TRANSMISSION MODELING

Conducted at IDA
Arlington, Virginia
28 January 1975

Vincent J. Corcoran
Program Chairman

WORKSHOP PROCEEDINGS

December 1975

INSTITUTE FOR DEFENSE ANALYSES
SCIENCE AND TECHNOLOGY DIVISION

IDA Log No. HQ 75-17974
Copy 74 of 100 copies

DISCLAIMER NOTICE

The work reported in this document was conducted under Contract DAHC15 73C 0200 for the Department of Defense. The publication of this IDA Paper does not indicate endorsement by the Department of Defense, nor should the contents be construed as reflecting the official position of that agency.

UNCLASSIFIED
SECURITY CLASSIFICATION OF THIS PAGE (When Data Entered)

REPORT DOCUMENTATION PAGE		READ INSTRUCTIONS BEFORE COMPLETING FORM
1. REPORT NUMBER PAPER P-1152	2. GOVT ACCESSION NO.	3. RECIPIENT'S CATALOG NUMBER 9
4. TITLE (and Subtitle) 6 Workshop on Atmospheric Transmission Modeling.		5. TYPE OF REPORT & PERIOD COVERED FINAL rept., ~~December 1975~~
		6. PERFORMING ORG. REPORT NUMBER 14 P-1152
7. AUTHOR(s) 10 Vincent J. Corcoran Program Chairman		8. CONTRACT OR GRANT NUMBER(s) 15 DAHC15-73-C-0200
9. PERFORMING ORGANIZATION NAME AND ADDRESS Institute for Defense Analyses 400 Army-Navy Drive Arlington, Virginia 22202		10. PROGRAM ELEMENT, PROJECT, TASK AREA & WORK UNIT NUMBERS Task T-36
11. CONTROLLING OFFICE NAME AND ADDRESS Defense Advanced Research Projects Agency Arlington, Virginia 22209	11	12. REPORT DATE Dec[redacted]75
		13. NUMBER OF PAGES 216
14. MONITORING AGENCY NAME & ADDRESS (if different from Controlling Office) Deputy Director (Research & Advanced Technology), ODDR&E 12 227p.		15. SECURITY CLASS. (of this report) UNCLASSIFIED
		15a. DECLASSIFICATION DOWNGRADING SCHEDULE None

16. DISTRIBUTION STATEMENT (of this Report)

Approved for public release; distribution unlimited.

17. DISTRIBUTION STATEMENT (of the abstract entered in Block 20, if different from Report)

None 18 IDA/HQ 19 75-17774

18. SUPPLEMENTARY NOTES

N/A

19. KEY WORDS (Continue on reverse side if necessary and identify by block number)

Atmospheric Transmission, Modeling, Optical Propagation, Attenuation

20. ABSTRACT (Continue on reverse side if necessary and identify by block number)

This is a report on a workshop on atmospheric transmission modeling. The workshop was divided into a morning session in which papers relating to the topic were presented and an afternoon workshop that was divided into a physics and engineering session and a session on computer modeling. The purpose of the workshop was to bring

DD FORM 1 JAN 73 1473 EDITION OF 1 NOV 65 IS OBSOLETE

UNCLASSIFIED
SECURITY CLASSIFICATION OF THIS PAGE (When Data Entered)

403 112

20.

together those people who have contributed to computer modeling of atmospheric transmission, those who use the programs, and those who have evaluated the programs so that a consensus could be obtained concerning present models, the problem areas, and what must be done to evolve a model or models that would be acceptable in the future.

PAPER P-1152

WORKSHOP ON ATMOSPHERIC TRANSMISSION MODELING

Conducted at IDA
Arlington, Virginia
28 January 1975

Vincent J. Corcoran
Program Chairman

WORKSHOP PROCEEDINGS

December 1975

IDA

INSTITUTE FOR DEFENSE ANALYSES
SCIENCE AND TECHNOLOGY DIVISION
400 Army-Navy Drive, Arlington, Virginia 22202

Contract DAHC15 73 C 0200
Task T-36

FOREWORD

This document consists of the papers presented at the Workshop on Atmospheric Transmission Modeling, held at IDA on 28 January 1975.

The Institute for Defense Analyses has published the material solely in the interest of information dissemination. The material has not been edited, and no technical review has been conducted nor is planned. Responsibility for technical content of the papers rests with the individual authors.

ACKNOWLEDGMENTS

I would like to acknowledge the cooperation of the people who helped in the operation of this workshop. They include Gene Barnes, George Aholtz, and Belton McKoy. I especially want to thank Ann Guida for the secretarial and administrative help that she has provided before, during, and after the workshop.

WORKSHOP ON ATMOSPHERIC TRANSMISSION MODELING
(Held at Institute for Defense Analyses)
28 January 1975

ATTENDEES

Mr. Dave Anding
Science Applications, Inc.
15 Research Drive
Ann Arbor, Michigan 48105

Dr. Robert L. Armstrong
New Mexico State University
Box 3D
Las Cruces, New Mexico 88003

Mr. Cyrus Beck
Code 0142
Naval Air Development Center
Warminster, Pennsylvania 18974

Dr. W. S. Benedict
University of Maryland
Institute for Molecular Physics
College Park, Maryland 20740

Mr. Richard Bergmann
Night Vision Laboratory
AMSEL-NV-VI
Ft. Belvoir, Virginia 22060

Mr. Lucien M. Biberman
Institute for Defense Analyses
400 Army-Navy Drive
Arlington, Virginia 22202

Mr. Richard E. Bird
U.S. Naval Weapons Center
China Lake, California 93555

Dr. Darrell Burch
Aeronutronic
Division of Philco-Ford
Ford Road
Newport Beach, California 92663

Capt. Roger E. Christensen
6585th Test Group
W. E. Holloman Air Force Base
Alamogordo, New Mexico 88330

Mr. Gerard Connell
Martin Marietta Corporation
P. O. Box 5837
Orlando, Florida 32805

Dr. Vincent J. Corcoran
Institute for Defense Analyses
400 Army-Navy Drive
Arlington, Virginia 22202

Mr. John D'Agostino
HQ U.S. Army Electronics Command
AMSEL-CT-L
Ft. Monmouth, New Jersey 07703

Mr. G. M. Daniels
AVCO Everett Research Labs
Revere Beach Parkway
Everett, Massachusetts 02149

Mr. Louis Drummeter
NRL
Code 5560
4555 Overlook Avenue, S.W.
Washington, D. C. 20375

Dr. Robert W. Fenn
Air Force Cambridge Research Labs.
(AFCRL/OPT)
L. G. Hanscom Field
Bedford, Massachusetts 01731

Mr. J. W. Fisk
Hughes Aircraft Company
Centinela & Teale Streets
Culver City, California 90230

Mr. Philip Freedenberg
Riverside Research Institute
80 West End Avenue
New York, New York 10023

Mr. James Gallagher
Engineering Experimentation Station
Georgia Institute of Technology
Atlanta, Georgia 30332

LTC. Frank T. Haloostock
P. O. Box 33557 AMCBR
Wright-Patterson AFB, Ohio 45433

Dr. Frank Harris
Old Dominion University
Norfolk, Virginia

Mr. Richard Jensen
Division 213
Naval Surface Weapons Center
White Oak Lab.
Silver Spring, Maryland 20910

Mr. Anthony J. LaRocca
Environmental Research Institute
of Michigan
Box 618
Ann Arbor, Michigan 48107

Dr. Peter Livingston
NRL
Code 5560
4555 Overlook Avenue, S.W.
Washington, D. C. 20375

Dr. Ronald K. Long
Dept. of Electrical Engineering-
ElectroScience
Ohio State University
1320 Kinnear Road
Columbus, Ohio 43212

Dr. Hirsch I. Mandelberg
National Security Agency
Fort George G. Meade, Maryland 20755

Capt. Lawrence D. Mendenhall
Environmental Technical Applications
Center
Bldg. 159
Navy Yard Annex
Washington, D. C. 20333

Mr. Robert E. Meredith
Science Applications, Inc.
15 Research Drive
Ann Arbor, Michigan 48105

Dr. Robert McClatchey
Air Force Cambridge Research Labs.
(AFCRL/OPT)
L. G. Hanscom Field
Bedford, Massachusetts 01731

Dr. Charles M. Randall
The Aerospace Corporation
P. O. Box 92957
Los Angeles, California 90009

Dr. Robert Rohde
HQ U.S. Army Electronics Command
AMSEL-CT-L
Ft. Monmouth, New Jersey 07703

Ms. Jean Rowe
The Aerospace Corporation
2350 E. El Segundo Blvd.
El Segundo, California 90245

Dr. Alvin D. Schnitzler
Institute for Defense Analyses
400 Army-Navy Drive
Arlington, Virginia 22202

Mr. John E. A. Selby
Air Force Cambridge Research Lab.
(AFCRL/OPT)
L. G. Hanscom Field
Bedford, Massachusetts 01731

Dr. S. T. Smith
U.S. Naval Weapons Center
China Lake, California 93555

Dr. John L. Walsh
NRL
Code 5503
4555 Overlook Avenue, S.W.
Washington, D. C. 20375

Dr. Cynthia Whitney
Charles Stark Draper Labs
75 Cambridge Parkway
Cambridge, Massachusetts 02142

Dr. Benjamin Winters
National Security Agency
Fort George G. Meade, Maryland 20755

Dr. Hans G. Wolfhard
Institute for Defense Analyses
400 Army-Navy Drive
Arlington, Virginia 22202

Mr. Douglas Woodman
GTE Sylvania, Inc.
Electronic Systems Group
Western Division
P.O. Box 188
Mountain View, California 94042

Dr. K. Yao
Hughes Aircraft Company
P. O. Box 92919
Los Angeles, California 90009

CALL TO ORDER AND OPENING REMARKS

V. J. Corcoran

I want to welcome all of you to the Workshop on Atmospheric Transmission Modeling.

The purpose of this workshop is to bring together those people who are actively involved in computer modeling of the atmosphere for optical propagation. This includes people who have generated models, those who have provided inputs to the models, and various users of the models. Also included are persons who have been critics of models and have expressed dissatisfaction with models as they now stand. It is hoped that the meeting will help to show what the similarities and differences of the models are, and that the criticisms that have been expressed can be aired by the group and especially by those who have generated the models.

As a result of the discussions means for improving current models and desired extensions of the models should become apparent. This future work should eventually result in a model, or models, that can be used to do system calculations which will not be in doubt because of the transmission model used.

We hope that this meeting is different from other meetings concerned with atmospheric propagation. If it is not it will be a waste of time. The best thing that could possibly happen is for us to conclude that no further meetings are necessary because of the progress that has been made toward having satisfactory models.

As you can see from the agenda we shall start in the morning with three users papers followed by a variety of papers on modeling and finally a comparison of two models. The afternoon is concerned with two workshops, one on the physics and engineering aspects and the other on the computational aspects of modeling the atmosphere. The discussions in the afternoon are expected to be the most important aspect of this meeting. After the two workshops we shall reconvene here in the IDA Board Room for the summary reports and closing remarks.

CONTENTS

MODELING THE EFFECTS OF WEATHER ON 8.5-11 MICROMETER FLIR PERFORMANCE

Lucien M. Biberman
George A. duMais

Institute for Defense Analyses
Arlington, Virginia

MODELING THE EFFECTS OF WEATHER ON 8.5-11 MICROMETER FLIR PERFORMANCE: AN ANALYSIS USING REAL WEATHER DATA

Lucien M. Biberman and George A. du Mais
Institute for Defense Analyses
Arlington, Virginia

ABSTRACT

This paper examines the detection probability of tanks versus range. It employs real weather data, a model developed by Sendall and Biberman growing out of the Rosell perceived signal-to-noise concept, and the LOWTRAN III atmospheric model.

The results show large variability in probability of detection caused by the large and frequent variations in weather examined hourly for a full year.

SUMMARY

The traditional way of thinking about the operational utility of infrared sensors such as FLIRs may very well be both inappropriate and incorrect.

The calculations based upon long-time averages of weather do not help one understand the probable utility at some particular hour.

Weather does change rapidly, and, more to the point, for infrared modeling it changes drastically within a single day often in a cyclic manner from day to day to day.

Further, aerosols dominate the FLIR performance far more than the absorption effects when one calculates the variations in FLIR performance that might be expected.

1. INTRODUCTION AND ACKNOWLEDGEMENTS

The Aerospace Applications Studies Committee of NATO AGARD sponsored a study on the use of sensors for low-flying fast aircraft at night. In the course of this study, it became clear that although adequate methodology was developed to carry out the study, the weather picture assumed appeared far too uniform, and indeed it was a highly smoothed ten-year average. Curiosity about the variations of unsmoothed data led to a proposal by L. M. Biberman of IDA and M. Deller of RAE, Farnborough to the AASC that this problem be investigated in some detail to study the effects of terrain masking for a number of real locations, the effect of cloud obscuration, and the effect of hour by hour weather variations.

This preliminary report outlines the early findings from calculations so far carried out for two sample months, January and August. These results are the daily and seasonal effects of real weather in the vicinity of Hannover, Germany that tend to control the applicability of the electro-optical sensors. The question is how much and how often. It is our hope to answer those questions.

This reporting of the work by Biberman and du Mais is actually based upon a larger cooperative effort with a long history. The final reporting will be by a committee. This preliminary reporting must however acknowledge the foundations upon which this work rests.

The model used in the study was created by the cooperation of a number of individuals supported by their parent organizations. The basic FLIR model was developed by Robert L. Sendall of the Xerox Corporation's Electro-Optical Systems Division (now of Hughes Aircraft Company) and Lucien M. Biberman of IDA.

The weather data was selected and assembled by ETAC through the efforts of Major Thomas E. Stanton and Clarence B. Elam. This data was further processed by the Westinghouse Aerospace & Electronic Systems Division of Baltimore under the supervision of Kenneth C. Leonard, Jr.

The need for cloud-free line of sight data was long unforeseen, and a cooperative effort by Colonel John T. McCabe of ETAC and Biberman of IDA led to the work "Estimating Mean Cloud and Climatalogical Probability of Cloud-Free Lines of Sight" in 1965 (Ref. 1).

In an effort to extend this work, Norman Sissenwine, then of AFCRL, proposed a data-collection program on a global scale to accumulate such data through routine observation by crews of commercial aircraft. The method was implemented, and Ivar Lund of AFCRL published three papers on the subject (Refs. 2, 3, 4).

Ref. 1. USAF/ETAC Technical Report 186.

Ref. 2. I.A. Lund, 1965; Estimating the Probability of Clear Line-of-Sight from Sunshine and Cloud Cover Observations, J. Appl. Meteor., 4, p. 714-722.

Ref. 3. I.A. Lund, 1966: Methods for Estimating the Probability of Clear Lines-of Sight, or Sunshine, through the Atmosphere, J. Appl. Meteor., 5, p. 769-777.

Ref. 4. I.A. Lund, and M.D. Shanklin, 1972; Photogrammetically Determined Cloud-Free Lines-of Sight Through the Atmosphere, J. Appl. Meteor., 11, p. 773-782.

The cloud-free line-of-sight data to be used with this model was prepared by ETAC on the basis of the AFCRL model.

The atmospheric transmission model initially used was the LOWTRAN Program of the AFCRL created by John Selby. This program was redone for Biberman by Selby to make better and fuller use of a broader base of scattering models developed at AFCRL under Robert Fenn and to allow greater flexibility to accept a variety of inputs and data formats commonly obtained in meteorological records. This new program will be known as the LOWTRAN III.

Overall program design was accomplished by George du Mais of IDA, who is primarily responsible for the final numerical analysis reported herein.

The overall base of the model grew from a long-range program of studies of system analysis and system synthesis by Rosell of Westinghouse; Sendall, then of Xerox, under the USAF AFAL Program 698 DF; and the work of Biberman and Schnitzler of IDA under a continuing study of infrared and night vision technology supported by the Office of Research and Technology, Director of Defense Research and Engineering, Department of Defense.

The work reported here is supported as part of an IDA-sponsored study under its internal central research program.

2. THE FOUNDATIONS OF THE BASIC METHOD

In past work, Rosell (Ref. 5) has developed and with Willson has shown (Refs. 6, 7, 8) that the ability of an observer to accomplish detection, recognition, or identification of a target object in a displayed image is best predicted by the signal-to-noise ratio of the target image. Further, Rosell develops the concept of equivalent bar pattern.

This concept goes back to the work of John Johnson (Ref. 9), who showed that an observer who could detect, recognize, or identify an object such as a man or a vehicle was also able to just resolve one, four, or six-and-one-half pairs of black and white bars (of a typical photographic resolution chart) when one, four, or six-and-one half pairs of such bar widths fit inside the critical (usually minimum) dimension. (See Tables I and II.)

Ref. 5. L. M. Biberman and S. Nudelman (Eds.), Photoelectronic Imaging Devices, Plenum Press, New York (1971), Vol. 1, Physical Processes and Methods of Analysis, Chapter 14, The Limiting Resolution of Low-Light-Level Imaging Sensors by F. A. Rosell, pp. 307-329.

Ref. 6. L. M. Biberman (Ed.), Perception of Displayed Information, Plenum Press, New York (1973), Chapter 5, Recent Psychophysical Experiments and the Display Signal-to-Noise Ratio Concept, by F. A. Rosell and R. H. Willson, pp. 175-232.

Ref. 7. F. A. Rosell and R. H. Willson, "Recent Psychophysical Experiments and the Display Signal-to-Noise Ratio Concept," (September 7, 1972), Report No. ADTM No. 110, Westinghouse Electric Corporation, Defense & Electronic System Center, Systems Development Division, P.O. Box 746, Baltimore, Md. 21203.

Ref. 8. F. A. Rosell and R. H. Willson, "Performance Synthesis of Electro-Optical Sensors," Report No. AFAL-TR-74-104, Contract No. F33615-73-C-4132, (April 1974), Westinghouse Electronic Corporation, Defense & Electronic Systems Center, Systems Development Division, P.O. Box 746, Baltimore, Md. 21203

Ref. 9. John Johnson (1958), Image Intensifier Symposium, Fort Belvoir, Va., October 6-7, 1958, AD 220160.

TABLE I. JOHNSON'S LEVELS OF OBJECT DISCRIMINATION

Classification of discrimination level	Meaning
Detection	An object is present
Orientation	The object is approximately symmetric or asymmetric and its orientation may be discerned
Recognition	The class to which the object belongs may be discerned (e.g., house, truck, man, etc.)
Identification	The target can be described to the limit of the observer's knowledge (e.g., motel, pickup truck, policeman, etc.)

TABLE II. JOHNSON'S CRITERIA FOR THE RESOLUTION REQUIRED PER MINOR OBJECT DIMENSION VERSUS DISCRIMINATION LEVEL

Discrimination level	Resolution per minor object dimension, TV lines
Detection	$2^{+1.0}_{-0.5}$
Orientation	$2.8^{+0.8}_{-0.4}$
Recognition	$8.0^{+1.6}_{-0.4}$
Identification	$12.8^{+3.2}_{-2.8}$

Little more was said about the concept in a quantitative sense until Rosell's work referenced above. Here it became clear that the work done by Johnson related the number of line pairs of a bar chart corresponding to the minor dimension of an object with the ability of an observer to liminally detect, recognize, or identify that object, i.e., perform that function at the level of 50 percent probability.

Rosell went further to establish the concept of the equivalent bar pattern illustrated in Fig. 1. This concept creates a bar pattern equivalent in dimensions to the object to be viewed. For the various increasingly difficult visual tasks, the bar pattern is composed of increasingly narrower bars, according to the demands of Johnson's criteria. If the device in question produces an image of the bar chart that permits an observer to "break out" the individual bars in the pattern 75 percent of the time, that observer should be able to, for example, recognize the real object 75 percent of the time if the equivalent bar pattern was composed of four pairs of black and white bars.

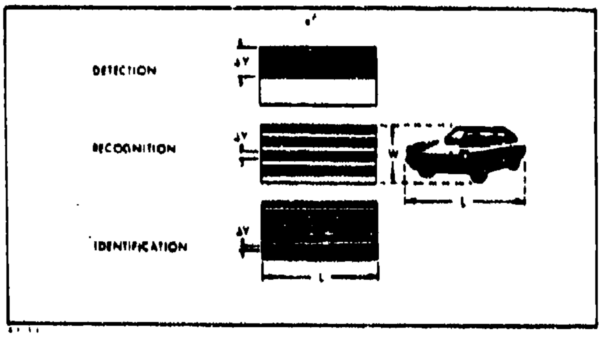

FIGURE 1a. RESOLUTION REQUIRED PER MINIMUM OBJECT DIMENSION TO ACHIEVE A GIVEN LEVEL OF OBJECT DISCRIMINATION EXPRESSED IN TERMS OF AN EQUIVALENT BAR PATTERN

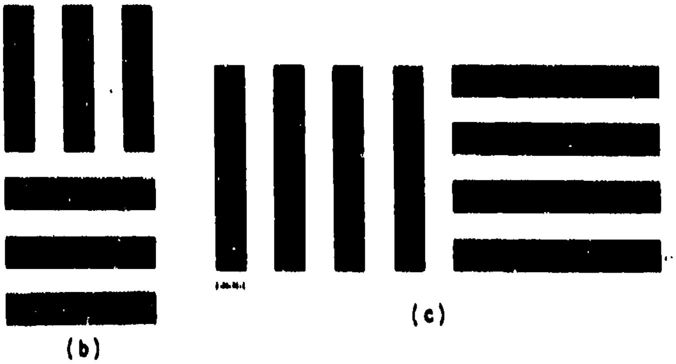

FIGURE 1b. USAF STANDARD THREE BAR TEST CHART

FIGURE 1c. MRT FOUR BAR TEST CHART

The equivalent bar pattern concept is a little more complex, in that it specifies that if the signal-to-noise ratio in the image of a single bar is some value as specified in Table IIIa, and the size (and therefore spatial frequency of that bar) is that required by the equivalent bar pattern, one can achieve the required function at the 50 percent probability level.

Table IIIb shows the spatial frequency of an equivalent bar pattern for a tank seen from front aspect as a function of range. Actually, since the tank from the front is about square, these frequencies would apply to the side aspect in detection or recognition, since the minor dimension is the same in both aspects.

TABLE IIIa. BEST ESTIMATE OF THRESHOLD SNR_D FOR DETECTION, RECOGNITION, AND IDENTIFICATION OF IMAGES

Discrimination Level	Background	k_d, TV Lines per Minimum Dimension	Threshold SNR_D[a] for a Single Bar of Spatial Frequency (in lines/picture height) equal to 100	300	500	700
Detection	Uniform[b]	1	2.8	2.8	2.8	2.8
Detection	Clutter	2	4.8	2.9	2.5	2.5
Recognition	Uniform	8	4.8	2.9	2.5	2.5
Recognition	Clutter	8	6.4	3.9	3.4	3.4
Identification	Uniform	13	5.8	3.6	3.0	3.0

[a]For a viewing-distance-to-picture-height ratio of 3.5.

[b]Treated as an aperiodic object.

TABLE IIIb. SPATIAL FREQUENCY AND LINES PER PICTURE HEIGHT FOR EQUIVALENT BAR PATTERN, TANK DETECTION, AS A FUNCTION OF RANGE

Distance, km	Target Angle, mrad	Bar Angle, mrad	Lines Per Picture Height for Field of View Indicated[a] 2.5°	5.0°	7.5°	10.0°
0.5	7.8	3.9	9	18	27	36
1.0	3.9	1.95	18	36	53	71
1.5	2.6	1.3	27	53	80	107
2.0	1.95	0.975	36	71	107	142
2.5	1.56	0.78	45	89	134	178
3.0	1.30	0.65	53	107	160	214
3.5	1.11	0.55	63	126	189	252
4.0	0.975	0.48	72	145	215	289
4.5	0.867	0.44	79	158	236	316
5.0	0.780	0.39	88	178	266	356
5.5	0.709	0.35	96	193	289	386
6.0	0.650	0.33	105	210	315	420
6.5	0.600	0.30	116	231	347	463
7.0	0.557	0.28	124	248	371	435
7.5	0.520	0.26	134	267	400	533
8.0	0.487	0.24	145	289	433	578
8.5	0.459	0.23	151	302	453	603
9.0	0.433	0.22	158	316	473	630
9.5	0.411	0.21	163	334	496	661
10.0	0.390	0.20	174	347	521	694

[a]The fields of view shown are in the horizontal dimension. Usually, the vertical dimension is three-fourths of the horizontal. The lines per picture height are therefore taken across three-fourths of the horizontal dimension.

For a distance indicated in Column 1, the front aspect of the tank target subtends an angle in milliradians shown in Column 2. The equivalent bar width for the detection model is shown in Column 3. The bar width in lines per picture height for four fields of view is shown in Columns 4, 5, 6, and 7.

For any probability other than 50 percent, the value of the signal-to-noise ratio needs to be adjusted according to the gaussian form shown in Fig. 2. Here the value of 50 percent probability is related to a normalized value of 1.0, and other probabilities require greater or lesser values, i.e., 90 percent probability corresponds to 1.5, and 10 percent probability corresponds to 0.5. These normalization constants would be applied to the signal-to-noise value for 50 percent probability to achieve the 90 percent or the 10 percent value. If a signal-to-noise ratio of 2.8 is required for 50 percent detection, then 1.5 x 2.8 is required for 90 percent probability of detection.

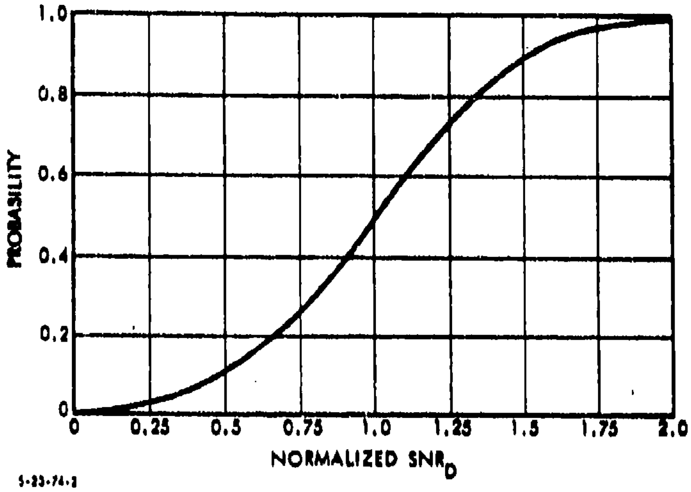

FIGURE 2. NORMALIZED DISPLAY SIGNAL-TO-NOISE RATIO

For a range of object sizes, and therefore a range of spatial frequencies, a range of signal-to-noise ratios, rather than a single value, is indicated. This effect is due to the decreasing efficiency of the eye as an integrator for images above a given angular size.

The details of this topic will not be repeated here but can be found primarily in Chapter 5 and the related Chapter 4 of Perception of Displayed Information (Ref. 10), and in "Low Light Level Devices: A Designers' Manual" (Ref. 11). These two texts give detailed equations, etc. for analyzing the performance of television-type devices.

Ref. 10. L. M. Biberman (Ed.), Perception of Displayed Information, Plenum Press, New York, (1973), Chapter 5, Recent Psychophysical Experiments and the Display Signal-to-Noise Ratio Concept by F. A. Rosell and R. H. Willson, pp. 175-232, and Chapter 4, Analysis of Noise-Required Contrast and Modulation in Image-Detecting and Display Systems, pp. 119-166.

Ref. 11. L. M. Biberman et al, Low-Light-Level Devices: A Designers' Manual, Institute for Defense Analyses Report R-169 (August 1971).

3. CALCULATIONS FOR FLIRS

For image-forming infrared devices such as forward-looking infrared (FLIR) devices, a new concept has grown up that is closely related to the material above. This concept is Minimum Resolvable Temperature (MRT). This MRT is the incremental temperature between a four-bar pattern and its background necessary to produce a just-discernible pattern to a viewer on a given display. Thus, MRT is related to the device and the size and quality of the display device producing the output image (see Fig. 3). This topic is covered in detail in an Appendix of the Final Report of Study Group No. 5 of the NATO/AGARD Aerospace Applications Studies Committee (Ref. 12), and in the Sendall-Rosell report "E/O Sensor Performance Analysis and Synthesis (TV/IR Comparison Study)," Ref. 13.

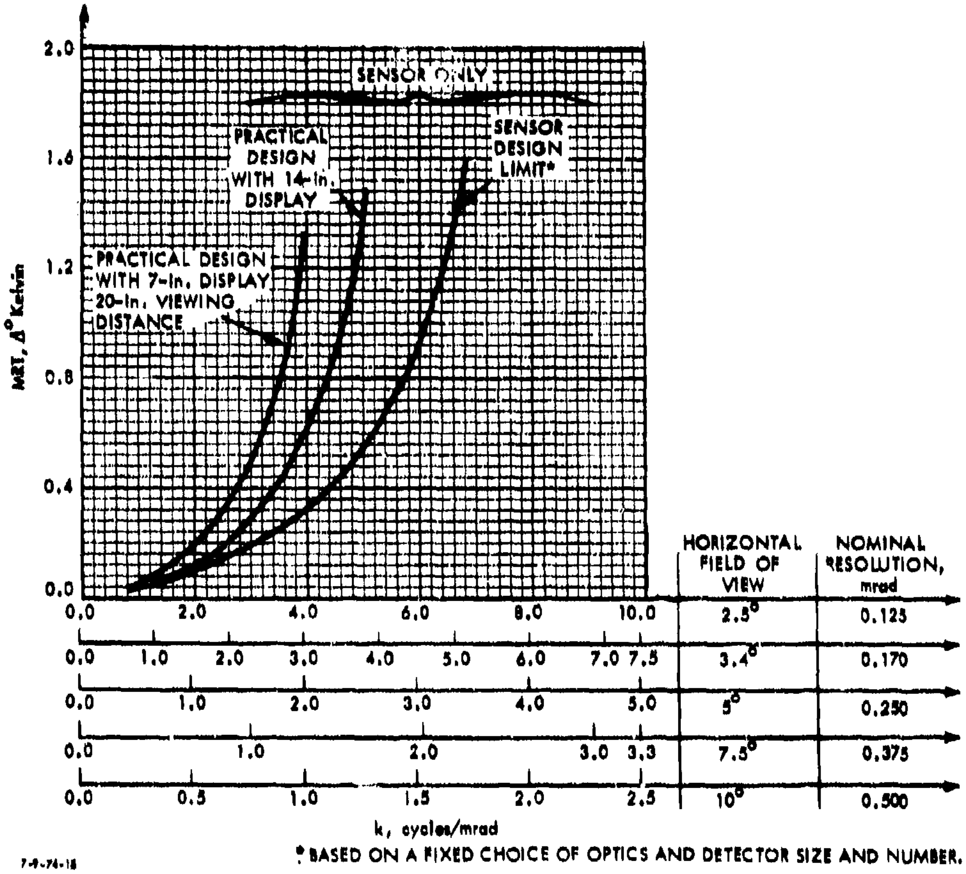

FIGURE 3. TYPICAL MRT CURVES

Ref. 12. NATO/AGARD Aerospace Applications Studies Committee No. 5, "Night Vision Devices for Fast Combat Aircraft, Final Report," AGARD AR-73, December 1975, NATO SECRET.

Ref. 13. Robert L. Sendall, Xerox Corporation, F. A. Rosell, Westinghouse Electric Corporation, Defense & Electronic Systems Division, "E/O Sensor Performance Analysis and Synthesis (TV/IR Comparison Study)," AFAL-TR-72-374, Final Report (April 1973).

Since MRT is that value of incremental temperature that produces a value of signal-to-noise ratio sufficient to allow an observer to break out the MRT test bar pattern at 50 percent probability, then $\frac{\Delta T}{MRT}$ corresponds to the normalization factor relating signal-to-noise to probability.

4. FIRST ORDER CORRECTIONS TO BAR PATTERN DATA

Though it is not the purpose of this paper to establish the theoretical basis of perception of displayed imagery, it is quite important to understand the means and the rationale for using MRT data to establish the probability of detecting, recognizing, or identifying real objects rather than the standard four-bar MRT test patterns.

In 1960, Coltman and Anderson reported (Ref. 14) that the detectability of a group of bars was a function of the number of such bars in the bar pattern.

To show the impact of reducing the number of bars available to the observer, Coltman and Anderson devised the experiment shown in Fig. 4. The displayed pattern was left fixed, and a series of cardboard apertures were employed to vary the number of lines seen by the observer (Ref. 14, p. 862). The mask was of square aspect ratio. The results as shown in Fig. 4 "show that the observer probably uses no more than seven line pairs in making an identification. As the number which he is permitted to see is decreased, the signal required rises rapidly, being greater by a factor of four when only one line pair is presented." (Ref. 14, p. 862.)

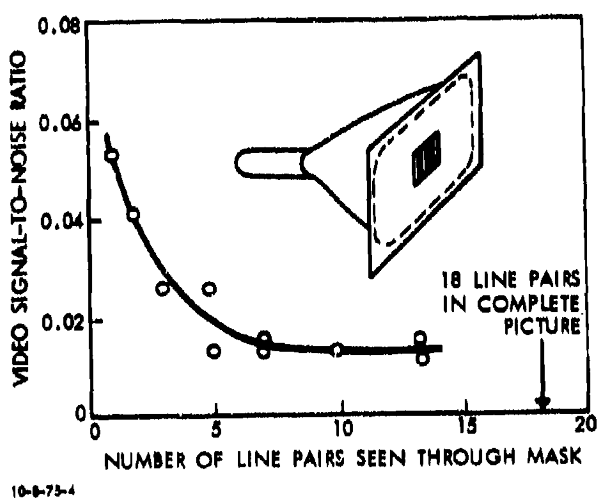

FIGURE 4. NUMBER OF LINE PAIRS SEEN THROUGH MASK (ADAPTED FROM REF. 14)

Schade (Ref. 15) also notes that "the sampling aperture of the eye for lines and edges is its line image, limited in length to fourteen equivalent point image diameters." These two observations

Ref. 14. J. W. Coltman and A. E. Anderson (1960), Noise Limitations to Resolving Power in Electronic Imaging, Proceedings IRE, 48(5), pp. 858-865.

Ref. 15. O. H. Schade, Sr. (1956), Optical and Photoelectric Analog of the Eye, Journal Optical Society of America, 46(9), p. 731.

give a possible explanation for the use of the elemental image of size $1/N_{TV} \cdot 1/N_{TV}$. However, if this is to hold over a wide range of spatial frequencies, it is necessary to conclude that, as the pattern spacing changes, the eye's ability to integrate along the line changes in direct proportion, or else it reaches some limit. This is at considerable variance with the results obtained in the rectangle experiment of Rosell and Willson, loc cit. In Rosell and Willson it was shown that the eye could integrate a line of length-to-width aspect ratio from 1:1 to at least 48:1 and perhaps even more, since no end point was determined.

The point of the above is that Coltman and Anderson reduced the number <u>and length</u> of the bars in their pattern and ascribed the variation in results to the number of bars, ignoring the effect of length. The work of Rosell and Willson predicts the same results based upon variation in bar length <u>ignoring the number of bars</u>, and further show similar results based upon as little as one bar of varying aspect ratio.

The aspect ratio of standard bar patterns is either 5:1 for the USAF three-bar pattern or 7:1 for the standard MRT test pattern. (See Fig. 1b, 1c.)

If we choose a more or less square cross section of a tank as a target and place one line pair across that target, the aspect one of those two bars is approximately 2:1 as opposed to the 7:1 of the MRT bar pattern.

Since the signal-to-noise ratio in the image of a bar is proportional to the square root of the aspect ratio, the signal-to-noise ratio in the 2:1 aspect bar will be the square root of 2/7 times that of the 7:1 aspect ratio or about 0.53. Thus, the signal-to-noise ratio from a 1:2 aspect bar would require a value of MRT greater than that measured by the ratio of $1/\sqrt{2/7}$.

One can correct for any value of aspect ratio, ϵ, when MRT data is used by correcting the value of MRT at any spatial frequency by the factor $1/\sqrt{\epsilon/7}$.

Thus, the important quantity in predicting the performance of devices like FLIRs is the value of

$$\frac{\Delta T}{MRT/\sqrt{\epsilon/7}}$$

Tables IVa and IVb show the values of MRT versus spatial frequency for the standard aspect bar target and for an equivalent bar pattern representing the front aspect of a tank in which the individual bars exhibit an aspect of approximately 2:1. These two sets of MRT values are used to show the uncorrected data as well as the bar aspect corrected data in Table Vb.

One may thus apply the $\Delta T/(MRT/\sqrt{\epsilon/7})$ to establish the signal to noise in an image and/or the probability that the equivalent bar pattern or its counterpart object will be, say, recognized.

One further important approximation is used in this work and it concerns the computation of ΔT at the sensor. It can be shown, and indeed Sendall does demonstrate (Refs. 12 and 13), that if a small incremental temperature ΔT between an object and its background is seen by a sensor through an attenuating atmosphere with a transmission at a given range of τ_R then the value of ΔT sensed at the sensor location is an apparent ΔT or ΔT_{AP} equal to ΔT_{τ_R}.

The material above described the perceptual factors associated with the aspect ratio of a bar in a bar pattern, the variation of MRT with that aspect ratio, and the method of correctly applying standard MRT data to nonstandard bar patterns and thus to the "equivalent bar pattern" stressed in this report.

TABLE IVa. MINIMUM RESOLVABLE TEMPERATURE, UNCOMPENSATED FOR ASPECT RATIO ε, TABULATED FOR FOUR FIELDS OF VIEW AND TWO DISPLAY SIZES AND FOR SPATIAL FREQUENCIES CORRESPONDING TO THE ANGLES SUBTENDED BY A SUBJECT AT VARIOUS RANGES

Range, km	Angle, mrad	Spatial Fre- quency, cycles/ mrad	Minimum Resolvable Temperature, $\Delta^{\circ}K$							
			2.5-deg FOV		5-deg FOV		7.5-deg FOV		10-deg FOV	
			Large Display	7-in. Display	Large Display	7-in. Display	Large Display	7-in. Display	Large Display	7-in. Display
.5	7.800	.128	.010	.019	.059	.015	.010	.019	.018	.019
1.0	3.900	.256	.010	.010	.010	.010	.010	.016	.051	.043
1.5	2.600	.385	.010	.010	.010	.010	.058	.079	.097	.127
2.0	1.950	.513	.010	.010	.061	.063	.097	.127	.131	.213
2.5	1.560	.641	.010	.010	.074	.095	.114	.185	.242	.349
3.0	1.300	.769	.010	.010	.087	.127	.157	.277	.322	.563
3.5	1.114	.897	.010	.010	.105	.159	.244	.389	.476	.834
4.0	.975	1.026	.061	.063	.131	.213	.327	.579	.671	1.248
4.5	.867	1.154	.068	.079	.157	.277	.432	.757	.953	
5.0	.780	1.282	.076	.095	.242	.349	.546	1.154	1.390	
5.5	.709	1.410	[illegible]	.111	.283	.428	.736	1.248		
6.0	.650	1.538	.087	.127	.322	.569	.963			
6.5	.600	1.667	.095	.143	.397	.707	1.191			
7.0	.557	1.795	.105	.159	.476	.834	1.390			
7.5	.520	1.923	.114	.185	.566	1.154				
8.0	.487	2.051	.131	.213	.671	1.248				
8.5	.459	2.179	.150	.245	.799					
9.0	.433	2.308	.197	.277	.963					
9.5	.411	2.436	.214	.311	1.206					
10.0	.390	2.564	.242	.349	1.380					

TABLE IVb. MINIMUM RESOLVABLE TEMPERATURE, COMPENSATED FOR ASPECT RATIO ε, TABULATED FOR FOUR FIELDS OF VIEW AND TWO DISPLAY SIZES AND FOR SPATIAL FREQUENCIES CORRESPONDING TO THE ANGLES SUBTENDED BY A SUBJECT AT VARIOUS RANGES

Range, km	Angle, mrad	Spatial Fre- quency, cycles/ mrad	Minimum Resolvable Temperature, Δ °K							
			2.5-deg FOV		5-deg FOV		7.5-deg FOV		10-deg FOV	
			Large Display	7-in. Display	Large Display	7-in. Display	Large Display	7-in. Display	Large Display	7-in. Display
.5	7.800	.128	.010	.010	.010	.010	.010	.010	.010	.013
1.0	3.900	.256	.010	.010	.010	.010	.010	.018	.115	.119
1.5	2.598	.385	.010	.010	.010	.010	.127	.149	.153	.235
2.0	1.950	.513	.010	.010	.115	.118	.153	.230	.245	.309
2.5	1.560	.641	.010	.019	.139	.178	.214	.305	.459	.653
3.0	1.300	.769	.010	.013	.163	.235	.349	.518	.602	1.065
3.5	1.114	.897	.010	.017	.196	.288	.474	.775	.831	1.560
4.0	.975	1.026	.115	.118	.245	.368	.592	1.055	1.256	2.329
4.5	.867	1.154	.127	.148	.349	.518	.898	1.417	1.837	
5.0	.780	1.282	.139	.178	.453	.653	1.050	2.158	2.592	
5.5	.709	1.410	.151	.208	.530	.881	1.376	2.328		
6.0	.650	1.538	.163	.238	.602	1.065	1.893			
6.5	.600	1.667	.178	.248	.723	1.322	2.593			
7.0	.557	1.795	.196	.268	.891	1.568	2.592			
7.5	.520	1.923	.216	.325	1.059	2.159				
8.0	.487	2.051	.245	.368	1.256	2.320				
8.5	.459	2.179	.297	.458	1.496					
9.0	.433	2.308	.349	.518	1.802					
9.5	.411	2.436	.401	.581	2.257					
10.0	.390	2.564	.453	.653	2.592					

If we now refer to the various sources of material on the value of signal to noise required for different visual tasks such as detection, recognition, etc. listed in Table IIIa, it becomes clear that the signal to noise required is different for the various tasks and further is different for different sized objects of interest.

Table IIIa. lists the perceived signal-to-noise ratio thresholds at 50 percent probability for a number of visual tasks. This material is explained in a number of publications such as Refs. 6, 7, 8, 11, 12, and 13. For the reasons explained in those references, the perceived signal-to-noise ratio, sometimes referred to as the signal-to-noise ratio at the display, SNR_D, or the signal-to-noise ratio in the displayed image must be larger for large images than for moderately small ones.

In the case of a FLIR, the measured value of MRT is the measured response of a human observer and thus the effects of the integration of the human eye are included in the measured response.

In the case of computed values of MRT, this factor must be introduced into the calculation.

In the case of predictions of observer performance computed from description of the scene and FLIR parameters, such corrections are also necessary.

5. DETAILS OF THE CALCULATION PROCEDURE

Based upon the factors discussed above we constructed an algorithm for the successive computation of atmospheric transmission, signal to noise at a series of ranges and thus at a series of appropriate spatial frequencies and, finally, the probability of detection of a tank for each range of interest. The successive operations are listed below.

1. Determine from tables, records, etc. the value of ΔT to be expected for a given target.
2. Determine the dimensions of the target.
3. Decide on the various ranges of interest.
4. Determine temperature, dew point and visibility for time and place of interest. See Figs. 6a-d for data over full year.
5. Using the LOWTRAN III model, calculate what the atmospheric transmission is for the chosen spectral band and range.
6. Calculate the angular subtense of the minimum dimension of the object at each range.
7. Calculate the "equivalent bar pattern" frequency for the target at each range.
8. Calculate the aspect ratio, ε, of the bar in the equivalent bar pattern.
9. Obtain or calculate the MRT as a function of spatial frequency for the sensor or sensors of interest.
10. For the ranges of interest and therefore for the "equivalent bar pattern" frequency, determine the values of $MRT/\sqrt{\varepsilon/7}$.
11. Calculate the value of ΔT_{Ap} by multiplying the ΔT of the object at zero range by the atmospheric transmission at the range of interest.
12. Calculate $\Delta T_{Ap}/(MRT/\sqrt{\varepsilon/7})$.
13. Enter the normalized probability curve. (See Fig. 5.)
14. Note the probability of achieving the given function.

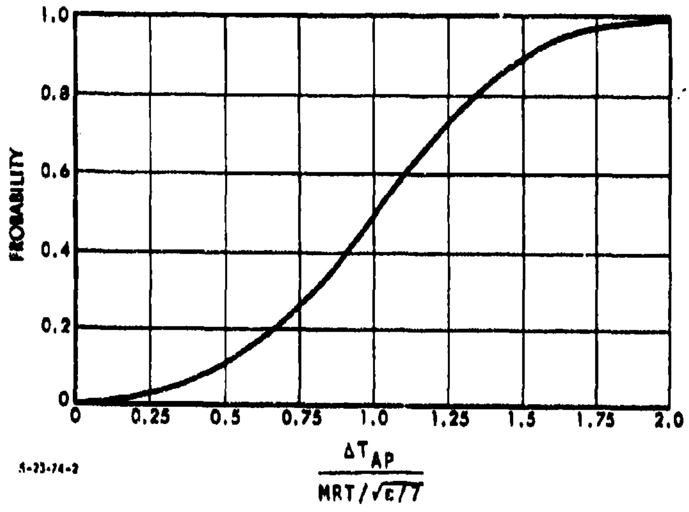

FIGURE 5. PROBABILITY OF DETECTION VS. $\frac{\Delta T_{AP}}{MRT/\sqrt{\epsilon/T}}$

6. FIRST RESULTS

The application of this algorithm to real data results in the data tabulated in Table Va and Vb. Table Va shows the probabilities of detection for a frontal aspect tank at one hour in January and one hour in August, uncorrected as well as corrected for aspect.

Although Table V is quite carefully calculated, it should not be taken very seriously. The reasons for its lack of credibility lie in the wide variations in that kind of data as weather conditions vary, and they do vary widely and rapidly. Although a glance at the sample weather data in Table VI doesn't seem to show much change, examine column 6. It is clear that although the humidity or temperature doesn't vary very widely, the visibility does, and that effect alone can at times put FLIRs out of business. Even though our study considers only the 8.5-11 micrometer and not visible band radiation, the same particulates and aerosols that cause trouble in visibility also cause trouble in 8.5-11, though not with a one-to-one correspondence.

Figures 6a and 6b show the hourly visibility, air temperature, dew point, and the corresponding computed atmospheric transmittance for January and August 1970. It is clear that if system performance is weather-dependent, the performance will vary widely and frequently. NOTE: DAY OF MONTH IS ALWAYS ABSCISSA.

7. DISCUSSION OF RESULTS

From the data on MRT weather and the equivalent bar patterns for given targets, we have computed and plotted a series of curves showing and comparing data as a function of the more important parameters of weather and sensor.

Figures 6a and 6b show the weather data and the computed transmittance data at 8.5-11 µm for distances (ranges) of 5 and 8 km. The choice of ranges was made on the basis of the exponential effect of range upon transmission. The next of this series, Figs. 7 and 8, show the range at 50

TABLE Va. PERCEIVED SIGNAL-TO-NOISE RATIO AND PROBABILITY OF FLIR DETECTION OF TANK IN FRONTAL ASPECT, HANNOVER, GERMANY, UNCOMPENSATED FOR ASPECT RATIO ε, FOR FOUR FIELDS OF VIEW AND TWO DISPLAY SIZES

8 JANUARY 1970, 1800 HOURS

Range, km	Apparent Target Temperature, °C	2.5-deg Field of View				5.0-deg Field of View				7.5-deg Field of View				10.0-deg Field of View			
		Large Display		7-in. Display		Large Display		7-in. Display		Large Display		7-in. Display		Large Display		7-in. Display	
		SNR	Probability	SNR	Probability	SNR	Probability	SNR	Probability	SNR	Probability	SNR	Probability	SNR	Probability	SNR	Probability
0.5	1.77	99.00	1.00	99.00	1.00	99.00	1.00	99.00	1.00	99.00	1.00	99.00	1.00	99.00	1.00	99.00	1.00
1.0	1.58	99.00	1.00	99.00	1.00	99.00	1.00	99.00	1.00	99.00	1.00	99.00	1.00	25.79	1.00	25.00	1.00
1.5	1.42	99.00	1.00	99.00	1.00	99.00	1.00	99.00	1.00	29.91	1.00	17.86	1.00	16.28	1.00	11.12	1.00
2.0	1.27	99.00	1.00	99.00	1.00	20.73	1.00	20.10	1.00	14.62	1.00	9.38	1.00	9.69	1.00	5.97	1.00
2.5	1.14	99.00	1.00	99.00	1.00	15.42	1.00	12.00	1.00	10.00	1.00	6.19	1.00	4.72	1.00	3.27	1.00
3.0	1.03	99.00	1.00	99.00	1.00	11.84	1.00	8.08	1.00	5.51	1.00	3.71	1.00	3.20	1.00	1.81	0.99
3.5	0.93	92.75	1.00	92.75	1.00	8.87	1.00	5.82	1.00	3.51	1.00	2.39	1.00	1.95	1.00	1.11	0.63
4.0	0.84	13.66	1.00	13.24	1.00	6.79	1.00	3.93	1.00	2.60	1.00	1.47	0.91	1.25	0.75	0.68	0.19
4.5	0.76	11.17	1.00	9.54	1.00	4.05	1.00	2.73	1.00	1.75	0.98	1.00	0.50	0.78	0.27	--	--
5.0	0.68	9.22	1.00	7.17	1.00	2.82	1.00	1.96	1.00	1.21	0.72	0.59	0.12	0.49	0.07	--	--
5.5	0.62	7.67	1.00	5.55	1.00	2.18	1.00	1.44	0.90	0.84	0.32	0.50	0.09	--	--	--	--
6.0	0.56	6.43	1.00	4.53	1.00	1.74	0.98	0.93	0.45	0.59	0.12	--	--	--	--	--	--
6.5	0.51	5.33	1.00	3.57	1.00	1.31	0.81	0.72	0.21	0.37	0.04	--	--	--	--	--	--
7.0	0.46	4.39	1.00	2.88	1.00	0.96	0.45	0.55	0.10	0.33	0.03	--	--	--	--	--	--
7.5	0.42	3.64	1.00	2.25	1.00	0.74	0.22	0.35	0.03	--	--	--	--	--	--	--	--
8.0	0.38	2.88	1.00	1.77	0.99	0.56	0.11	0.30	0.02	--	--	--	--	--	--	--	--
8.5	0.34	2.16	1.00	1.40	0.97	0.43	0.05	--	--	--	--	--	--	--	--	--	--
9.0	0.31	1.67	0.97	1.12	0.64	0.32	0.03	--	--	--	--	--	--	--	--	--	--
9.5	0.28	1.32	0.82	0.91	0.40	0.23	0.01	--	--	--	--	--	--	--	--	--	--
10.0	0.26	1.06	0.57	0.74	0.25	0.19	0.01	--	--	--	--	--	--	--	--	--	--

8 AUGUST 1970, 0100 HOURS

Range, km	Apparent Target Temperature, °C	2.5-deg Field of View				5.0-deg Field of View				7.5-deg Field of View				10.0-deg Field of View			
		Large Display		7-in. Display		Large Display		7-in. Display		Large Display		7-in. Display		Large Display		7-in. Display	
		SNR	Probability	SNR	Probability	SNR	Probability	SNR	Probability	SNR	Probability	SNR	Probability	SNR	Probability	SNR	Probability
0.5	1.65	99.00	1.00	99.00	1.00	99.00	1.00	99.00	1.00	99.00	1.00	99.00	1.00	99.00	1.00	99.00	1.00
1.0	1.39	99.00	1.00	99.00	1.00	99.00	1.00	99.00	1.00	99.00	1.00	99.00	1.00	22.69	1.00	22.00	1.00
1.5	1.18	99.00	1.00	99.00	1.00	99.00	1.00	99.00	1.00	17.44	1.00	14.30	1.00	13.59	1.00	9.28	1.00
2.0	1.01	99.00	1.00	99.00	1.00	16.43	1.00	15.93	1.00	11.58	1.00	7.91	1.00	7.58	1.00	4.73	1.00
2.5	0.86	86.04	1.00	86.04	1.00	11.61	1.00	9.03	1.00	7.53	1.00	4.66	1.00	3.55	1.00	2.46	1.00
3.0	0.74	73.66	1.00	73.66	1.00	8.47	1.00	5.79	1.00	3.95	1.00	2.66	1.00	2.29	1.00	1.29	0.80
3.5	0.63	63.17	1.00	63.17	1.00	6.04	1.00	3.96	1.00	2.39	1.00	1.63	0.96	1.33	0.82	0.76	0.24
4.0	0.54	8.85	1.00	8.58	1.00	4.14	1.00	2.55	1.00	1.69	0.98	0.95	0.45	0.81	0.29	0.44	0.05
4.5	0.47	6.88	1.00	5.88	1.00	2.50	1.00	1.68	0.97	1.08	0.59	0.62	0.14	0.48	0.07	--	--
5.0	0.40	5.40	1.00	4.20	1.00	1.65	0.97	1.15	0.66	0.71	0.20	0.35	0.03	0.29	0.02	--	--
5.5	0.34	4.28	1.00	3.10	1.00	1.22	0.73	0.80	0.29	0.47	0.06	0.28	0.02	--	--	--	--
6.0	0.30	3.41	1.00	2.33	1.00	0.92	0.41	0.52	0.09	0.31	0.02	--	--	--	--	--	--
6.5	0.26	2.69	1.00	1.78	0.99	0.66	0.17	0.36	0.05	0.19	0.01	--	--	--	--	--	--
7.0	0.22	2.11	1.00	1.58	0.96	0.45	0.06	0.25	0.02	0.16	0.01	--	--	--	--	--	--
7.5	0.19	1.66	0.97	1.03	0.53	0.34	0.03	0.16	0.01	--	--	--	--	--	--	--	--
8.0	0.16	1.25	0.76	0.77	0.26	0.24	0.02	0.13	0.01	--	--	--	--	--	--	--	--
8.5	0.14	0.89	0.38	0.58	0.11	0.18	0.01	--	--	--	--	--	--	--	--	--	--
9.0	0.12	0.65	0.16	0.44	0.06	0.13	0.01	--	--	--	--	--	--	--	--	--	--
9.5	0.11	0.49	0.07	0.34	0.03	0.09	0.00	--	--	--	--	--	--	--	--	--	--
10.0	0.09	0.36	0.04	0.26	0.02	0.07	0.00	--	--	--	--	--	--	--	--	--	--

TABLE Vb. PERCEIVED SIGNAL-TO-NOISE RATIO AND PROBABILITY OF FLIR DETECTION OF TANK IN FRONTAL ASPECT, HANNOVER, GERMANY, COMPENSATED FOR ASPECT RATIO ε, FOR FOUR FIELDS OF VIEW AND TWO DISPLAY SIZES

8 JANUARY 1970, 1800 HOURS

Range, km	Apparent Target Temperature, °C	2.5-deg Field of View				5.0-deg Field of View				7.5-deg Field of View				10.0-deg Field of View			
		Large Display		7-in. Display		Large Display		7-in. Display		Large Display		7-in. Display		Large Display		7-in. Display	
		SNR	Probability	SNR	Probability	SNR	Probability	SNR	Probability	SNR	Probability	SNR	Probability	SNR	Probability	SNR	Probability
0.5	1.77	99.00	1.00	99.00	1.00	99.00	1.00	99.00	1.00	99.00	1.00	99.00	1.00	99.00	1.00	99.00	1.00
1.0	1.58	99.00	1.00	99.00	1.00	99.00	1.00	99.00	1.00	99.00	1.00	13.78	1.00	13.78	1.00	13.35	1.00
1.5	1.42	99.00	1.00	99.00	1.00	99.00	1.00	99.00	1.00	9.55	1.00	8.70	1.00	8.70	1.00	5.94	1.00
2.0	1.27	99.00	1.00	99.00	1.00	11.08	1.00	10.74	1.00	5.33	1.00	5.18	1.00	5.18	1.00	3.19	1.00
2.5	1.14	99.00	1.00	99.00	1.00	8.24	1.00	6.41	1.00	3.51	1.00	2.52	1.00	2.52	1.00	1.75	0.98
3.0	1.03	99.00	1.00	99.00	1.00	6.33	1.00	4.32	1.00	1.99	1.00	1.71	0.98	1.71	0.98	0.97	0.46
3.5	0.93	92.75	1.00	92.75	1.00	4.74	1.00	3.11	1.00	1.28	0.79	1.04	0.55	1.04	0.55	0.59	0.12
4.0	0.84	7.30	1.00	7.08	1.00	3.41	1.00	2.10	1.00	0.79	0.27	0.67	0.17	0.67	0.17	0.36	0.03
4.5	0.76	5.97	1.00	5.10	1.00	2.16	1.00	1.46	0.91	0.53	0.09	0.42	0.05	0.42	0.05	—	—
5.0	0.68	4.93	1.00	3.83	1.00	1.51	0.93	1.05	0.55	0.32	0.03	0.26	0.02	0.26	0.02	—	—
5.5	0.62	4.10	1.00	2.97	1.00	1.17	0.68	0.77	0.26	0.27	0.02	—	—	—	—	—	—
6.0	0.56	3.44	1.00	2.35	1.00	0.93	0.42	0.53	0.09	—	—	—	—	—	—	—	—
6.5	0.51	2.85	1.00	1.89	0.99	0.70	0.20	0.38	0.04	—	—	—	—	—	—	—	—
7.0	0.46	2.35	1.00	1.54	0.94	0.51	0.08	0.29	0.02	—	—	—	—	—	—	—	—
7.5	0.42	1.95	1.00	1.20	0.72	0.39	0.04	0.19	0.01	—	—	—	—	—	—	—	—
8.0	0.38	1.54	0.94	0.95	0.44	0.30	0.02	0.16	0.01	—	—	—	—	—	—	—	—
8.5	0.34	1.15	0.67	0.75	0.24	0.23	0.01	—	—	—	—	—	—	—	—	—	—
9.0	0.31	0.89	0.38	0.60	0.13	0.17	0.01	—	—	—	—	—	—	—	—	—	—
9.5	0.28	0.70	0.20	0.49	0.07	0.13	0.01	—	—	—	—	—	—	—	—	—	—
10.0	0.26	0.57	0.11	0.39	0.04	0.10	0.01	—	—	—	—	—	—	—	—	—	—

8 AUGUST 1970, 0100 HOURS

Range, km	Apparent Target Temperature, °C	2.5-deg Field of View				5.0-deg Field of View				7.5-deg Field of View				10.0-deg Field of View			
		Large Display		7-in. Display		Large Display		7-in. Display		Large Display		7-in. Display		Large Display		7-in. Display	
		SNR	Probability	SNR	Probability	SNR	Probability	SNR	Probability	SNR	Probability	SNR	Probability	SNR	Probability	SNR	Probability
0.5	1.65	99.00	1.00	99.00	1.00	99.00	1.00	99.00	1.00	99.00	1.00	99.00	1.00	99.00	1.00	99.00	1.00
1.0	1.39	99.00	1.00	99.00	1.00	99.00	1.00	99.00	1.00	99.00	1.00	99.00	1.00	12.13	1.00	11.75	1.00
1.5	1.18	99.00	1.00	99.00	1.00	99.00	1.00	99.00	1.00	9.32	1.00	7.96	1.00	7.26	1.00	4.95	1.00
2.0	1.01	99.00	1.00	99.00	1.00	8.78	1.00	8.52	1.00	6.19	1.00	4.23	1.00	4.10	1.00	2.53	1.00
2.5	0.86	86.04	1.00	96.04	1.00	6.21	1.00	4.83	1.00	4.03	1.00	2.49	1.00	1.90	0.99	1.32	0.82
3.0	0.74	73.66	1.00	73.56	1.00	4.53	1.00	3.09	1.00	2.11	1.00	1.42	0.59	1.22	0.74	0.69	0.19
3.5	0.63	63.17	1.00	63.17	1.00	3.23	1.00	2.12	1.00	1.28	0.79	0.87	0.36	0.71	0.20	0.40	0.04
4.0	0.54	4.73	1.00	4.59	1.00	2.21	1.00	1.36	0.85	0.90	0.39	0.51	0.08	0.43	0.05	0.23	0.01
4.5	0.47	3.68	1.00	3.14	1.00	1.33	0.83	0.90	0.39	0.58	0.11	0.33	0.03	0.26	0.02	—	—
5.0	0.40	2.89	1.00	2.25	1.00	0.88	0.37	0.61	0.13	0.38	0.04	0.19	0.01	0.16	0.01	—	—
5.5	0.34	2.29	1.00	1.56	0.97	0.65	0.16	0.43	0.05	0.25	0.02	0.15	0.01	—	—	—	—
6.0	0.30	1.82	0.99	1.25	0.76	0.49	0.07	0.28	0.02	0.16	0.01	—	—	—	—	—	—
6.5	0.26	1.44	0.89	0.95	0.45	0.35	0.03	0.19	0.01	0.10	0.01	—	—	—	—	—	—
7.0	0.22	1.13	0.64	0.74	0.23	0.25	0.02	0.14	0.01	0.09	0.00	—	—	—	—	—	—
7.5	0.19	0.89	0.38	0.55	0.10	0.18	0.01	0.09	0.00	—	—	—	—	—	—	—	—
8.0	0.16	0.67	0.17	0.41	0.05	0.13	0.01	0.07	0.00	—	—	—	—	—	—	—	—
8.5	0.14	0.48	0.07	0.31	0.02	0.09	0.00	—	—	—	—	—	—	—	—	—	—
9.0	0.12	0.35	0.03	0.24	0.01	0.07	0.00	—	—	—	—	—	—	—	—	—	—
9.5	0.11	0.26	0.02	0.18	0.01	0.05	0.00	—	—	—	—	—	—	—	—	—	—
10.0	0.09	0.20	0.01	0.14	0.01	0.04	0.00	—	—	—	—	—	—	—	—	—	—

TABLE VIa. SAMPLE, ILLUSTRATIVE WEATHER DATA FOR JANUARY 8, 1970, HANNOVER, WEST GERMANY

Month	Day	Hour	Dew Point °C	Air Temp. °C	Visibility Km	Cloud Cover (eighths)	Lumb Factor	Wind Velocity (knots)	Wind Direction (Degrees)	Barometric Pressure Millibars (every 3rd hour)
1	8	0100	-5.	-4.	1.6	8.	5.	5.	60.	
1	8	0200	-5.	-4.	1.6	8.	5.	4.	80.	
1	8	0300	-5.	-4.	2.	8.	5.	5.	80.	1027.
1	8	0400	-5.	-5.	1.6	8.	5.	7.	70.	
1	8	0500	-6.	-5.	1.2	8.	5.	8.	100.	
1	8	0600	-8.	-7.	0.4	8.	5.	9.	110.	1027.
1	8	0700	-8.	-7.	0.4	8.	5.	8.	90.	
1	8	0800	-8.	-7.	0.3	8.	5.	8.	90.	
1	8	0900	-8.	-7.	0.4	8.	5.	9.	90.	1028.
1	8	1000	-9.	-8.	0.6	8.	5.	8.	90.	
1	8	1100	-9.	-8.	0.6	8.	5.	7.	100.	
1	8	1200	-9.	-8.	1.3	8.	5.	10.	90.	1028.
1	8	1300	-9.	-8.	1.8	8.	5.	8.	90.	
1	8	1400	-9.	-8.	2.	7.	4.	8.	90	
1	8	1500	-8.	-7.	1.8	7.	4.	13.	90.	1026.
1	8	1600	-8.	-8.	1.6	7.	3.	14.	80.	
1	8	1700	-8.	-7.	1.8	7.	3.	12.	100.	
1	8	1800	-8.	-7.	2.5	6.	2.	12.	100.	1026.
1	8	1900	-8.	-7.	2.0	6.	2.	15.	110.	
1	8	2000	-8.	-7.	3.5	3.	2.	15.	110.	
1	8	2100	-8.	-7.	3.0	6.	2.	17.	90.	1025.
1	8	2200	-8.	-8.	3.0	7.	3.	13.	90.	
1	8	2300	-8.	-7.	3.0	7.	3.	17.	100.	
1	8	2400	-8.	-6.	4.0	7.	3.	17.	90.	1024.

TABLE VIb. SAMPLE, ILLUSTRATIVE WEATHER DATA FOR AUGUST 8, 1970, HANNOVER, WEST GERMANY

Month	Day	Hour	Dew Point °C	Air Temp. °C	Visibility Km	Cloud Cover (eighths)	Lumb Factor	Wind Velocity (knots)	Wind Direction (Degrees)	Barometric Pressure Millibars (every 3rd hour)
8	8	0100	16.	17.	6.00	8.	4.	0.	0.	
8	8	0200	15.	16.	6.00	8.	4.	2.	90.	
8	8	0300	15.	16.	5.00	8.	4.	2.	90.	1012.
8	8	0400	15.	16.	5.00	8.	4.	2.	40.	
8	8	0500	15.	16.	5.00	7.	4.	2.	90.	
8	8	0600	17.	17.	4.00	7.	4.	5.	50.	1012.
8	8	0700	17.	19.	4.00	7.	4.	4.	70.	
8	8	0800	19.	20.	4.00	6.	3.	6.	60.	
8	8	0900	19.	22.	5.00	7.	4.	7.	90.	1012.
8	8	1000	19.	23.	7.00	6.	4.	9.	100.	
8	8	1100	16.	24.	9.00	6.	3.	10.	90.	
8	8	1200	16.	23.	7.00	8.	4.	10.	100.	1011.
8	8	1300	17.	19.	3.00	8.	6.	8.	220.	
8	8	1400	17.	17.	7.00	8.	6.	4.	90.	
8	8	1500	17.	17.	8.00	8.	5.	1.	90.	1012.
8	8	1600	17.	18.	8.00	6.	4.	2.	90.	
8	8	1700	17.	18.	8.00	8.	5.	4.	10.	
8	8	1800	17	18.	7.00	7.	4.	2	360.	1012.
8	8	1900	16.	16.	3.80	5.	3.	4.	350.	
8	8	2000	16.	16.	3.00	8	5.	5.	270.	
8	8	2100	15.	16.	3.00	8.	5.	6.	310.	1012.
8	8	2200	16.	16.	4.00	8.	5.	5.	310.	
8	8	2300	16.	16.	2.00	8.	5.	5.	250	

JANUARY 1970

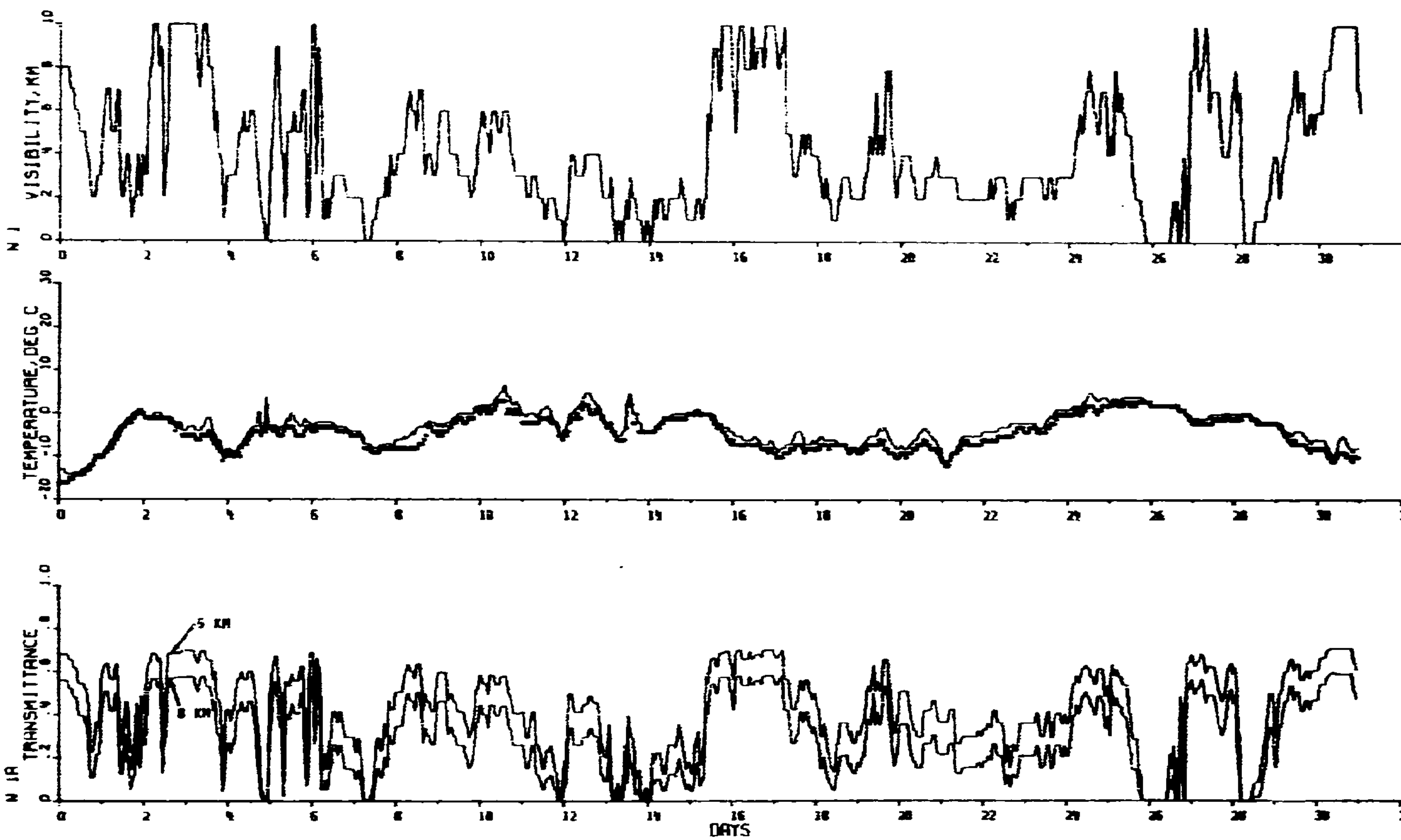

1-26-76-2

FIGURE 6a. HOURLY VISIBILITY, AIR TEMPERATURE (—), DEW POINT (o), AND CORRESPONDING COMPUTED ATMOSPHERIC TRANSMITTANCES AT 8.5-11 μm FOR RANGES OF 5 AND 8 km; HANNOVER, GERMANY, JANUARY 1970. (VISIBILITY CURVE IS TRUNCATED AT 10 km. EACH TICK ON ABSCISSA MARKS END OF A DAY.)

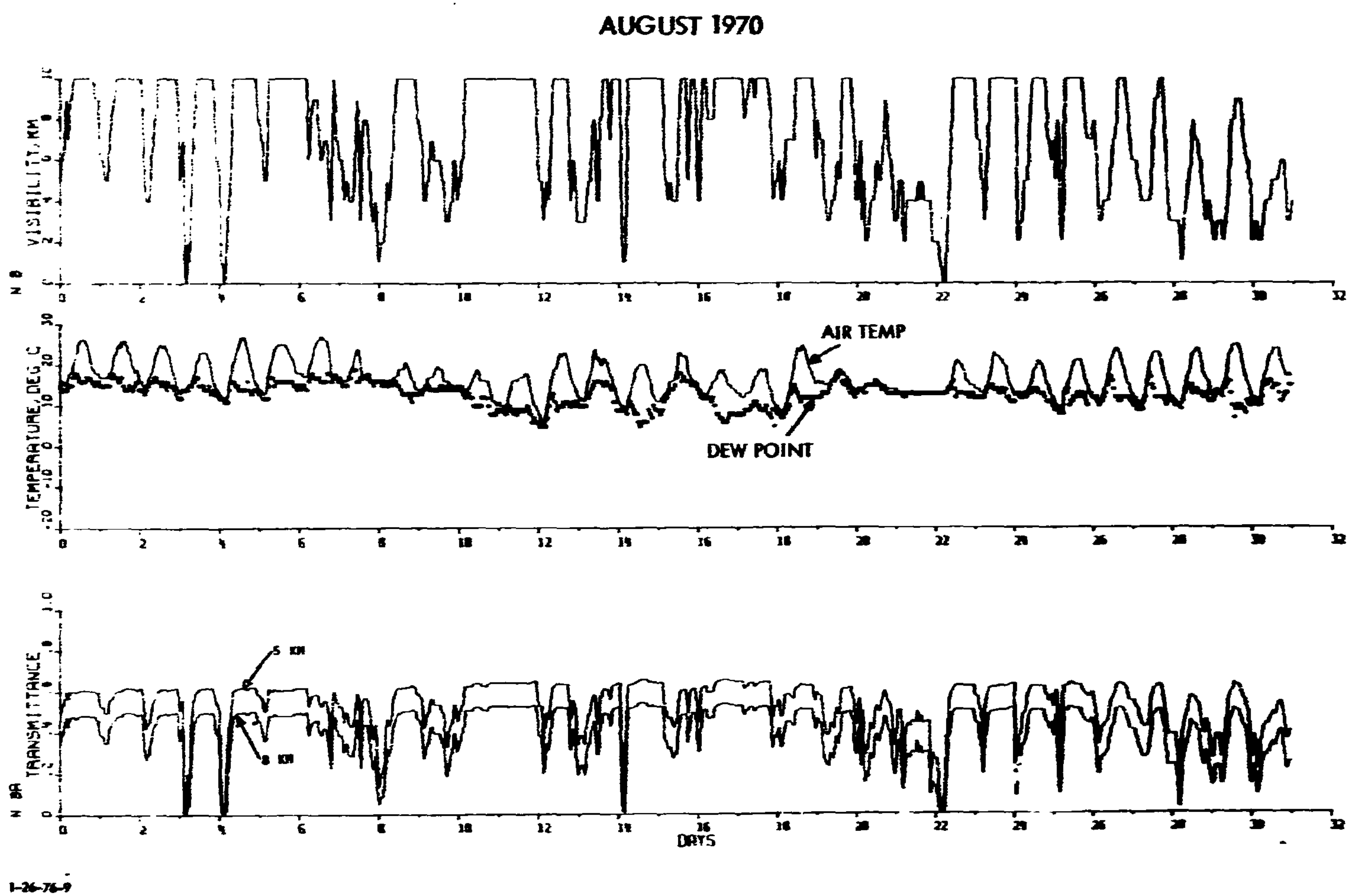

FIGURE 6b. HOURLY VISIBILITY, AIR TEMPERATURE (—), DEW POINT (o), AND CORRESPONDING COMPUTED ATMOSPHERIC TRANSMITTANCES AT 8.5-11 μm FOR RANGES OF 5 AND 8 km; HANNOVER, GERMANY, AUGUST 1970. (VISIBILITY CURVE IS TRUNCATED AT 10 km. EACH TICK ON ABSCISSA MARKS END OF A DAY.)

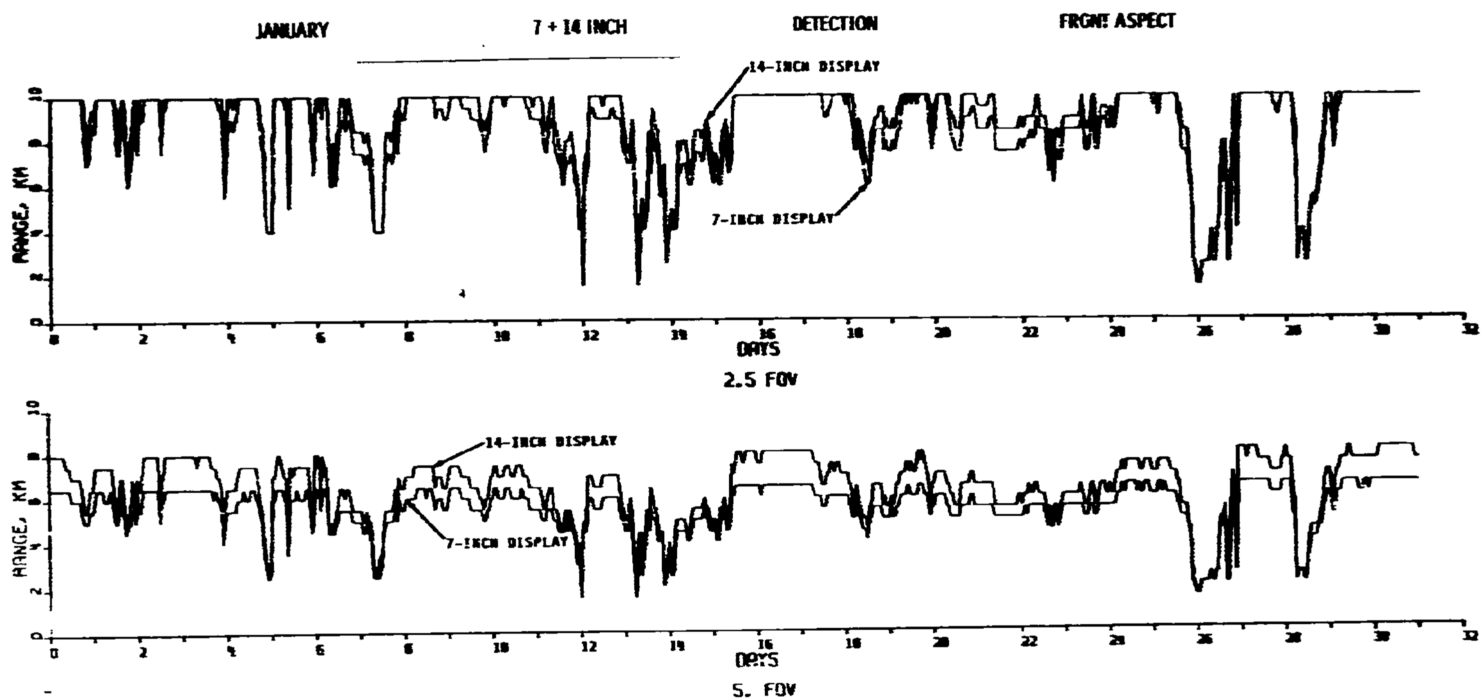

4-13-76-13

FIGURE 7. RANGE FOR 50 PERCENT PROBABILITY OF DETECTION OF TANK IN FRONTAL ASPECT, HANNOVER, GERMANY, JANUARY 1970; FLIR, 8.5-11 μm, 2.5-DEG AND 5-DEG FOV, 7-IN. AND 14-IN. DISPLAYS.

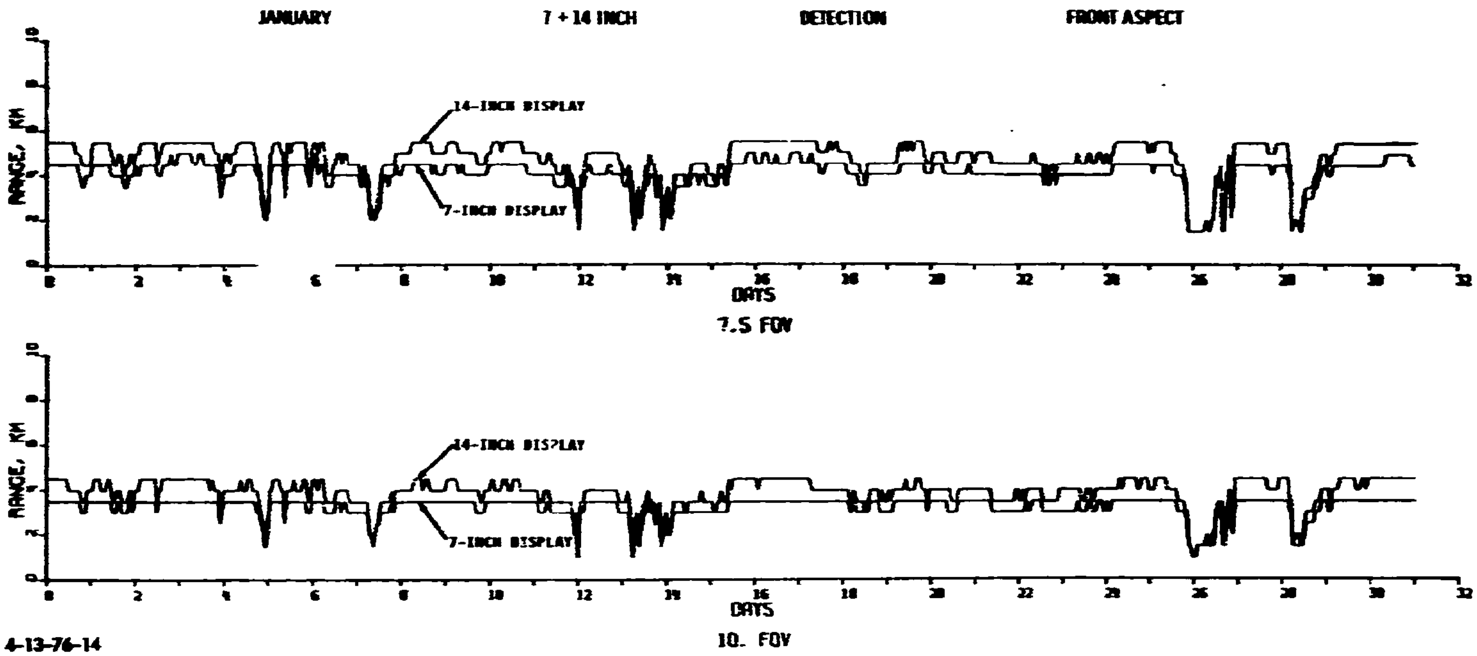

FIGURE 8. RANGE FOR 50 PERCENT PROBABILITY OF DETECTION OF TANK IN FRONTAL ASPECT, HANNOVER, GERMANY, JANUARY 1970; FLIR, 8.5-11 μm, 7.5-DEG AND 10-DEG FOV, 7-IN. AND 14-IN. DISPLAYS.

percent probability of front aspect detection of a tank in January 1970 for four different fields of view from 2-1/2 degrees to 10 degrees with displays of 7 and 14 inches. The range is greatest for the smallest field of view and the larger display and least for the largest field of view and the smaller display.

Although we started by showing the data as range at 50 percent probability, we believe that showing probability at specified ranges is more meaningful and the rest of the series of first results, i.e., Figs. 9 through 13, show the probability at various ranges and conditions with sufficient comparison data presented simultaneously for the major effects to be clearly obvious to the reader.

Figure 9 shows the probability of detection for a tank seen in frontal aspect with a 2-1/2 degree FOV FLIR at a range of 8 km, and it also shows similar data for a 7-1/2 degree FOV FLIR at a range of 4 km.

When the SNR_D or value of $\Delta T/MRT$, corrected and uncorrected, is significantly greater than about 2.0, the correction matters little, and the probability of detecting appears to be 100 percent for any case.

When, however, $\Delta T/MRT$ falls off appreciably below that point, the slopes get increasingly steep and the difference in corrected and uncorrected data can be a factor of five and more. For example, the values that previously indicated a probability of detection of, say, 0.63 now become 0.12 when corrected.

8. CONCLUSIONS

It is important to note that there are two major different but important factors affecting the detection of a target by infrared through a real atmosphere. These factors apply to any spectral band but here we consider only the 8.5-11 micrometer window.

The first factor is gaseous absorption such as that caused by atmospheric water or carbon dioxide, etc. The second is that due to scatter caused by aerosols and particulate material.

We all learned that water was the real villian in infrared system performance, and thus the wintertime with cold weather and little water should be much better than summer with much humidity.

Out data shows that the facts do not support these contentions, and that the haze, mists, fogs, and smokes of winter are far more serious, see Figs. 11-14. These figures show the probability of detection: 1) limited by the total atmospheric attenuation, 2) limited just by scatter, and 3) limited just by absorption. Note the effects of scatter tend to cause the most severe degradation, i.e., the calculated transmissions of Figs. 6e and 6f bob up and down not with humidity but with computations scaled to visibility.

One may question the wisdom of scaling from data taken at 0.55 micrometers to 10 micrometers. We worried about that. Therefore we asked Selby and Fenn of the Air Force Cambridge Research Laboratories to examine the question in more detail. The response follows.

John Selby has compared the new extinction coefficient provided by Bob Fenn for rural and urban aerosols with those currently in LOWTRAN III (average continental aerosol). He found* that although the three models exhibit small differences in their spectral characteristics in the 7-14 micrometer

*Personal correspondence, 24 February 1975.

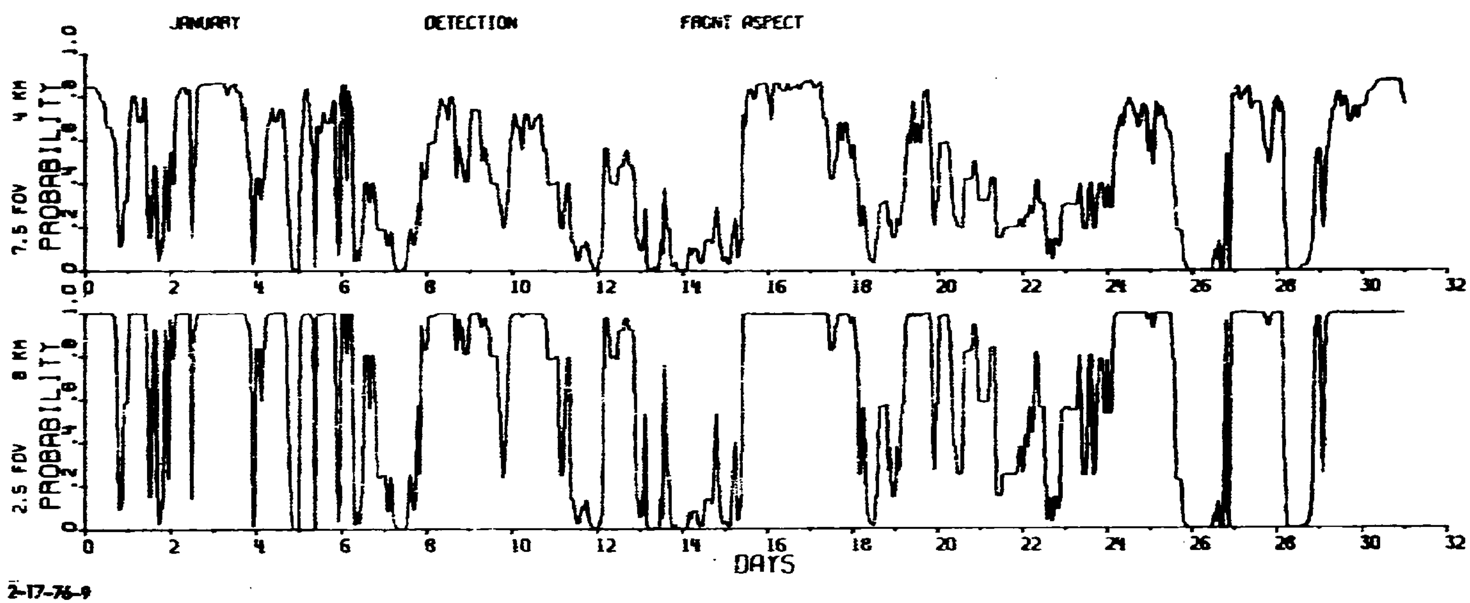

FIGURE 9. PROBABILITY OF DETECTION OF TANK IN FRONTAL ASPECT, HANNOVER, GERMANY, JANUARY 1970; FLIR, 8.5-11 μm, 7.5-DEG FOV AT 4-km RANGE, 2.5-DEG FOV AT 8-km RANGE, 7-IN. DISPLAY.

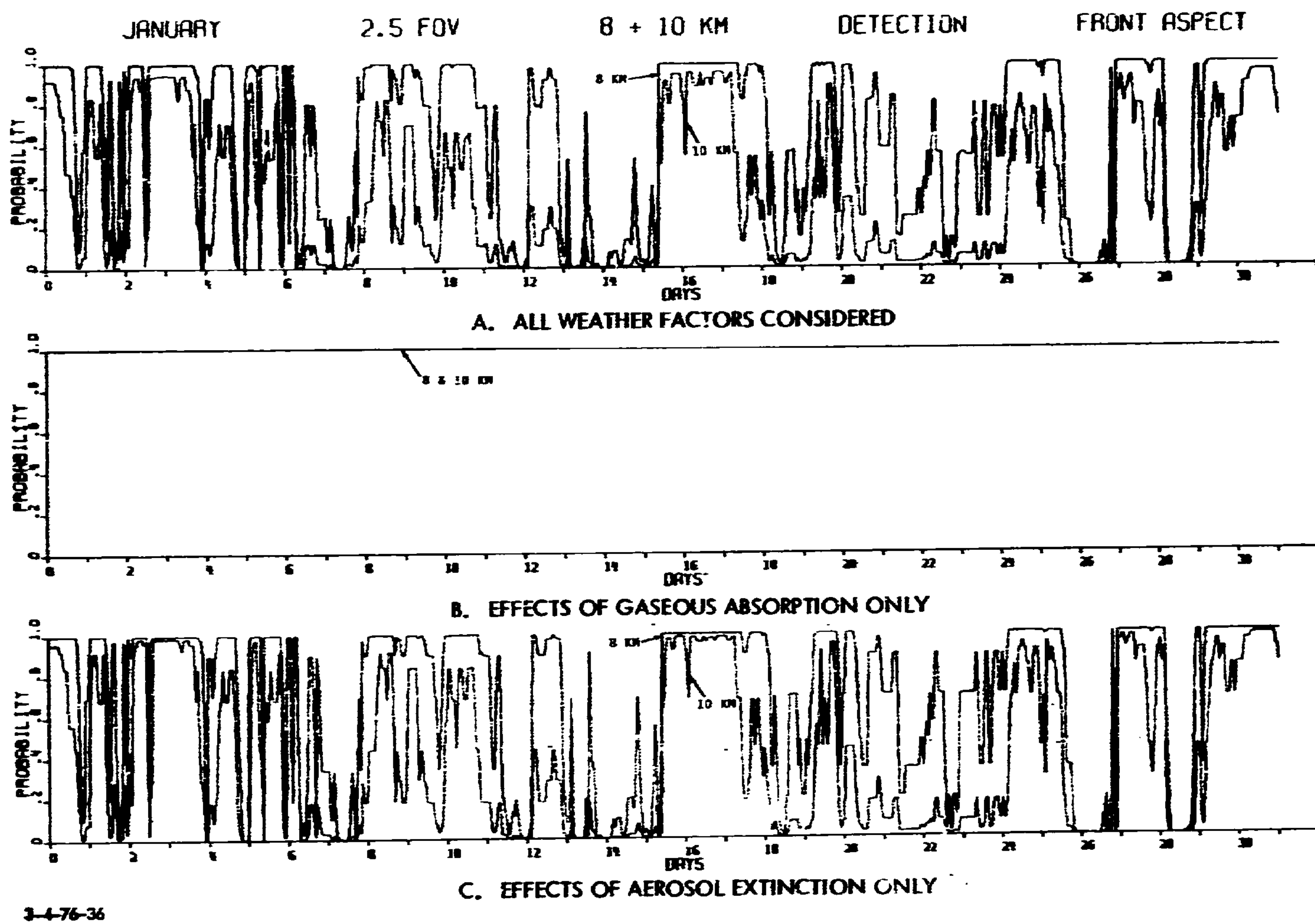

FIGURE 10. PROBABILITY OF DETECTION OF TANK IN FRONTAL ASPECT, HANNOVER GERMANY, JANUARY 1970; FLIR, 2.5-DEG FOV, 7-IN. DISPLAY, 8.5-11 μm, RANGES OF 8 AND 10 km.

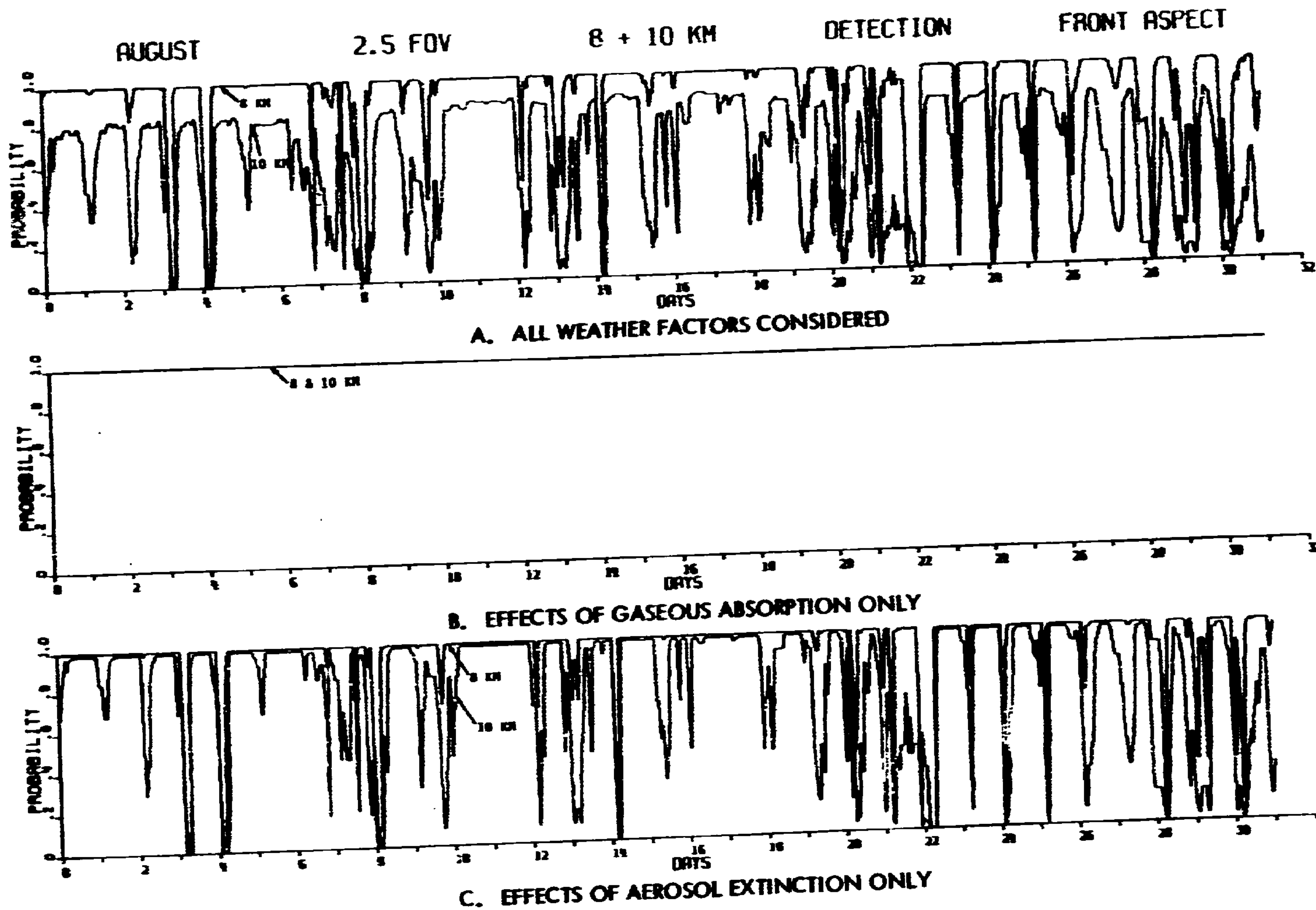

3-4-76-43

FIGURE 11. PROBABILITY OF DETECTION OF TANK IN FRONTAL ASPECT, HANNOVER, GERMANY, AUGUST 1970; FLIR, 2.5-DEG FOV, 7-IN. DISPLAY, 8.5-11 μm, RANGES OF 8 AND 10 km.

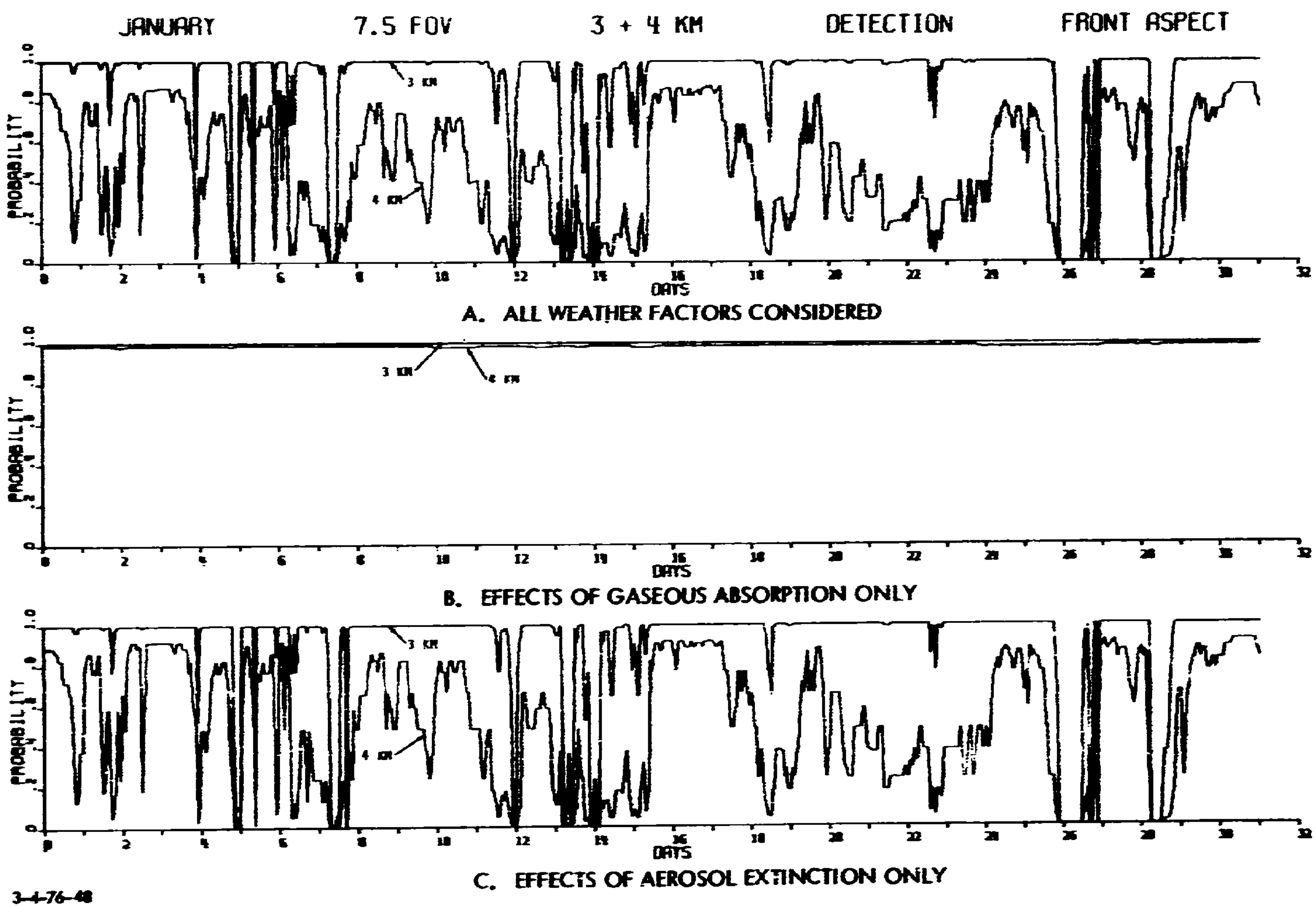

FIGURE 12. PROBABILITY OF DETECTION OF TANK IN FRONTAL ASPECT, HANNOVER, GERMANY, JANUARY 1970; FLIR, 7.5-DEG FOV, 7-IN. DISPLAY, 8.5-11 μm, RANGES OF 3 AND 4 km.

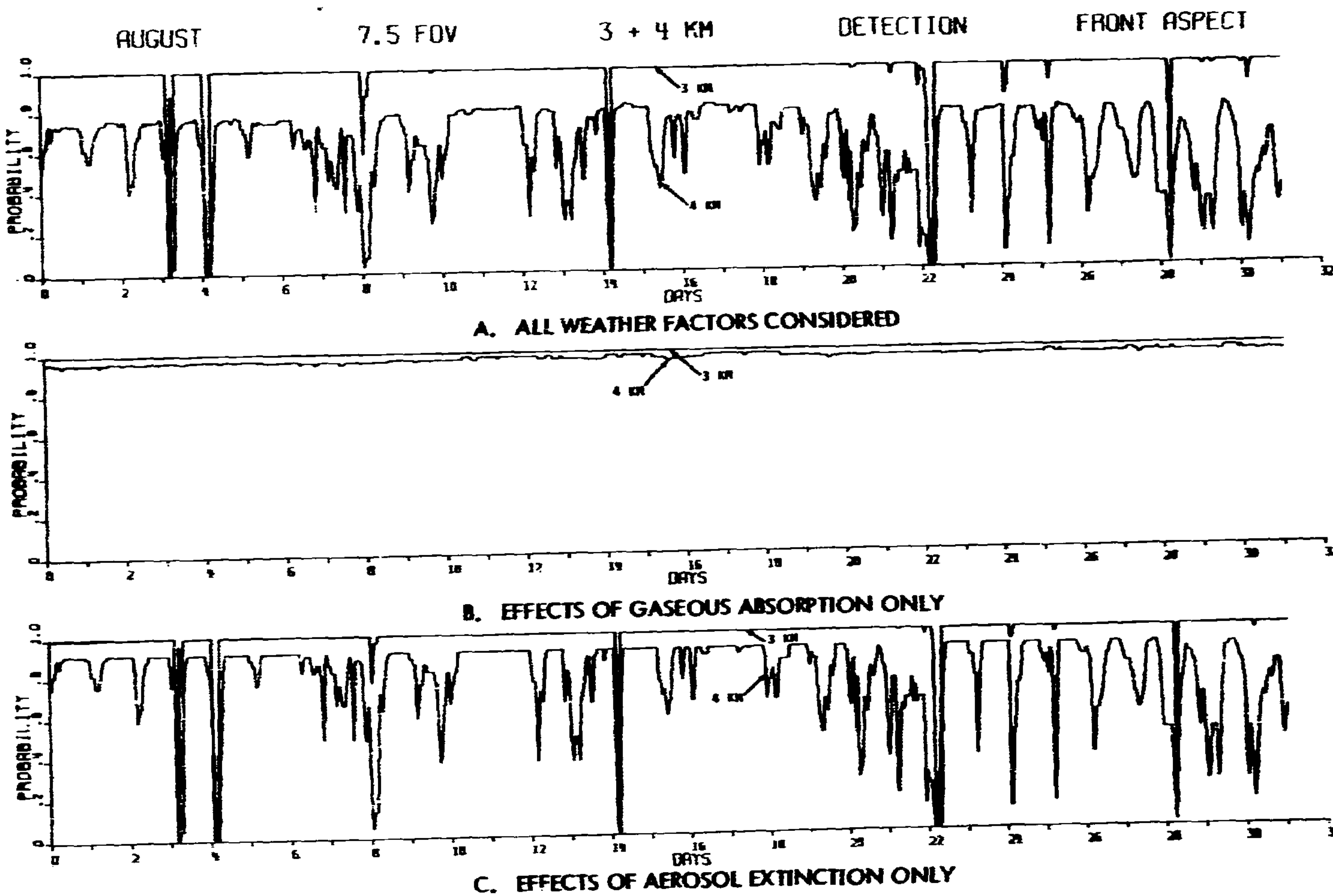

3-4-76-55

FIGURE 13. PROBABILITY OF DETECTION OF TANK IN FRONTAL ASPECT, HANNOVER, GERMANY, AUGUST 1970; FLIR, 7.5-DEG FOV, 7-IN. DISPLAY, 8.5-11 μm, RANGES OF 3 AND 4 km.

region, the average broadband transmittance appears to be the same. Each of these models in Tables VIIa-c in fact contains a different size distribution and particle number density: urban - 2.3×10^5 particles/cm^3; rural - 2.7×10^5; average continental - 2.8×10^3.

The differences between these models as a function of wavelength result from the different particle size distributions and refractive indices. For example, the maritime model has more large particles than the others. In order to use these curves, the visual range must be given, and the data all compared at 0.5 micrometers.

Although the three models considered above give the same average extinction coefficient in the 8.5-11 micrometer region, these models differ more significantly at other wavelengths. These will be examined (especially the 3.4-4.2 micrometer band) in another paper.

It should be clear from that data that the model is not very sensitive to variations in particle size distribution, and thus we believe quite strongly that our results, though possibly not as complete as might be hoped for, do show the effects we wished to demonstrate.

Later on in 1976-77, NATO Project OPAQUE will provide more experimental data against which we can test our results. In the interim, we present these findings above to show as best we can the effects of weather.

NOTE IN PROOF

Since this paper was first presented, detailed studies by Robert Roberts and Lucien Biberman (Ref. 16) have lead to the discovery that the LOWTRAN II and III models were erroneous in the values used for the 8-14 micron region of the water vapor continuum. These corrections have since been applied to the figures presented herein. The results for August, when humidity is significant, are considerably improved over prior calculations using the LOWTRAN II and III models. Figure 14 shows a comparison of atmospheric transmission by LOWTRAN II and III and our corrected calculations.

Ref. 16. R.E. Roberts, L.M. Biberman (IDA) and J.E.A. Selby (AFCRL), "Infrared Continuum Absorption by Atmospheric Water Vapor in the 8-12 μm Window," IDA P-1184, in press.

TABLE VIIa, b, c. TRANSMITTANCE AS A FUNCTION OF VISIBILITY AND RANGE (KM), CONTINENTAL (LOWTRAN III)

VIS / RANGE	.1	.5	1.0	5.0	10.0	15.0	20.0
.5	.91475	.63909	.41199	.01570	.00041	.00001	.00000
1.0	.95644	.79739	.63996	.11694	.01652	.00265	.00046
2.0	.97802	.89139	.79415	.33445	.11975	.04410	.01698
3.0	.98527	.92524	.85155	.43909	.23720	.11995	.06174
4.0	.98878	.94241	.89211	.57597	.33784	.20077	.12072
5.0	.99077	.95321	.91425	.64299	.41880	.27516	.18220
6.0	.99202	.96034	.92595	.69195	.48393	.34035	.24072
7.0	.99285	.96544	.93491	.72979	.53658	.39655	.29436
8.0	.99345	.96935	.94111	.75889	.58024	.44521	.34267
9.0	.99388	.97237	.94914	.78259	.61667	.48746	.38595
10.0	.99421	.97479	.95390	.80215	.64753	.52387	.42467
11.0	.99447	.97678	.95779	.81853	.67397	.55596	.45937
12.0	.99468	.97844	.96104	.83246	.69687	.58427	.49054
13.0	.99485	.97985	.96179	.84443	.71698	.60940	.51864
14.0	.99499	.98106	.96617	.85443	.73451	.63194	.54407
15.0	.99510	.98211	.96823	.85935	.75015	.65128	.56716
20.0	.99576	.98578	.97447	.89675	.80769	.72793	.65635
25.0	.99587	.98890	.97739	.91702	.84441	.77787	.71680
30.0	.99594	.98948	.98278	.93079	.86996	.81315	.76030
35.0	.99599	.99051	.98494	.94374	.88855	.83937	.79305
RURAL							
.5	.91336	.64254	.40321	.01958	.00414	.00000	.00000
1.0	.95573	.79392	.63147	.13676	.01179	.00141	.00019
2.0	.97767	.88951	.79471	.32992	.10662	.03593	.01221
3.0	.98505	.92407	.85722	.47049	.22421	.10770	.05208
4.0	.98864	.94173	.89139	.57922	.32995	.18712	.10836
5.0	.99053	.95250	.91399	.63946	.40810	.26245	.16920
6.0	.99195	.95978	.92474	.68648	.47431	.32940	.22777
7.0	.99280	.96498	.93483	.72453	.52815	.38557	.28192
8.0	.99341	.96891	[illegible]	[illegible]	.57254	.43437	.33075
9.0	.99385	.97198	.94441	.77895	.60973	.47790	.37459
10.0	.99419	.97445	.95121	.79979	.64119	.51211	.41407
11.0	.99445	.97647	.95716	.81547	.66815	.54792	.44939
12.0	.99456	.97815	.96146	.82454	.69150	.57659	.48114
13.0	.99483	.97934	.96327	.84143	.71199	.60231	.50978
14.0	.99497	.98081	.96584	.85242	.72996	.62519	.53570
15.0	.99509	.98188	.96777	.85171	.74590	.64577	.55926
20.0	.99579	.98541	.97514	.89509	.80452	.72315	.65019
25.0	.99587	.98746	.97754	.91574	.84141	.77405	.71181
30.0	.99544	.98917	.98256	.92471	.86771	.80998	.75614
35.0	.99599	.99044	.98470	.93493	.88672	.83066	.78952
URBAN							
.5	.91507	.63637	.41137	.01161	.00016	.00000	.00000
1.0	.95662	.79759	.63424	.10907	.01263	.00134	.00020
2.0	.97812	.89158	.79436	.32939	.11996	.03786	.01305
3.0	.98535	.92549	.85495	.47744	.23057	.11207	.05476
4.0	.98886	.94282	.89940	.57451	.33292	.19352	.11294
5.0	.99094	.95338	.91257	.64220	.41525	.26917	.17491
6.0	.99208	.96049	.92519	.69145	.48129	.33549	.23415
7.0	.99291	.96551	.93605	.72931	.53494	.39274	.28867
8.0	.99349	.96947	.94132	.75999	.57892	.44208	.33784
9.0	.99392	.97247	.94917	.78675	.61574	.48475	.38186
10.0	.99425	.97499	.95407	.80237	.64698	.52197	.42122
11.0	.99450	.97687	.95795	.81950	.67354	.55416	.45645
12.0	.99471	.97852	.96118	.83274	.69660	.59300	.48808
13.0	.99487	.97992	.96373	.84473	.71674	.60839	.51637
14.0	.99501	.98113	.96670	.85514	.73446	.63105	.54232
15.0	.99512	.98217	.96835	.85427	.75019	.65137	.56559
20.0	.99577	.98593	.97557	.89705	.80793	.72794	.65579
25.0	.99589	.98804	.97933	.91732	.84470	.77502	.71695
30.0	.99595	.98951	.98294	.93103	.87015	.81140	.76038
35.0	.99599	.99056	.98493	.94095	.88441	.83956	.79325

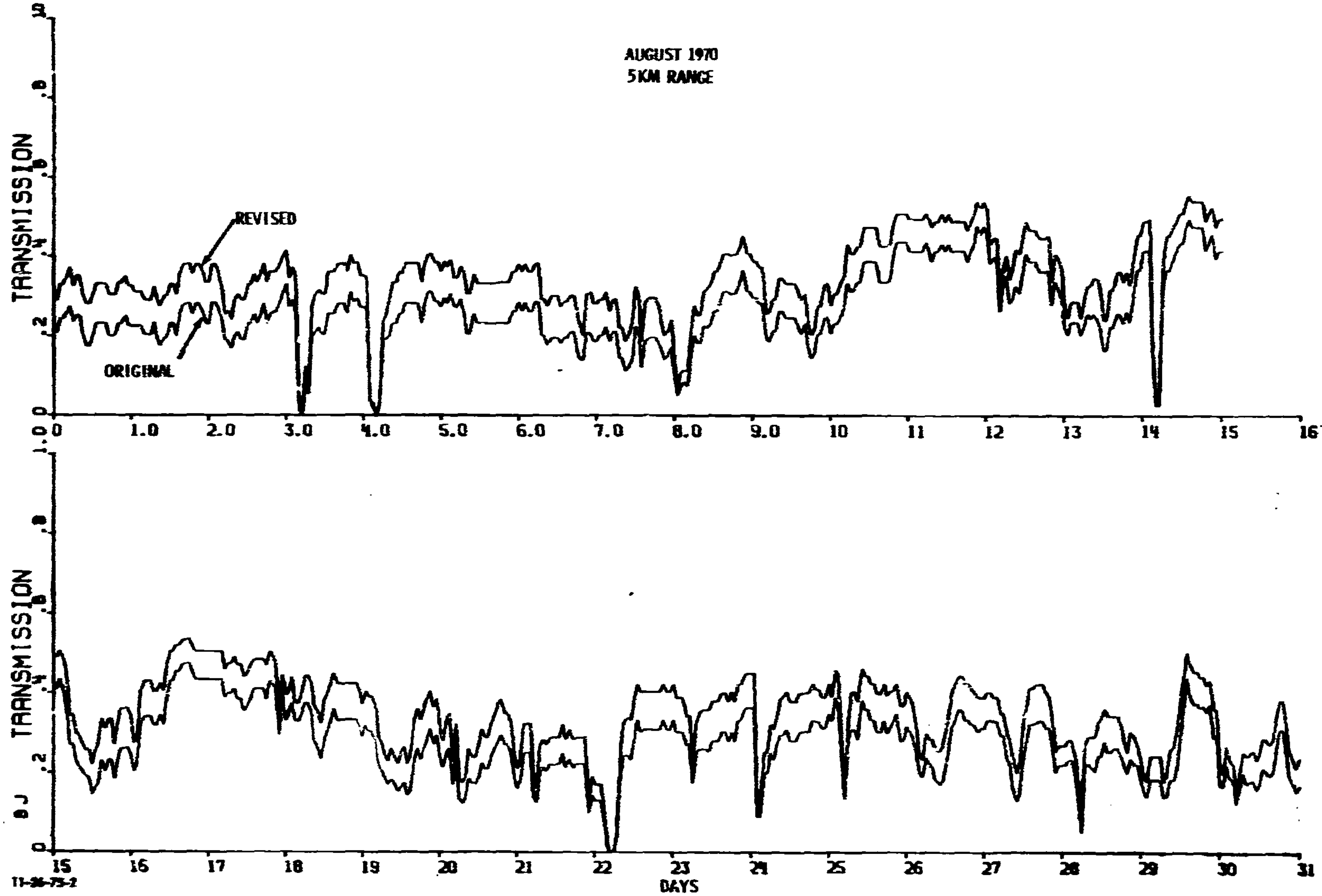

FIGURE 14. TRANSMISSION IN 8.5-11 μm BAND ACCORDING TO LOWTRAN II AND III (MARKED ORIGINAL) AND TO ROBERTS (MARKED REVISED) VERSUS DAY OF MONTH.

THE TRANSMISSION OF AIRCRAFT OR ROCKET PLUME RADIATION THROUGH THE ATMOSPHERE

Hans G. Wolfhard

Institute For Defense Analyses
Arlington, Virginia

SUMMARY OF PRESENTATION AT WORKSHOP ON ATMOSPHERIC TRANSMISSION MODELING

The presentation concerns the transmission of aircraft or rocket plume radiation through the atmosphere. Cambridge Research Laboratories have developed line by line transmission calculations that are very useful. In principle these calculations are applicable for a continuum emitter or a spectral line emitter provided every single emitting rotational line is known. This follows from the fact that emitting and absorbing rotational lines are not always identical in wavelength position or width of the lines. We will now discuss the limitations of the knowledge of the detailed emission spectrum of plumes and restrict ourselves mainly to the 4.3μ CO_2 band.

At ambient temperature and small optical depth the 4.3μ CO_2 band consists essentially of the $001 \rightarrow 000$ (or CRL notation $00011 \rightarrow 00001$) transition. This band has a R-branch that extends to shorter wavelengths and converges towards a band head. The P-branch extends towards longer wavelength and the spacing between the lines increase slowly. Higher rotational lines are not sufficiently included in the CRL computer tape and the position of the presently listed higher rotational lines is not sufficiently accurate to decide on the coincidence of lines (such as emission and absorption lines). An example of this can be seen in fig. 1 which is taken from recent results by G. Lindquist of ERIM under an ARPA contract. One sees the missing R-branch lines near the band head and the mismatch between calculated and experimental line positions due to inaccuracies in the rotational constants.

The CRL line by line calculation contains about 25 transitions between upper vibrational levels (the so-called hot bands) with the upper levels going up to about 6000 cm^{-1}. These hot bands become important under two circumstances. The first is

connected with transmission over large absorbing path lengths. This causes the fundamental 001 → 000 band to become strongly saturated whereas the weaker upper transition lines grow with path length until even very weak lines absorb strongly. The second arises from elevated temperatures. At plume temperatures high vibrational levels are excited and all transitions leading to a reduction of one vibrational level in the ν_3 levels cause emission at or near 4.3μ. Differences in vibrational levels decrease in magnitude for higher levels as the levels converge towards the dissociation energy of the molecule. Thus all (or nearly all) upper state transitions have their origin at longer wavelengths than the 001 → 000 transition. This in turn is the reason why the band head of the R-branch is unperturbed by the hot bands (fig. 1).

The P-branch region at wavelength > 4.3μ behaves differently and all the various upper state transitions (hot bands) overlap and mask the P-branch of the fundamental. The full half width at sealevel of a CO_2 line is about 0.14 cm^{-1}. As lines are on the average 2 cm^{-1} apart, it takes about 14 lines on the average to fill in the spaces between the lines. Thus the P-branch of the 4.3μ CO_2 band should become quite continuous at elevated temperatures. Figure 2 shows a line by line calculation by J. Selby, CRL of part of the P-branch for a 1000°K emitter for thin optical conditions. For optical thicknesses as represented in plumes the spectrum will become less spiky as weaker lines increase whereas stronger lines become limited by the black-body condition. One sees that for all practical conditions the region has become a pseudo-continuous emitter (although of rather rugged appearance). For relatively short absorbing path length (say of the order of a kilometer) the atmospheric CO_2 will absorb mainly through its 000 → 001 and 010 → 011 bands (including the isotop $^{13}CO_2$. Thus the pseudo continuum emitter is absorbed

by relatively few lines and transmission losses are less than if a line by line correlation between emitting and absorbing lines would pertain. Thus transmission depends on minor spectral details of the emitting plume and depends on the temperature as well as optical depth of the emitter. There is little value in measuring atmospheric transmission experimentally unless one can simulate the structure of the emitter i.e., a near continuum in the P-branch and a line structure in the R-branch.

A further example will be shown for the CO molecule. Figure 3, taken from preliminary data by Aerodyne, Inc. shows the emission of the fundamental band centered at 4.7μ for a $2000^{\circ}K$ hot emitter of 2.8 meter total thickness with 5 mole % CO present. Many of the 1-0 and 2-1 lines become optically thick. As the atmosphere contains a small amount of CO one will expect that 1-0 lines will become partially absorbed after an absorbing path length of a few kilometer. It will be the 2-1, 3-2, 4-3, 5-4 and even 6-5 transition lines that will be transmitted and although in this case the line density is not enough to render the spectrum pseudo-continuous nevertheless it will be of sufficient complexity to render the transmission problem quite complex.

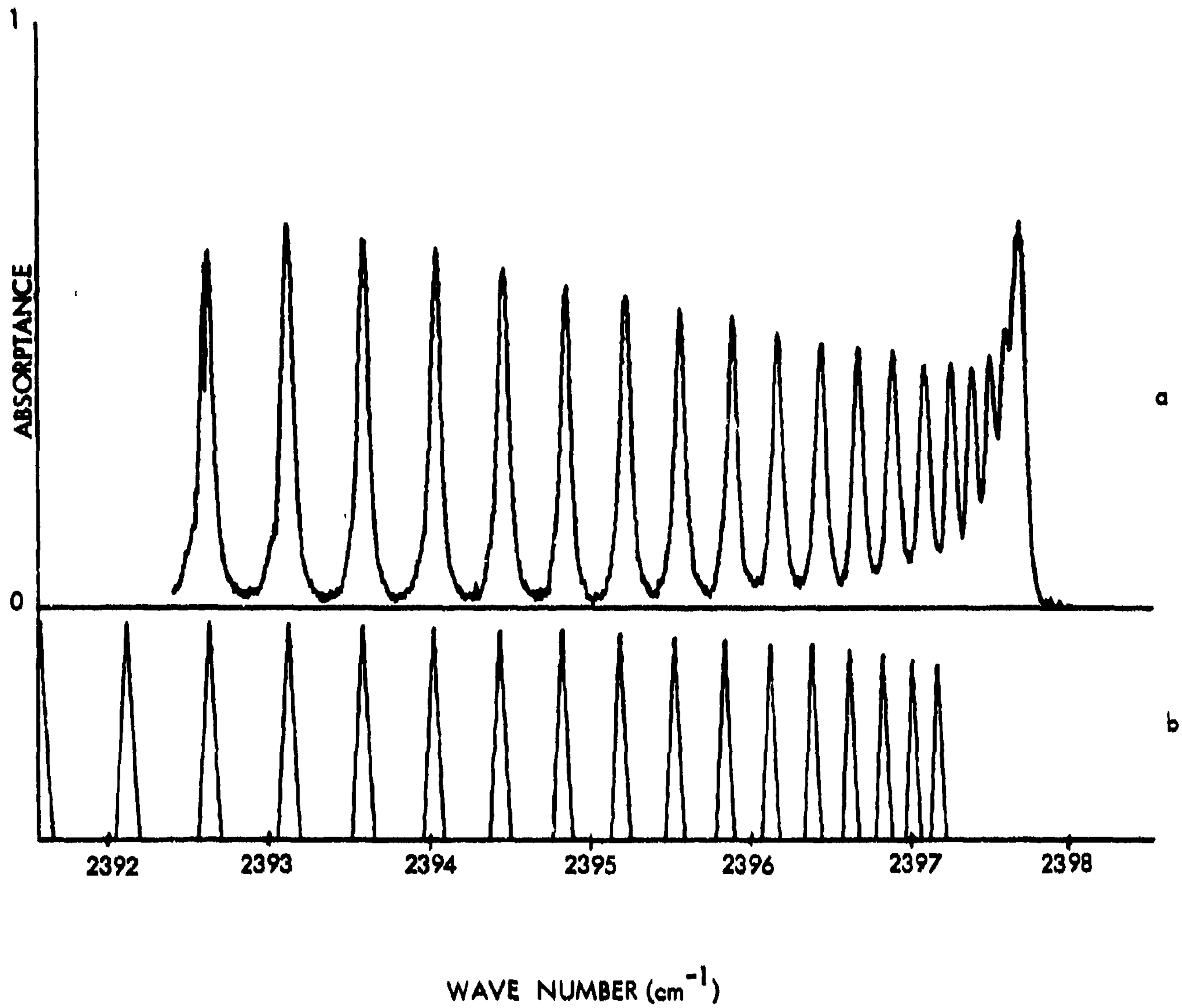

FIGURE 1a. Absorptance as Measured Near the CO_2 R-Branch Band Head in a CO-O_2 Flame at 0.3 cm Optical Depth of 2500° K Temperature. The lines can be seen to be well separated and undisturbed by hot bands. (from G. Lindquist, ERIM)

FIGURE 1b. CO_2 R Branch as Calculated by CRL Line-By-Line Code. Lines near the band head are seen to be missing and the last line near 2397.2 cm^{-1} coincides with a minimum of the measured spectrum. Thus its position is not sufficiently correct for detailed emission-absorption calculations. (from G. Lindquist, ERIM)

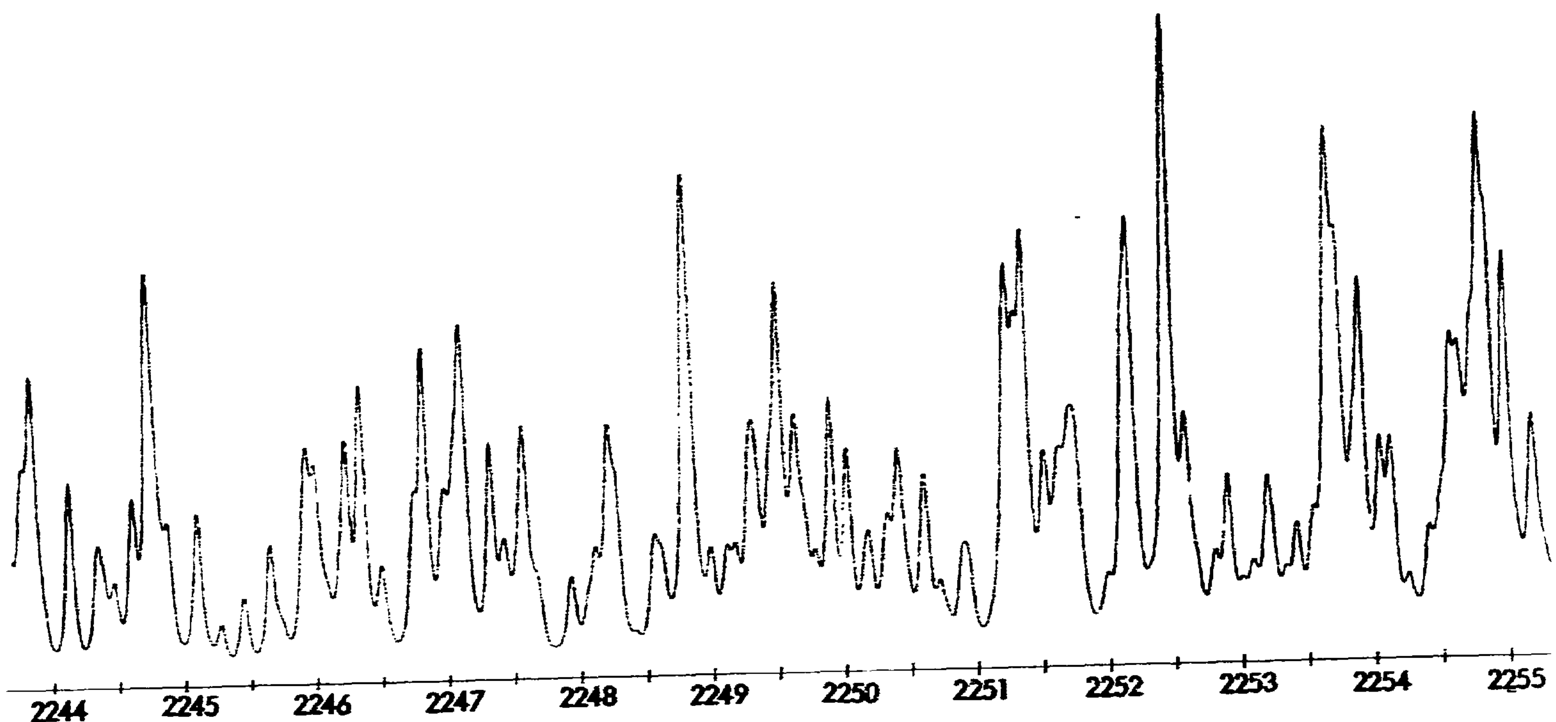

FIGURE 2. CO_2 Spectrum at 1000°K as Calculated from Line-By-Line Computer Code for Thin Optical Layer (near 4.44μ). (from J. Selby, CRL). The spectrum becomes so crowded with lines from hot bands that for realistic plumes with thick optical layer the spectrum becomes pseudo-continuous.

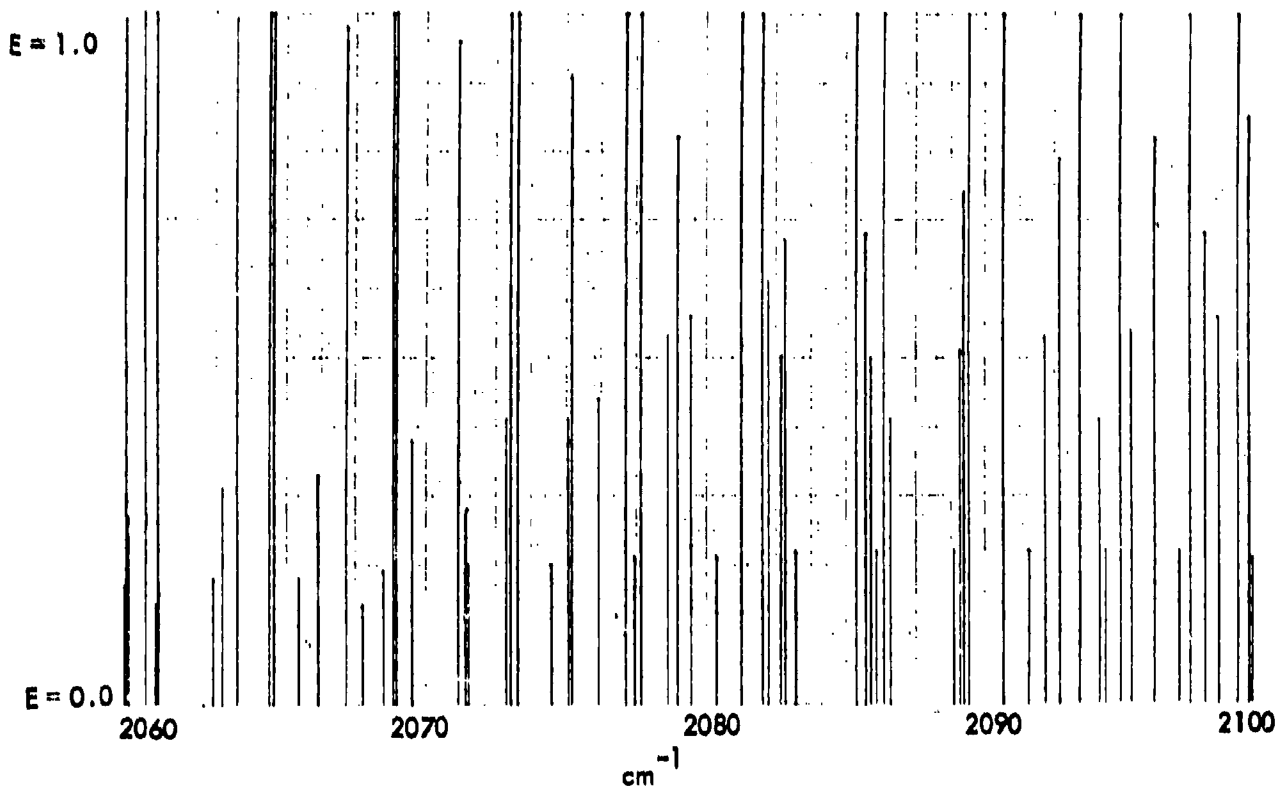

FIGURE 3. Spectrum of CO Molecules at about 2000°K and 2.8 Meter Optical Thickness. Weaker lines from 3-2, 4-3, 5-4, and 6-5 vibrational transitions are seen to render the spectrum complete. (from J. Draper, Aerodyne, Inc.)

THE USER'S VIEW OF ATMOSPHERIC MODELING--LASER SYSTEMS

Vincent J. Corcoran

Institute for Defense Analyses
Arlington, Virginia

THE USERS VIEW OF ATMOSPHERIC MODELING - LASER SYSTEMS

Vincent J. Corcoran
Institute For Defense Analyses
Arlington, Virginia 22202

I would like to point out a couple of problem areas associated with using the high resolution codes to calculate the atmospheric transmittance for laser systems.

The first point is illustrated in Fig. 1 which shows a table taken from the December issue of Applied Optics in which a comparison between measured values of the absorption coefficient for DF laser lines is compared to the values calculated by the group at AFCRL. The two columns on the right show that there is a difference in the calculated and measured values by as much as a factor of two. There are two DF laser lines, the $P_1(8)$ and $P_2(7)$, that are only 7 wavenumbers apart. Now if a person is off by a factor of two in the one way transmission and the receiver is located at the same point as the transmitter, then the prediction of the system capability will be off by a factor of 4. That may not sound like much to someone who only wants to get a ballpark feeling for the system performance but for a soldier who expects to carry a 10 lb pack and ends up with a 40 lb pack because of a factor of 4 uncertainty the difference can be significant.

The other point I want to make is illustrated in Fig. 2, which is a plot of the transmission vs visibility over 12 km horizontal paths at sea level for 10.6 micron radiation using the line by line program. It shows that for a subarctic winter where there is little water vapor the transmission can approach one for a clear day; however for a tropical atmosphere where there is a large water vapor content, the transmission can be down by a factor of 500 for the same visibility.

Incidentally if the curve is plotted for a 100% humidity condition, you obtain virtually the same curve as for the tropical atmosphere. You know that if you do a calculation that is off by a factor of 300 you are not going to be believed for very long.

The third figure shows a photograph of a scene under clear conditions and foggy conditions. It also indicates that the increased propagation loss for an 11 mile path was only 4 db. This points out an apparent discrepancy between the calculations made by the AFCRL program and the experimental measurements since the fog, in addition to being a high humidity condition, has water droplets that would further increase the attenuation. I know that there is a partial explanation of this discrepancy based on particle size, and I would like to see this problem addressed during the workshop.

The fourth figure summarizes the two points that I wanted to make. First, the calculations of any model must provide accurate transmission vs wavelength, and second, the transmission at any wavelength must be accurately predictable as the meteorological conditions are changed.

EXPERIMENTAL ABSORPTION COEFFICIENTS FOR SEVENTEEN DF LASER LINES COMPARED WITH THEORETICAL PREDICTIONS[a]

Line	Experimental[b]					Summation	Theory[c]
	$K \times 10^4$ (km^{-1})					$K_T \times 10^4$	$K_M \times 10^4$
	N_2O	CH_4	HDO	CO_2	N_{Sum}	(km^{-1})[d]	(km^{-1})
$P_1(3)$	0.591	30.5[e]	21	0	0	52.1	89.8
$P_1(4)$	0.145	32.9[e]	54.4[e]	0	0	87.4	65.3
$P_1(5)$	0	6.27	24.4[e]	0	0	30.7	17.1
$P_1(6)$	0	21.4	155[e]	0	7	184	139
$P_1(10)$	0	45.7	4.3	0	16	65.9	75.2
$P_2(7)$	0	13.9	56.8[e]	0	18	88.7	134
$P_2(8)$	0	9.56	11.5	0	20[e]	41.1	34.8
$P_1(12)$	1.30	0.982	33.6[e]	0	20[e]	55.9	37.7
$P_2(9)$	6.36	10.3	15.7	0	22[e]	54.4	77.6
$P_3(6)$	26.3[e]	2.89	37.4	0	28[e]	94.6	55.7
$P_2(10)$	500[e]	2.39	4.78	0	39	546	295
$P_3(7)$	359[e]	3.67	0	0	54	417	560
$P_2(11)$	132[e]	2.26	21.4	0	75	231	163
$P_3(8)$	248[e]	40.7	58.8	0	86	433	356
$P_3(9)$	7.12	0.740	29.0	35.5	161[e]	233	164
$P_3(10)$	6.24	1.65	16.1	71.0	269[e]	363	298
$P_3(11)$	28.0	5.43	29.4	106.0	463[e]	632	491

[a] Horizontal path at sea level 0.35 cm precipitable water/km, 272.2K.

[b] Results of The Aerospace Corporation DF laser experiments of N_2O, CH_4, HDO, and CO_2.

[c] R.A. McClatchey and J.E.A. Selby (Environmental Research Paper 400, AFCRL, 23 May 1972).

[d] $K_t = K_{N2O} + K_{CH4} + K_{HDO} + K_{N2}$.

[e] Principal absorber.

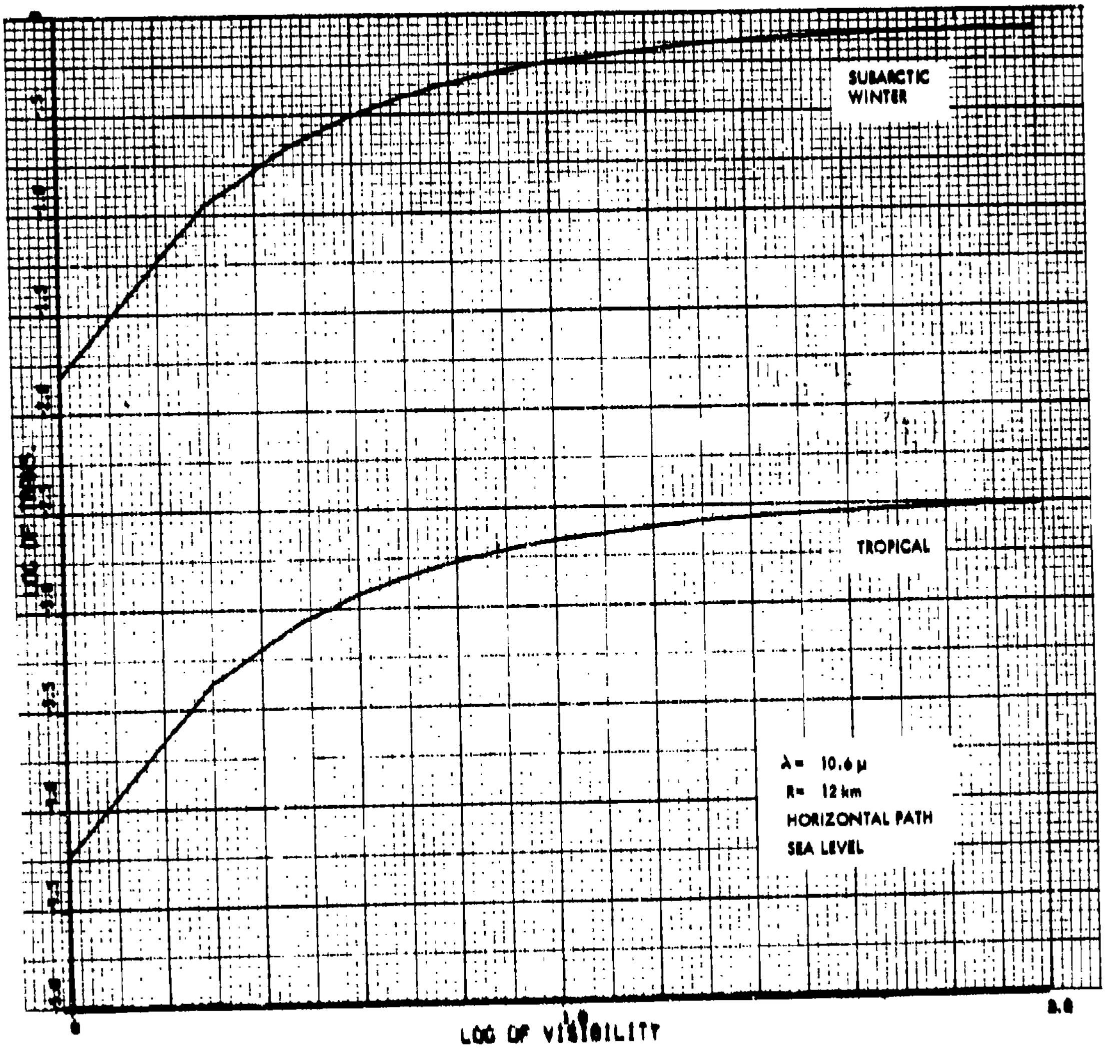

Atmospheric Transmission of 10.6μ Radiation
Over 12 km Horizontal Path at Sea Level

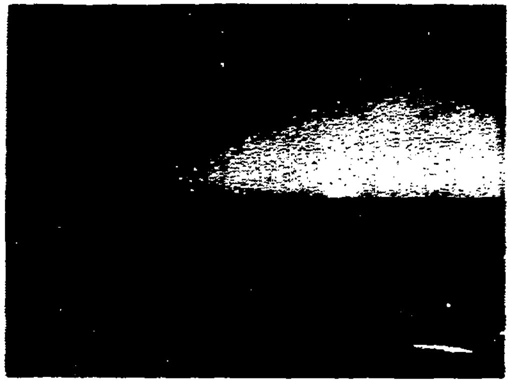

S/N = 28dB

S/N = 24dB

OCCULT COMMUNICATION

REQUIREMENTS FOR LASER

SYSTEMS CALCULATIONS

- ACCURATE TRANSMISSION VS λ

- ACCURATE TRANSMISSION FOR VARIOUS METOROLOGICAL CONDITIONS

TRANSMITTANCE MODELING

Robert A. McClatchey

Air Force Cambridge Research Laboratories (AFSC)
Hanscom Air Force Base, Massachusetts

TRANSMITTANCE MODELING

A general overview of the AFCRL transmittance modeling activity will be given. The first slide describes the tools that have been developed for dealing with this problem:

A) LINE LIST - A compilation of Atmospheric Absorption Line Parameters has been developed (McClatchey et al., 1973) for dealing with the problem of atmospheric transmittance modeling. In order to apply this line list, it is first necessary to define the atmosphere in terms of molecular abundances, pressure and temperature. In practice there are many applications where uncertainties in atmospheric models are larger than the uncertainties in the molecular parameters in terms of transmittance calculations. There are exceptions, particularly as concerns laser (monochromatic) transmittance calculations in certain spectral regions.

B) HITRAN - This is a computational technique (computer code) capable of using the line list as input data together with an appropriate model atmosphere and creating a synthetic spectrum through repeated monochromatic calculations. It is very time-consuming on the computer, but provides the only method for synthetically generating high resolution transmittance spectra (spectral resolution between 0 and 5 cm^{-1}).

C) BAND MODELS - Band models have been used in the past in lieu of detailed molecular spectroscopic data to provide low spectral resolution transmittance models. They have fundamental limitations, because they depend on a variety of assumptions regarding the spectral distribution and intensity distribution of molecular absorption lines. Perhaps more accurate band models can be developed using the line list as input data. In this way, models could be built based on the real spectral and intensity statistics of a particular absorption band belonging to a particular molecular species.

D) LOWTRAN - This is a particular low spectral resolution (20 cm^{-1}) transmittance model (see McClatchey et al., 1972). It is a one-parameter model in which an attempt has been made to optimize the transmittance accuracy in terms of the most appropriate single parameter for a given molecular species. LOWTRAN was built as a computer program (Selby and McClatchey, 1972) in order to address a wide variety of systems applications in which atmospheric transmittance plays an important role and also in order to provide a very rapid and efficient computational capability. John Selby will describe some recent modifications to the LOWTRAN code included in a new version of the code, LOWTRAN 3. The modifications are primarily in the 2.7-μm water vapor absorption, the introduction of a revised aerosol model and more flexible input requirements in terms of meteorological parameters and atmospheric models.

The second slide is a diagram showing the flow of information from the generation of the fundamental spectroscopic data through the generation of transmittance and background codes to be used in connection with system design and operation. An important point indicated here is the feedback loop indicating that comparisons of transmittance models with field measurements is made and may lead to appropriate modifications in the developed codes. Scattering data are also provided as input.

The third slide indicates the molecules included in the ARCRL Atmospheric Absorption Line Parameters Compilation and the number of molecular absorption lines currently included in the compilation. It should be noted that the lines included in this compilation are based on their importance on the atmospheric transmittance problem and therefore, are not necessarily sufficient for use in dealing with the emission of hot plumes containing the same molecular species. Some special studies have been carried out which indicate that the line data currently available (As of April 1975) can be used with some confidence up to temperatures around 1000K, but that their use as higher temperatures will require additional investigation and probably inclusion of additional hot lines.

The fourth slide shows a series of solar spectra observed from different altitudes (and displaced by 20% with respect to each other). These spectra result from a contractual program with the Denver Research Institute. The point to be made is simply the complexity of the atmospheric transmittance and therefore, the need to obtain information of the many absorption lines involved in accurate transmittance calculations are to be performed.

The fifth slide shows the equations that relate the line parameters to the monochromatic absorption coefficient. It indicates the need for the following four fundamental parameters: line position or frequency, ν, line intensity, S, line half-width, α, and the energy of the lower state of the transition, E''.

The sixth slide provides the fundamental equations associated with the line-by-line (HITRAN) computational technique. Equation 1 defines the monochromatic transmittance; Equation 2 indicates the necessity of summing over all i lines belonging to all j molecular species in order to determine the monochromatic transmittance at the frequency, ν; Equation 3 indicates the necessity of integrating through a nonhomogeneous atmospheric path (in which pressure, temperature and molecular abundances are not uniformly distributed); Equation 4 indicates the usual requirement (except for laser transmittance calculations) of performing a convolution of the monochromatic transmittances with an appropriate slit function (or filter function).

The seventh slide shows the results of a HITRAN calculation corresponding to a 10-km horizontal path at an altitude of 12 km in the 4.8-μm region. Similar plots covering the entire spectral region from 0.76 μm to 31.25 μm have been published by McClatchey & Selby, 1974. Several additional reports on laser transmittance are also referenced.

Slide Number 8 demonstrates the potential applicability of band model techniques through use of the molecular line parameters by comparing the results with a line-by-line calculation in the 15-μm spectral region.

Slide Number 9 shows a similar band model comparison in the 9.6-μm band of ozone.

Slide Number 10 describes the general applications of this transmittance modeling activity. In addition to the obvious laser transmittance and low resolution transmittance modeling capability, the same tools can be used with slight modification to address the problem of atmospheric emission modeling. With the reservations and limitations expressed above, the same data and techniques can also be used for exhaust plume modeling.

Slide Number 11 compares an emission calculation with measurements made at about 0.5 cm^{-1} spectral resolution. It is likely that any discrepancies indicated here are more likely a measure of the uncertainty of atmospheric temperature and molecular abundance than an indication of uncertainties in the molecular absorption parameters.

Slide Number 12 shows a similar emission comparison in the 16-30-μm region where the measurement was made from a balloon platform at an altitude of 70.2 kft.

Slide Number 13 shows the results of a general atmospheric emission survey computed with the molecular line list and degraded in spectral resolution to 5 cm^{-1}. Additional background calculations are provided in the report by Garing et al., 1972 (Secret Report).

Slide Number 14 shows the results of applying the molecular line data to the emission of a hot (600K) source as viewed through a 2-km horizontal atmospheric path at sea level. The overall spectral feature is the "blue spike" and at high (infinite) resolution the individual emission lines can be seen on the short wavelength side and the individual atmospheric absorption lines can be seen on the long wavelength side.

TRANSMITTANCE MODELLING

- LINE LIST
- HITRAN
- BAND MODELS
- LOWTRAN

SLIDE No. 1.

Laboratory and Theoretical
Molecular Spectroscopic Parameters

↓

Data Bank of Spectral Line Parameters

↓

Optical/IR Atmospheric Transmission Computer Code	← Atmospheric Model ← Scattering Data and Theory

↓

Comparison with Field Measurements → (Scattering Data and Theory)

↓

Atmospheric Transmittance and Background

↓

System Design and Operation

SLIDE No. 2.

Table I

MOLECULES INCLUDED IN COMPILATION

Molecule	Abundance (ppm)	No. Entries
H_2O	Variable (3×10^{24} molecules/cm^2)	38,145
CO_2	330	32,839
O_3	Variable (1×10^{20} molecules/cm^2)	19,328
N_2O	0.28	14,969
CO	0.075	354
CH_4	1.6	1,741
O_2	2.1×10^5	490

SLIDE No. 3.

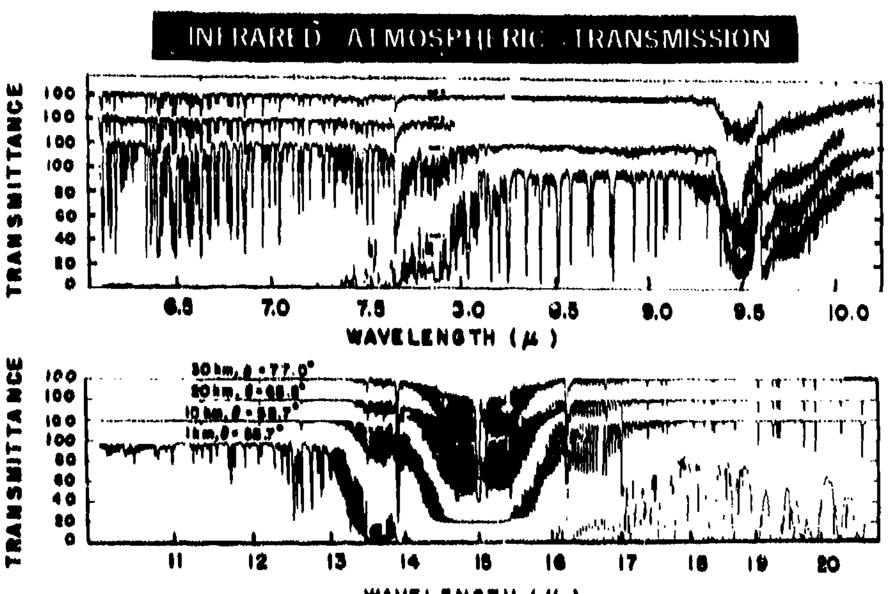

SLIDE No. 4.

$$k = \frac{S\alpha}{\pi\left[(\nu-\nu_0)^2+\alpha^2\right]} \quad (1)$$

$$S(T) = S(T_0)\left(\frac{T_0}{T}\right)^n \exp\left[-\frac{hc}{\kappa}E''\left(\frac{T_0-T}{T_0 T}\right)\right] \quad (2)$$

$$\alpha_L = \frac{\alpha_0 P}{P_0}\sqrt{\frac{T_0}{T}} \qquad \alpha_D = \frac{\nu}{c}\left[\frac{2\kappa T}{m}\right]^{1/2} \quad (3)$$

SLIDE No. 5.

$$\tau(\nu) = \exp-\left[k(\nu)m\right] \quad (1)$$

$$\tau(\nu) = \exp-\left[\sum_j\sum_i k_{ji}(\nu)m_j\right] \quad (2)$$

$$\tau(\nu) = \exp-\sum_j\left[\int\left(\sum_i k_{ji}(\nu)\,dm_j\right)\right] \quad (3)$$

$$\bar{\tau}(\nu) = \frac{\int\tau(\nu)\,g(\nu-\nu_0)\,d\nu}{\int g(\nu-\nu_0)\,d\nu} \quad (4)$$

SLIDE No. 6.

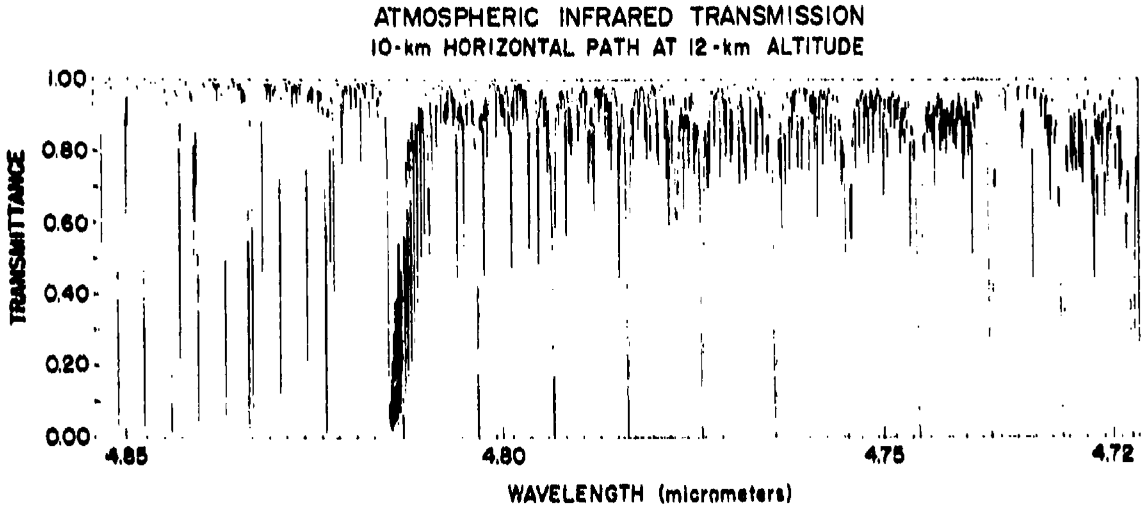

SLIDE No. 7.

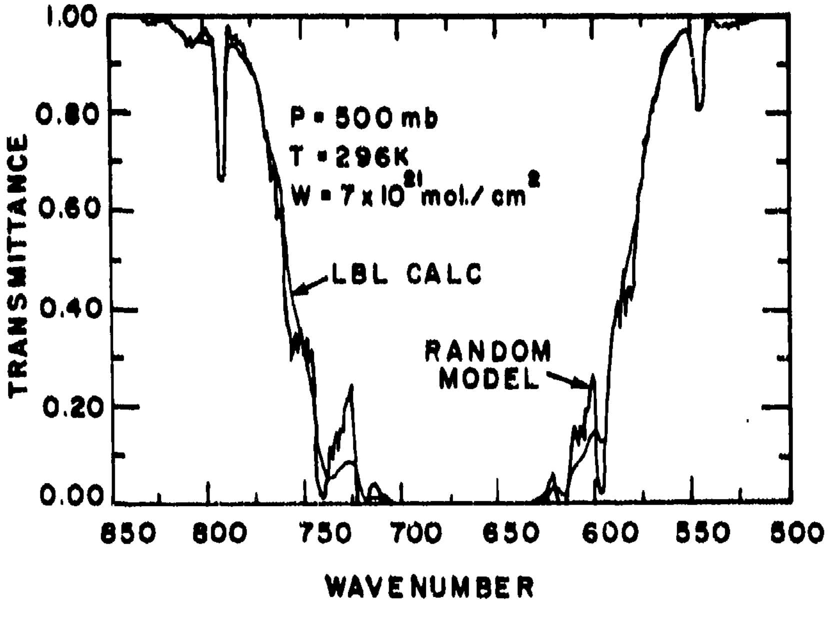

SLIDE No. 8.

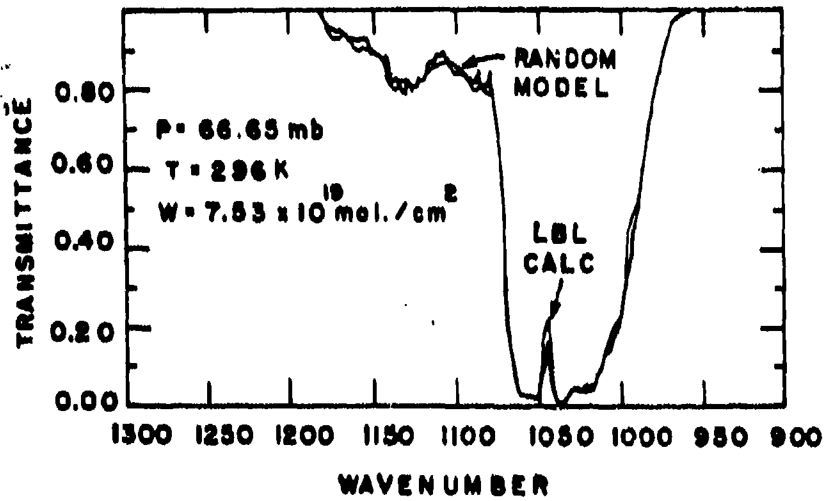

SLIDE No. 9.

APPLICATIONS

- LASER TRANSMITTANCE
- LOW RESOLUTION TRANSMITTANCE
- EMISSION MODELLING
- EXHAUST PLUME-ATMOSPHERE

SLIDE No. 10

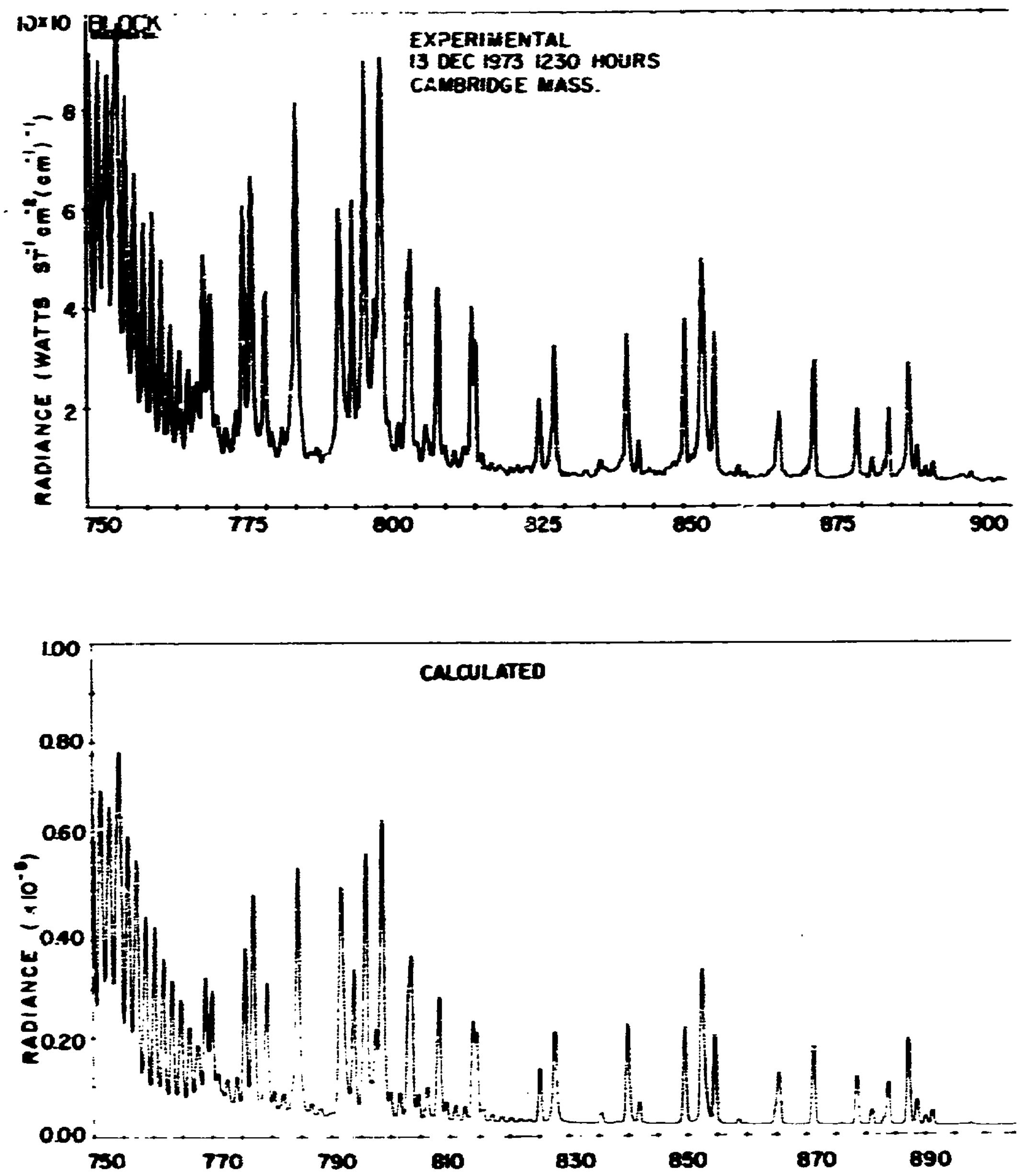
EXPERIMENTAL
13 DEC 1973 1230 HOURS
CAMBRIDGE MASS.
BLOCK
RADIANCE (WATTS $st^{-1} cm^{-2} (cm^{-1})^{-1}$)
2
4
6
8
750
775
800
825
850
875
900
CALCULATED
RADIANCE
0.00
0.20
0.40
0.60
0.80
1.00
750
770
790
810
830
850
870
890

SLIDE No. 11.

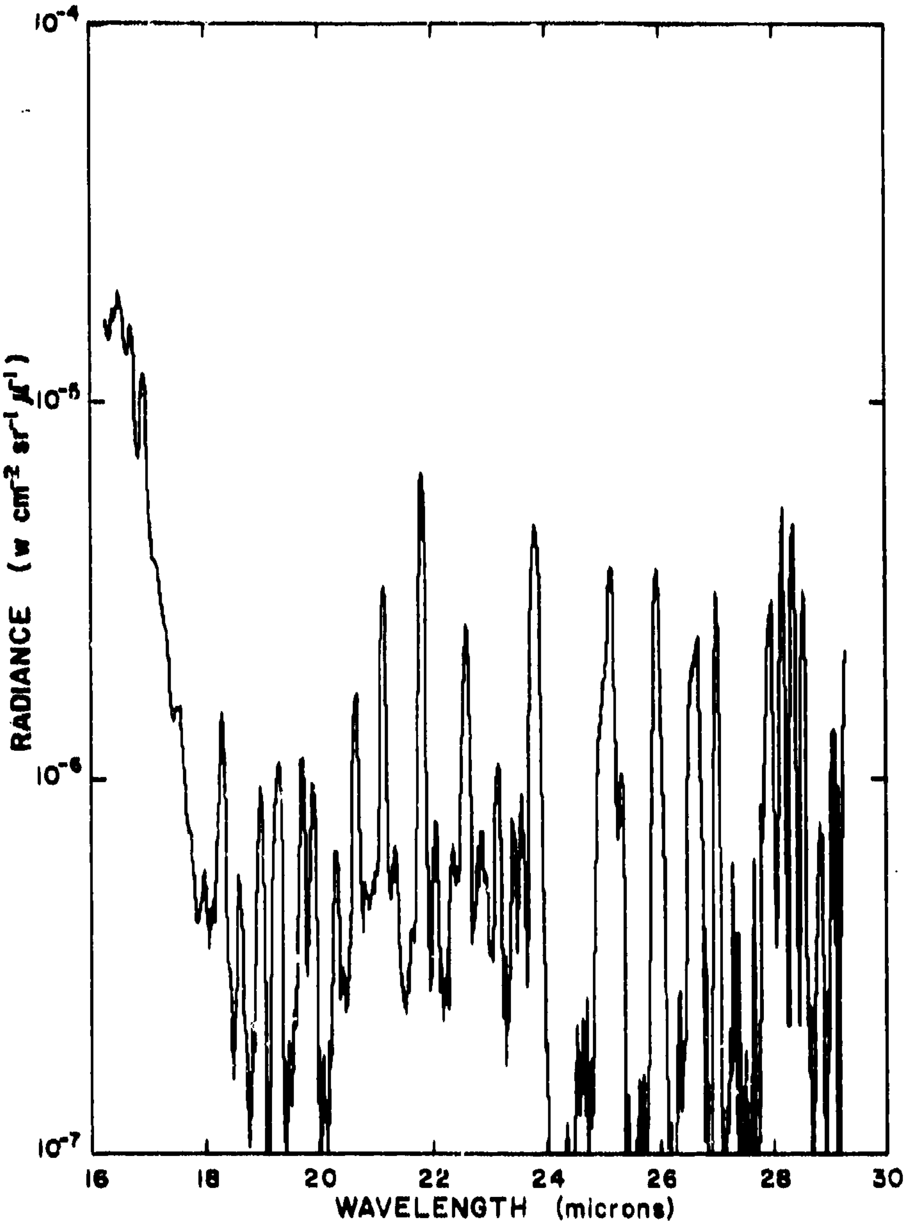

Radiance vs Wavelength at 70.2 kft and 0607 MST.

SLIDE No. 12.

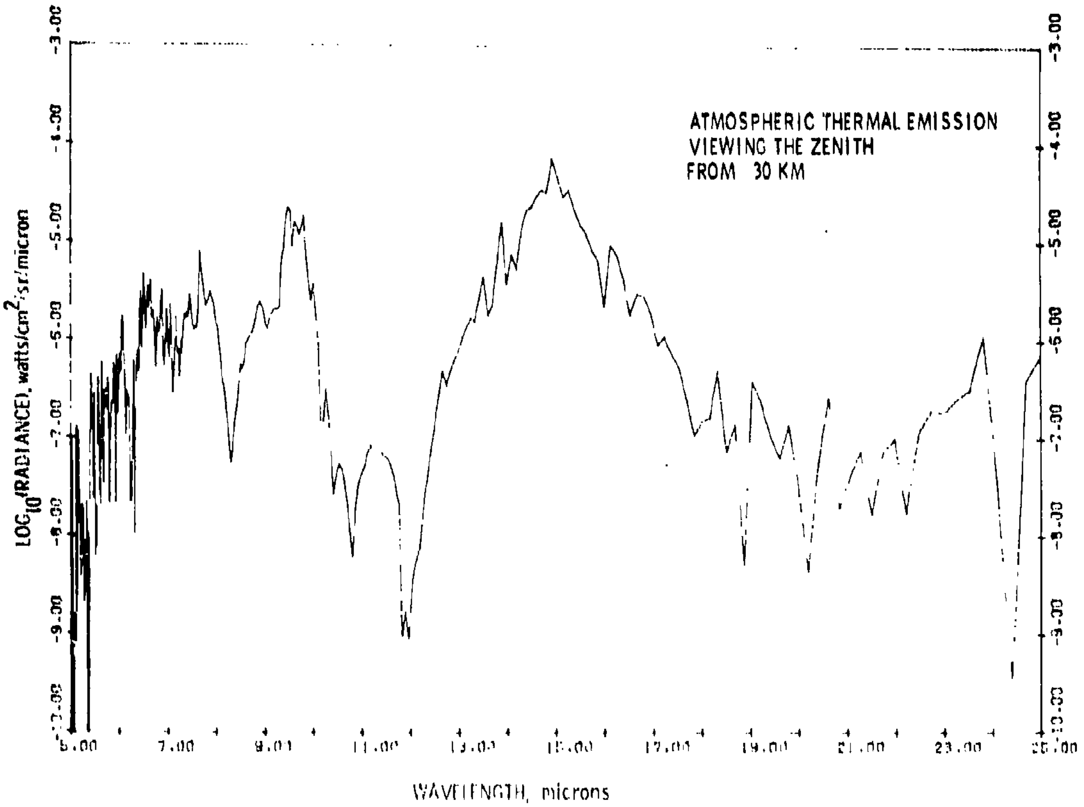
ATMOSPHERIC THERMAL EMISSION
VIEWING THE ZENITH
FROM 30 KM
LOG10(RADIANCE), watts/cm²·sr/micron
WAVELENGTH, microns

SLIDE No. 13.

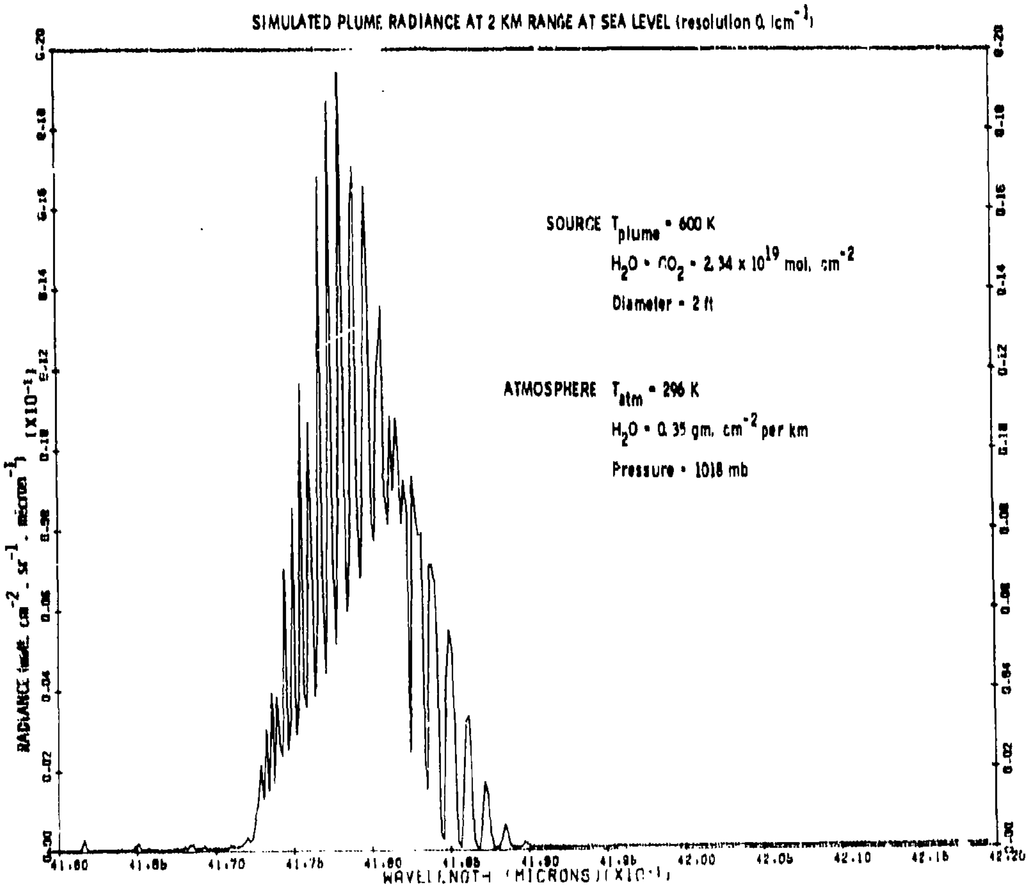

SIMULATED PLUME RADIANCE AT 2 KM RANGE AT SEA LEVEL (resolution 0.1cm^{-1})
SOURCE T_{plume} = 600 K
H_2O = CO_2 = 2.34 x 10^{19} mol. cm^{-2}
Diameter = 2 ft
ATMOSPHERE T_{atm} = 296 K
H_2O = 0.35 gm. cm^{-2} per km
Pressure = 1018 mb
RADIANCE (watt cm^{-2}. sr^{-1}. micron^{-1}) (X10^{-1})
WAVELENGTH (MICRONS)(X10^{-1})

SLIDE No. 14.

REFERENCES

Garing, J.S., et al. (1972), Long Wavelength Infrared Backgrounds -- Measurement Program (U), AFCRL-72-0588, AF Survey in Geophysics 248 (s).

McClatchey, R.A. (1971), Atmospheric Attenuation of CO Laser Radiation, AFCRL-71-0370, Environmental Research Paper 359.

McClatchey, R.A., et al. (1973), AFCRL Atmospheric Absorption Line Parameters Compilation, AFCRL-TR-73-0096, Environmental Research Paper 434.

McClatchey, R.A., R.W. Fenn, J.E. Selby, F.E. Volz and J.S. Garing (1972) Optical Properties of the Atmosphere, Third Edition, AFCRL-72-0497, Environmental Research Paper 411.

McClatchey, R.A., and J.E. Selby (1972a), Atmospheric Attenuation of HF and DF Laser Radiation, AFCRL-72-0312, Environmental Research Paper 400.

McClatchey, R.A., and J.E. Selby (1972b), Atmospheric Transmittance, 7-20 μm: Attenuation of CO_2 Laser Radiation, AFCRL-72-0611, Environmental Research Paper 419.

McClatchey, R.A., and J.E. Selby (1974), Atmospheric Attenuation of Laser Radiation from 0.76 to 31.25 μm, AFCRL-TR-74-0003, Environmental Research Paper 460.

Selby, J.E., and R.A. McClatchey (1972), Atmospheric Transmittance from 0.25 to 28.5 μm: Computer Code LOWTRAN 2, AFCRL-72-0475.

THE EFFECT OF SOURCE SPECTRUM ON APPARENT ATMOSPHERIC TRANSMITTANCE

C. M. Randall
S.J. Young

The Aerospace Corporation
Los Angeles, California 90009

I Introduction

In my experience the users of atmospheric transmittance computations can be separated into two quite distinct groups: the system planners and the data gatherers. Those of us who are expected to give technical advice concerning atmospheric transmittance should be aware of the different types of information required by members of these two groups.

The system planner is concerned with the conditions which will limit the performance of his system, not the ability to know the transmittance with great accuracy at any particular time or place. The planner needs parametric studies based on climatic data to tell him the limits of transmittance his system is likely to encounter under operational conditions. If inaccuracies in transmittance codes do not unduly bias results, then some uncertainty in transmittance computation is acceptable in view of the uncertainty inherent in the use of climatological information.

The data gatherer, on the other hand, wishes to extract all the information possible from observations made through the atmosphere. The data gatherer cares little for climatic data, but requires the best possible meteorological data for the particular event of interest to him. He also requires the best possible transmittance codes consistent with the accuracy of the data available to him.

The accuracy of computed atmospheric transmittance is limited by a number of factors. Applicable meteorological data may not be available for the time and place of particular interest. This is particularly true of ocean areas viewed by space based sensors. Even if meteorological data are available at the time and place of interest, the data itself may be of limited accuracy. As others at this conference have pointed out, there is little information in the routinely recorded meteorological data to permit the estimation of infrared attenuation due to the particles in the atmosphere. If, in the spectral region of interest, water is an important absorber, the meteorological data may still be inadequate even through radiosonde data including humidity observations are available. For example the hygrometers on radiosondes are useless when the ambient temperature is below -40 C, a condition which usually occurs within 10 km above the

*This work was sponsored by the Defense Advanced Research Projects Agency Order No. 2843 and SAMSO Number FO4701-74-C-0075.

II Source-Absorber Line Correlation Effects - Line by Line Calculations

The problem being considered is summarized in figure 1. Of the several emission and attenuation mechanisms implied by figure 1, only the molecular absorption by gases in the atmosphere of radiation emitted by hot gas in the target is considered. Figure 2 summarizes the basically simple equations of radiative transfer applicable for a single frequency of light when the assumption of local thermodynamic equilibrium is valid. Quasi-monochromatic target radiance spectra and transmittance spectra of slant paths through the atmosphere have been computed for the 2.7 μm spectral region based on the relations shown in figure 2 and the Air Force Cambridge Research Laboratories atlas of spectroscopic line parameters. The specific conditions for which spectra discussed here were computed are shown in figure 3. A detailed discussion of the techniques may be found in reference 1. The quasi-monochromatic emission and transmission spectra can then be combined to provide the apparent radiance at the end of an atmospheric path. Figure 4 shows a short segment of such an apparent radiance spectrum.

Since most sensors have bandwidths much wider than the width of individual lines, it is convenient to consider the atmospheric transmittance averaged over some interval, typically a few wavenumbers wide and including a number of lines. However, as soon as the bandwidth exceeds that of an individual line, the numerical value of the "average" transmittance depends on the assumptions made about the spectral characteristics of the source. We illustrate this by considering several different definitions of average transmittance and demonstrating the quantitative difference in transmittance computed by these various definitions from the correct quasi-monochromatic spectra computed for the conditions listed in figure 3.

The effective average transmittance T_e is the applicable value if the objective of sensor measurements is the inference of the source radiance.

earth's surface. Because of the difficulty of measuring extremely low humidities with sensors which have passed through a region of high humidity, many of the older models of the stratosphere are unrealistically wet. Much of the meteorological data routinely provided by the USSR also indicates impossibly wet stratospheric conditions. Personnel of the Air Force Air Weather service inform me that even in the troposphere when the ambient temperature is above -40 C some of the hygrometer systems employed in the past could be significantly affected by solar illumination and thus produce erroneous results. There are a number of reasons why meteorological data of the desired accuracy may not be available for many events of interest.

The conversion of meteorological measurements to the required input for transmittance modelling codes must be done carefully to avoid introducing errors. For example, if relative humidities are reported for temperatures below 0 C, are they referred to saturation vapor pressures over ice or over water?

Finally, the transmittance codes themselves have limitations. One limitation is in the area of aerosol attenuation computation discussed by others at this conference. Another is the limitations imposed by the approximations required to obtain computationally efficient band models.

The spectrum of the source observed through the atmosphere can affect the apparent transmittance of the atmosphere, as alluded to previously by Dr. Wolfhard. The rest of this paper is devoted to a quantitative demonstration of the size of this particular effect by means of quasi-monochromatic spectral computations and subsequently a discussion of a band model transmittance approach which includes these effects.

$$\overline{T}_e = \frac{\int_{\nu_1}^{\nu_2} L_a(\nu)\, d\nu}{\int_{\nu_1}^{\nu_2} L_t(\nu)\, d\nu} = \frac{\int_{\nu_1}^{\nu_2} L_t(\nu)\, T(\nu)\, d\nu}{\int_{\nu_1}^{\nu_2} L_t(\nu)\, d\nu} \qquad (1)$$

is the ratio of the integrated apparent radiance $L_a(\nu)$ to the integrated target radiance $L_t(\nu)$. Spectra of $\overline{T}_e$ for two optical paths are indicated by solid lines in Figs. 5 and 6. The value $\Delta\nu = \nu_2 - \nu_1 = 20\ cm^{-1}$ was used in computing these spectra. Three values of $\overline{T}_e$ obtained for bandwidths greater than 20 cm^{-1} in the two wings and the center of the absorption region shown in Figs. 5 and 6 are listed in Table 1. The entry in Table 1 titled "20 cm^{-1} Intermediate Average" is the average of the $\overline{T}_e$ curve from Fig. 5 or 6 for the same radiometer bandwidth. This indicates that the average of low resolution spectra does not produce the same results as the average obtained from high resolution spectra.

The average transmittance $\overline{T}$ is the most frequently computed or approximated transmittance.

$$\overline{T} = \frac{1}{\Delta\nu} \int_{\nu_1}^{\nu_2} T(\nu)\, d\nu \qquad (2)$$

The average transmittance for the two sample paths was computed from the high resolution transmittance spectra by averaging over $\Delta\nu = 20\ cm^{-1}$. Results are indicated by dashed curves in Figs. 5 and 6. Average transmittances for wider bands are shown in Table 1. For sources of uniform spectral radiance, $\overline{T}$ should be the same as $\overline{T}_e$, but for line sources such as hot gases, they clearly are not the same.

The factor $\overline{T}$ is the quantity approximated by most atmospheric transmittance band model procedures. Estimates of $\overline{T}$ by two such programs for the two sample paths are included for comparison in Table 1. In the table,

LOWTRAN refers to the program developed by R.A. McClatchey at the Air Force Cambridge Research Laboratories,[2,3] and ATLES refers to a band model developed at Aerospace to account for source effects.[4] Spectra computed with the use of LOWTRAN are indicated by the broken curves in Figs. 5 and 6. The comparisons given in Table 1 indicate that the band models approximate $\bar{T}$ reasonably well. The discrepancy between the $\bar{T}$ spectrum and the LOWTRAN estimate for the 75-deg slant path is not understood at present.

An attempt to include source effects can be made by using low resolution source and transmittance functions to compute low resolution effective transmittance $\bar{T}_{eL}$.

$$\bar{T}_{eL} = \frac{\sum_i T(\Delta\nu_i)\, L_t(\Delta\nu_i)}{\sum_i L_t(\Delta\nu_i)} \tag{3}$$

The results of carrying this out for the wings and center of the 2.7-μm absorption are given in Table 1. The accuracy of estimating $\bar{T}_e$ in this way is only a little better than the average transmittance $\bar{T}$ obtained without considering the source spectrum in any way.

The techniques of band modelling can be applied directly to the definition of the effective average transmittance, Eq. (1), to obtain $\bar{T}_{eB}$. These procedures are discussed later in this paper and in detail in Ref. 4. Included in Table 1 is the radiometer transmittance predicted by this special band model, which is the only band model procedure that explicitly takes into account line-correlation relations between the source and atmosphere in estimating $\bar{T}_e$. It is also the only procedure that does not overestimate the transmittance. In fact, if any conclusions may possibly be drawn about the band model from this limited set of data, it would appear that the model overestimates the effects of line correlation.

Based on the limited test cases presented in this discussion, one may conclude that all average transmittance procedures, which do not account for possible line correlations, tend to overestimate the effective transmittance of the atmosphere for a line source. In some spectral regions

and over some atmospheric paths, this can lead to errors of up to 79 percent in the estimated effective transmittance.

III Source-Absorber Line Correlation Effects - Band Model ATLES

Presented now are spectra produced by the band model approach for estimating the effective average transmittance. This band model[4] is based on the work of Lindquist and Simmons[5]. In this model, the hot plume is assumed to be part of the optical path to the observer. The resulting path is therefore highly inhomogeneous due primarily to the high temperatures in the plume. The usual Curtis-Godson approximation for accounting for inhomogeneities along the optical path is no longer valid. The quantity which must be estimated accurately in the equation of radiative transport is the derivative of the transmittance along the optical path. The ATLES band model program is based on making an estimation of this derivative using the Lindquist-Simmons approximation.

Figures 7 and 8 compare the average transmittance, $\bar{T}$, spectra computed with the ATLES band model with that computed by quasi-monochromatic means on the basis of individual lines for the conditions specified in figure 3. It is this transmittance that is applicable for determining the attenuation of radiation from continuum sources. The agreement between the band model calculations and the quasi-monochromatic computations is satisfactory.

Figures 9 and 10 compare the average effective transmittance, $\bar{T}_e$, as obtained with the ATLES band model with that obtained from quasi-monochromatic calculations for the conditions specified in figure 3. For both atmospheric paths, the band model estimate of $\bar{T}_e$ is lower than that obtained by the line by line calculations, even though they are both based on the same spectral line compilation.

Up to this point, only a source at 20 km altitude has been considered. Figure 11 shows the average transmittance, $\bar{T}$, and the average effective transmittance, $\bar{T}_e$, for a spectral interval in the wing of the 2.7μm atmospheric absorption band. Results obtained with the ATLES model and

with the AFCRL program LOWTRAN2 for $\bar{T}$ are shown. Shown as isolated points are results obtained from quasi-monochromatic computations. The agreement between the line by line results and ATLES is adequate except for the tendency of ATLES to underestimate $\bar{T}_e$. As expected, the LOWTRAN2 results agree well with the $\bar{T}$ curve.

The surprising feature in figure 11 is the large absorption at high altitudes evidenced in the $\bar{T}_e$ results. This large apparent absorption results from two sources. The first is the inappropriateness of the Lorentz pressure broadened line shape used in the calculations of figure 11 for the high altitude region. The second effect is the improved correlation of source and absorber line positions and strengths as the plume temperature decreases at increasing altitude.

The effect of the line shape function has been investigated and results shown in figure 12. The effect, as expected, is to increase the high altitude transmittance. However, even with the more appropriate Voigt line shape there is still an appreciable absorption due to line correlation at an altitude of 60 km as indicated by both the ATLES and line by line computations.

IV Summary

Significant reductions in effective atmospheric transmittance occur when there is a correlation between the emitting and absorbing spectral features and when the sensor has a bandwidth greater than a single spectral line. The conditions leading to this effect are common in the observation of aircraft and missile plumes through the atmosphere by many types of sensors. These effects can be demonstrated by quasi-monochromatic spectral computation and modelled efficiently by improved band model techniques described briefly here.

The reduction in transmittance due to line correlation occurs even at very high altitudes where the atmosphere is often considered completely transparent.

At Aerospace, we are continuing to examine this problem by using improved plume models, by improving the band model formulation, and by obtaining a consistent set of band model parameters for both high and low temperatures.

References

1. C.M. Randall, "Monochromatic Transmittance/Radiance Computations" Aerospace Corporation Technical Report TR-0075(5647)-3, 31 December 1974.

2. R.A. McClatchey, et al, "Optical Properties of the Atmosphere (Third Edition)", Air Force Cambridge Research Laboratories Environmental Research Paper 411, AFCRL-72-0497, 24 August 1972.

3. J.E.A. Selby and R.A. McClatchey, "Atmospheric Transmittance from 0.25 to 28.5 μm: Computer Code LOWTRAN2", Air Force Cambridge Research Laboratories Environmental Research Paper 427, AFCRL-72-0745, 29 December 1972.

4. S.J. Young, "Band Model Calculations of Atmospheric Transmittance for Hot Gas Line Emission Sources." Aerospace Corporation Technical Report TR-0075(5647)-1, 31 December 1974.

5. G.H. Lindquist and F.S. Simmons, "A Band Model Formulation for Very Nonuniform Paths," J. Quant. Spectrosc. Radiat. Trans. 12, 807(1972).

Figure Captions

1. Atmospheric Attenuation problem summary

2. Basic equations describing the transfer of radiation for a single frequency under conditions of local thermodynamic equilibrium.

3. Conditions employed to compute the atmospheric transmittance curves presented in this report.

4. Apparent spectral radiance of a typical target after traversing a path through the atmosphere from 20 km to space at a 75-deg zenith angle.

5. Transmittance computed in several ways for a horizontal path 100 km long at 20 km altitude (the solid curve ——— is the effective average transmittance for a typical missile plume. The dashed curve ------ is the average transmittance. These two curves were obtained from high resolution calculations averaged over 20 cm^{-1}. The - ——— - curve is the approximation to the average transmittance provided by the AFCRL LOWTRAN computer program).

6. Transmittance computed in several ways for a slant path from 20 km to space at a 75-deg zenith angle (the solid curve ——— is the effective average transmittance for a typical missile target. The dashed curve ------ is the average transmittance. These two curves were obtained from high resolution calculations. The - ——— - curve is the approximation to the average transmittance provided by the AFCRL LOWTRAN code).

7. Comparison of the average transmittance, $\overline{T}$, computed by means of the ATLES band model with the results of line by line computations for a 100 km horizontal path at 20 km altitude.

8. Comparison of the average transmittance, $\overline{T}$, computed by means of the ATLES band model with the results of line by line computations for a path from 20 km to space at a 75 deg zenith angle.

9. Comparison of the effective average transmittance, $\overline{T}_e$, computed by means of ATLES with the results of line by line computations for a 100 km horizontal path at 20 km altitude.

10. Comparison of the effective average transmittance, $\overline{T}_e$, computed by means of ATLES with the results of line by line computations for a slant path from 20 km to space at a 75 deg zenith angle.

11. The variation in atmospheric transmittance with source altitude for a path from the source altitude to space at a 73.7 deg zenith angle.

12. The effects of line shape function on the computed transmittance at high altitudes.

Table 1. Radiometer Transmittance

Path	20 km to Space, 75-Deg Zenith Angle						100-km Horizontal at 20 km					
Band Limits (cm^{-1})	3350 - 3575		3575 - 3725		3725 - 3950		3350 - 3575		3575 - 3725		3725 - 3950	
	Trans.	% Diff.	Trans.	% Diff.	Trans.	% Diff.	Trans.	% Diff.	Trans.	% Diff	Trans.	% Diff.
Effective Average, $\overline{T}_e$	0.8303	---	0.3971	---	0.5608	---	0.7508	---	0.1561	---	0.4337	---
20 cm^{-1}, Intermediate Av.	0.8661	4.3	0.4033	1.6	0.6119	9.11	0.8020	6.8	0.1631	4.5	0.4954	14.2
ATLES Estimate, $\overline{T}_{eb}$	0.7534	-9.3	0.2745	-30.9	0.4321	-22.9	0.6324	-15.8	0.08103	-48.1	0.2602	-40.0
Average, $\overline{T}$	0.9325	12.3	0.5579	40.5	0.8707	55.3	0.8658	15.3	0.2375	52.1	0.7756	78.8
LOWTRAN, Estimate, $\overline{T}$	0.9351	12.6	0.4683	17.9	0.8652	54.3	0.8329	10.9	0.1714	9.8	0.7429	71.3
ATLES, Estimate, $\overline{T}$	0.9377	12.9	0.5832	46.9	0.8704	55.2	0.8666	15.4	0.2695	72.6	0.7693	77.4
Low Resolution Effect. Average, T_{eL}	0.9119	9.8	0.5508	38.7	0.8081	44.1	0.8262	10.0	0.2290	46.7	0.6818	57.2

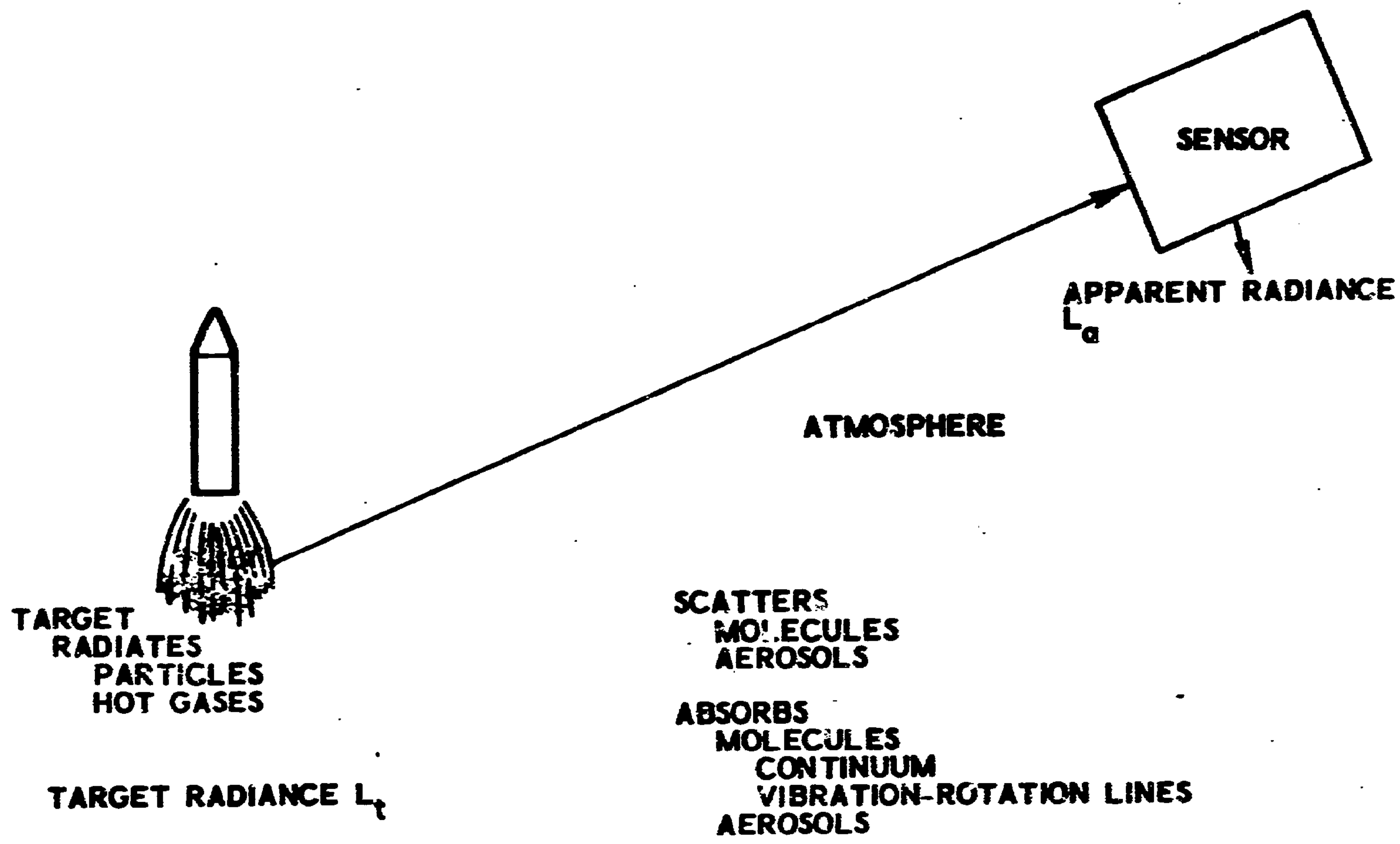
SENSOR
APPARENT RADIANCE
L_a
ATMOSPHERE
TARGET
RADIATES
PARTICLES
HOT GASES
TARGET RADIANCE L_t
SCATTERS
MOLECULES
AEROSOLS
ABSORBS
MOLECULES
CONTINUUM
VIBRATION-ROTATION LINES
AEROSOLS

FIGURE 1.

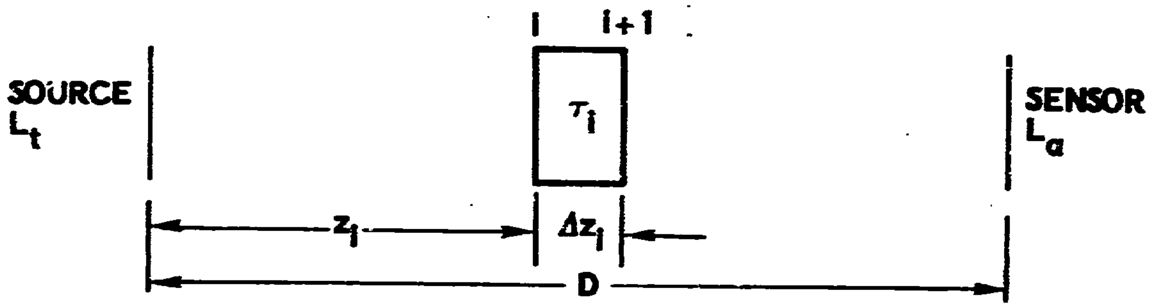

$$L_a(\nu) = L_t(\nu)\, T_{0,D}(\nu) + \sum_{i=0}^{N-1} T_{z_{i+1},\, D}(\nu)\,(1 - \tau_i(\nu))\, L_B(\nu, \theta(z_i))$$

$$T_{z_i,\, z_j}(\nu) = \mathrm{EXP}\left(-\int_{z_j}^{z_j} k(\nu, z)\, dz\right) = \tau_i \tau_{i+1} \cdots \tau_j$$

$k(\nu, z)$ IS ATTENUATION COEFFICIENT

$L_B(\nu, \theta)$ IS BLACKBODY RADIANCE AT TEMPERATURE θ

ν IS FREQUENCY

FIGURE 2.

Monochromatic Atmospheric Effects Program

INITIAL TEST CASE

SOURCE

- TYPICAL TARGET AT 20 km
- EQUIVALENT ISOTHERMAL PLUME MODEL
- EMITTING SPECIES: H_2O, CO_2

TRANSMITTANCE

- TROPICAL MODEL
- 20 km TO SPACE, 75° ZENITH ANGLE
- 100 km HORIZONTAL PATH AT 20 km
- ABSORBING MOLECULAR SPECIES: H_2O, CO_2, O_3, N_2O, CO, CH_4, O_2
- CONTINUUM ABSORPTION AND AEROSOLS OMITTED

SPECTRAL REGION 3325 - 3975 cm^{-1} (2.516 - 3.008)

- AVERAGE TRANSMITTANCES IN WINGS AND BAND CENTER

FIGURE 3.

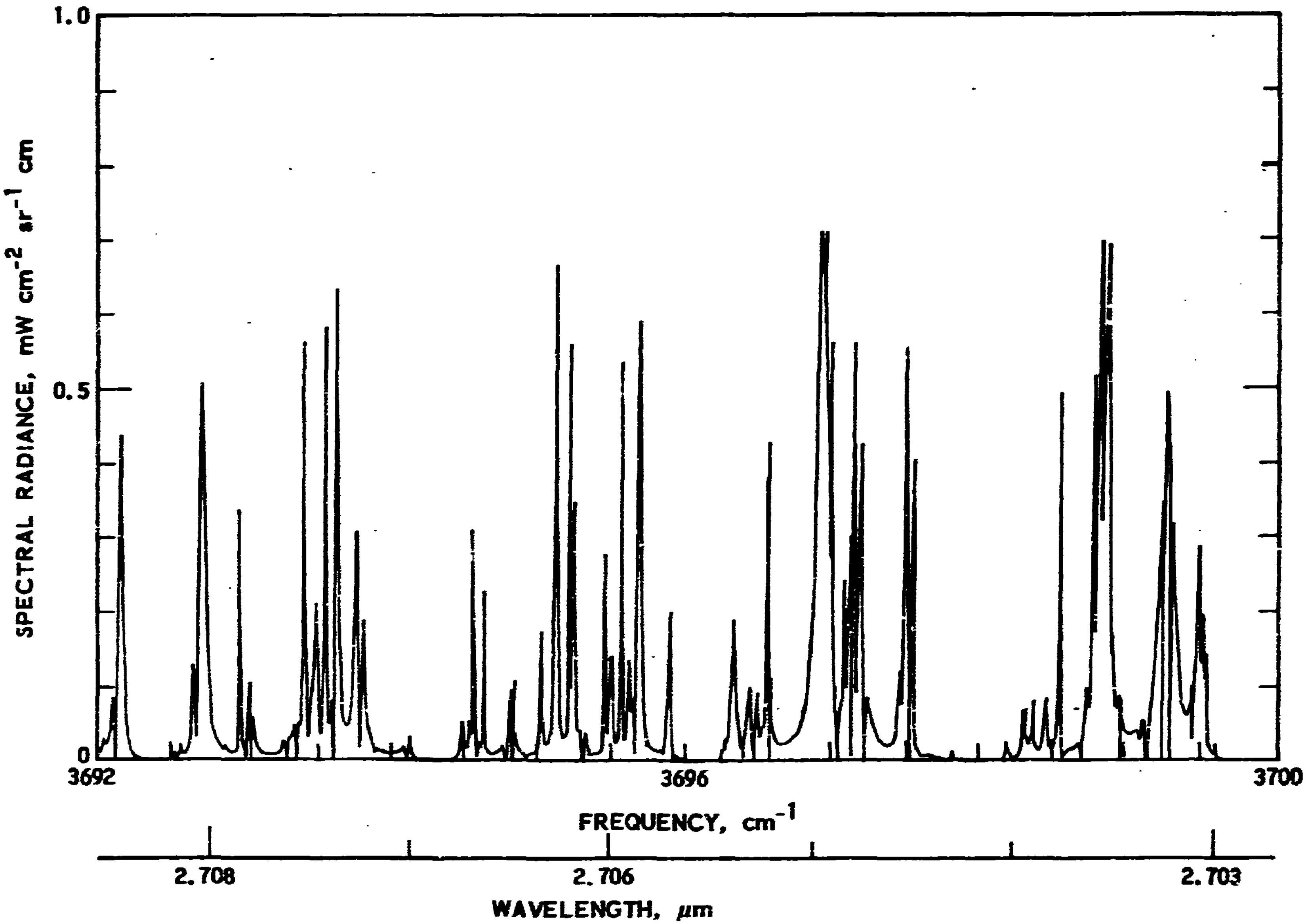
1.0
0.5
0
SPECTRAL RADIANCE, mW cm^{-2} sr^{-1} cm
3692
3696
3700
FREQUENCY, cm^{-1}
2.708
2.706
2.703
WAVELENGTH, μm

FIGURE 4.

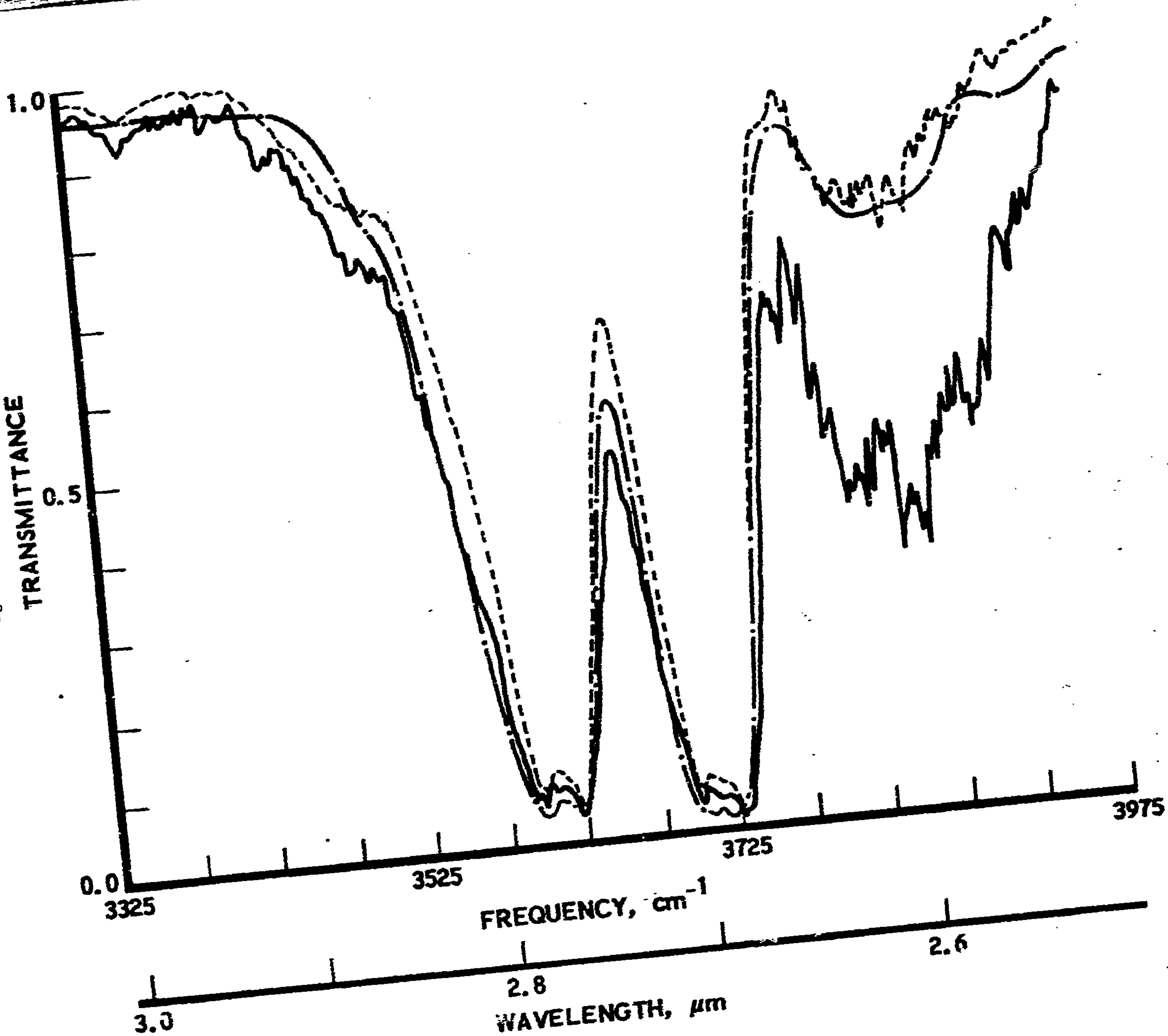
1.0
0.5
0.0
TRANSMITTANCE
3325
3525
3725
3975
FREQUENCY, cm^{-1}
3.0
2.8
2.6
WAVELENGTH, μm

FIGURE 5.

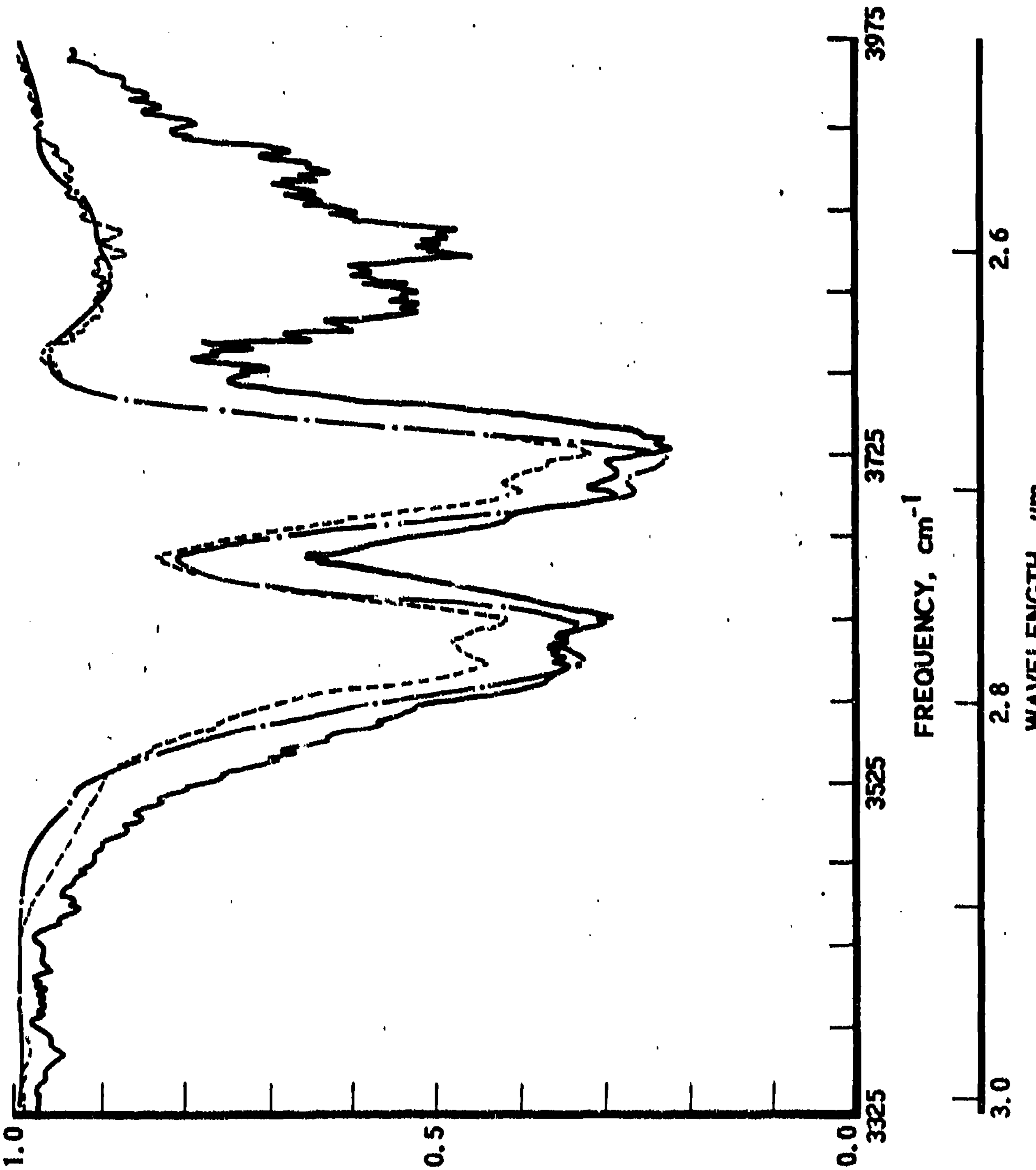
TRANSMITTANCE
1.0
0.5
0.0
3325
3525
3725
3975
FREQUENCY, cm-1
3.0
2.8
2.6
WAVELENGTH, μm

FIGURE 6.

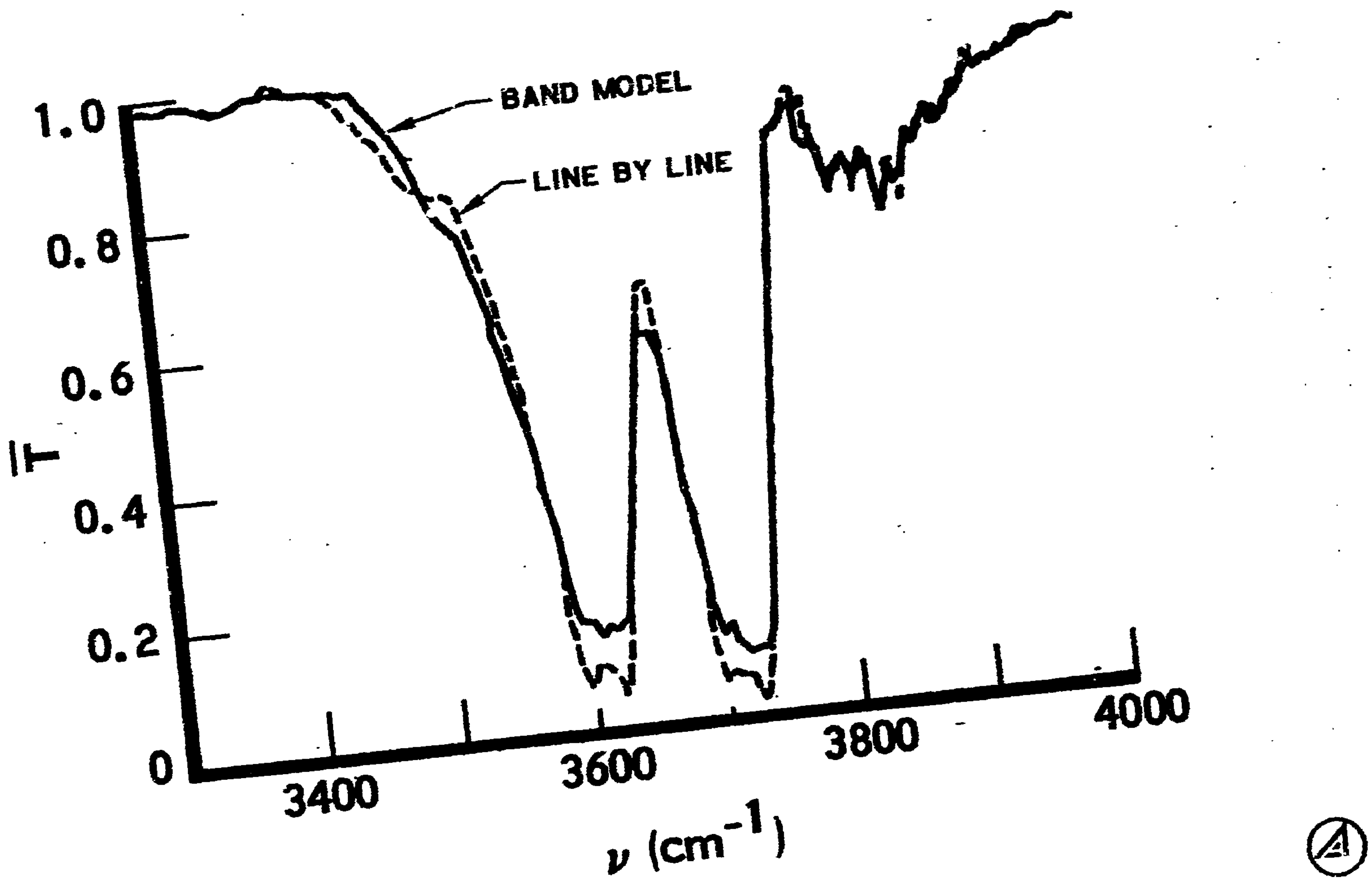
BAND MODEL
LINE BY LINE
1.0
0.8
0.6
0.4
0.2
0
$\overline{T}$
3400
3600
3800
4000
ν (cm^{-1})

FIGURE 7.

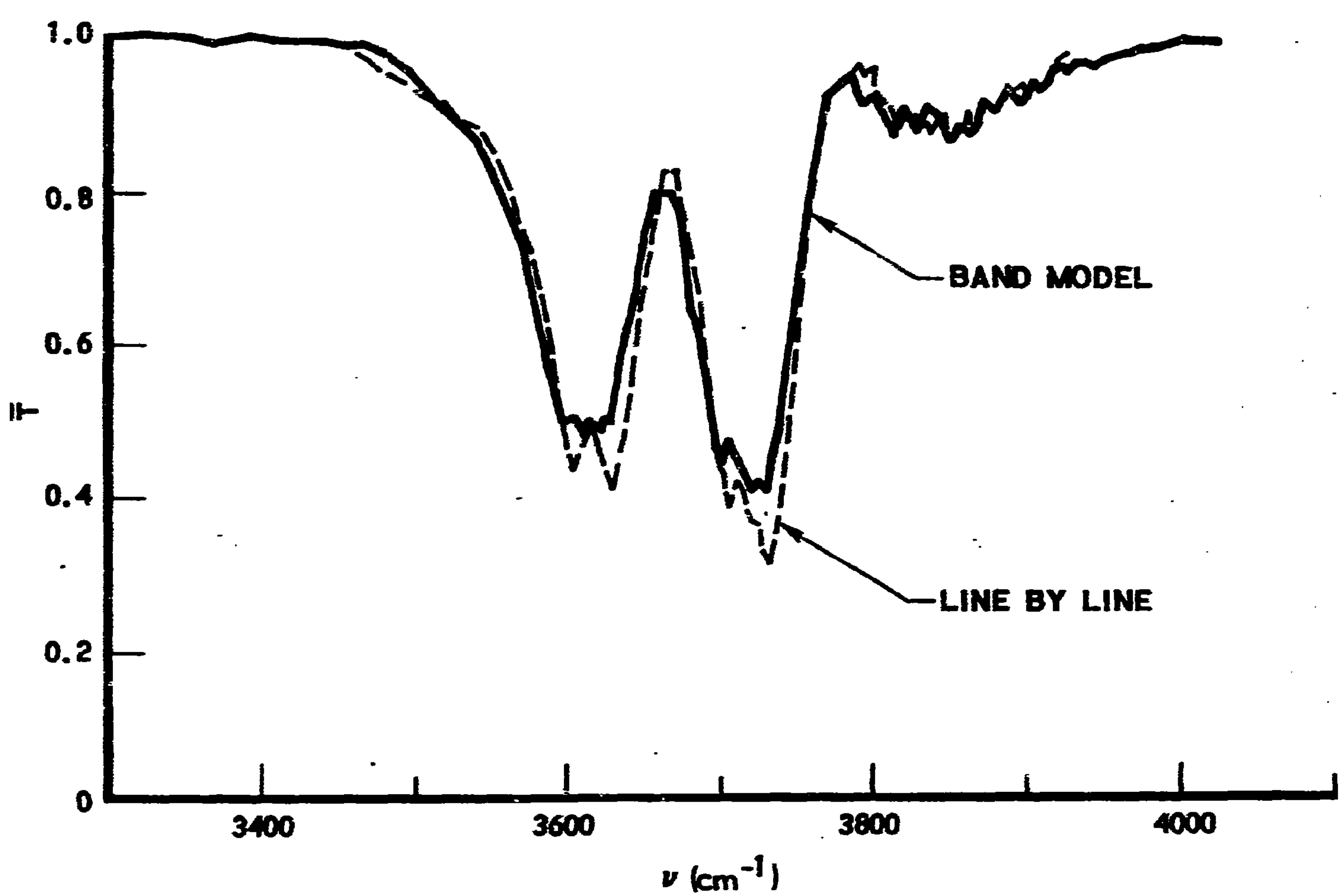
1.0
0.8
0.6
0.4
0.2
0
T
3400
3600
3800
4000
ν (cm^{-1})
BAND MODEL
LINE BY LINE

FIGURE 8.

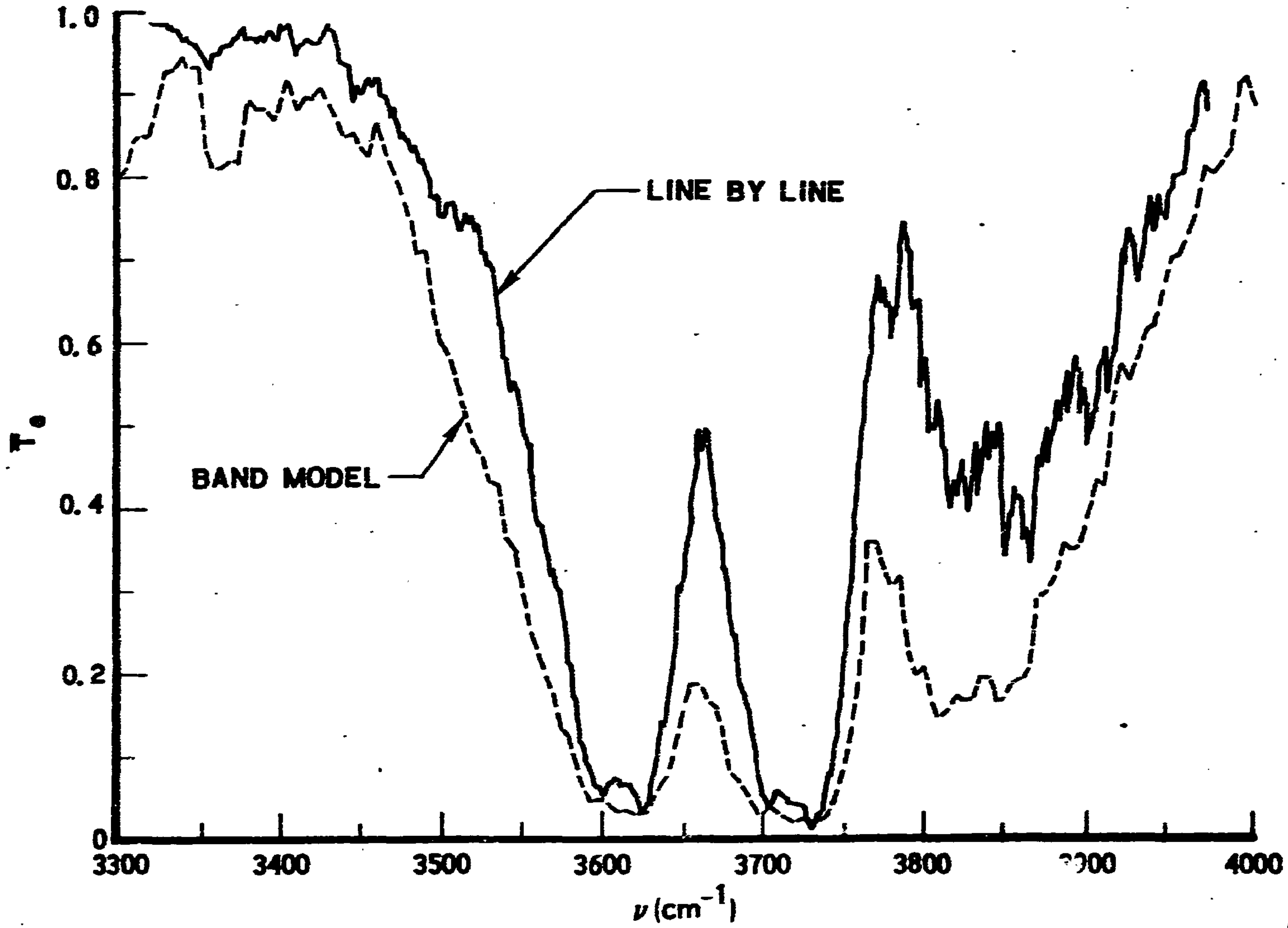
1.0
0.8
0.6
0.4
0.2
0
T_e
LINE BY LINE
BAND MODEL
3300
3400
3500
3600
3700
3800
3900
4000
ν (cm^{-1})

FIGURE 9.

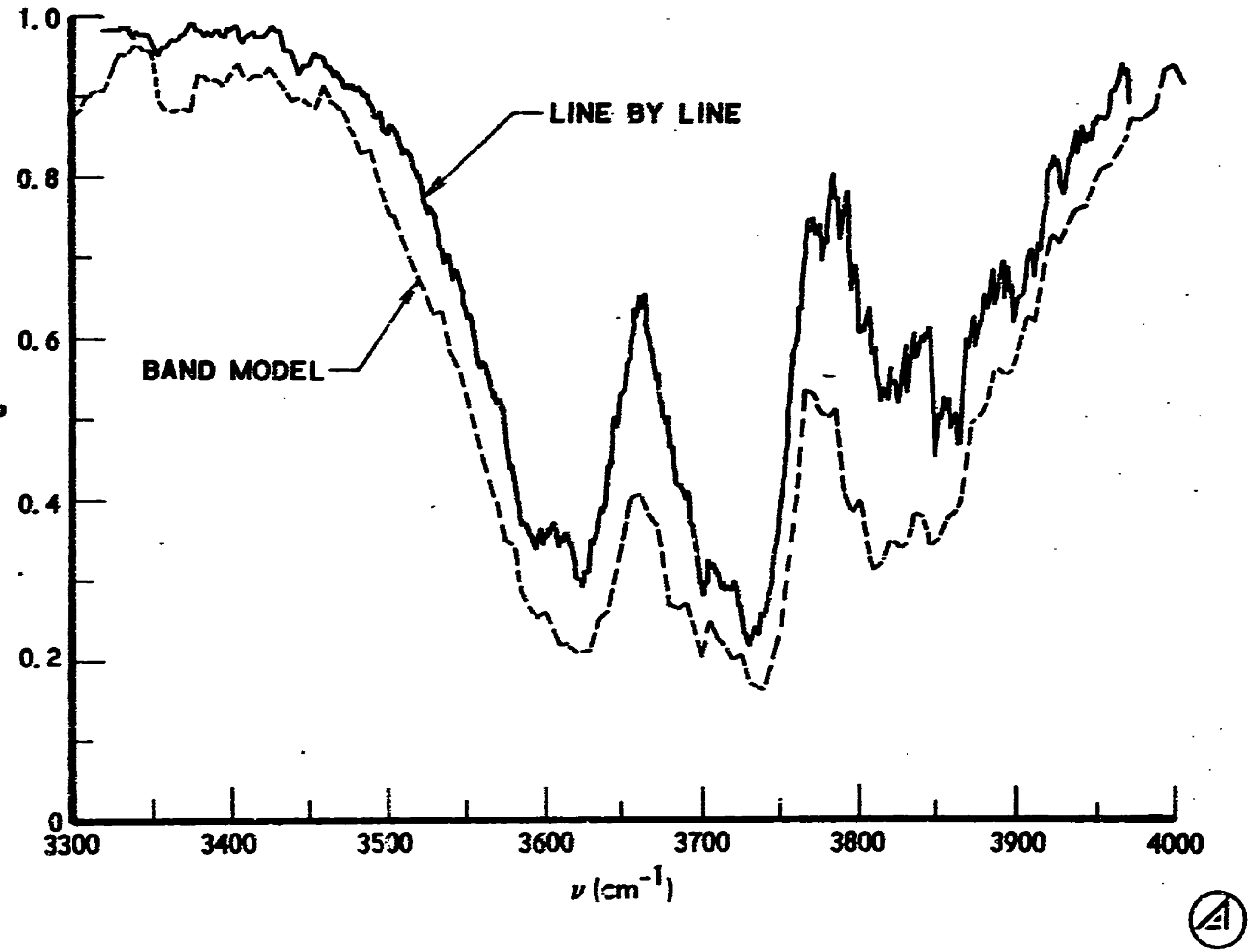
LINE BY LINE
BAND MODEL
1.0
0.8
0.6
0.4
0.2
0
τ_e
3300
3400
3500
3600
3700
3800
3900
4000
ν (cm^{-1})

FIGURE 10.

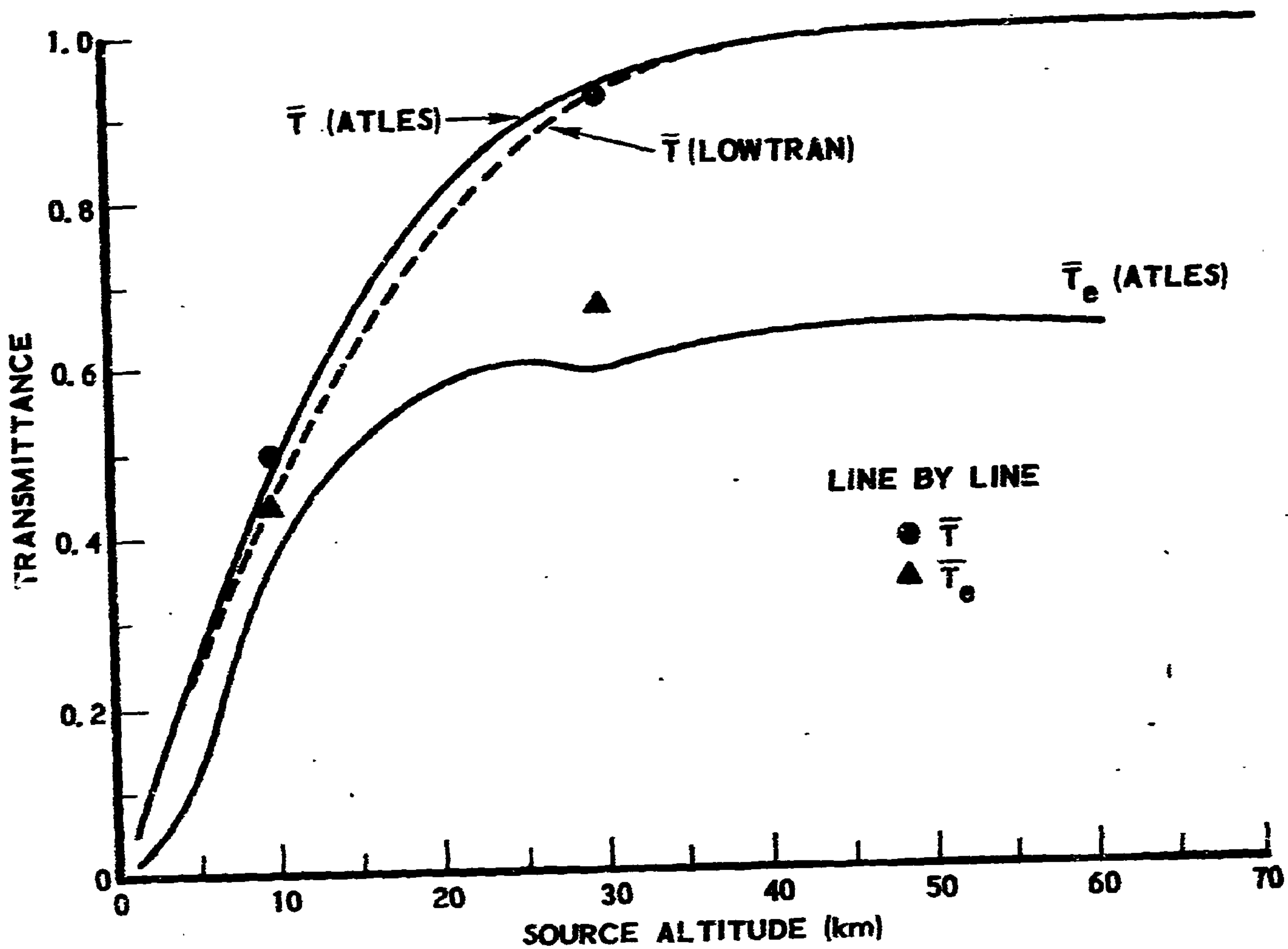

$\bar{T}$ (ATLES)
$\bar{T}$ (LOWTRAN)
$\bar{T}_e$ (ATLES)
LINE BY LINE
● $\bar{T}$
▲ $\bar{T}_e$
TRANSMITTANCE
1.0
0.8
0.6
0.4
0.2
0
0
10
20
30
40
50
60
70
SOURCE ALTITUDE (km)

FIGURE 11.

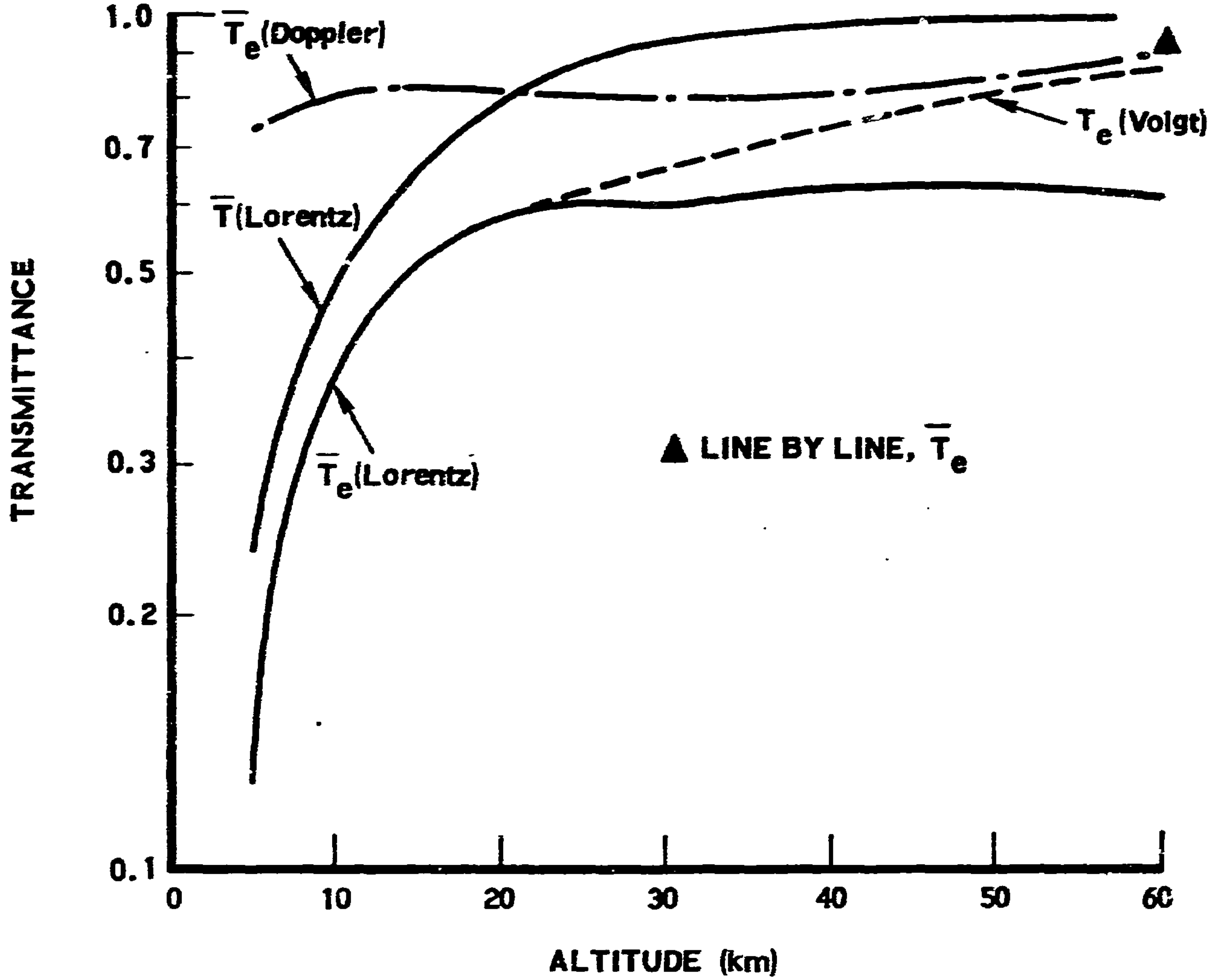

$\overline{T}_e$(Doppler)
T_e(Voigt)
$\overline{T}$(Lorentz)
$\overline{T}_e$(Lorentz)
▲ LINE BY LINE, $\overline{T}_e$
TRANSMITTANCE
1.0
0.7
0.5
0.3
0.2
0.1
0
10
20
30
40
50
60
ALTITUDE (km)

FIGURE 12.

ATMOSPHERIC TRANSMISSION AND EMISSION PROGRAM

David C. Anding

Science Applications, Inc.
La Jolla, California

ATMOSPHERIC TRANSMISSION AND EMISSION PROGRAM

David C. Anding
Science Applications, Inc.
La Jolla, California

Described herein is an atmospheric transmission and emission computer code which is an outgrowth of a study performed at the Infrared Information and Analysis Center (IRIA) at The University of Michigan's Willow Run Laboratories, in 1967. Since its conception in 1967 the code has undergone many revisions and improvements in selected spectral regions. The result is a code which may be considered state-of-the-art for wavelengths greater than 4.0 μm, but remains in its conceived form for shorter wavelengths. The code has been published in an Aerospace report. *

Slide 1 delineates the basic capabilities of the code. The effects of molecular absorption, aerosol extinction, and thermal emission from both molecules and aerosols are included. The applicable spectral region extends from 1 to 30 μm. The molecules whose effects are represented include H_2O, CO_2, O_3, CH_4, N_2O, HNO_3 and N_2. The basic assumptions inherent in the calculational procedure are local thermodynamic equilibrium and single scattering for aerosols. The effects of refraction are not included. The inputs required for a given calculation are the altitude distributions of pressure, temperature, aerosol density, H_2O, O_3 and HNO_3 densities, and the mixing ratios of the uniformly mixed gases - CO_2, N_2O and CH_4. The outputs of the code are transmission and path radiance versus wavelength.

---

* J. Hamilton, J. Rowe and D. Anding, Atmospheric Transmission and Emission Program, Aerospace Report No. TOR-0073 (3050-02)-3, June 1973.

The code is divided into two sub-codes, CATM and ATMRAD, which operate in tantum. The next two slides present the specific calculations that are performed by each of these codes. CATM converts rudimentary atmospheric data to a spherically shelled model atmosphere which is required as input to ATMRAD, the code which performs the transmission and radiance calculation. The inputs to CATM are pressure, temperature and H_2O, O_3 and HNO_3 densities, each expressed as a function of altitude (at whatever altitudes they are available to the user), and the mixing ratios of CO_2, N_2O and CH_4. The outputs are the input parameter values re-evaluated at the prescribed spherical shells. In essence, CATM constructs a spherical shelled model atmosphere from rudimentary atmospheric data. Five standard atmospheres have been compiled for general usage. These are denoted Arctic Summer, Arctic Winter, Temperate Summer, Temperate Winter, and Tropic Mean.

ATMRAD (Atmospheric Radiance) calculates spectral path transmission and radiance from 1 to 30 μm for any geometric path within a spherically shelled model atmosphere. ATMRAD also includes the radiance contribution of a Planckian radiator within the optical line-of-sight. The inputs required are the model atmosphere for CATM, the geometric path, the wavelength interval, and the spectral emissivity of the Planckian source. The outputs are spectral path transmission and total radiance at the point of observation along the direction of the line-of-sight. A schematic of the geometry is shown in slide 4. A Planckian source is denoted Target, located at the nth shell, and the point of observation is denoted Detector, located at the earth's surface. The radiance at the detector (in the direction of the line-of-sight) is calculated, including the atmospheric modified target radiance and the atmospheric radiance originating along the line-of-sight (radiance originating at points off the line-of-sight impinging upon the detector are not included). The number of shells (n) into which the model atmosphere is divided for any given altitude regime is an option of

the user. Generally, as the path becomes more horizontal the shell density is increased in proportion to the secant of the zenith angle.

As shown in slide 5 the path transmission is the product of the individual transmissions. This approximation introduces little error if either the transmission is slowly varying over the wavelength interval of the applicable transmission model, or there is minimal correlation between the spectral absorption lines. Also shown in slide 5 is the equation evaluated for the computation of radiance.

Slide 6 displays the transmission models used by the code. In total there are seven; Goody model, strong-line Goody, Elsasser, strong-line Elsasser, the continuum models for H_2O and N_2, and the aerosol extinction model. All parameters have the common interpretation. Slide 7 presents the transmission models that are used for the respective molecules, listing the approximate resolution for each wavelength interval, the procedure that was used to obtain the transmission model coefficients, and the source of the data used in the coefficient evaluation. The asterisk denotes those transmission models and coefficients which have been modified since the code was conceived in 1967.

Slide 8 is a comparison of the one set of aerosol extinction coefficients used by ATMRAD with those published by McClatchey in 1974.* This comparison is given to demonstrate the sensitivity of the extinction coefficient to particle size distribution and aerosol complex index, both of which are considerably different for the two cases shown. Wavelength dependent extinction and scattering coefficients are specified as input and as such, ATMRAD can perform calculations for any aerosol. Five additional sets of aerosol coefficients are available for use ranging from 100%

---

* R. A. McClatchey and J. E. A. Selby, Atmospheric Attenuation of Laser Radiation from 0.76 to 31.25 μm, AFCRL-TR-74-0003, January 1974.

maritime haze to 100% continental haze. These coefficients are from the work of B. Finn of AFCRL.

Possibly the single most important coefficients in the 8 to 14 μm spectral region are those for the water vapor continuum. Shown in slide 9 is the self broadening absorption coefficient used by ATMRAD (solid line) which is a least-squares fit to the measurement data. In slide 10 transmission at 10.59 μm (as calculated by ATMRAD) is compared with measurements of McCoy* using a foreign to self broadening ratio of 0.005. Observe that the absorption is overestimated, which when extrapolated to long paths at high humidity can be considerable. Because of the consistency and repeatability of the McCoy data, and hence the likelihood of its correctness, it was felt a modification to either the self-broadening coefficients or the K_f/K_s ratio was in order to bring ATMRAD results in agreement with the McCoy data. This was achieved by reducing the ratio of K_f to K_s to a value of 0.001. Subsequent discussions with Burch and Long indicated that a least-squares fit to the data of slide 9 probably yielded a self-broadening coefficient that is too high because of possible systematic errors for the larger data points. By reducing the self-broadening coefficients to coincide with the lowest values shown in slide 9, agreement between ATMRAD computations and McCoy's measurements can be achieved using a value for K_f/K_s of 0.005. It is recommended that the available data base be carefully reviewed and the best values for both self and foreign broadening be selected for use in future computations. As a further refinement to H_2O continuum absorption a temperature dependence has been adopted which is shown in slide 11.

Since the publication of the Aerospace report certain improvements have been made to the code as part of SAI's internally funded R & D

---

* J. McCoy, D. Rensch, R. Long, Applied Optics, Vol. 8, No. 7, 1969.

activities. These are shown in slide 12. The re-evaluation of the CO_2 and H_2O coefficients was done primarily to increase the resolution capability. The data base and procedure used are noted on the slide.

Slides 13 through 20 present example results from the ATMRAD, including comparisons with measurement data, line-by-line calculations, and LOWTRAN II. Slide 13 displays the spectral region from 1.0 to 4.0 μm, simply to typify the resolution capability for this spectral region. Slide 14 displays a comparison between ATMRAD results and open air field measurements performed by Convair. The measurement path parameters are noted on the slide. The results presented in slides 15, 16, 17 and 18 were generated subsequent to the recent code modifications to demonstrate consistency between band model results and the data base used to generate the band model coefficients. Slide 15 is a comparison of band model results for CO_2 with the measurement data of Burch. Slides 16, 17, and 18 are comparisons between band model results and line-by-line results (degraded to the band model resolution) for H_2O in three different spectral regions. For each case the parameters are noted on the slides.

Slide 19 is a comparison of radiance values computed by ATMRAD with measurement data from Nimbus. The measurement data were acquired by the Infrared Interferometer Spectrometer (IRIS) over a cloud-free ocean area for which the surface temperature and atmospheric temperature and humidity were known. These known parameters were used in ATMRAD to perform the radiance calculations. It is felt that the results are very satisfying, particularly in the window region centered at 1150 cm^{-1}.

Slide 20 is a comparison of transmission calculations made by ATMRAD and LOWTRAN for a zenith path through a common atmosphere. The precise reason for the difference between the two calculations is not known. However, it is felt that the discrepancy probably arises from slight differences in the treatment of all the contributing mechanisms, i.e., continuum absorption, local line absorption, and aerosol extinction.

Of considerable importance to many applications is accurate prediction of 8-14 μm window transmission, particularly when the transmission is less than 10%. To achieve this both an accurate scattering model is required and an accurate representation of H_2O continuum absorption. The scattering models are discussed elsewhere in these proceedings and will not be considered further here. Based upon a brief, yet reasonably thorough, study of the literature, a few statements concerning our understanding of H_2O continuum have been made. These are given in slide 21.

First, there still remains a lack in the understanding of the mechanism of continuum absorption. Is it H_2O dimer, the far wings of neighboring lines, or caused by contributions of both? Second, based upon the laboratory data of Long and Burch, self-induced absorption is known to an accuracy of approximately 20% at room temperature for wavelengths longer than 8.0 μm. Because of the sparsity of data, the accuracy is considerably worse at shorter wavelengths and at temperatures cooler than approximately 296 Kelvins. In general, for terrestrial temperatures, the temperature dependence of the continuum is poorly known. Third, the foreign-induced absorption coefficient is known to within about a factor of 2. This uncertainty arises because the foreign-induced coefficient has not been measured directly, but must be inferred from measurements in which both self- and foreign-induced absorption are present, using the self-induced coefficient as a basis. Small errors in the self-induced coefficient can cause large errors in the foreign-induced coefficient. Lastly, and of considerable relevance, measurements of continuum absorption have not been made for H_2O partial pressures greater than approximately 75 percent of the saturation vapor pressure. Therefore, the application of the data base to predictions of atmospheric transmission in tropical atmospheres where the humidities are near 90% results in an extrapolation of the data and may result in considerable error, particularly for long paths.

In summary, ATMRAD may be considered a state-of-the-art band model transmission and emission code for wavelengths greater than 4.0 μm in regard to its treatment of molecular absorption and emission. For shorter wavelengths ATMRAD is vintage 1967. For aerosol extinction ATMRAD yields results that are consistent with the accuracy of the extinction and scattering coefficients used as input. As new aerosol parameters are disseminated from AFCRL, these can be used as input to ATMRAD.

1. Atmospheric Transmission and Emission Code Capabilities

CALCULATIONAL CAPABILITIES

- MOLECULAR ABSORPTION (1 - 30 μm)
  H_2O, CO_2, O_3, CH_4, N_2O, N_2, HNO_3
- AEROSOL EXTINCTION (1 - 30 μm)
  WATER HAZE
- THERMAL EMISSION (1 - 30 μm)
  MOLECULES AND AEROSOL

ASSUMPTIONS

- LOCAL THERMODYNAMIC EQUILIBRIUM
- SINGLE SCATTERING FOR AEROSOLS
- REFRACTION NOT INCLUDED

INPUTS REQUIRED

- PRESSURE PROFILE
- TEMPERATURE PROFILE
- AERCSOL DENSITY PROFILE
- MIXING RATIO (CO_2, N_2O, CH_4)
- DENSITY PROFILES (H_2O, O_3, HNO_3)

OUTPUTS

- TRANSMISSION VS WAVELENGTH (1 - 30 μm)
- PATH RADIANCE VS WAVELENGTH (1 - 30 μm)

2. Basic Capability of Model Atmosphere Code CATM

CONVERTS RUDIMENTARY MODEL ATMOSPHERE PROFILES TO SPHERICAL SHELLED MODEL REQUIRED FOR TRANSMISSION AND RADIANCE CALCULATION

INPUTS

- PRESSURE PROFILES
- TEMPERATURE PROFILES
- H_2O, O_3, HNO_3 PROFILES
- CO_2, CH_4, N_2O MIXING RATIOS

OUTPUTS

- REQUIRED INPUT PARAMETER VALUES EVALUATED FOR PRESCRIBED SHELLS

FIVE STANDARD ATMOSPHERES HAVE BEEN COMPILED FOR GENERAL USAGE:

- ARCTIC SUMMER
- ARCTIC WINTER
- TEMPERATE SUMMER
- TEMPERATE WINTER
- TROPIC MEAN

3. Basic Capability of Transmission/Radiance Code ATMRAD

CALCULATES TRANSMISSION AND/OR RADIANCE VERSUS WAVELENGTH FROM 1 TO 30 μm FOR ANY GEOMETRIC PATH WITHIN DEFINED SPHERICAL SHELLED ATMOSPHERE

INPUTS

- COMPILED ATMOSPHERE FROM CATM
- DEFINITION OF GEOMETRIC PATH
- WAVELENGTH INTERVAL
- SOURCE EMISSIVITY

OUTPUTS

- TRANSMISSION AND/OR RADIANCE VERSUS WAVELENGTH

4. Schematic of Optical Path for Transmission and Radiance Calculations

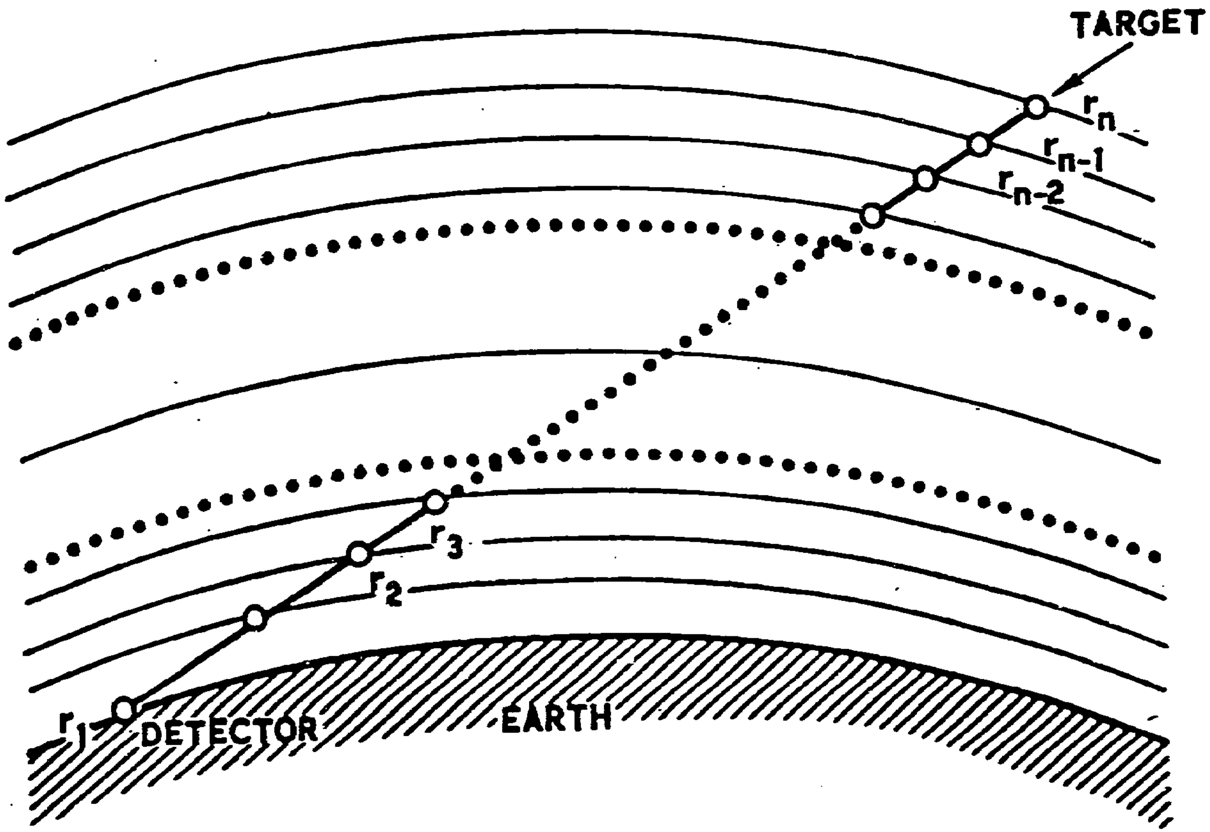

5. Equations Used to Compute Transmission and Radiance

TRANSMISSION:

$$\tau = \tau_{H_2O}\, \tau_{H_2O\ \text{continuum}}\, \tau_{CO_2}\, \tau_{O_3}\, \tau_{CH_4}\, \tau_{N_2O}\, \tau_{HNO_3}\, \tau_{N_2}\, \tau_{a}\, \tau_{s}$$

RADIANCE:

$$L_{\Delta\lambda} = L_{\Delta\lambda}^{bb}(T_{source})\, \epsilon_{source}\, \tau_{obs\text{-}source} + \sum_{i=1}^{n} L_{\Delta\lambda}^{bb}(T_i)(\tau_i - \tau_{i+1})$$

6. Transmission Models Used by ATMRAD

GOODY MODEL:

$$T = \mathrm{EXP}\left[-\frac{(S/d)\,W}{\sqrt{1+\left(\frac{S}{\pi\alpha}\right)\frac{W}{P}}}\right]$$

$$T = \mathrm{EXP}\left[-\sqrt{\left(\frac{S}{\pi\alpha d^2}\right)\frac{W}{P}}\right] \qquad \text{(STRONG LINE)}$$

ELSASSER MODEL:

$$T = 1 - \mathrm{SINH}\,\beta \int_0^Y I_0(y)\ \mathrm{EXP}\,(-\,y\ \mathrm{COSH}\beta)\,dy$$

$$\beta = \frac{2\pi\alpha}{d}\,P$$

$$y = \beta x/\mathrm{SINH}\beta$$

$$x = \frac{S}{2\pi\alpha}\,\frac{W}{P}$$

$$T = 1 - \mathrm{ERF}\,\sqrt{1/2\beta^2 x} \qquad \text{(STRONG LINE)}$$

H_2O CONTINUUM: $T = \mathrm{EXP} - [(k_s p_s + k_f P_f)\,W]$

N_2 CONTINUUM: $T = \mathrm{EXP} - [(C_s p_s + C_f P_f)\,W]$

AEROSOL EXTINCTION: $T = \mathrm{EXP} - [(k_s + k_a)\,W]$

7. Transmission Band Models Used by Code

GAS	SPECTRAL REGION (μm)	APPROXIMATE RESOLUTION (μm)	MODEL	COEFFICIENT ACQUISITION PROCEDURE	SOURCE OF DATA
H_2O	1 to 2	0.10	Strong-Line Goody	Empirical Fit to Lab Data	Howard, et. al.
	2 to 4.0	0.05	Goody	Empirical Fit to Lab Data	Burch, et. al.
	4.0 to 15	0.10	Goody	*Direct from Line Parameters	AFCRL
	15 to 30	1.0	Goody	*Direct from Line Parameters	AFCRL
	6.7 to 15.0	-	H_2O Continuum	*Empirical Fit to Lab Data	Burch and Bignell
CO_2	1.9 to 2.1	0.20	Strong-Line Elsasser	Empirical Fit to Lab Data	Howard, et. al.
	2.64 to 2.88	0.01	Elsasser	Empirical Fit to Lab Data	Burch, et. al.
	4.0 to 5.5	0.02	Elsasser	*Empirical Fit to Lab Data	Burch, et. al.
	9.13 to 11.67	0.50	Strong-Line Elsasser	Empirical Fit to Lab Data	Howard, et. al.
	11.67 to 19.92	0.10	Elsasser	*Empirical Fit to Line by Line Spectra	Drayson
N_2O	4.228 to 4.73	0.50	Strong-Line Elsasser	*Empirical Fit to Lab Data	Plyer
	7.53 to 8.91	0.50	Elsasser	*Empirical Fit to Lab Data	Burch
	15.4 to 19.3	0.50	Goody	*Empirical Fit to Lab Data	Burch
N_2	3.76 to 4.83	-	N_2 Continuum	*Empirical Fit to Lab Data	Burch
O_3	8.398 to 10.19	0.10	Elsasser	Empirical Fit to Lab Data	Walshaw
	11.7 to 15.4	0.50	Goody	*Empirical Fit to Lab Data	McCaa and Shaw
CH_4	5.91 to 9.1	0.10	Elsasser	*Empirical Fit to Lab Data	Burch
HNO_3	5.8 to 5.944 7.45 to 7.80 10.9 to 11.67	0.50	Goody	*Empirical Fit to Lab Data	Goldman

8. Extinction Coefficients Versus Wavelength

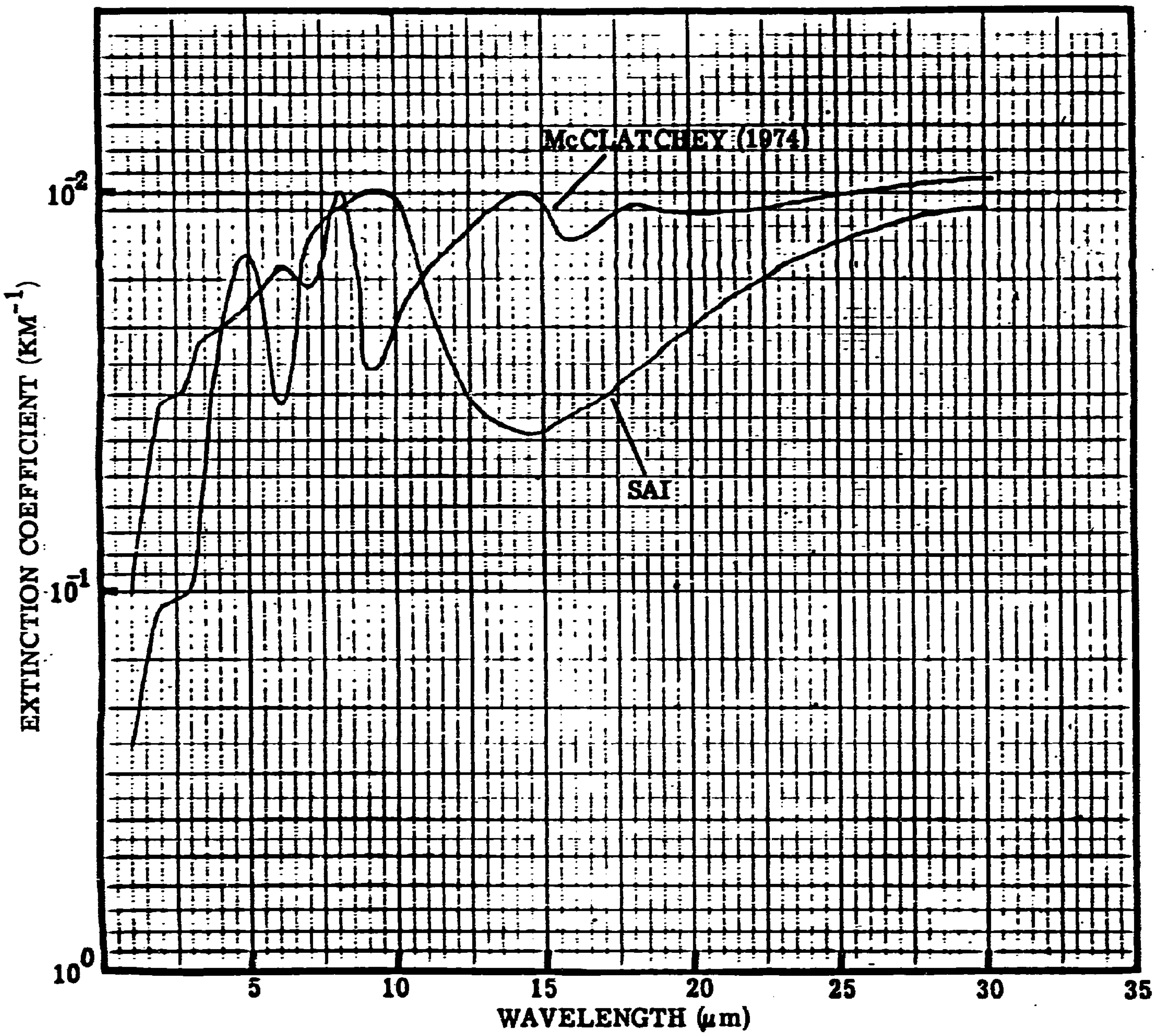

9. Absorption Coefficient for Self Broadening

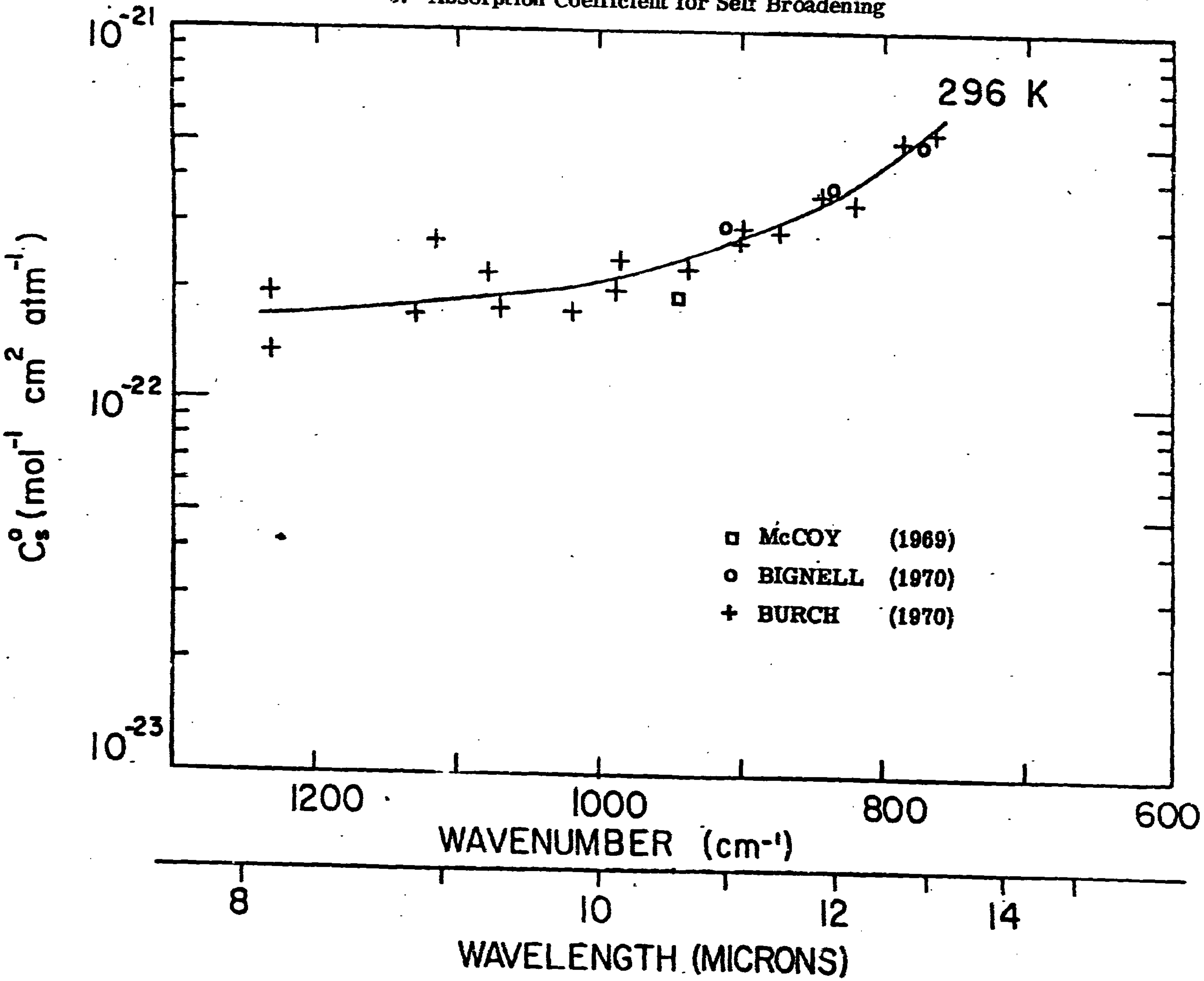

10. Transmission at 10.59 μm Versus Water Vapor Pressure for Pure Water

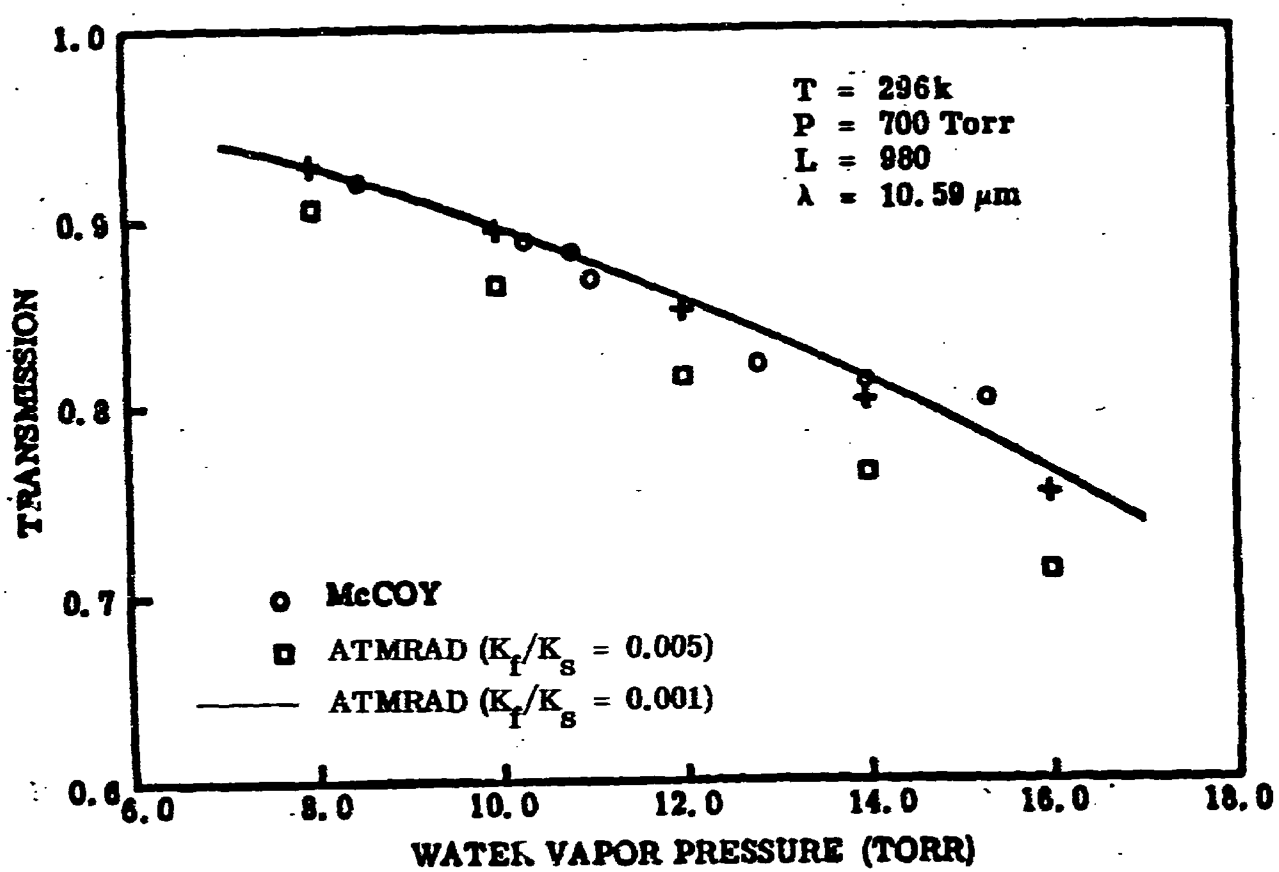

11. Temperature Dependence of H_2O Continuum

- FOR SELF-INDUCED ABSORPTION, TEMPERATURE DEPENDENCE ADOPTED FROM WORK OF BIGNELL.* ADOPTED DEPENDENCE - NEGATIVE AT 2 PERCENT PER DEGREE KELVIN.

- FOR FOREIGN-INDUCED ABSORPTION, TEMPERATURE DEPENDENCE SCALED FROM TEMPERATURE DEPENDENCE OF ROTATIONAL WATER LINES. ADOPTED DEPENDENCE - POSITIVE AT 2 PERCENT PER DEGREE KELVIN.

---

* K. J. Bignell, QJRSM, 96, 390 (1970).

12. Code Improvements Since Aerospace Report Publication

- NEW ELSASSER BAND MODEL COEFFICIENTS WERE INCLUDED FOR CO_2 FROM 4.0 TO 5.0 μm.

  COEFFICIENTS EVALUATED BY EMPIRICALLY FITTING ELSASSER FUNCTION TO LABORATORY DATA OF BURCH (1966).

  RESOLUTION = 10 cm^{-1}.

- NEW GOODY BAND MODEL COEFFICIENTS WERE INCLUDED FOR H_2O FROM 4.0 TO 15.0 μm.

  COEFFICIENTS WERE EVALUATED DIRECTLY FROM AFCRL LINE PARAMETERS (1973) USING PROCEDURE OF GOODY.

  RESOLUTION = 10 cm^{-1}.

13. Example ATMRAD Transmission Spectrum

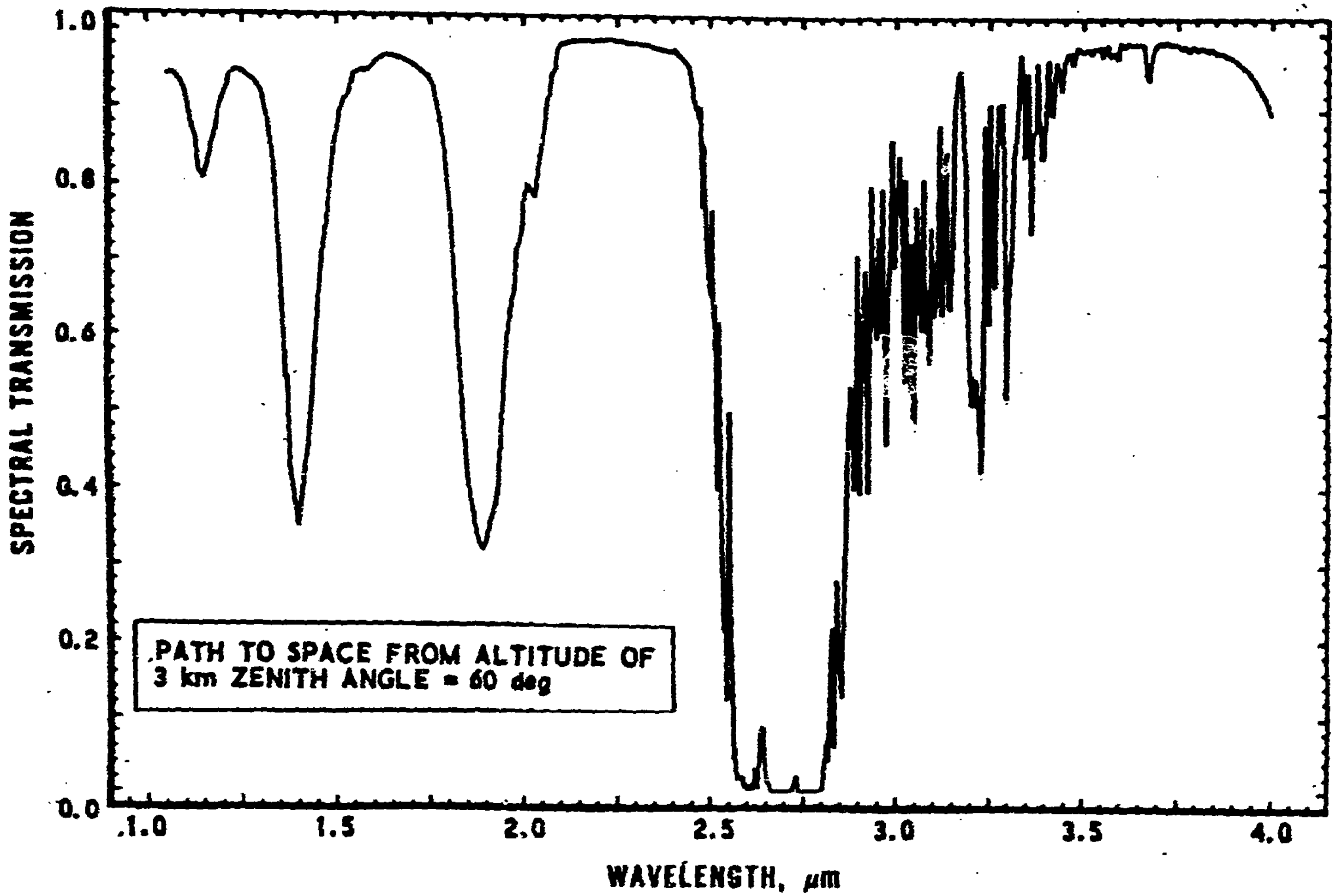

14. Comparison of ATMRAD Results with Open Air Measurements

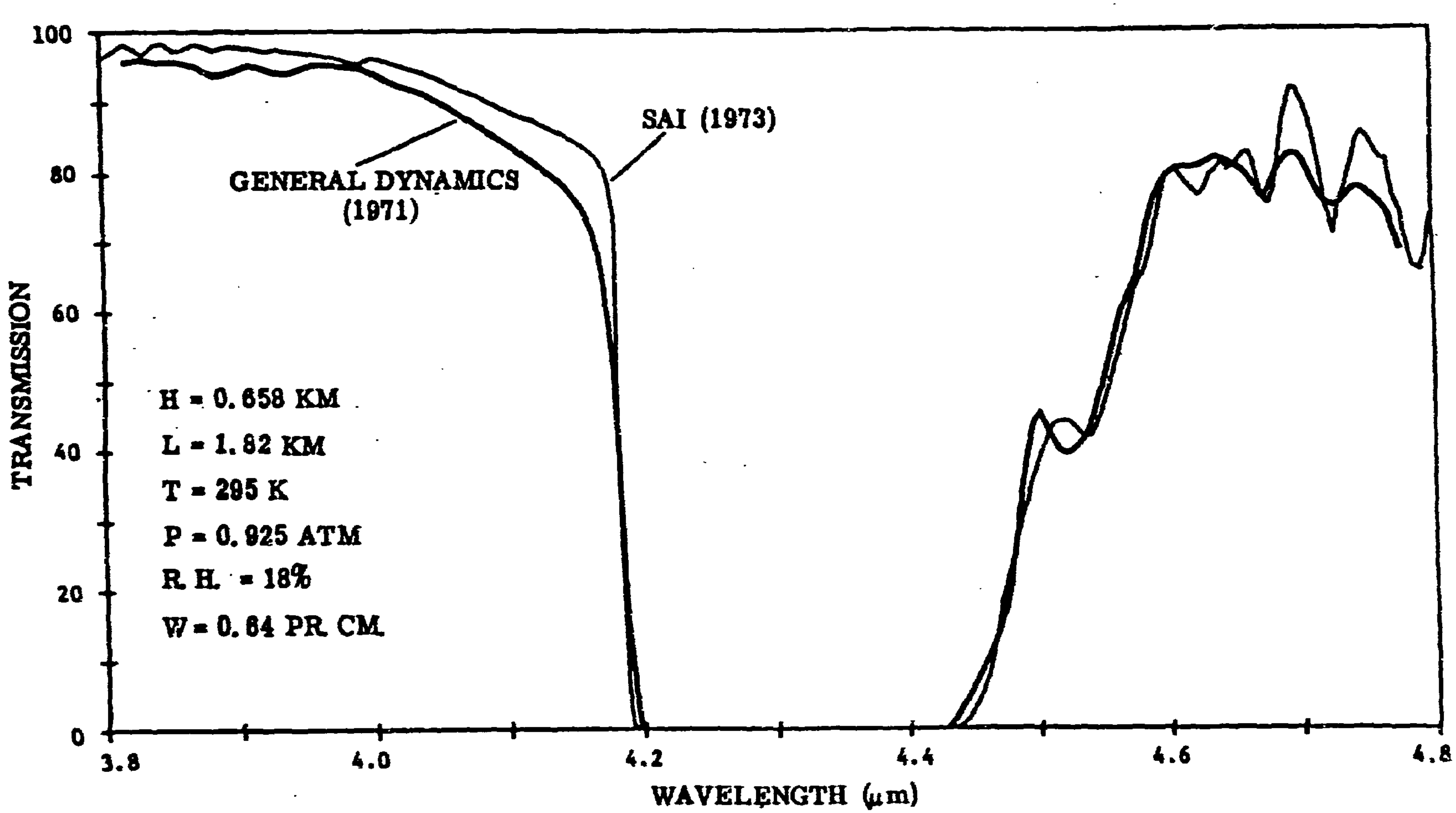

15. Comparison of CO_2 Band Model Results with Data of Burch

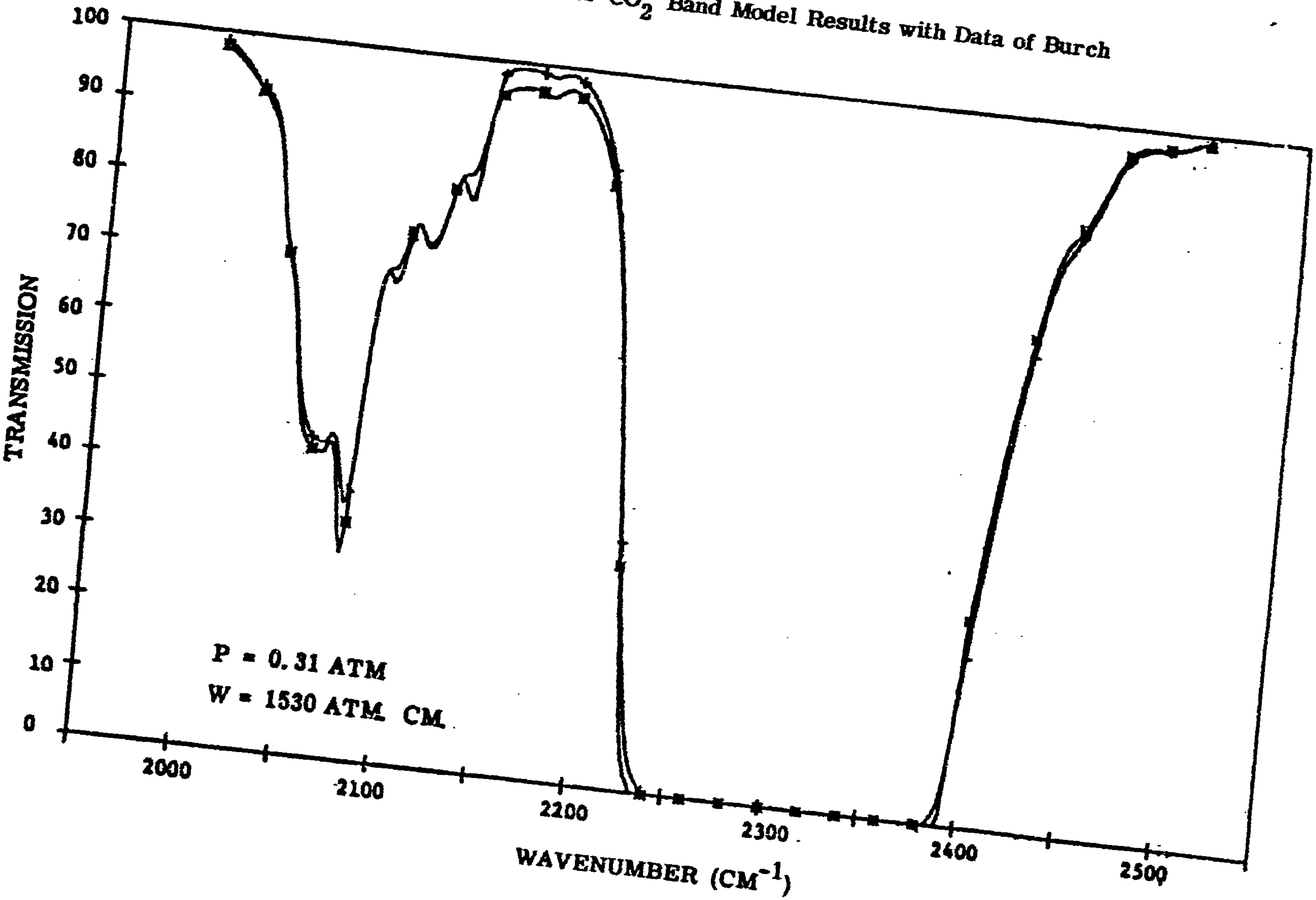

16. Comparison of Band Model Results with Line-by-Line Results for H_2O

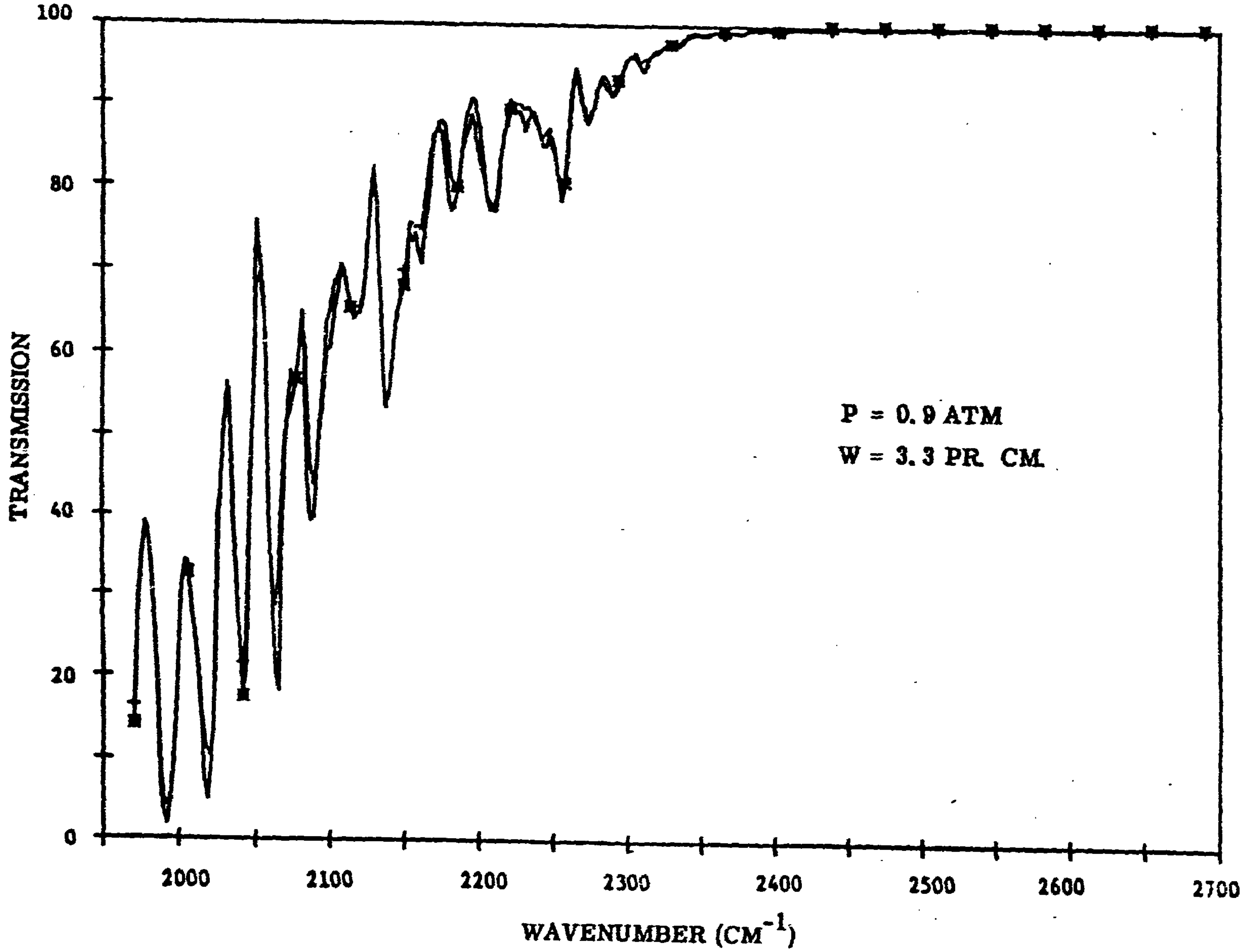

17. Comparison of Band Model Results with Line-by-Line Results for H_2O

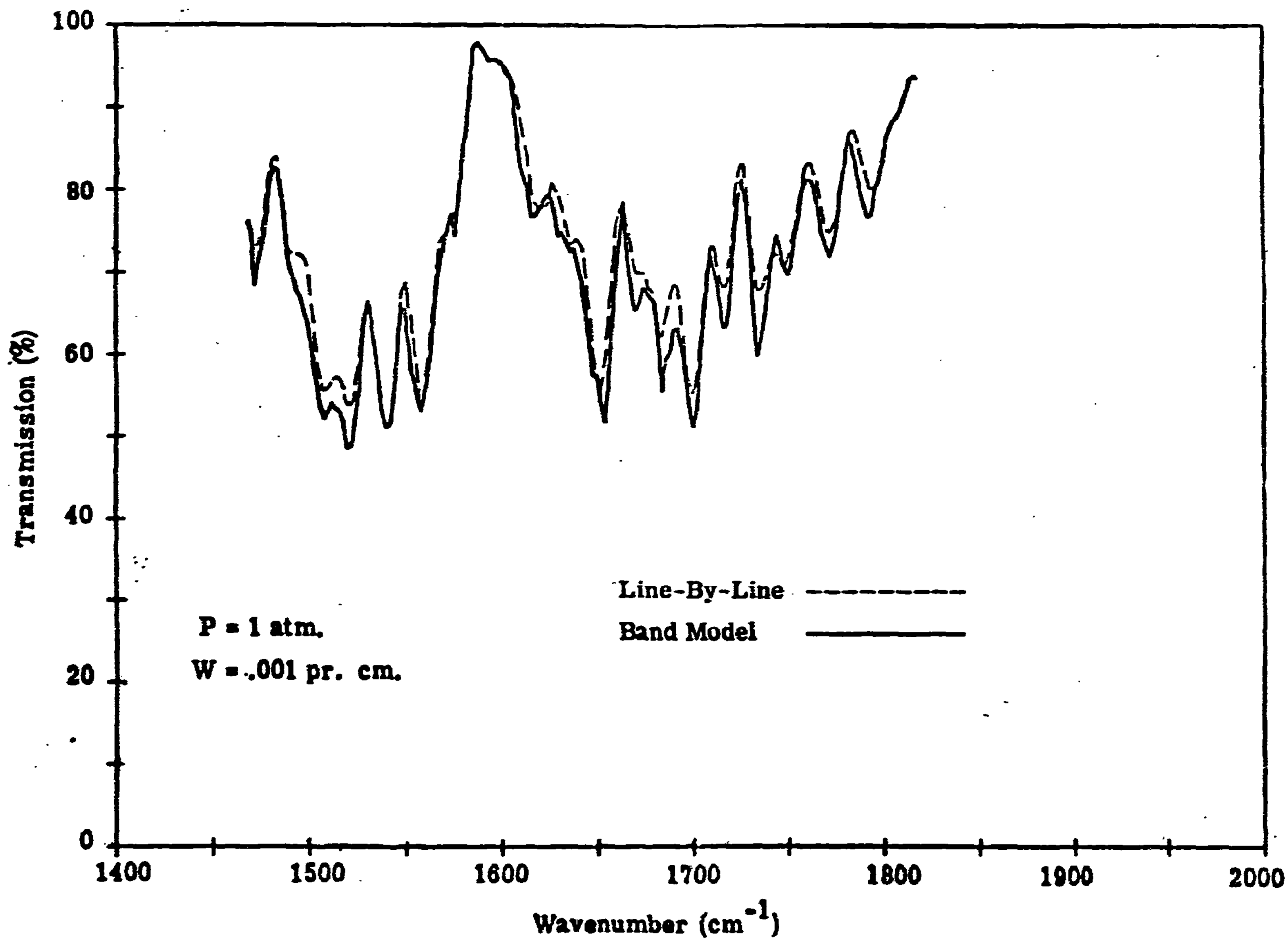

18. Comparison of Band Model Results with Line-by-Line Results for H_2O

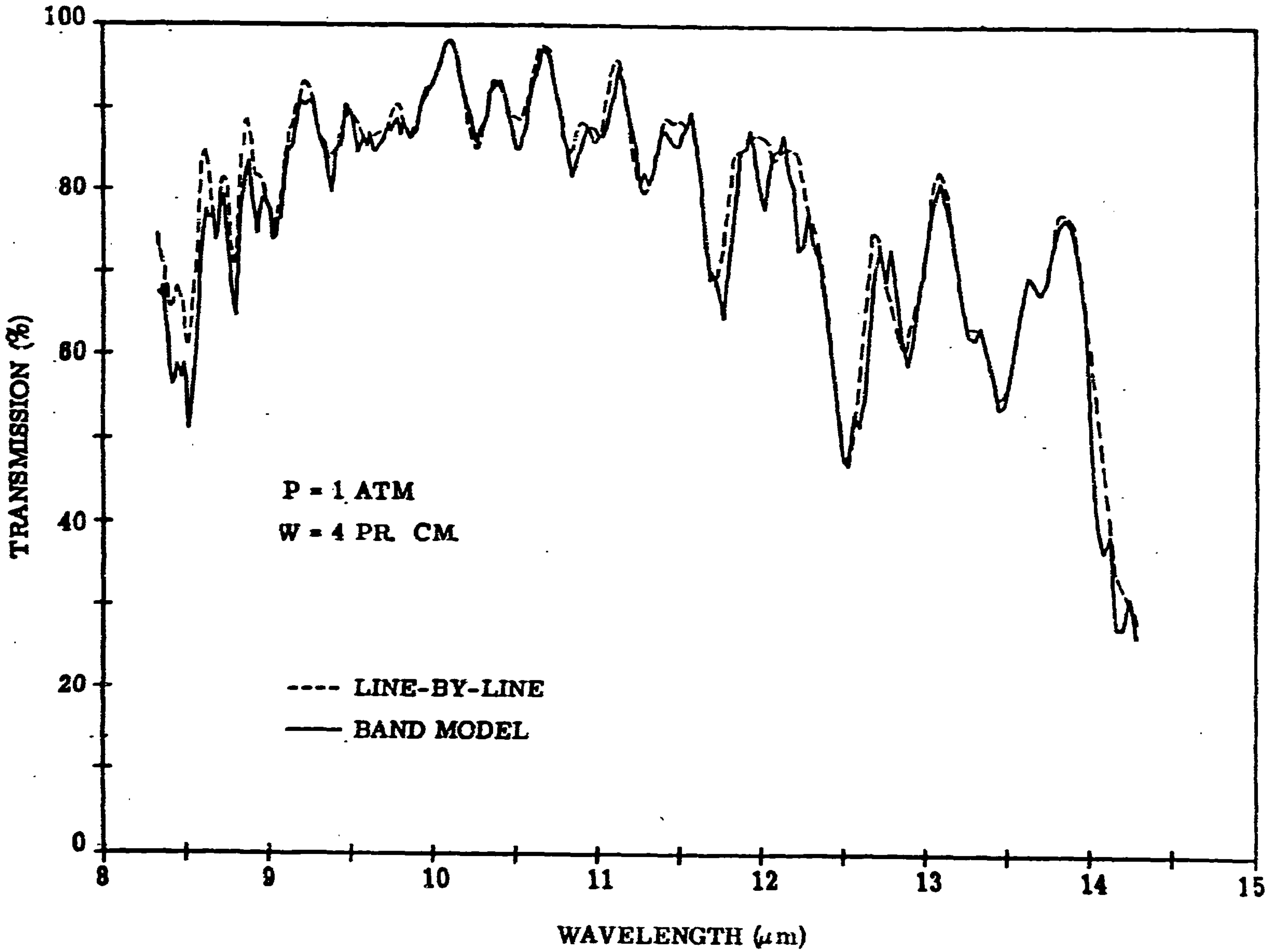

19. Comparison of ATMRAD Radiance Calculations with Measurement Data from Nimbus

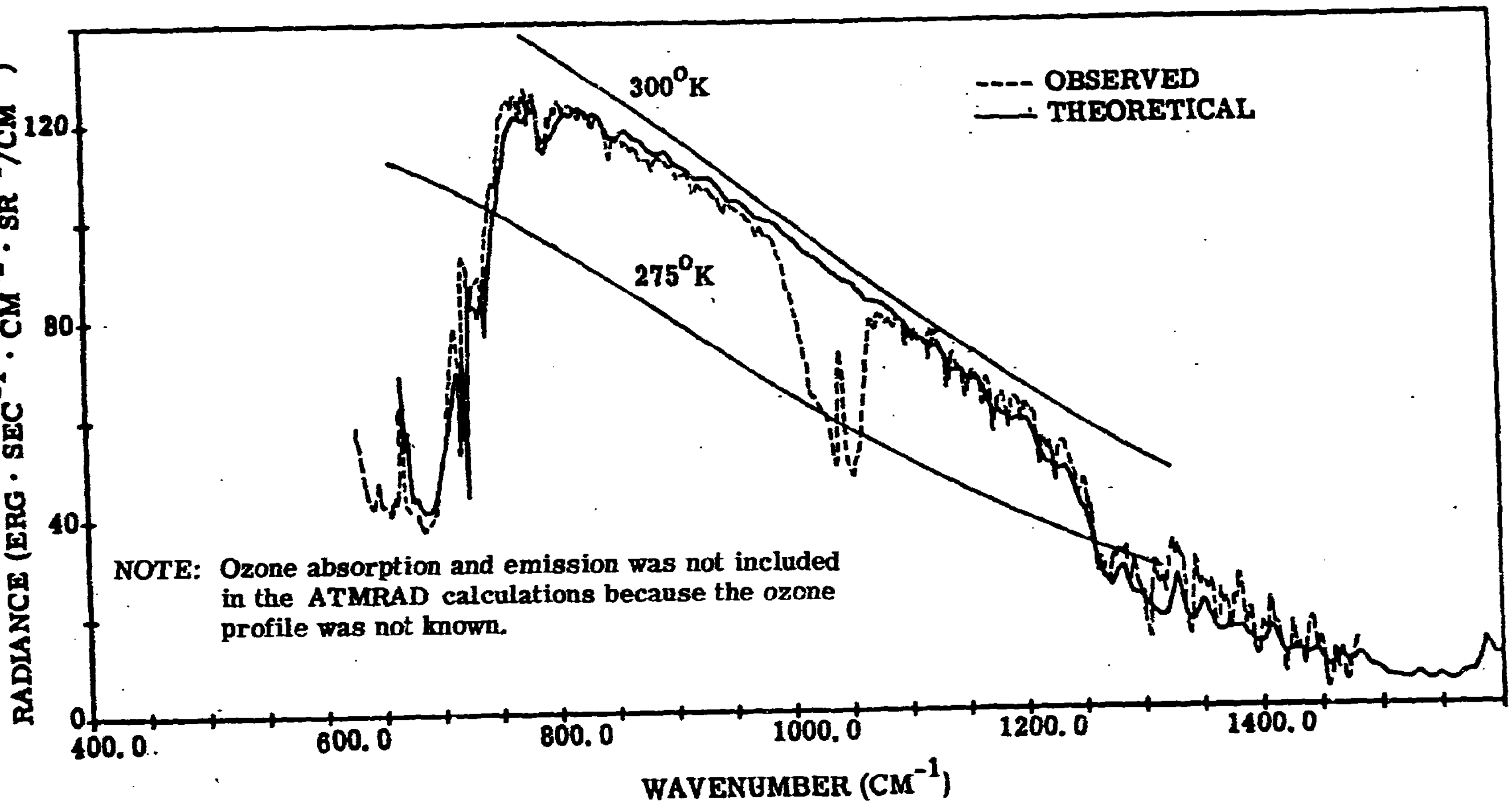

20. Comparison of ATMRAD and LOWTRAN Transmission Calculations

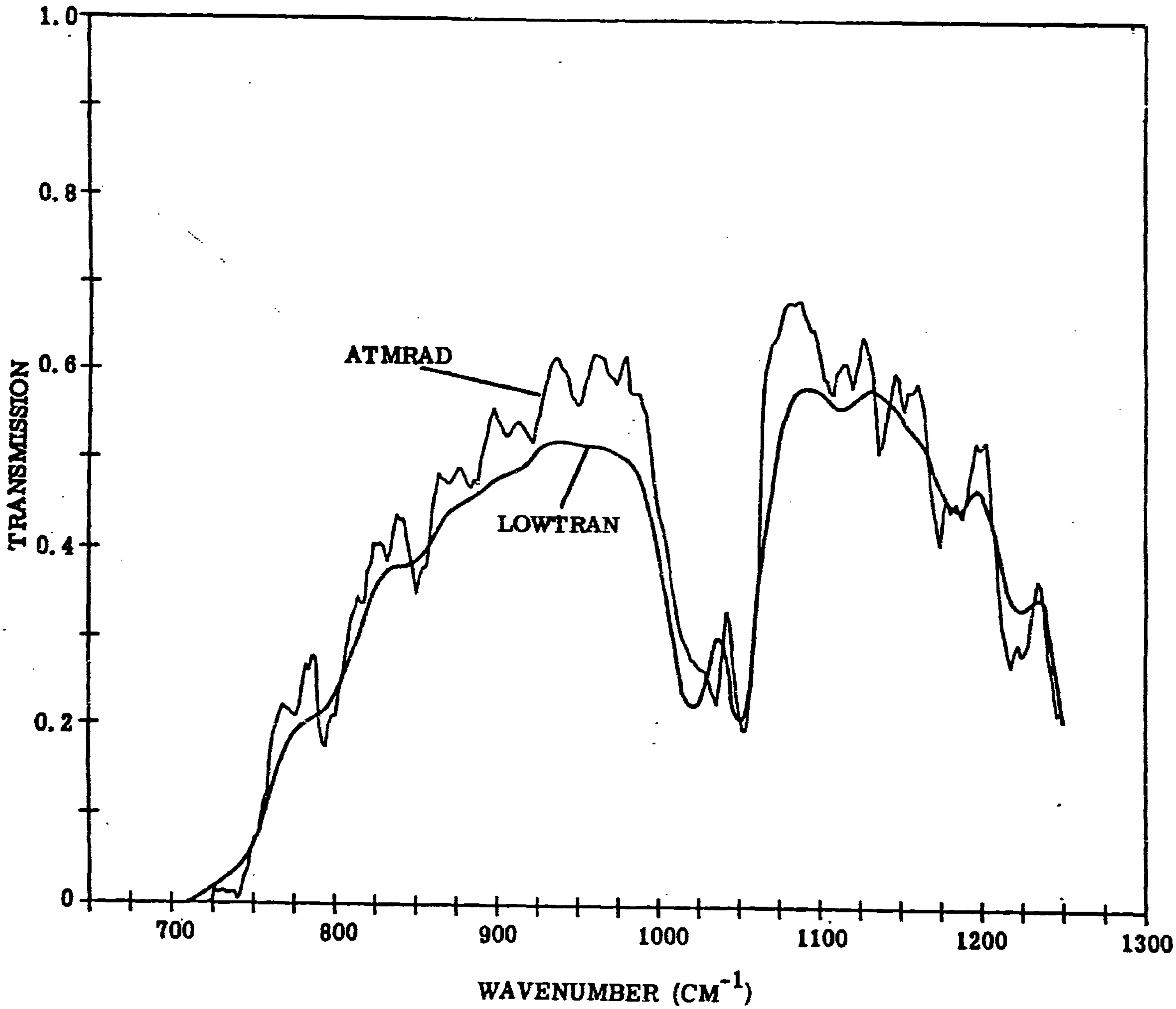

21. Summary of H_2O Continuum Knowledge

- LACK OF UNDERSTANDING OF H_2O CONTINUUM ABSORPTION.
- SELF-INDUCED ABSORPTION IS KNOWN TO AN ACCURACY OF APPROXIMATELY 20 PERCENT FOR $\lambda \geq 8.0\,\mu m$. FOR SHORTER WAVELENGTHS ACCURACY IS CONSIDERABLY WORSE BECAUSE OF SPARSITY OF DATA.
- FOREIGN-INDUCED ABSORPTION COEFFICIENT IS KNOWN TO WITHIN ABOUT A FACTOR OF 2.
- LACK OF INFORMATION NECESSARY TO DEFINE ACCURATELY THE TEMPERATURE DEPENDENCE OF CONTINUUM.
- LACK OF DATA FOR H_2O PARTIAL PRESSURES GREATER THAN APPROXIMATELY 75 PERCENT OF THE SATURATION VAPOR PRESSURES.

ATMOSPHERIC AEROSOLS: MODELS OF THEIR OPTICAL PROPERTIES

Eric P. Shettle
Robert W. Fenn
Frederic E. Volz

Air Force Cambridge Research Laboratories (AFSC)
Hanscom Air Force Base, Massachusetts

ATMOSPHERIC AEROSOLS: MODELS OF THEIR OPTICAL PROPERTIES

Eric P. Shettle, Robert W. Fenn and Frederic E. Volz

AFCRL

In previous AFCRL reports (Elterman 1964, 1968, and 1970, McClatchey a.o. 1970) atmospheric models have been presented which can be used to derive the transmission of visible and infrared radiation along a given path through the atmosphere. The models developed by Elterman consider atmospheric light attenuation due to scattering by aerosol particles and air molecules and absorption by ozone molecules. IR transmission calculations in these models, therefore, were limited to a few wavelength values in watervapor windows where it was assumed that molecular absorption is negligible. The models developed by McClatchey and others included the absorption by all major molecular constituents in the atmosphere in addition to aerosol scattering and absorption.

The aerosol component in these models was based on experimental measurements which were made during and prior to the mid 1960's. At this time there was sufficient experimental data available to define an average stratospheric and upper tropospheric aerosol profile with some different haze concentrations in the lower troposphere (up to a few km altitude) with exponential vertical decrease in particle concentration.

The vertical distribution of aerosol attenuation in the upper troposphere and stratosphere in these models was primarily based on several years of searchlight measurements in a fixed location (Elterman 1966, and 1968; also Elterman et al. 1969). Ivlev (1967 and 1969) has made

a review of the available experimental data up through 1967. Based on this review Ivlev presented a model of the vertical distribution of aerosol particles and their extinction of visible light. Ivlev's model is similar to Elterman's (1968, 1970), which also forms the basis for aerosol models used by McClatchey et al. (1970), up to a height of about 30 km. Above this height Ivlev's model diverges rapidly becoming several orders of magnitude larger than the model of McClatchey et al. (1970).

During the past decade in this country and elsewhere extensive additional measurements from ground as well as airborne and space platforms have been made of aerosol concentrations, their size distribution, and optical properties, to warrant the development of updated aerosol models which also describe some of the temporal and spatial variations in atmospheric aerosol distributions and properties.

One result of particular significance from these recent measurements is that the stratospheric aerosol concentration during the middle and late 1960's was still above normal background levels (see Elterman et al., 1973; Fox et al., 1973; Hofmann et al., 1974; and Russell et al., 1974), due to a residual of the aerosols injected into the stratosphere by the eruption of Mt. Agung during the spring of 1963. It was measurements made during this time period of elevated aerosol concentration which served as the major input to Elterman's and Ivlev's models.

In this study a number of different aerosol models for each of 4 different altitude regimes has been developed. The vertical distribution of the attenuation coefficients for these models is shown in Fig. 1.

(1) For the Boundary Layer (below 2 km) 10 models have been defined which describe rural and urban environments as well as the maritime sea

aerosol, for several surface visibilities between 2 and 50 km.

(ii) For the upper troposphere there are two models which represent spring and summer conditions versus fall and winter conditions.

(iii) In the stratosphere (up to 30 km) models are presented for background, moderate and high volcanic conditions for each of the two seasonal models. The vertical distribution for the moderate volcanic models for both seasons is essentially that of Elterman's model.

(iv) For the upper atmosphere (above 30 km) two models are being used: One of these corresponds to the most likely background conditions and the other represents the high aerosol concentrations which may be observed at times in shallow layers at various altitudes and which can be of significance for long horizontal propagation paths.

The vertical aerosol concentration profiles and the size distribution are described by analytic functions.

The data will be presented so that any model for one region can be used with any of the models in a different altitude regime. So in effect it is possible to compose 100 different combinations of aerosol models, covering the altitudes between 0 and 100 km.

For each of these models the coefficients of extinction and scattering as a function of altitude will be presented for 20 wavelength values between 0.25 and 40μm, including 11 laser wavelengths (Fig. 2). For each of the aerosol components, composing the various models, the coefficients for extinction, scattering, absorption, the particle albedo and the scattering asymmetry coefficient will be presented as a function of wavelength. The angular scattering function will be shown for each model for a few significant wavelength values.

These aerosol models and their optical parameters are being published in a format similar to that of the AFCRL Report: Optical Properties of the Atmosphere, by McClatchey et al. (1970) to allow for transmittance calculations including molecular absorption and aerosol attenuation. The optical properties of these models will be compiled into a computer program subroutine suitable for use with the LOWTRAN program (Selby & McClatchey, 1972) for more detailed calculations. The report on these new models will also present a discussion of the aerosol models and of the experimental data foundation for them, and it will give guidelines for the selection of the proper model for a specific environmental condition.

These atmospheric optical models in their present form do not give any information with regard to the probability of occurrence of any particular condition. Yet such information is frequently needed by the users of such models.

For lack of better data, one is presently forced to resort to statistical data on surface visibility and humidity distributions. However, these parameters are not adequate to derive or predict slant path visibility, spectral contrast reduction, IR transmission or other complex quantities. An improvement of this situation can only come from measurements which are directed towards obtaining statistical data on some of the basic atmospheric optical/IR properties, and which can be used to derive correlations between these specific optical quantities and the more routinely observed atmospheric parameters.

A measurement program which has these objectives is presently being implemented under a NATO Research Study Group effort in western Europe. Under this measurement program of the Optical Atmospheric Quantities in Europe (OPAQUE) a network of at least 6 stations will be set up to measure on an hourly basis 24 hours a day a minimum sot of visible and IR atmospheric parameters (Fig. 3). Some stations will also record some additional properties such as angular light scattering functions, aerosol content, IR sky and terrain radiance. These stations will be instrumented jointly by several NATO countries (Fig. 4) and located in various regions of western Europe. The measurements are scheduled to start in fall 1975 and continue for a 2-year period.

REFERENCES

Elterman, L. (1964): "Atmospheric Attenuation Model, 1964, in the Ultraviolet, Visible, and Infrared Regions for Altitudes to 50 km;" Tech. Report AFCRL-64-740 (Sept 1964).

Elterman, L. (1966): "An Atlas of Aerosol Attenuation and Extinction Profiles for the Troposphere and Stratosphere;" Tech. Report AFCRL-66-828 (Dec. 1966).

Elterman, L. (1968): "UV, Visible, and IR Attenuation for Altitudes to 50 km, 1968;" Tech. Report AFCRL-68-0153 (April 1968).

Elterman, L. (1970): "Vertical Attenuation Model with Eight Surface Meteorological Ranges 2 to 13 Kilometers;" Tech. Report AFCRL-70-0200 (March 1970).

Elterman, L., R. Wexler, and D.T. Chang (1969): "Features of Tropospheric and Stratospheric Dust;" J. Applied Optics, 8 (No. 5), 1969.

Elterman, L., R.B. Toolin, and J.D. Essex (1973): "Stratospheric Aerosol Measurements with Implications for Global Climate;" Applied Optics, 12, 330-337.

Fox, R.J., G.W. Grams, B.G. Schuster, and J.A. Weinman (1973): "Measurements of Stratospheric Aerosols by Airborne Laser Radar;" J. Geophys. Research, 78, 7789-7801.

Hofmann, D.J., J.M. Rosen, and T.J. Pepin (1974): "Global Measurements of the Time Variations and Morphology of the Stratospheric Aerosol;" Proceedings of the Third Conference on the Climatic Impact Assessment Program: Feb. 26 - Mar. 1, 1974. Ed. by A. J. Broderick and T.M. Hard (DOT-TSC-OST-74-15).

Ivlev, L.S. (1967): "Aerosol Model of the Atmosphere;" Prob. Fiz. Atmos., No. 7, Leningrad, pp. 125-160, translated by Foreign Science and

Technology Center, Dept. of the Army, available from U.S. National Technical Information Service (AD 760-393).

Ivlev, L.S. (1969): "Atmospheric Aerosol;" pp. 28-42 in Radiation Characteristics of the Atmosphere and the Earth's Surface, Ed. K. Ya Kondratev, Amerind Publishing Co., New Delhi, available from U.S. National Technical Information Service (No. TT-71-58003).

McClatchey, R., R. Fenn, J. Selby, F. Volz, and J. Garing (1970): "Optical Properties of the Atmosphere;" Tech. Report AFCRL-70-0527, (1970). Also follow-on editions AFCRL-71-0279 and AFCRL-72-0497.

Russell, P.B., W. Viezee, R.D. Hake (1974): "Lidar Measurements of Stratospheric Aerosols over Menlo Park, California, Oct 1972-March 1974;" Final Report, June 1974, under Contract NAS2-7261.

Selby, J.E.A., and R.M. McClatchey (1972): "Atmospheric Transmittance from 0.25 to 28.5μm: Computer Code LOWTRAN 2;" Tech. Report AFCRL-72-0745 (29 Dec 72).

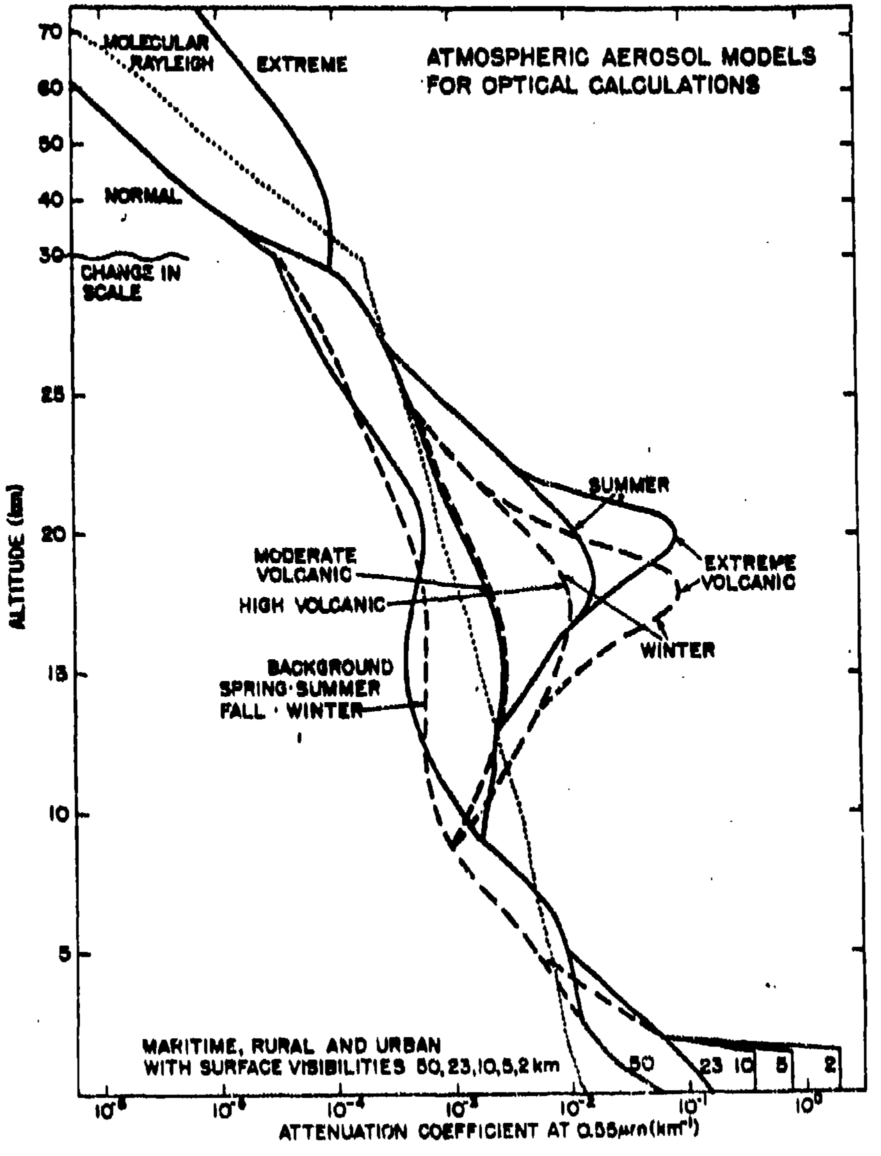

ATMOSPHERIC AEROSOL MODELS
FOR OPTICAL CALCULATIONS
MOLECULAR
RAYLEIGH
EXTREME
NORMAL
CHANGE IN
SCALE
SUMMER
EXTREME
VOLCANIC
MODERATE
VOLCANIC
HIGH VOLCANIC
WINTER
BACKGROUND
SPRING·SUMMER
FALL · WINTER
MARITIME, RURAL AND URBAN
WITH SURFACE VISIBILITIES 50,23,10,5,2 km
50
23
10
5
2
ALTITUDE (km)
70
60
50
40
30
25
20
15
10
5
ATTENUATION COEFFICIENT AT 0.55μm (km⁻¹)

DATA PRESENTATION

MODEL OPTICAL PROPERTIES

20 Tables, 1 for each of 20 Wavelengths

λ 1, 2 . . . 20

	Model 1			Model 10	
H	σ_E	σ_S		σ_E	σ_S

6 Tables, One for each Aerosol Type

	σ_E	σ_S	σ_A	Albedo	Asym. Factor
λ					

Figures Normalized Scattering Functions

PARAMETERS MEASURED

VISIBLE PHOTOPIC EXTINCTION COEFFICIENT

IR - TRANSMITTANCE (3 - 5, 8 - 12 μm)

ILLUMINANCE ON HORIZONTAL AND VERTICAL SURFACE

TOTAL ATMOSPHERIC TURBIDITY

PATH RADIANCE IN 4 HORIZONTAL DIRECTIONS (DAY)

PATH RADIANCE TOWARDS EAST (NIGHT)

TURBULENCE STRUCTURE CONSTANT C_T

METEOROLOGICAL PARAMETERS

RAWINSONDE FLIGHTS

2 MEASUREMENTS (<5 MIN) EVERY HOUR

NATO COUNTRY COMMITMENTS

AS OF 15 MAY 1974

CANADA DENMARK:	JOINT STATION IN BALTIC SEA
GERMANY:	STATION IN SW-GERMANY, 2ND STATION UNDER DISCUSSION
NETHERLANDS:	STATION NEAR THE HAGUE
UNITED KINGDOM:	STATION AT SRDE, DATA BANK
USA:	STATION AT MEPPEN OPERATED BY GERMANY
ITALY:	PLANNING A STATION ON SARDINIA
FRANCE:	PLANNING A STATION IN NW-FRANCE
NORWAY:	OFFER TO OPERATE A STATION
BELGIUM:	PROVIDE LIMITED INSTRUMENTATION

MODELING THE EFFECTS OF AEROSOLS ON OPTICAL SYSTEMS

R. E. Bird

Advanced Systems Division
Fuze Department
Naval Weapon Center
China Lake, California

ABSTRACT

This report describes computer models which have been developed to determine the effects of atmospheric constituents on optical sensor systems and used primarily to model the effects of aerosols, such as clouds, fogs, and smokes. Models which calculate response to only single-order scattering are described, and sample results obtained by applying these models are presented. A more sophisticated model which uses Monte Carlo techniques is also described. This latter model possesses the capability of modeling a plane-parallel atmosphere of up to 100 layers containing both aerosol and molecular constituents.

INTRODUCTION

Several computer models have been developed at NWC and have been used extensively to model the effects of aerosols (clouds, fogs and smokes) on various active optical sensor systems. The investigation has three major goals:

1. To develop viable methods of discriminating between aerosol and target reflections.

2. To develop computer models that characterize sensor system performance.

3. To perform design-optimization studies of sensor systems.

All of these have been accomplished to some extent; however, work is continuing on the development of better techniques for discriminating between aerosol and target backscatter.

The purpose of this report is to explain the utility and applications of these modeling techniques. Illustrations of typical results are presented and suggestions for other areas of application are put forward.

The rationale for performing theoretical analysis of this nature is that optical system designers must determine the effects of aerosols on most optical systems. Experimental data collected in natural environments are difficult and expensive to obtain. On the other hand, theoretical models provide information rapidly and are inexpensive to exercise. Use of modeling capabilities allows the optical designer first to perform a design optimization and then to collect experimental data as needed at a much lower cost.

Figure 1 illustrates the aerosol problem for a generic optical sensor system. The target signal is attenuated by the aerosol, and backscatter from the aerosol produces clutter and false alarms. Figure 2 illustrates the aerosol problem in communications systems. Here, the aerosol attenuates the desired signal and also distorts the modulation content of the signal. Other systems investigations where aerosol modeling techniques might be applicable include active and semiactive seekers, target designators, range finders, landing systems, use of smoke screens as countermeasures, and laser detection systems.

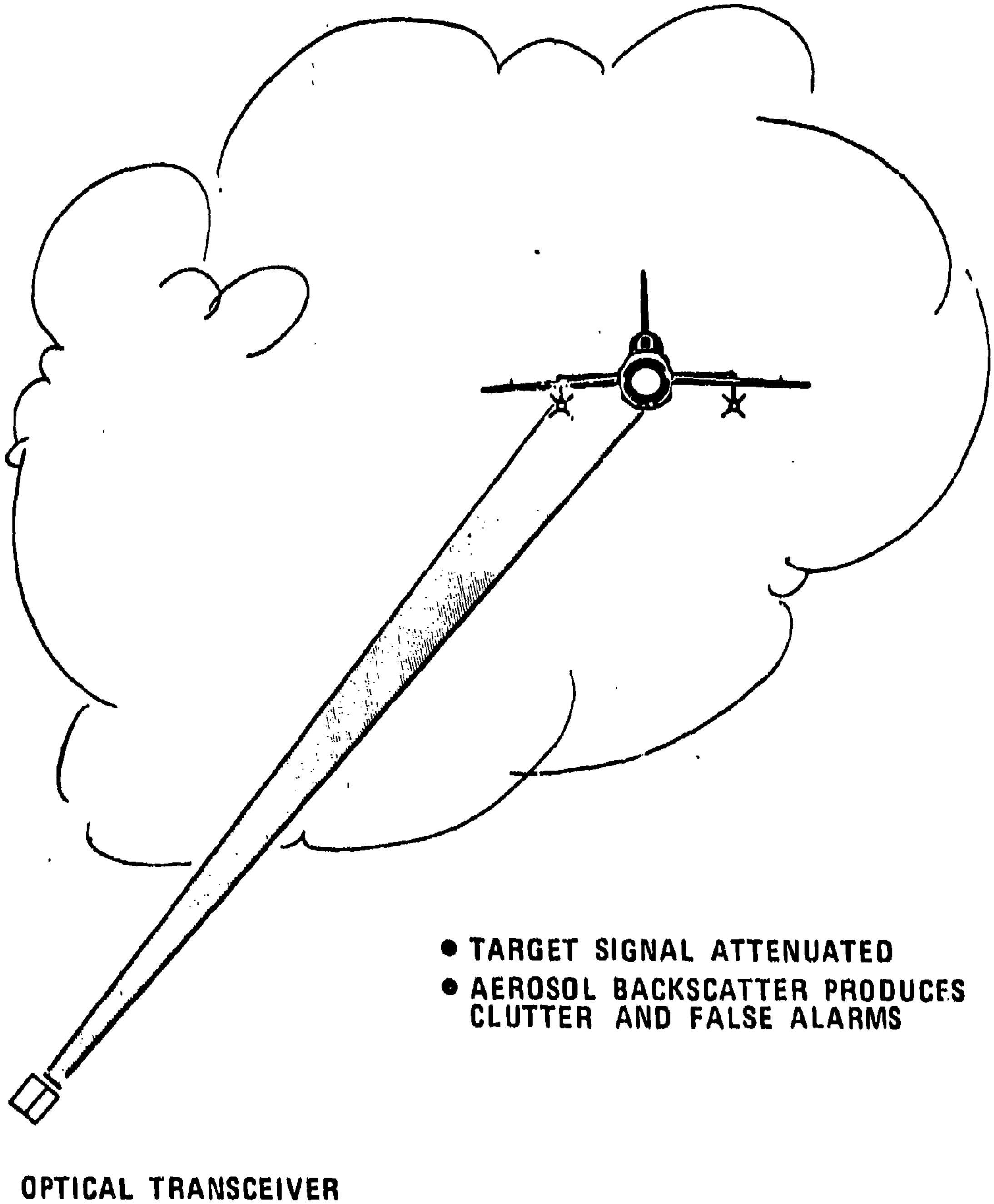

FIGURE 1. Aerosol Problem for Optical Radar.

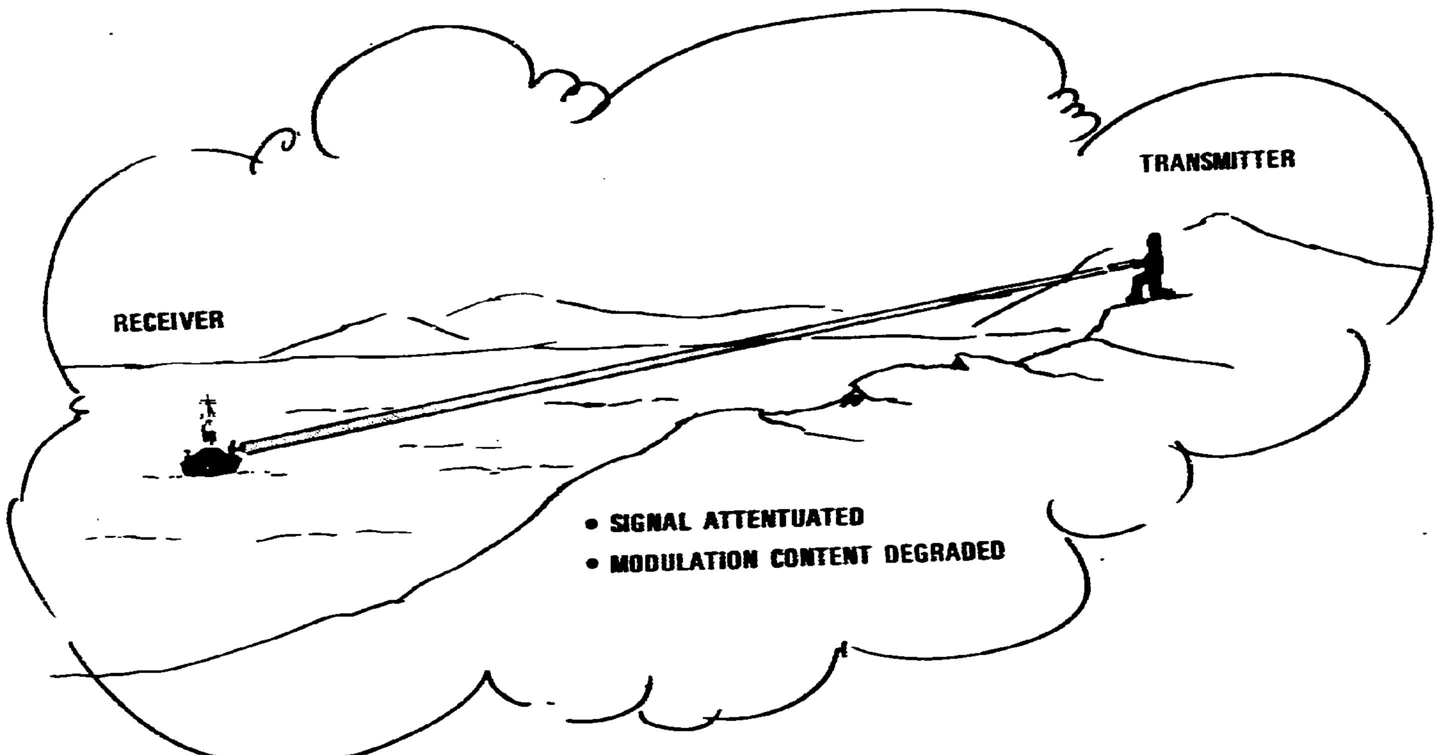

FIGURE 2. Aerosol Problem in Communications.

SINGLE SCATTERING MODEL

The first type of model discussed is one that calculates only first-order scattering from homogeneous aerosol clouds.[1] This model uses Mie light scattering theory to calculate the intensity of light scattered from spherically shaped particles. The particle-size distribution and the complex index of refraction of the scattering medium are required for use of this model. With a particular beam geometry defined, this model will calculate the extinction of a target signal due to the aerosol, and the intensity of the light scattered from the aerosol itself. These calculations can be performed at any desired discrete wavelength and for various types of aerosols. Figures 3 and 4 illustrate the capability for calculating the extinction coefficient and the backscatter phase function at several wavelengths in the visible and infrared regions. These calculations were performed using a Deirmendjian Model C_1, fair weather cumulus cloud particle-size distribution.[2] The extinction coefficient is fairly constant at all wavelengths, but the backscatter phase function has several deep minima that are very significant. To illustrate the effect of these minima, the beam geometry illustrated in Figure 5 was modeled at wavelengths of 0.905, 3.0, and 10.5 micrometers. The system is immersed in the fair weather cumulus cloud, and a 100-nanosecond square pulse is emitted. The cloud and target returns are shown in Figures 6 through 8, as the leading edge of the pulse moves out in range. This corresponds to target returns from all ranges from zero to 45 feet, and cloud return from the depth of the cloud penetrated by the leading edge of the pulse. A comparison of these results reveals that the cloud backscatter is approximately a factor of 40 lower at 3.0 micrometers than at 0.905 micrometer and a factor of 25 lower at 10.5 micrometers than at 0.905 micrometer. However, the transmission of the target signal is approximately a factor of 2.5 larger at 10.5 micrometers than at the other two wavelengths, which results in an additional improvement in the target/cloud backscatter ratio at 10.5 micrometers.

The effect of modeling different particle-size distributions is shown in Figure 9. Deirmendjian size distributions[1] are used in these calculations to represent a sea fog in various stages of development. The mode radius is the radius at which the greatest number of particles are concentrated. Five size distributions with five different mode

---

[1]Naval Weapons Center. *Analytical Models for the Design of Lidar Systems* (U) by R. E. Bird. China Lake, Calif., NWC, October 1973. (NWC TP 5576, publication CONFIDENTIAL.)

[2]Deirmendjian, D. *Electromagnetic Scattering on Spherical Polydispersions*. New York, Elsevier, 1969. 290 pp.

radii have been used to generate these data. An interesting result is that the extinction coefficient becomes larger at a wavelength of 10.6 micrometers than that for a wavelength of 0.905 micrometer for size distributions, with their major concentration of particles with radius greater than 6 micrometers. However, the backscatter coefficient continues to improve at 10.6 micrometers relative to 0.905 micrometer as the particle size increases.

MULTIPLE SCATTERING MODEL

In some applications, multiple-order scattering can play a significant role. A computer model has been constructed that uses Monte Carlo techniques to calculate all orders of scattering that are of interest.[3] This technique traces photon trajectories through random scattering events with built-in efficiency techniques which greatly reduce the computer time required to produce a good statistical sample. An infinite plane-parallel atmosphere with up to 100 layers can be modeled. The aerosol and molecular content can be varied in each successive layer, and scattering and absorption due to both of these constituents can be calculated. The model can simulate conical, fan, and point-beam geometries with no restrictions on the beam orientation. The polarization state of the scattered light is calculated through the use of Stokes parameters. An illustration of these capabilities is shown in Figure 10. Figure 11 illustrates one possible profile for naturally occurring aerosols as a function of altitude; Figure 12 is a possible profile for ozone as a function of altitude. A good representation of these profiles as well as other atmospheric constituents can be modeled in this program.

Experimental data were taken under controlled conditions in a fog simulation facility for the purpose of checking the accuracy of this model. The results of this comparison are shown in Figures 13 and 14 for two different beam geometries. The Monte Carlo results agree very well with the experimental data in most situations.

Comparisons were also made between several second-order scattering theories and the Monte Carlo results. An example of a comparison with data generated at the University of Florida[4] is shown in Figure 15.

---

[3] Naval Weapons Center. *Calculations of Multiple-Scattering Effects on Active Optical Sensors in Cloud Environments* (U) by R. E. Bird. China Lake, Calif., NWC, August 1974. (NWC TP 5667, publication UNCLASSIFIED.)

[4] Anderson, R. C. and E. V. Browell. "First-and-Second-Order Backscattering from Clouds Illuminated by Finite Beams," APPL OPT, Vol. II (1972), pp. 1345-51.

The agreement is quite satisfactory for this particular comparison, but poorer agreement was obtained with other second-order scattering models.

One application where multiple scattering can have an important effect is in the shape of the return for a short-pulse system. Figure 16 illustrates the pulse shape calculated using the single scattering model and the Monte Carlo model for exiting a cloud. The returned pulse as a function of time is plotted for a 10-nanosecond square pulse for both models, and for a 15-nanosecond sine pulse for the multiple-scattering case. The effect of multiple scattering on both the leading and trailing edges of this pulse is readily apparent.

CONCLUSION

The computer models described here have proven extremely useful for optical design optimization studies and for modeling the effects of aerosols on optical systems under various conditions. These models are suitable for application to optical trackers, seekers, target designators, landing systems, communications systems, and laser detection systems.

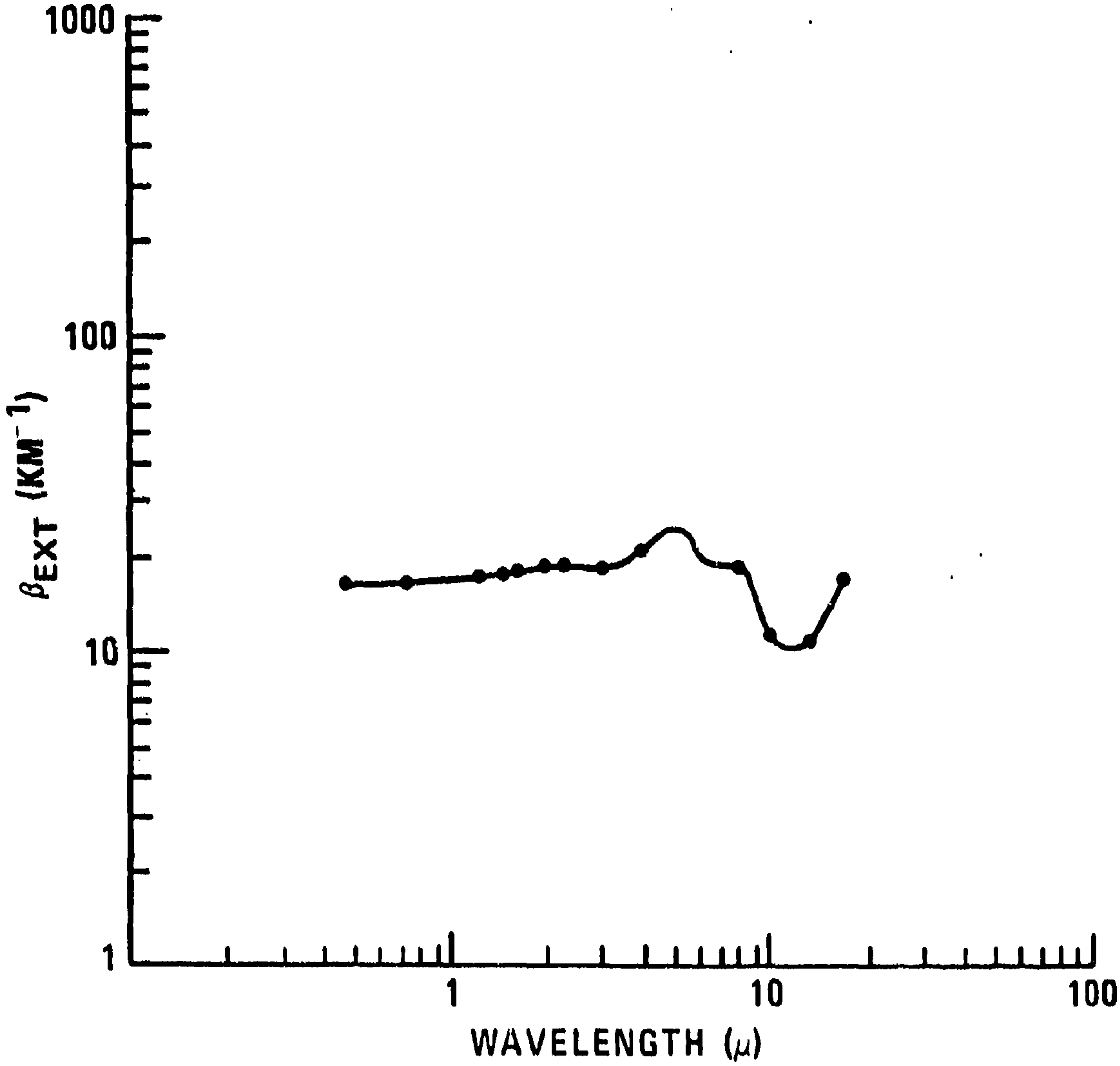

FIGURE 3. Calculated Extinction Coefficient for Model C_a Fair Weather Cumulus Cloud.

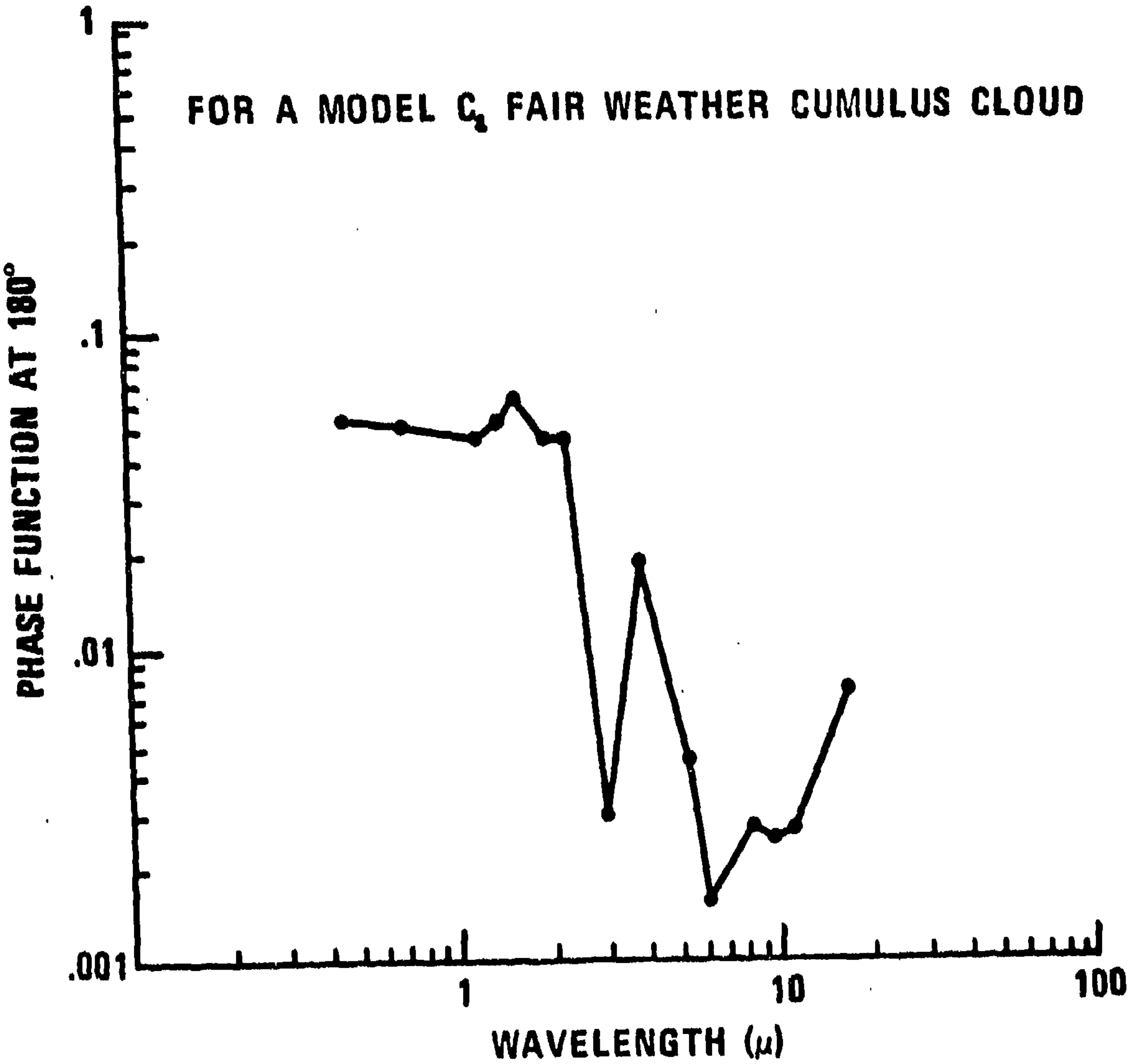

FIGURE 4. Calculated Ratio of Volume Backscatter Coefficient to Scattering Coefficient.

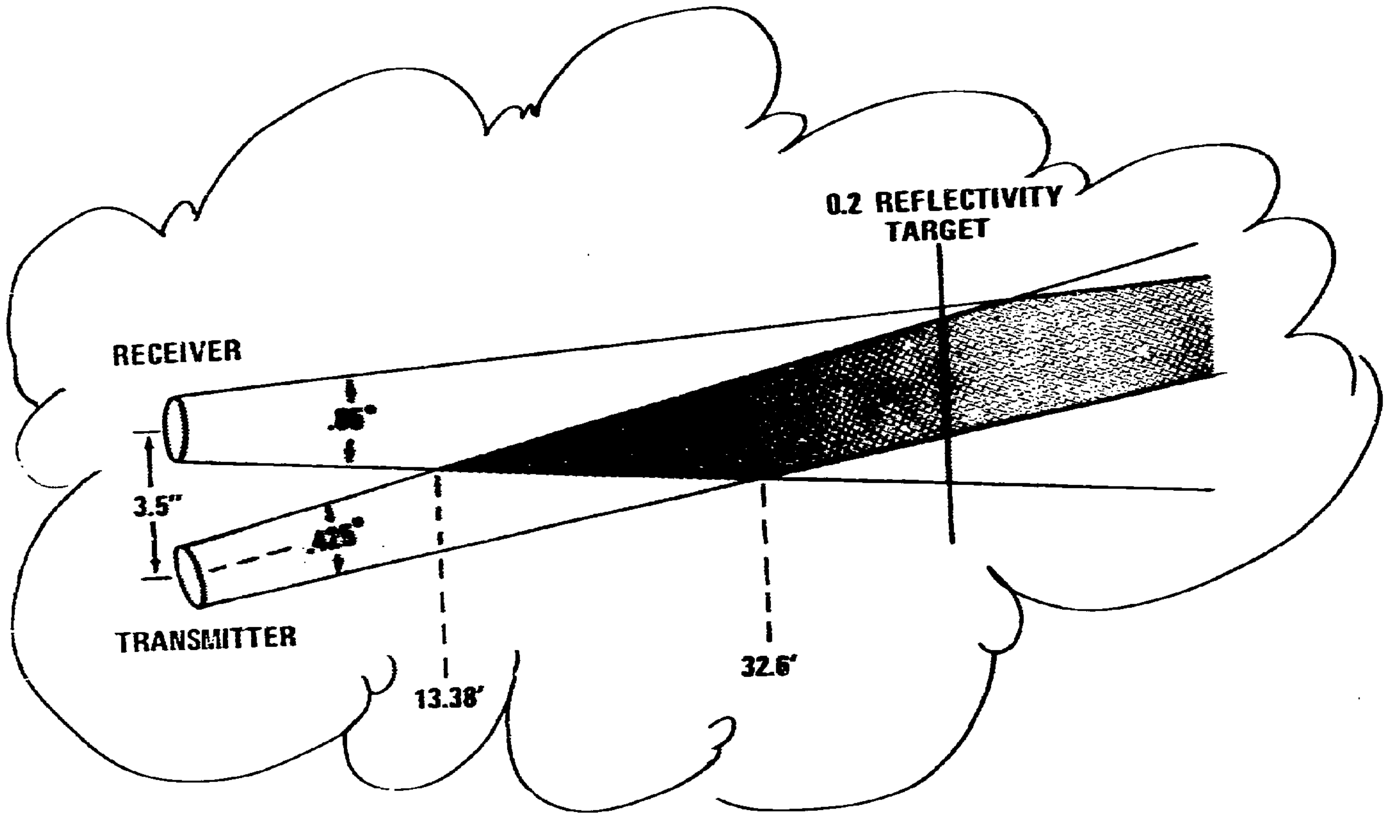

FIGURE 5. Sample Problem Geometry.

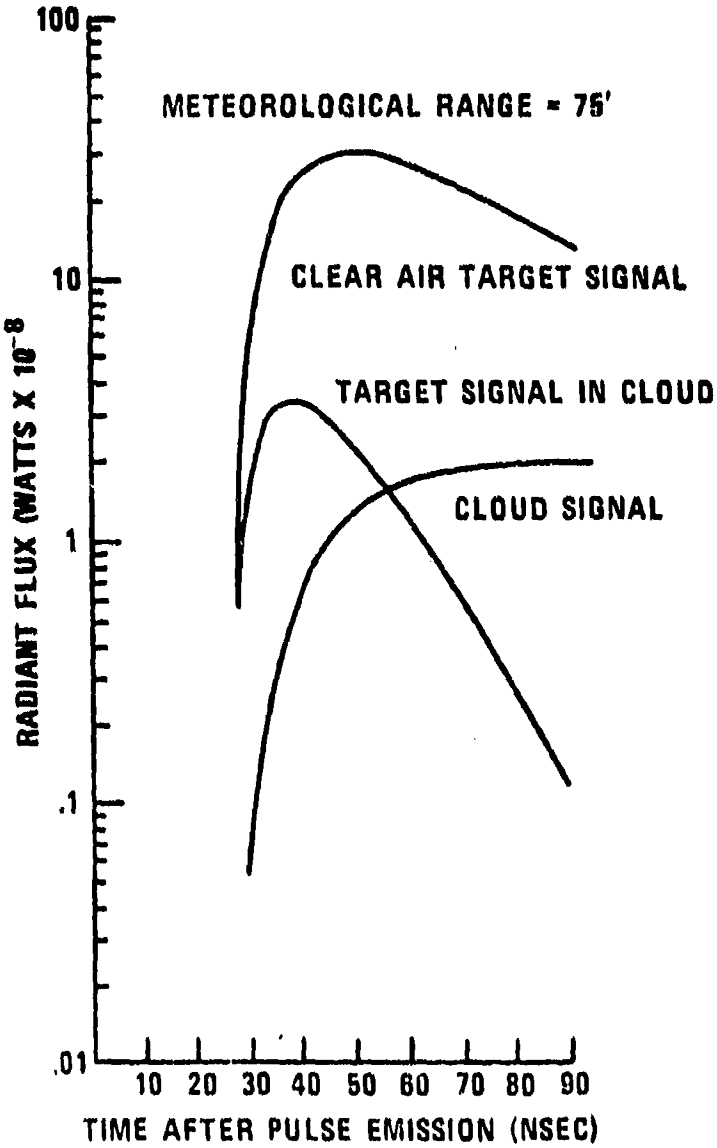

FIGURE 6. Target and Cloud Return for Pulsed 0.905-Micrometer Light with Optics Immersed.

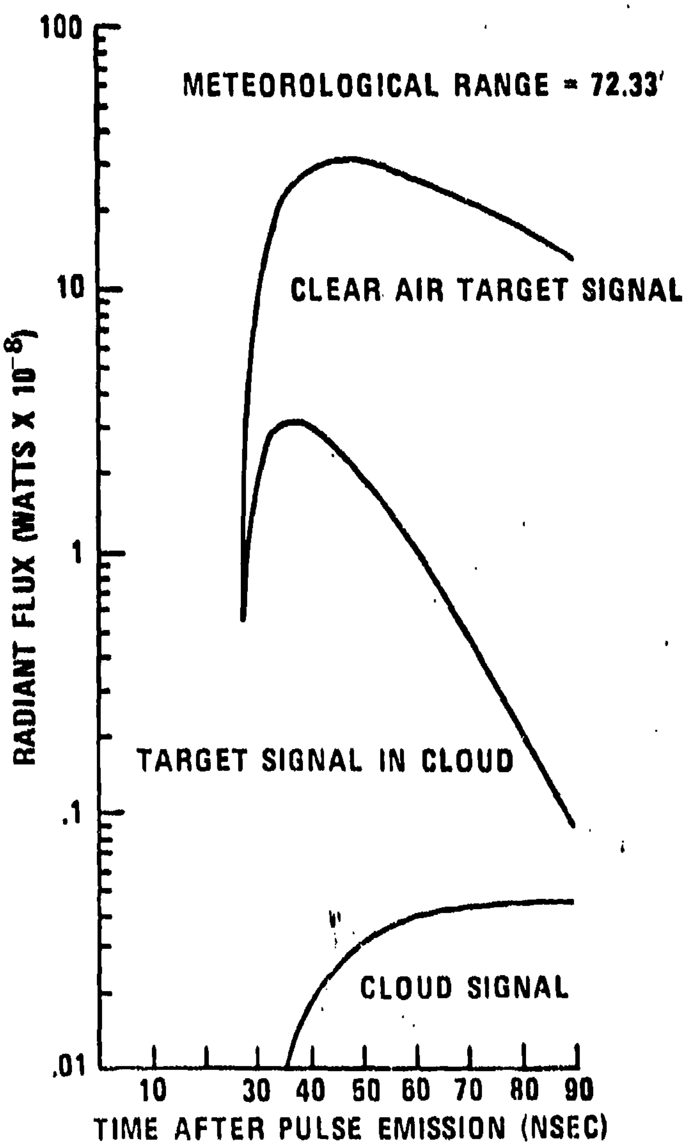

FIGURE 7. Target and Cloud Return for Pulsed 3.0-Micrometer Light with Optics Immersed.

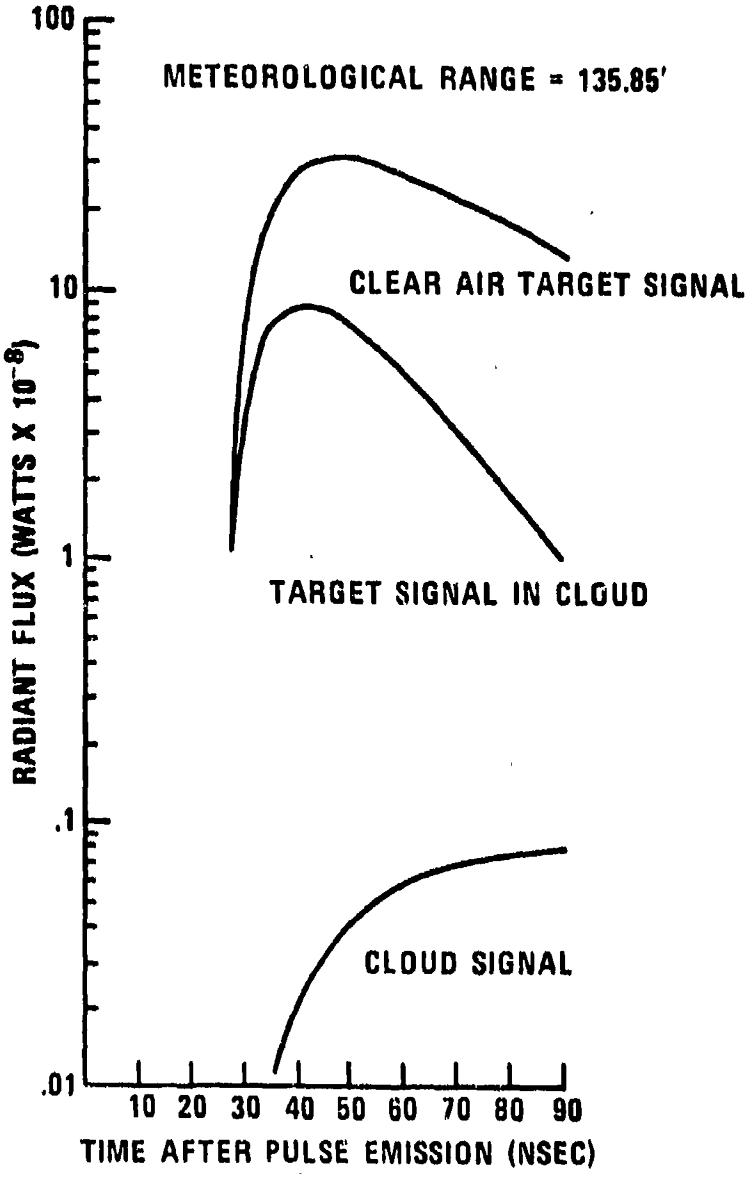

FIGURE 8. Target and Cloud Return for Pulsed 10.5-Micrometer Light with Optics Immersed.

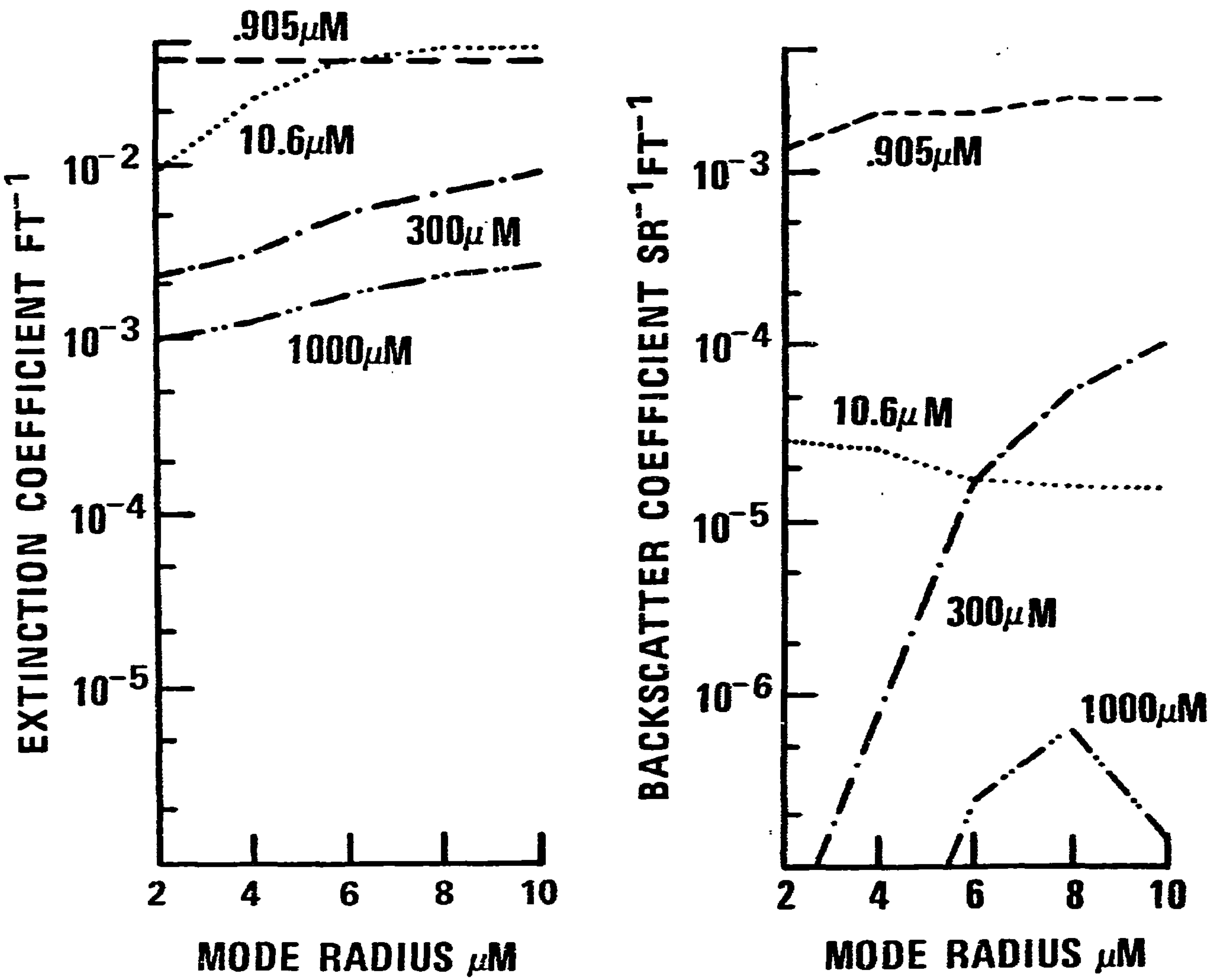

FIGURE 9. Fog Optical Extinction and Backscatter.

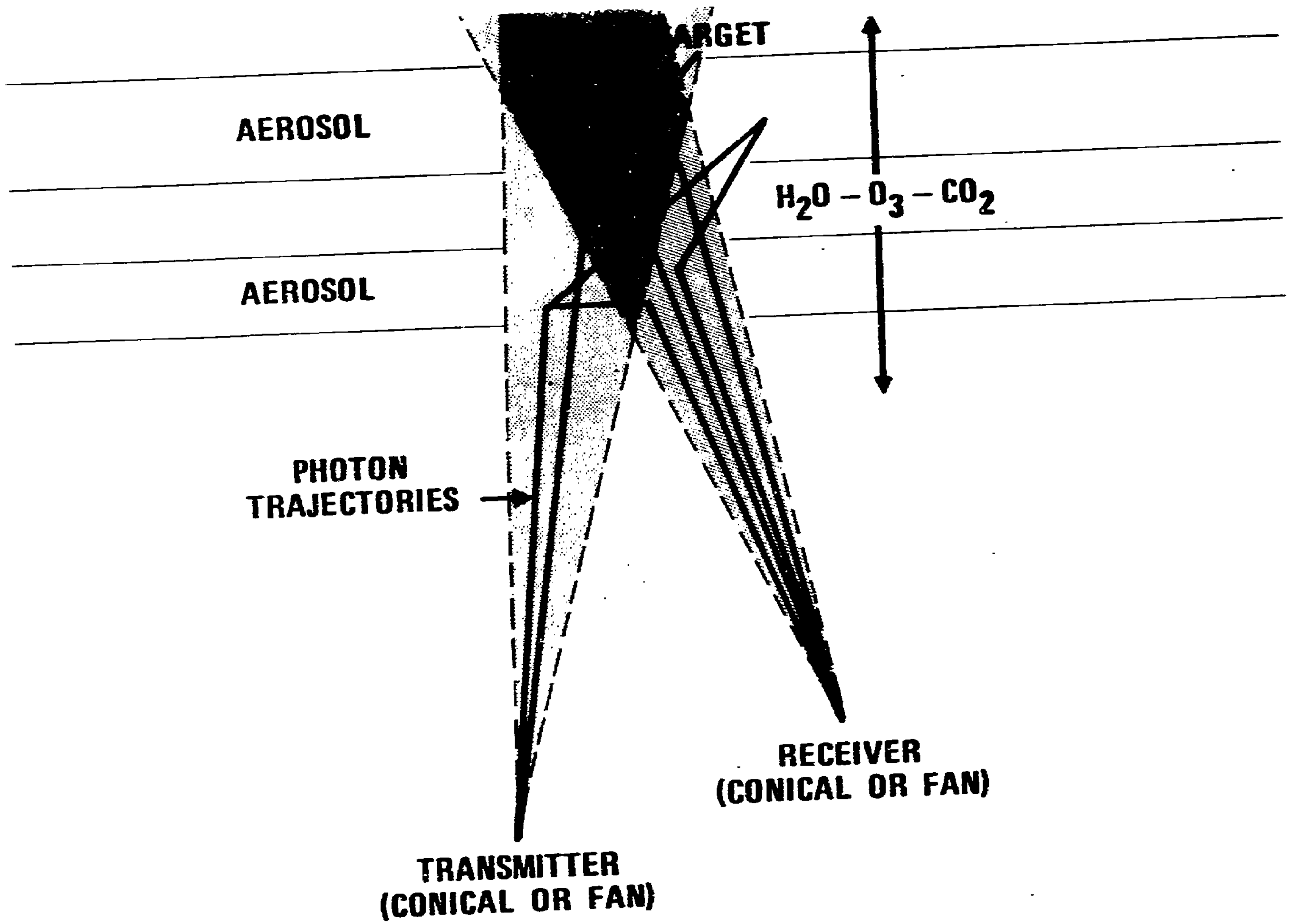

FIGURE 10. Multiple Scattering Analysis.

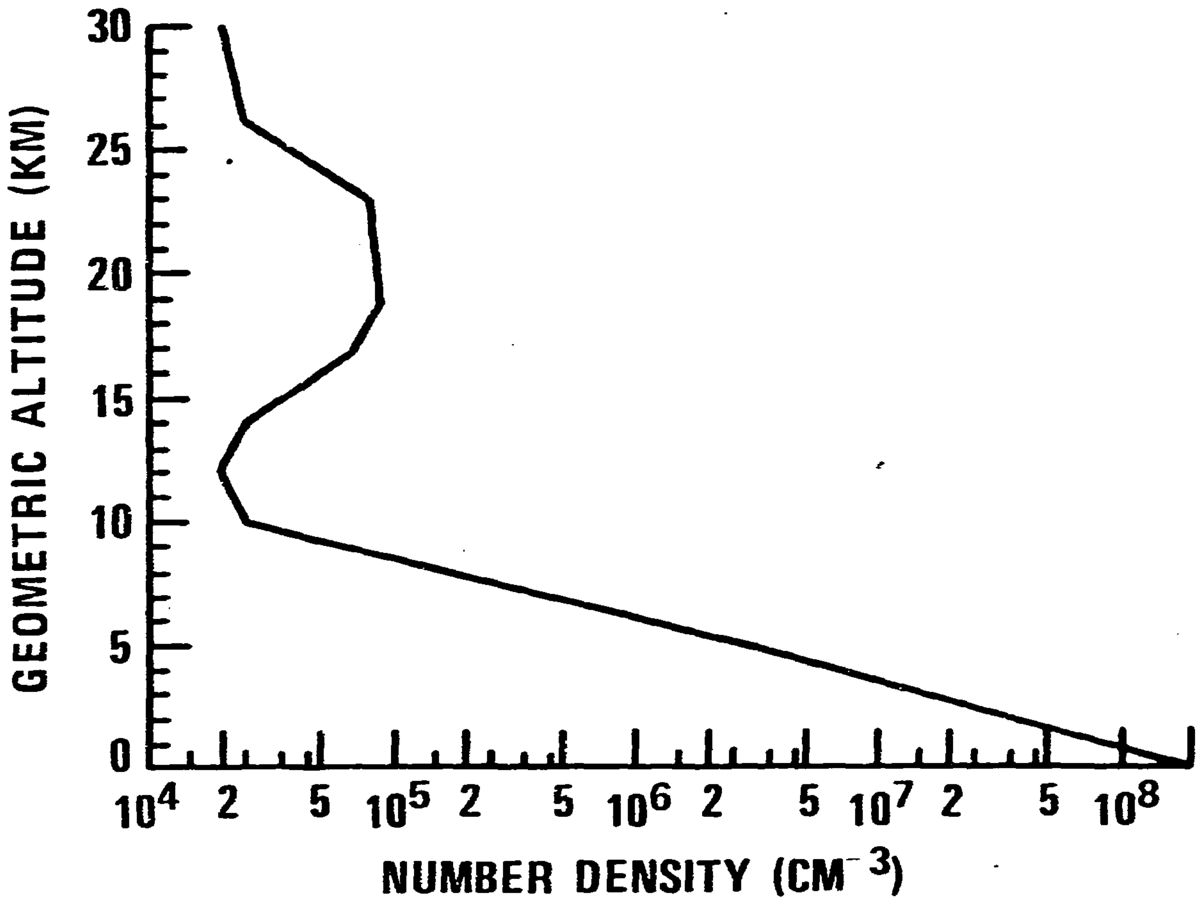

FIGURE 11. Aerosol Number Density Versus Altitude for the Atmospheric Attenuation Model.

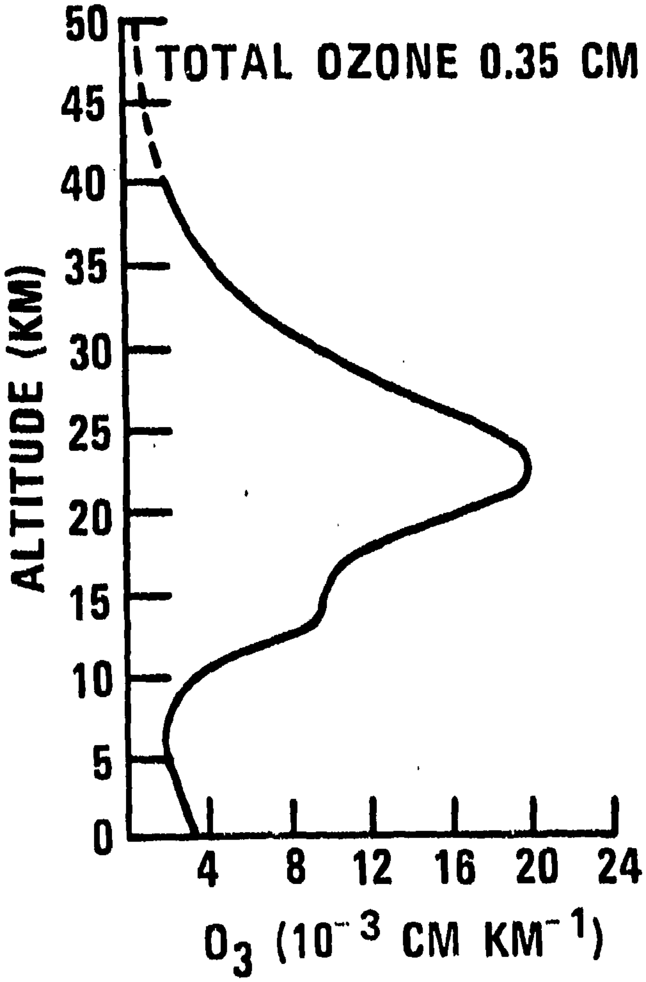

FIGURE 12. Ozone Concentration Versus Altitude for Atmospheric Model.

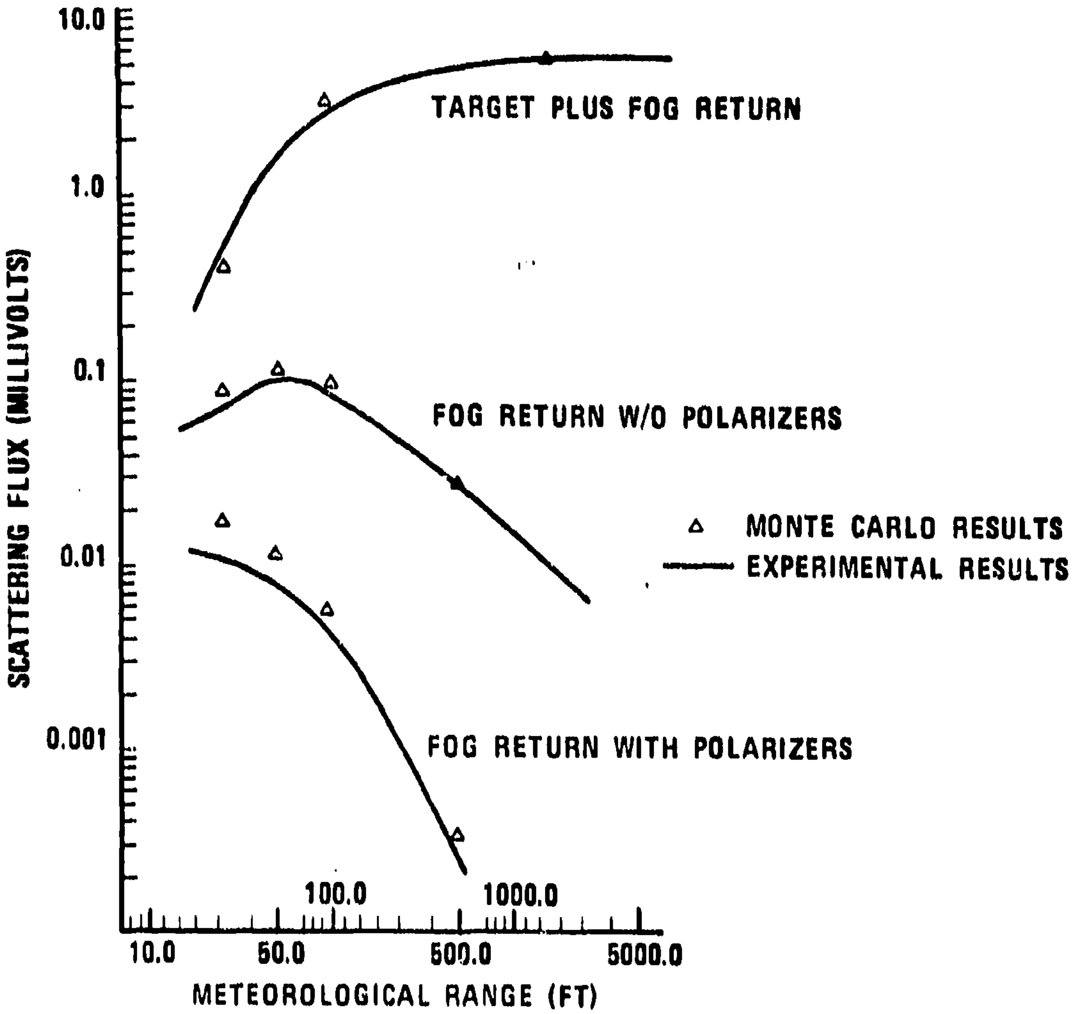

FIGURE 13. Target and Fog Return Signal Versus Meteorological Range Through 18 Feet of Fog for 2-Degree Source and 2-Degree Receiver.

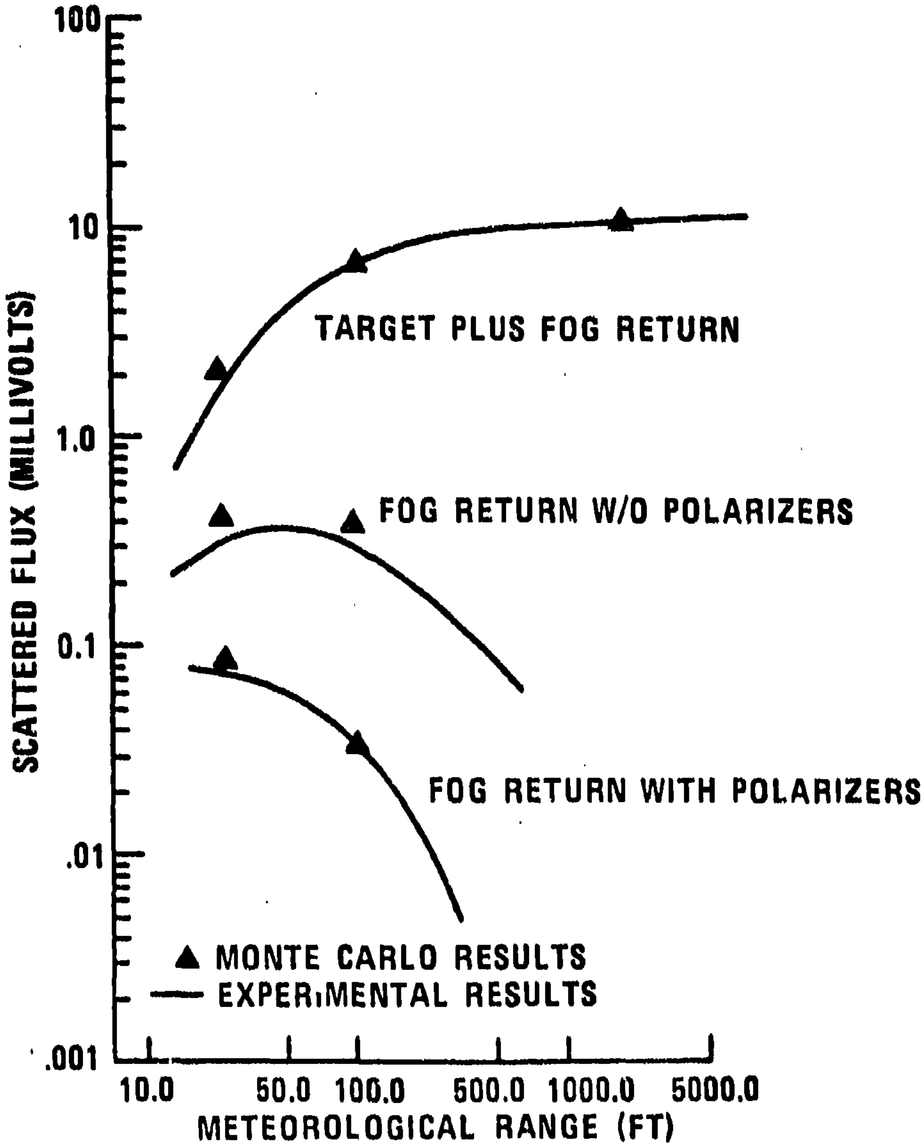

FIGURE 14. Target and Fog Return Signal Versus Meteorological Range Through 18 Feet of Fog for 2-Degree Source and 4-Degree Receiver.

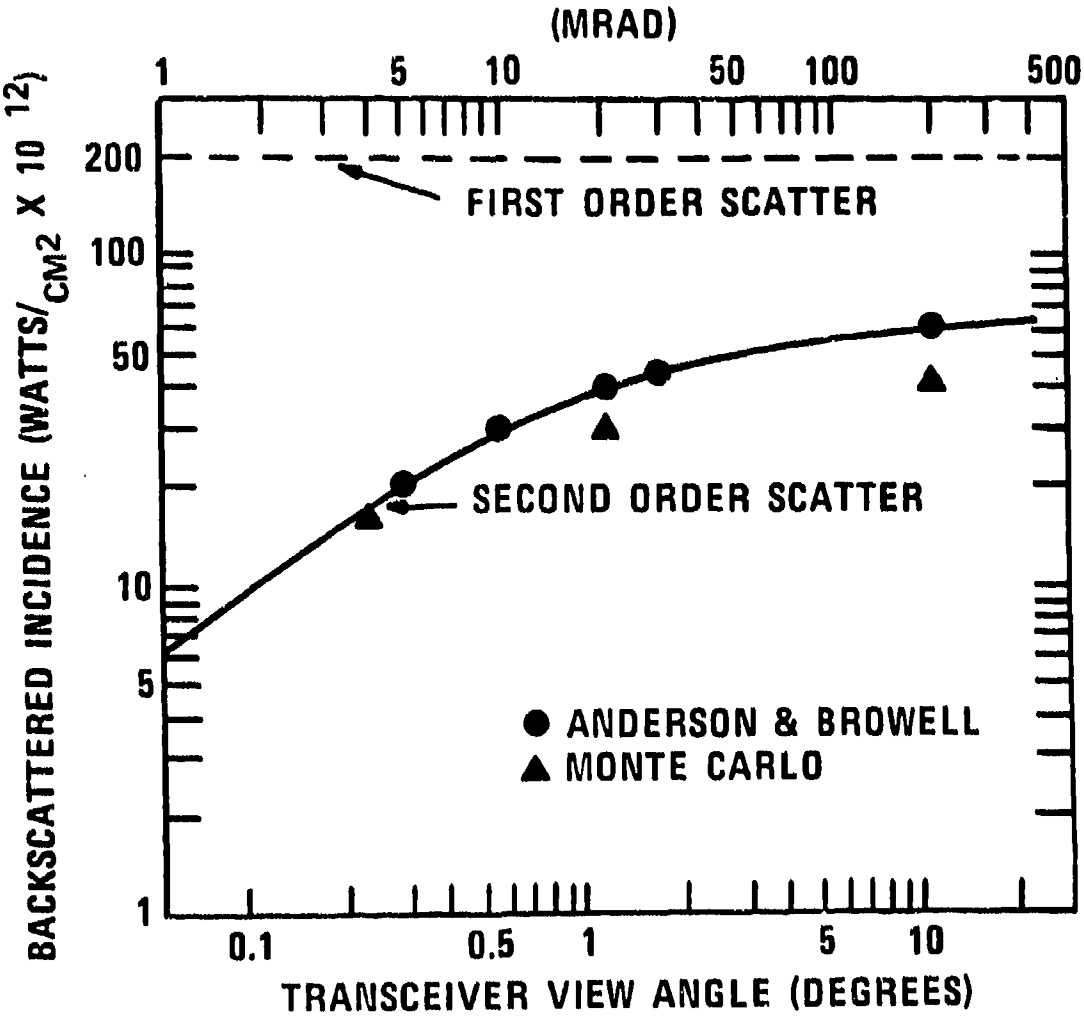

FIGURE 15. Comparison Between Second-Order Scatter and Monte Carlo.

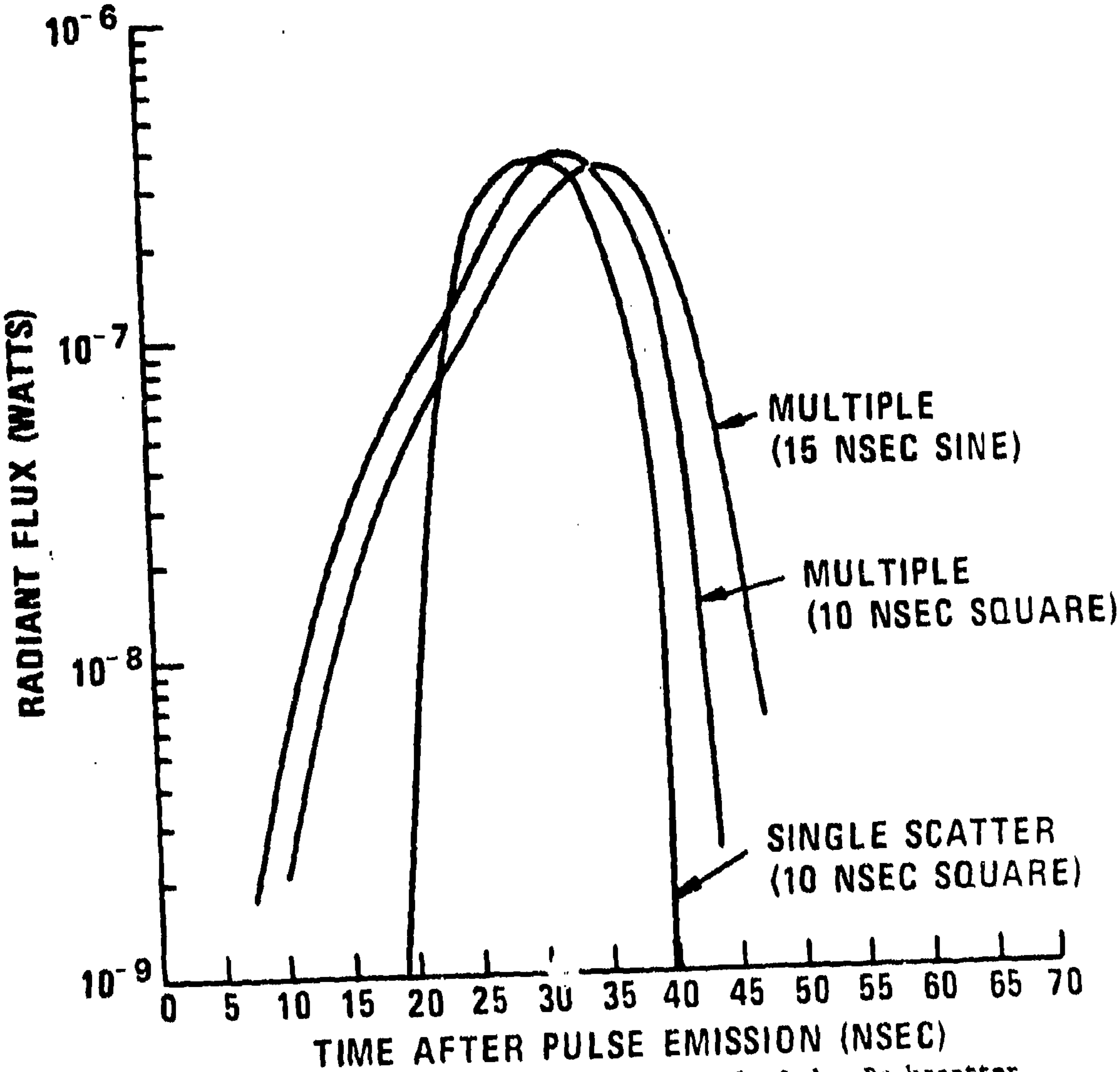

FIGURE 16. Pulse Stretching Due to Multiple Order Backscatter for System Immersed in Cloud, and Cloud 15 Feet Deep.

REFERENCES

1. Naval Weapons Center, Analytical Models for the Design of Lidar Systems (U) by R. E. Bird. China Lake, Calif., NWC, Oct 1973 (NWC TP 5576, publication CONFIDENTIAL).
2. Deirmendjian, D., Electromagnetic Scattering on Spherical Polydispersions. New York, Elsevier, 1969. 290 pp.
3. Naval Weapons Center, Calculations of Multiple-Scattering Effects on Active Optical Sensors in Cloud Environments (U) by R. E. Bird. China Lake, Calif., NWC, Aug 1974 (NWC TP 5667, publication UNCLASSIFIED).
4. Anderson, R. C. and E. V. Browell. "First-and-Second-Order Backscattering from Clouds Illuminated by Finite Beams," APPL OPT, Vol. II (1972), pp. 1345-51.

AEROSOL EXTINCTION:
COMPARISON OF MODELING METHODS

D. P. Woodman

GTE Sylvania
Mountain View, California

Aerosol Extinction:

Comparison of Modeling Methods

D. P. Woodman
GTE Sylvania

Mountain View, California

While very impressive progress has been made in modeling atmospheric molecular absorption, the aerosol portions of existing atmospheric models apply only to long-term average conditions. It has been pointed out (reference 1) that optical system designers require information regarding the departure of local meteorological optical conditions from the long-term average conditions currently represented by our atmospheric models. This paper compares techniques for modeling aerosol transmission effects and compares Filippov and Mirumyants models with those of Elterman (3) and McClatchey, et al (4).

The modeling techniques currently in use can be grouped according to the fundamental experimental data on which the model is based. Both Elterman and Filippov's models rely on direct attenuation vs wavelength measurements. In contrast, McClatchey, et al, and the techniques used by Barnhardt and Streete (5), and Hodges (6), for example, rely on experimental measurements of particle size distributions and indices of refraction. In the latter case, the attenuation versus wavelength is calculated using Mie theory.

The development of useful atmospheric models requires a blend of both experimental data and theory. It is the author's opinion that the current aerosol models should be extended to include an indication of expected departures from long-term average conditions. Fillipov has attempted to improve aerosol models using direct attenuation measurements.

Filippov's data indicates that a classification of "optical weather" at a particular site by season and weather type is possible. One can obtain an indication of expected deviations of local conditions from long-term average conditions by comparing Filippov's data with the McClatchey, et al, model.

Filippov used an empirically derived expression for the attenuation coefficient,

$$\alpha (\lambda) \approx \frac{3.9}{V} [K_0 + K_1 \lambda^{-n}] \tag{1}$$

where λ is the wavelength in microns and V is the meteorological range. The values of K_0, K_1, and n depend on the weather type and are listed in Table I. The transmission is given by

$$T = e^{-\alpha(\lambda)R} \tag{2}$$

where R is the range. Figure 1 shows a comparison of equation (2) with the Elterman and McClatchey models for horizontal propagation where V = 5 KM and R = 10 KM. It is apparent that the transmission for a DF laser could vary from 80% to ~20% depending on the weather classification even though the meteorological range is 5 KM for all conditions. The McClatchey, et al model preducts T ≈ 40% for the same conditions. Figure 2 illustrates an extreme example which illustrates the impact of local "optical weather" on a practical system. The case considered is a DF laser radar propagating over a 10 KM path (R = 20 KM for two-way path) with a meteorological range of 5 KM. The McClatchey model preducts T = 15%, whereas Filippov's data covers the range of T = 5% to 60%. These comparisons, while strictly applicable only to a specific geographical location, do indicate the kind of deviation from long-term average conditions which can be encountered.

Two specific measures should be pursued to improve our current ir aerosol attenuation models. First, data regarding the sensitivity of the results of existing aerosol models to changes in the assumed aerosol characteristics should be published. Secondly, a direct attenuation measurement program should be initiated to begin to provide data on the geographical and seasonal variations of ir attenuation. This data should be used to derive empirical models for local conditions and to check the theoretical predictions which are based on assumed particle size distributions.

TABLE I

WEATHER CONDITIONS	K_O	K_1	n
SPRING AND FALL HAZE	0.04	0.585	1.02
WINTER HAZE	0.0	0.4	1.24
STABLE SUMMER HAZE	0.06	0.36	1.88
NEW SUMMER HAZE	0.0	0.4	1.88

FROM REFERENCE 2

References:

(1) D. P. Woodman, Limitations in Using Atmospheric Models for Laser Transmission Estimates, Appl. Opt. 13, No. 10, October, 2193-2195, (1974)

(2) Vil. Filippov and S. O. Mirumyants, Analysis of Mean Statistical Spectral Dependences of Coefficients of Aerosol Absorption in the Range 0.59 - 10 μm, Izvestiya Vysshykh Uchebnykh Zavedenii, Fizika, No. 10, pp. 103-106, October, 1972

(3) L. Elterman, Vertical Attenuation Mo[illegible] with Eight Surface Meteorological Ranges 2 to 13 Kilometers, AFCRL-70-0200, Environmental Research Paper 318 (March 1970).

(4) R. A. McClatchey, R. W. Fenn, J. E. A. Selby, F. E. Volz, and J. S. Garing, Optical Properties of the Atmosphere, AFCRL-71-0279, Environmental Research Paper 354 (May 1971).

(5) E. A. Barnhardt and J. L. Streete, Appl. Opt. 9, 1337 (1970).

(6) J. A. Hodges, Appl. Opt. 11, 2304 (1972).

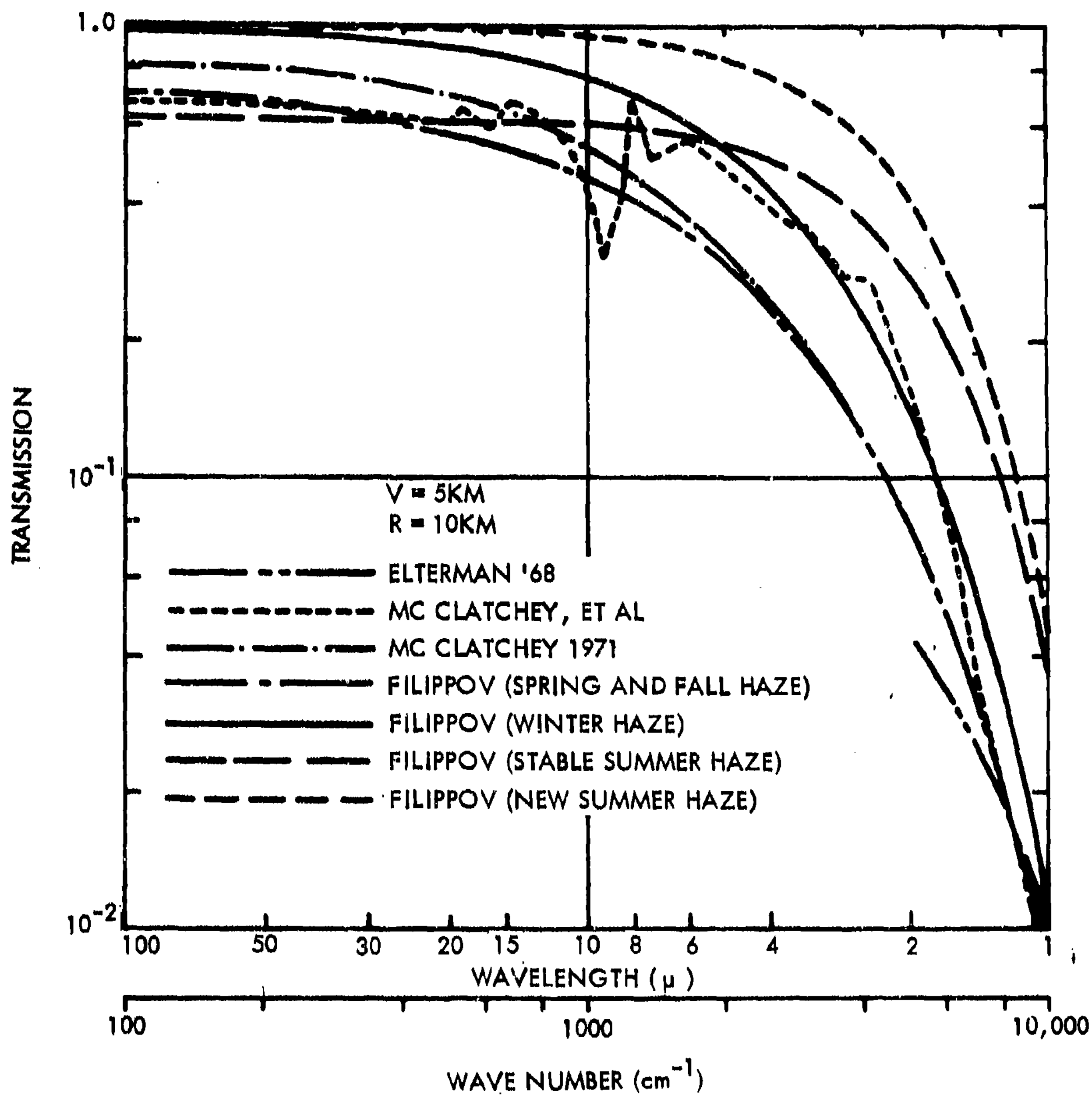

FIGURE 1. Attenuation Model Comparison

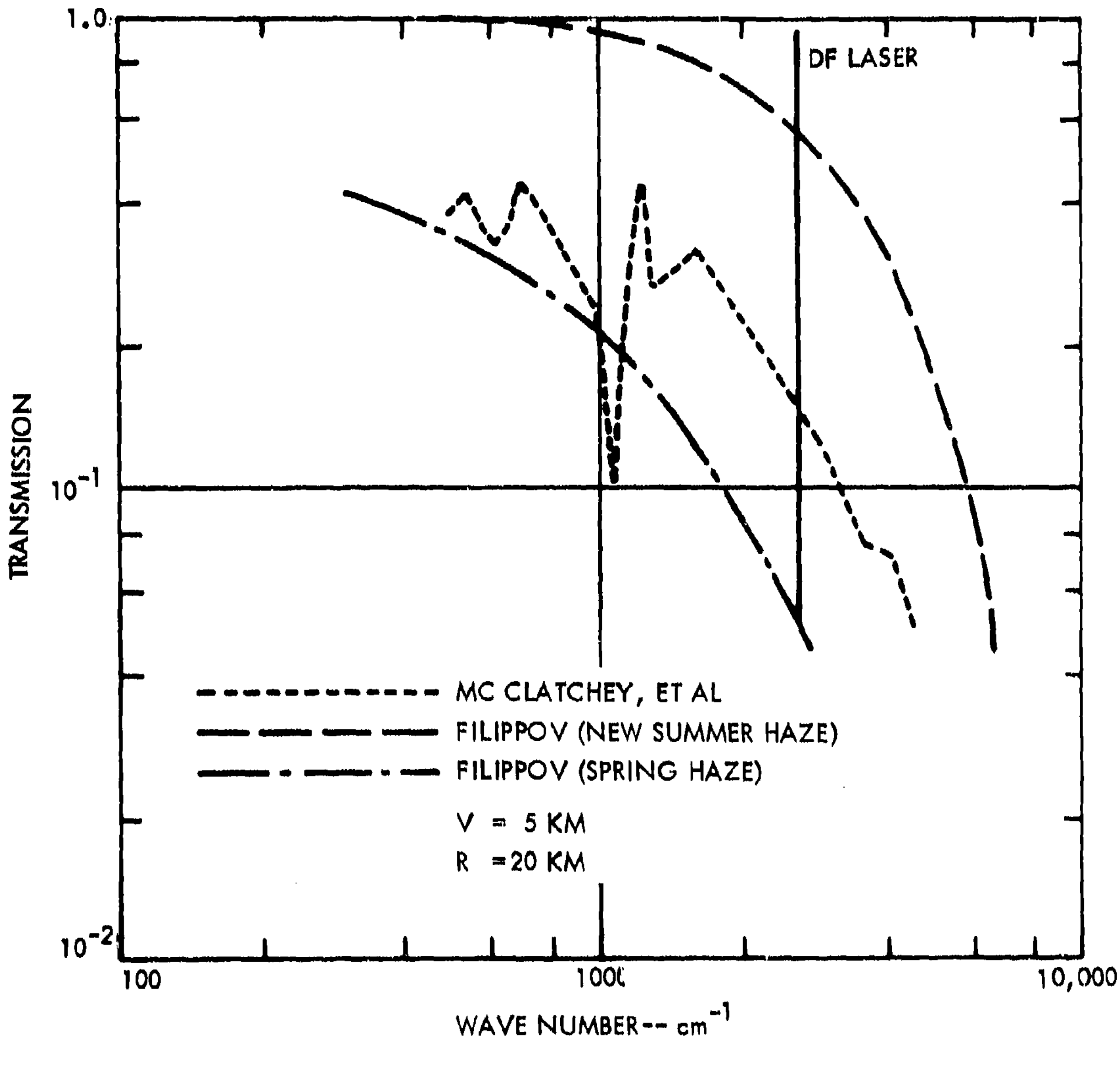

FIGURE 2. Radar Transmission Example

A DESIGN STUDY FOR AN AIRBORNE INFRARED TRANSMISSOMETER

Roger E. Christensen, Captain, USAF
6585th Test Group (AFSC)
Holloman Air Force Base, New Mexico

BACKGROUND PAPER

ON

A DESIGN STUDY FOR AN AIRBORNE INFRARED TRANSMISSOMETER

1. This paper concerns a design study for an airborne instrument to measure the transmissivity of the atmosphere to infrared radiation between the wavelengths of 2 and 13 micrometers. The design study was accomplished by Block Engineering, Incorporated, of Cambridge, MA for the 6585th Test Group (AFSC) at Holloman AFB, NM. This paper addresses the potential benefits of the instrument, its specifications, its principles of operation, its possible configurations, and its costs of procurement and operation. This paper recommends that DOD designate and fund an agency to buy and fly the transmissometer to improve and verify the accuracy of widely used transmissivity models.

2. Benefits of an Airborne Infrared Transmissometer:

a. The immediate benefit of a transmissometer would be measurements of atmospheric transmissivity during tests of infrared systems. Systems sensitive to atmospheric transmission conditions are Forward Looking Infrared Imaging Systems (FLIRs), imaging infrared guidance units for missiles, air to air missile guidance units, infrared trackers, and remote atmospheric sensors. For example, atmospheric transmissivity must be known in order to properly analyze results of comparative tests of infrared systems that are not accomplished simultaneously. Also, knowledge of transmissivity during tests of IR systems allows analysts to define their performance capabilities under various atmospheric conditions. Such knowledge is important for determining proper inventories, deployments, and employments of infrared guided munitions.

b. The most important benefit of a transmissometer would be its capability to provide data needed to verify models of atmospheric transmissivity. Models of infrared transmissivity are currently used by developers, testers, and weapons performance analysts to assess potential and real capabilities of infrared systems. The accuracy of these models as functions of various atmospheric constituents has not been established. Their parameterization of the effects of certain atmospheric constituents, such as aerosols, needs to be improved. Measurements of atmospheric transmissivity in a variety of atmospheric conditions could provide the data needed to verify and improve the models. Once verified, the models could be used with full confidence.

A special program to build and fly the airborne infrared transmissometer to gather the required data is considered appropriate. Simultaneous measurements of atmospheric parameters with transmissivity would be required.

c. A third benefit of a transmissometer would be its capability to provide basic scientific information pertaining to spectral locations of absorption/emission lines, pressure and doppler broadening of these lines, and information on the kind and concentrations of atmospheric constituents. It could provide the first spectral information available on infrared transmissivity in various aerosols.

d. A particular benefit of this transmissometer is that its design study is finished and paid for.

3. Specifications of the Airborne Infrared Transmissometer are illustrated in Figure I. They are as follows:

a. Spectral interval: 2-13μm

b. Wavenumber resolution: $\geq 0.5\ cm^{-1}$

c. Signal to noise ratio: $>$ 10 to 1 (design goal = 100 to 1)

d. Range:

(1) Air to air: 500 to 25,000 feet when extinction coefficient $< 0.1\ km^{-1}$

(2) Air to ground: 500 to 50,000 feet when extinction coefficient $< 0.1\ km^{-1}$

e. Scanning time: 1 to 60 seconds (integration time for an interferometer)

f. Calibration:

(1) Internal reference: ±5%

4. Basic Operating Principles of Recommended Design: The recommended design by Block Engineering, Incorporated is called the Source-Interferometer-Retroreflector (SIR) configuration. Four

SPECIFICATIONS

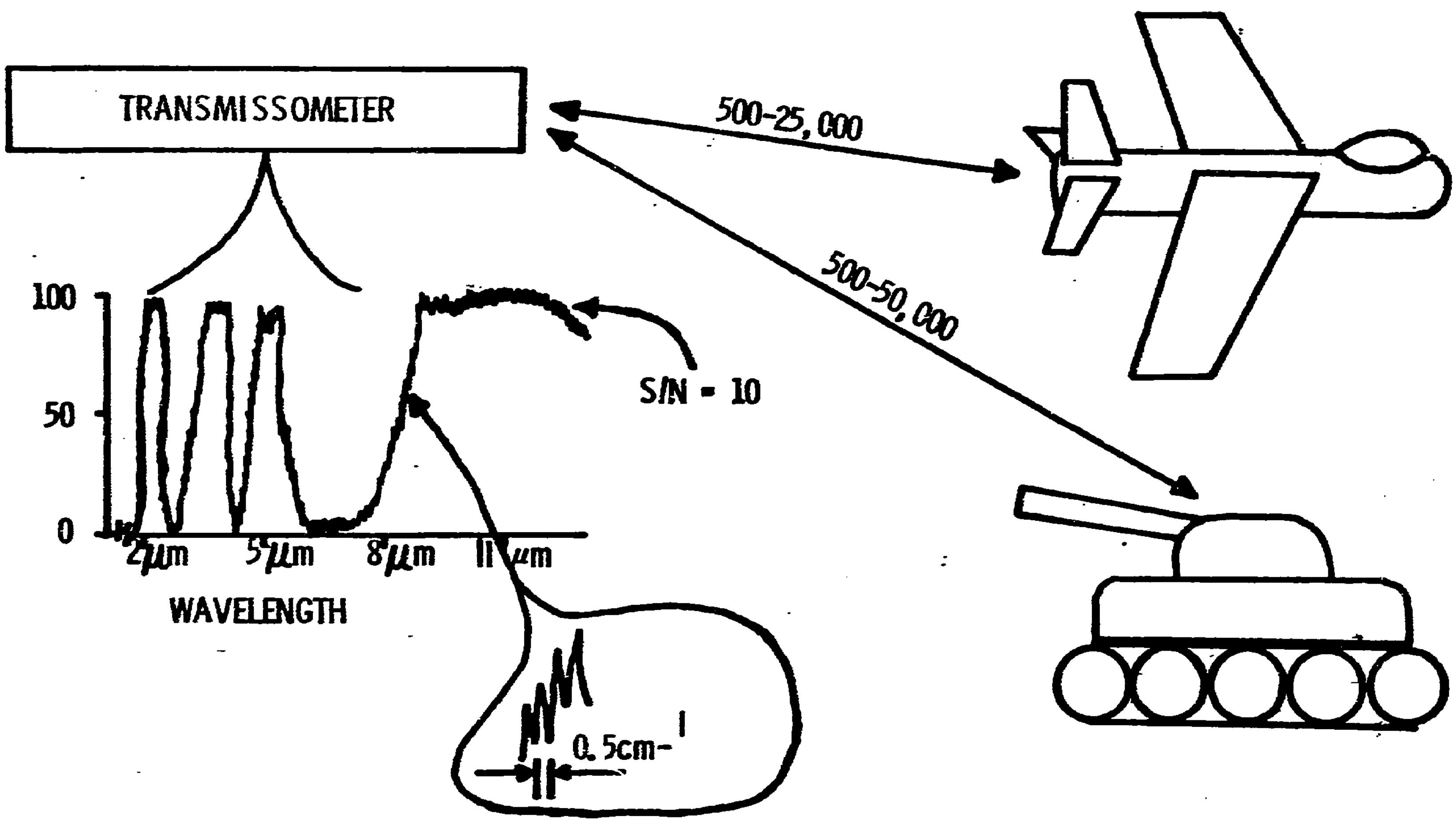

6585TG
015
FIGURE I

additional configurations were addressed in the design study as possibilities for performing transmissivity measurements. The SIR design is illustrated by Figure II. A 2500 degree Kelvin, incandescent source is moduled by a moving mirror in the Block type Michelson interferometer to produce an interferogram of the source radiation, which passes through transmitter optics into the atmosphere for transmission to a retroreflector aboard a target vehicle or on the ground. The retroreflector returns the radiation through the atmosphere to receiver optics ahead of a detector which senses the interferogram. Appropriate electronics are employed behind the detector to distinguish the interferogram (AC signal) from background radiation (DC signal) within the field of view of the detector optics. A Fourier transform of the interferogram and proper geometric scaling yields a high resolution transmissivity spectrum.

5. Airborne Infrared Transmissometer Test Bed Aircraft:

a. The design study assumes the transmissometer will be carried in a space stabilized gimbal platform in the nose of a C-130 aircraft. This gimbal moves in two dimensions for pointing and tracking purposes, and is aimed by a visual or infrared tracker carried with and boresighted to the transmissometer optics. This arrangement is illustrated by Figure III.

b. An alternate approach, illustrated in Figure IV, requiring additional design work, would be to use pods to carry the transmissometer as well as the retroreflector. This would allow for more flexibility in the choice of the test bed aircraft. Some difficulty may be encountered in the design of appropriate protective windows ahead of the transmissometer and the retroreflector. A stabilized gimbal may or may not be required in the pod holding the transmissometer, depending upon the abilities of the pilot to properly point the aircraft at the retroreflector in an airborne pod or at a retroreflector array on the ground.

6. Costs: Figure V indicates likely costs to be incurred by the transmissometer. The basic design study cost \$70K. Design of the alternate pod configuration is estimated to cost approximately \$30K. Costs of building the transmissometer and retroreflector are estimated to be \$170K. Various configurations of data processing and graphics display equipment are estimated to cost anywhere between \$80K and \$300K, the latter for a ruggedized, airborne real-time system.

SOURCE - INTERFEROMETER - RETROREFLECTOR (SIR)

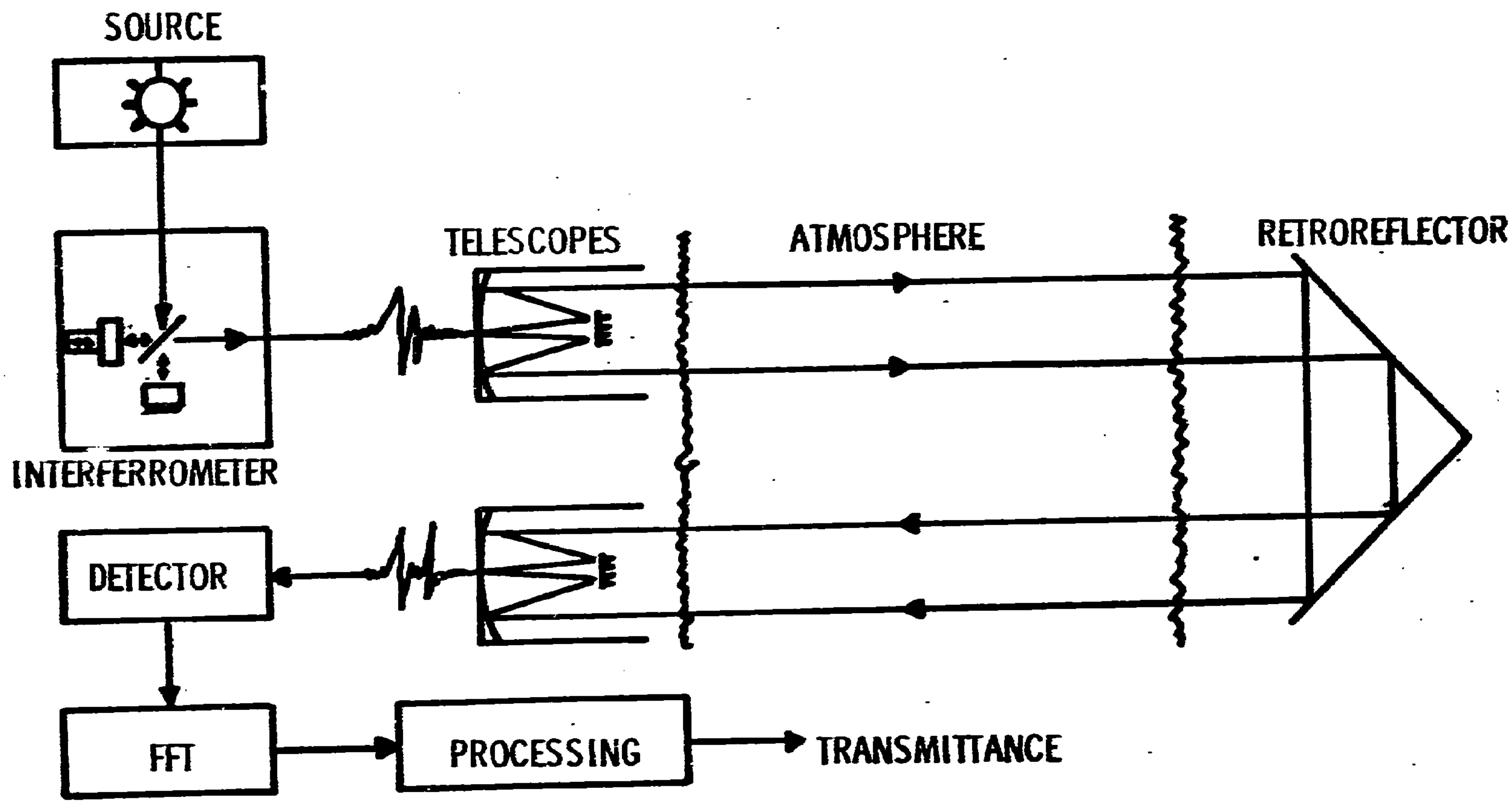

FIGURE II
6585TG
015

C-130 TEST BED

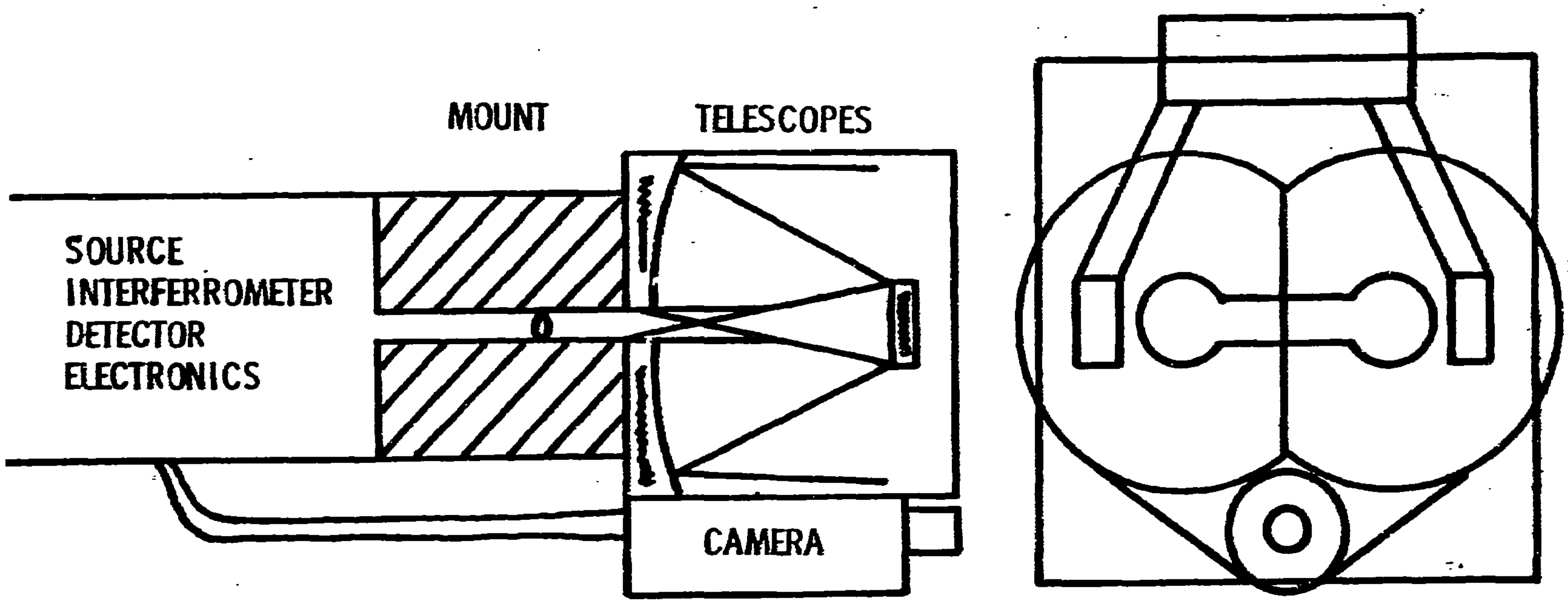

FIGURE III
6585TG
015

AIRCRAFT PODS

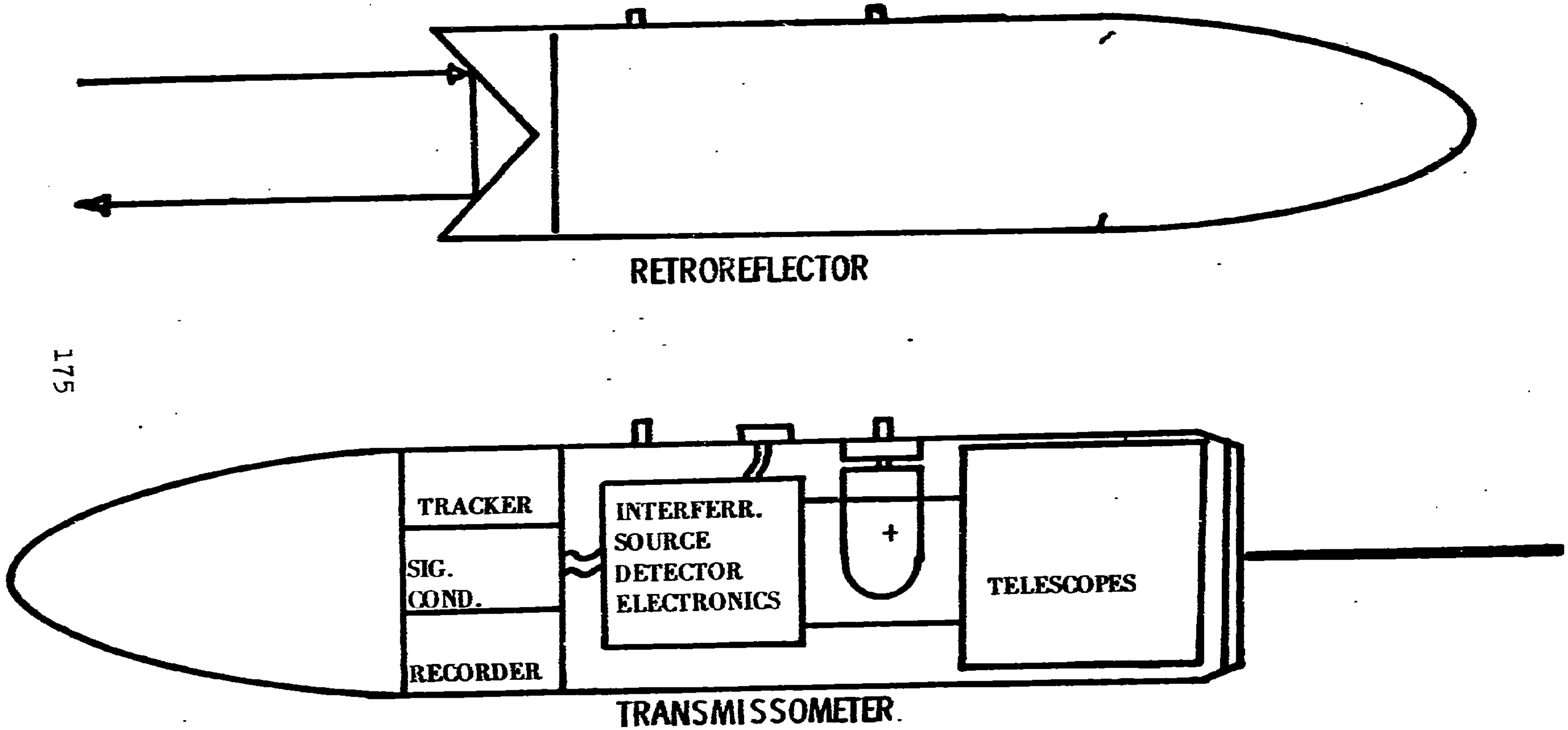

FIGURE IV
6585TG
015

COSTS

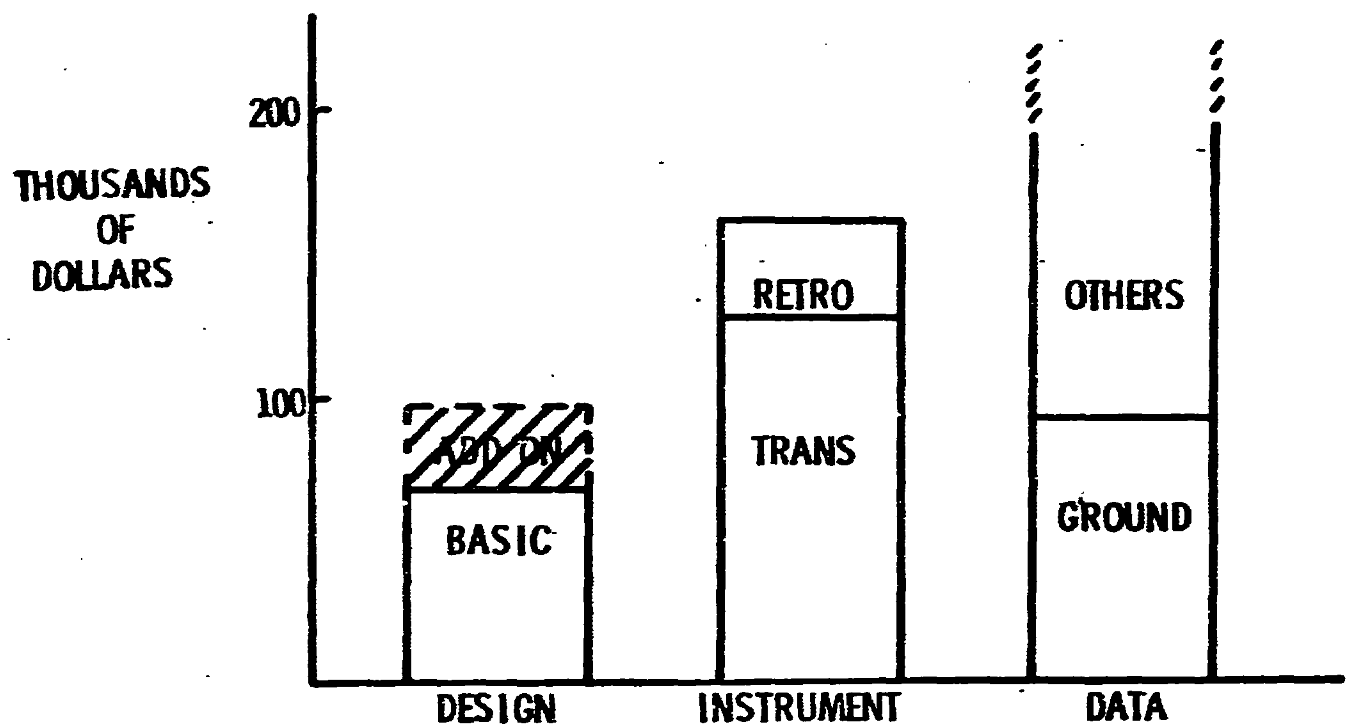

FIGURE V
6585TG
015

7. Other Configurations: Several other instrument configurations were investigated by Block as possibilities to accomplish the transmissivity measurements. These are discussed and illustrated in the design study. Their primary advantage is greater range capability. Their disadvantages involve greater cost, lower accuracy, and higher pointing and tracking requirements.

8. Summary: The design of an instrument capable of measuring the transmissivity of the atmosphere in an airborne environment has been completed. Its design costs have been paid. This instrument would be capable of providing basic spectral transmissivity data important for establishing transmissivity information during tests of infrared systems or to verify the accuracy of various computer models of transmissivity. We believe the most important and most economical use of the transmissometer would be to improve the accuracy of existing transmissivity models. These models could then be used with full confidence by systems developers, testers, and performance analysts. Transmissivity of the atmosphere must be considered when deciding (1) which weapons to develop, (2) which weapons perform the best, and (3) what proper force levels to procure and maintain in various operational environments. In the future, streamlined transmissivity models might also be used by weather support personnel to indicate proper employment tactics of available weapons to operations personnel. Accurate transmissivity models are essential in order to relate standard meteorological variables observed world-wide to the performance capability of infrared guided munitions. For these reasons, this paper recommends that DOD designate and fund an agency like the Air Force Cambridge Research Laboratories to build and fly the Airborne Transmissometer, in order to gather data required to improve and verify their widely used transmissivity models. This approach would seem to be more economical than for one or more test agencies to buy and fly a transmissometer during tests of infrared systems.

COMPARISONS OF TRANSMITTANCE CALCULATIONS BY TWO METHODS

A. J. LaRocca

Environmental Research Institute of Michigan
Ann Arbor, Michigan

COMPARISONS OF TRANSMITTANCE CALCULATIONS BY TWO METHODS

A. J. LaRocca
Environmental Research Institute of Michigan

I was invited to attend this meeting after hearing from Dave Anding, who suggested that I present some of my results showing comparison of calculated values of transmittances using the LOWTRAN 2 model and the model developed by him and others while he was at the Environmental Research Institute of Michigan (ERIM). The comparisons are part of the product of a State-of-the-Art Report, sponsored under a contract with the Infrared Information and Analysis (IRIA) Center, entitled "Atmospheric Transmittance and Radiance: Methods of Calculation," by LaRocca and Turner. The report is now in publication and will be distributed to IRIA-IRIS subscribers in about a month or so.

Because the report is pertinent to the subject matter of this meeting, a few brief statements about its content are in order. This is probably best done by quoting the abstract which is reproduced as follows:

"The effort represented by this report was a result of the need to bring a description of the state-of-the-art of methods of calculating atmospheric transmittance and radiance up-to-date. The report is broadly divided into the categories of scattering and absorption, with the greater stress laid on absorption. The essential material is presented in Sections 3, 6, 7, and 8, in which specific methods are described. Section 3 is devoted to scattering calculation techniques, while Sections 6, 7, and 8 cover methods of calculating transmittance. The first of these is the so-called line-by-line direct integration method, which requires a detailed compilation of the characteristics of individual molecular lines. Some familiar numerical integration techniques are used to effect quadrature in the most convenient and economical way.

"The second of the absorption methods of calculation presented is the band-model technique. In this method, the line spectrum is approximated by some mathematically manipulatable distribution function with undetermined band-model parameters. By comparison of calculated results with laboratory experimental data the parameters are defined, and the band-model is used for calculating transmittance under any required meteorological conditions.

"The third general set of techniques is given the heading 'Multi-Parameter Analytical Procedures.' These techniques are derived from the band-model concept, incorporating a larger number of parameters, with presumably greater accuracy in the resultant calculations.

"The rest of the report is either tutorial or supportive, presenting details of information which is required as input to the calculation procedures. The major input is the meteorology required to describe absorber concentrations, pressures, temperatures, and other necessary physical entities.

"An assessment is made of the various techniques of calculation in terms of accuracy, computer time needed to perform calculations, adaptability to specific problems, and practicality."

The specific purpose of this presentation is to show a comparison between the results alluded to above. The method developed by Anding is entitled the Aggregate Method in the State-of-the-Art report because of the nature of the approach to the calculation. In the Foreword to the report it is stated that the cut-off period for material contained in it is around mid-1974. This makes the results about to be shown a bit out-of-date because Anding has since changed his make-up of the Aggregate method to some extent, as he related to me shortly before the meeting. And we have heard in the course of this meeting that LOWTRAN 2 is about to be changed to LOWTRAN 3.

The calculations were made with all meteorological inputs the same so that the comparisons would point out differences only in the techniques for performing the calculations. In order to show in this presentation the range of whatever differences occur I have included two standardized atmospheric models, one relatively dry and one relatively wet. The dry model is represented by what is called an Arctic-Winter atmosphere and the wet by a Tropic atmosphere. Figure 117 shows a comparison between the transmittance calculated by the Aggregate and LOWTRAN 2 method. The figure is divided into an (a) and (b) parts representing respectively the long and short wavelength parts of the infrared spectrum. Figure 117 is for an Arctic Winter atmosphere. The comparison is reasonable good showing some compatibility in the two methods for a fairly dry atmosphere.

Figure 113, (a) and (b), shows the same type of comparison for a Tropic atmosphere. The divergence in transmittance values here is somewhat larger, especially in certain spectral regions. Some of this difference, according to Anding, is attributed to differences in the method of handling the H_2O continuum, as well as differences in the coefficients considered in the two methods. It is most difficult to resolve these differences, because comparisons with an independent method, say the results of field measurements, is inadequate. Reliable field measurements, in which the atmospheric conditions can be reproduced by calculation, are hard to come by.

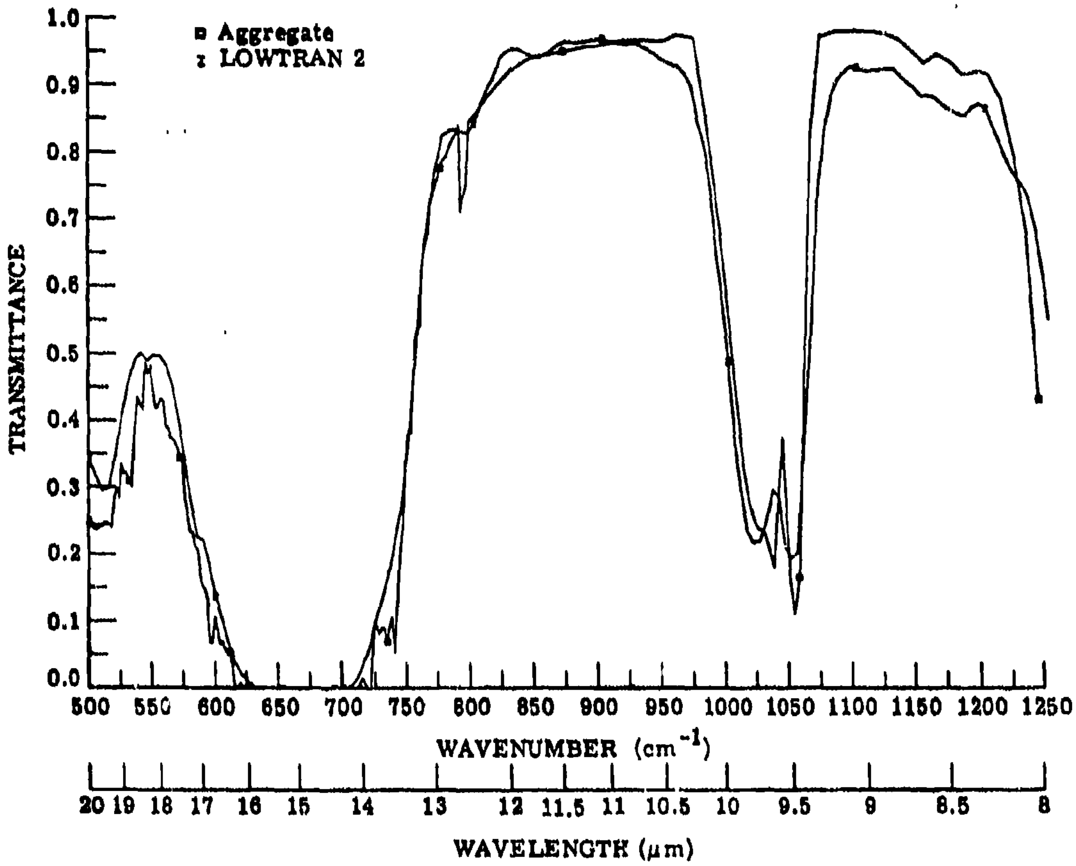

(a)

FIGURE 117. TRANSMITTANCE FOR A VERTICAL PATH LOOKING DOWN FROM 100 km. Arctic Winter atmosphere.

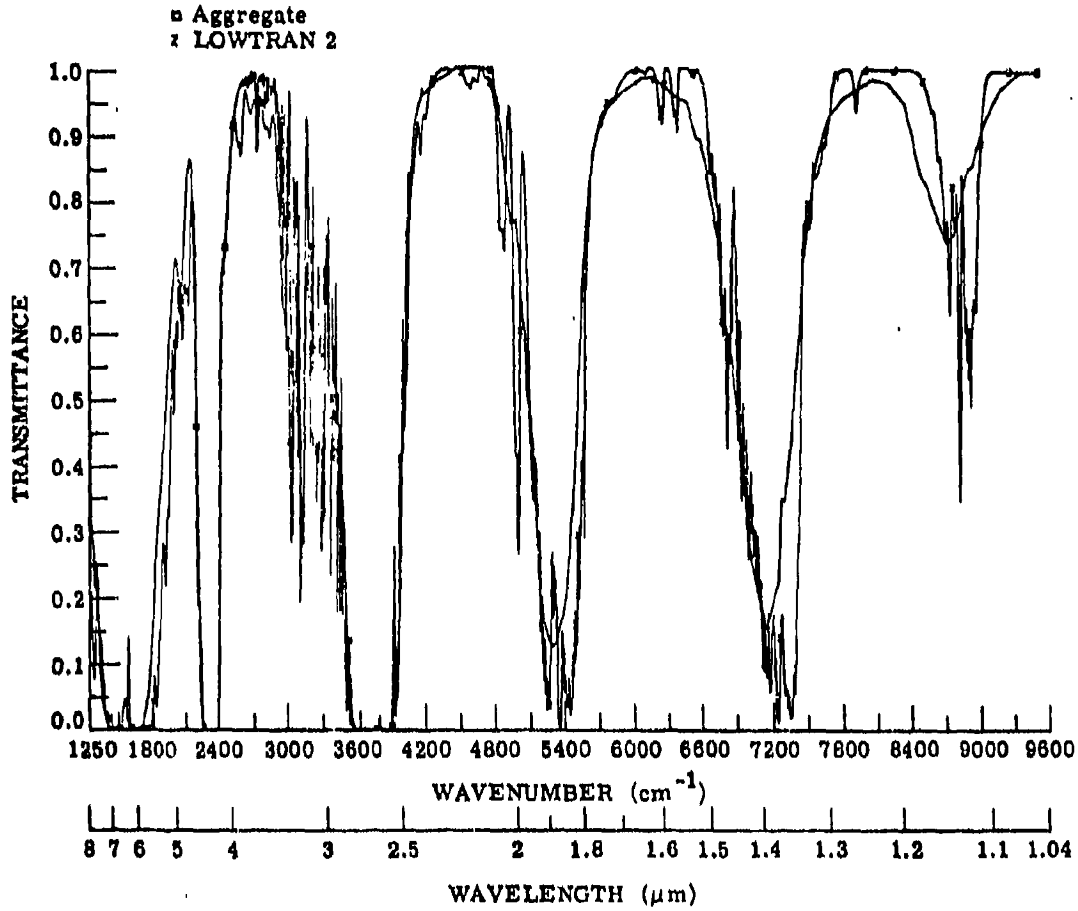

(b)

FIGURE 117. TRANSMITTANCE FOR A VERTICAL PATH LOOKING DOWN FROM 100 km. Arctic Winter atmosphere. (Concluded)

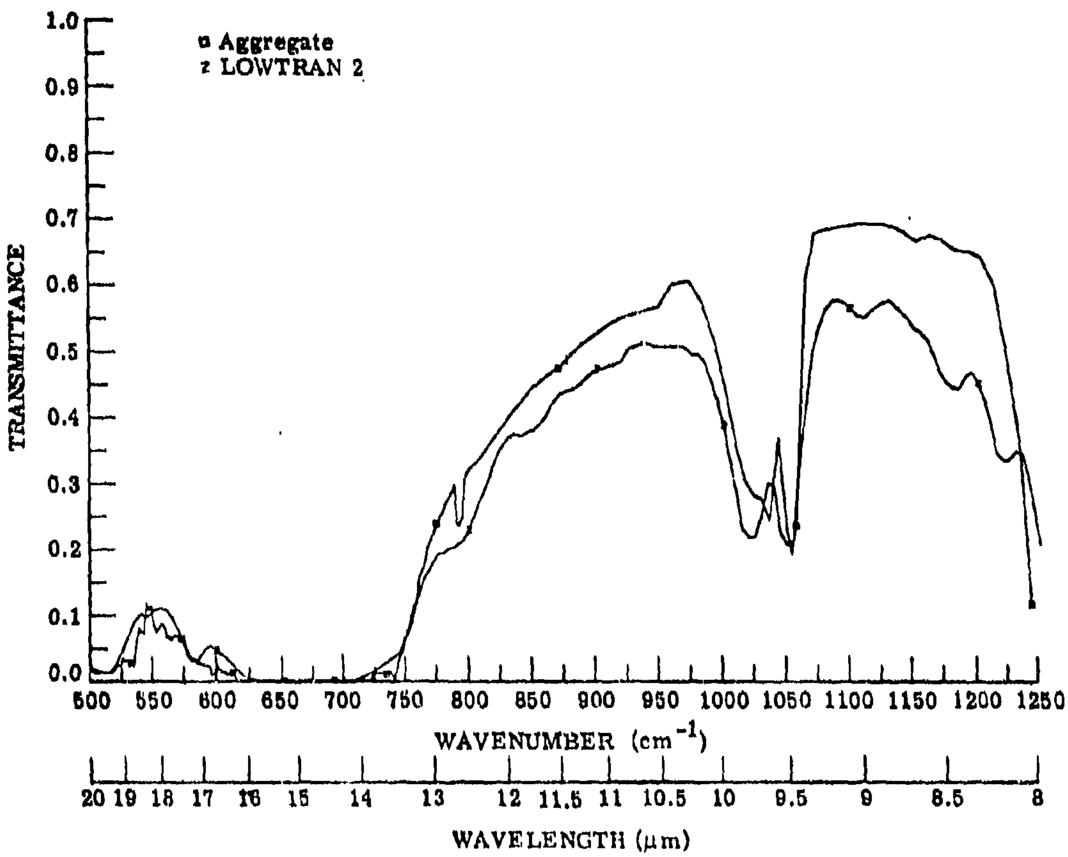

(a)

FIGURE 113. TRANSMITTANCE FOR A VERTICAL PATH LOOKING DOWN FROM 100 km. Tropic model atmosphere.

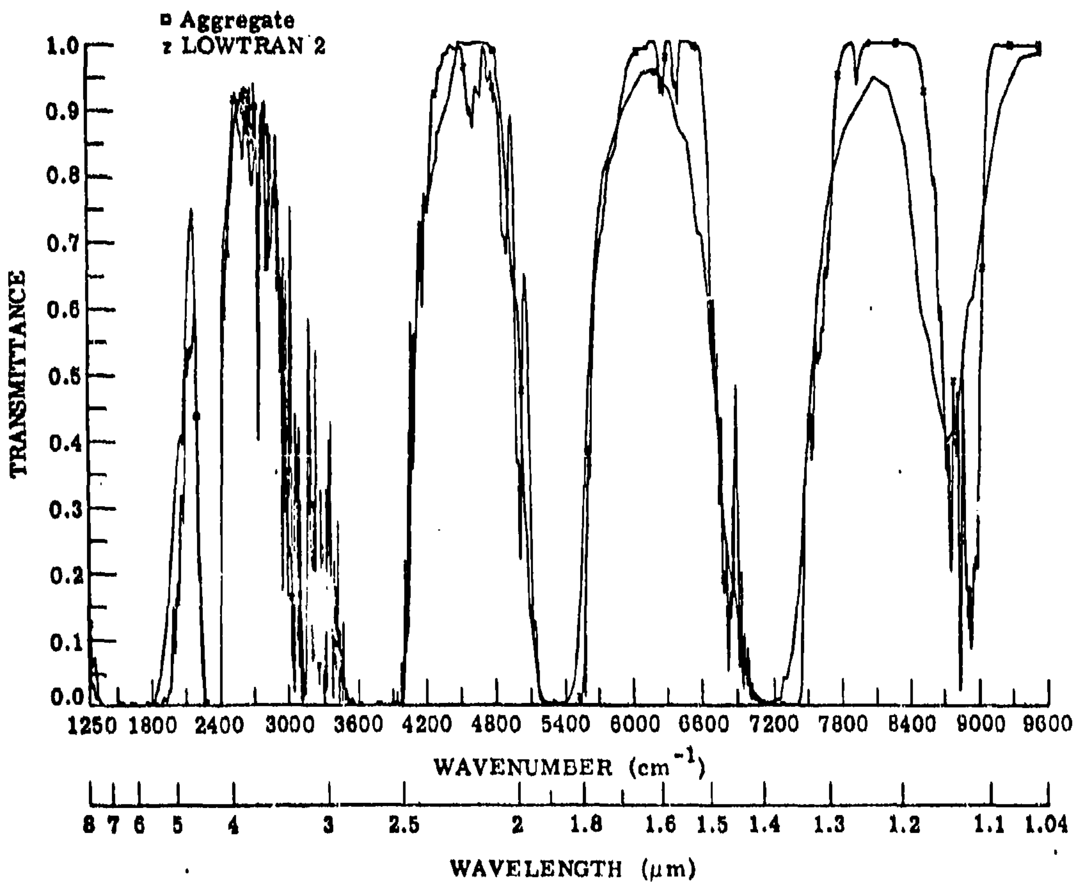

(b)

FIGURE 113. TRANSMITTANCE FOR A VERTICAL PATH LOOKING DOWN FROM 100 km. Tropic model atmosphere. (Concluded)

WORKSHOP ON PHYSICS AND ENGINEERING OF MODELING THE ATMOSPHERE

J. J. Gallagher, Moderator

Engineering Experiment Station
Georgia Institute of Technology
Atlanta, Georgia

WORKSHOP ON ATMOSPHERIC TRANSMISSION MODELING

January 28, 1975
Institute for Defense Analysis

Afternoon Session: Workshop on Physics and Engineering of Modeling the Atmosphere

Moderator: J. J. Gallagher
Engineering Experiment Station
Georgia Institute of Technology

The afternoon session was an open session on the physics and engineering of modeling the atmosphere. The session was taped, however, one tape did not record satisfactorily, resulting in considerable difficulty in transcribing the session. The difficulties of Rosemary Wood were deeply appreciated in this effort.

The session was started with a call for questions and comments on the papers presented in the morning. The first paper addressed was that of Dr. L. Biberman, entitled "The User's View of Atmospheric Models: 1. Thermal Imaging Systems." A question was asked how Biberman's IR measurements were made.

Biberman: In 1970, a decision was made to gather meteorological data for one year. I have the data on visibility, relative humidity, dew point, temperature, all the usual parameters. I used the LOWTRAN III Model. These are calculated results and the validity hinges quite clearly on validity of the scattering model, and I pointed out that when things get bad, they get bad because of scattering. There's not much water in January. When stuff goes out for six hours, it's snowing or there's bad ground fog or similar atmospheric conditions. So when the equipment is about to go out of operation or it's only operating for half its normal range or less, its because of scattering, and therefore, when one wants to take a look at how long the equipment will be of no value to serve, one really has to consider this on the basis of the scattering model that dominates, and therefore it's necessary that the scattering model be reasonably appropriate or reasonably accurate. When I go back to the Air Force and say that you better not build that, because the Air Force model is no damned good, that's

about where we stand. Now, it turns out that we had six-seven years of scatter modeling work, and we still can't use it. I'm going to put all the pressure that I can into getting a scattering model that will plug into a computable program.

Walsh: Can we ask you to give a few thoughts on what the content of a scatter model should be? One difficulty with the scatter model is that it's continuously variable from 100% transmission to zero. People talk about London fogs in which you cannot see your hand in front of your face.

Biberman: OK, John, that's critical.

Walsh: You need to reach some understanding on what kind of model you want to have. It has to go all the way from zero to one. Do you want a highly refined model that correlates with visibility? Can you in fact correlate with visibility because you know that at 10 micrometers it's somewhat different than what happens in the visible. What should be try to do to get to the model? What should the model contain?

Woodman: Can I ask one question first? When you say scatter model, are you talking about probability of occurrence, or are you talking about scattering by particles in air?

Biberman: Scattering by particles in air. I know when the scattering gets bad because any weather station tells me that the visibility is bad.

Woodman: The LOWTRAN III does not have a hydrometeor subroutine in it. Does it?

Selby: No.

Woodman: So when you say that it's snowing or foggy...

McClatchey: That's another set of conditions that one might address. It could be handled by LOWTRAN III. I think one might...

Fenn: You didn't have any infinite fog situation in those cases. Did you?

Biberman: All I can tell you is that when you get meteorological data recorded, they tell you what the relative humidity is, what the temperature

is, what the ground temperature is, and what the visibility is. Very seldom there is a little thing that says it's raining.

Selby: The visibilities that you had were from zero or 2-10 km?

Biberman: Correct. Visibility in a couple cases went to zero. As far as I'm concerned, that's either fog or snow, and I'm not worried about that. I'm worried when the visibility is 2 km, and I would like to see a model that says this model is typical of a high sea state at low altitude above the ocean, and that ain't distilled water. Someone said it's boulibais, and it is. If you take a look at all models of what aerosol content is, of sea and why bubbles break and they throw stuff up, and water evaporates and you leave salt nuclei all over the place, and they are not small in size and they're serious, then you need a model like that. We have a model somewhere over White Sands, New Mexico, but I don't believe this for Hanover, Germany or coastal regions around the North Sea, so I think that we have to have something like coastal, we have to have something like continental, they have to say that we are using a scatter that is typified when the visibility runs between 2 and 4, and it is in suburban or rural continental mid-lattitude, and we have urban under some conditions. I think the scatter for 2-4 kilometers is different from one that has 10 kilometer visibility, and so I don't think that we have one continuous model. We may have a series of step functions, but your program must be able to correlate.

Walsh: It's still a problem no matter how much you know that people will continue to ignore it. I had a call last week from a Navy contractor way down the line on building some system for a CO_2 laser, and he is suddenly concerned about the high attenuation that he's going to encounter in rain and fog. I told him that years ago they should never have started such a development.

Biberman: There will always be stupid people. Let's not address those. Let's try to address more responsible people in the world who can see that things happen properly. There's no point in taking a look at the dumb heads. There's enough dumb heads around, and no matter what we do, we will not impress the dumb heads. What I think we have to do is supply data for the

thinking individuals who know how to use real data and understand constraints, and all the other things that you have to apply to the data.

Fenn: The problem that arises though, I think, is to evolve too many models, a large number of them, and I fully agree that I do not think that it's possible to ascribe a large variety of conditions to one model by just varying some parameters. There's just different physical conditions that require different models but if one can describe these different models, then one problem that we run into is the difficulty in educating the users to use the proper model for this situation.

Biberman: Listen, there's a lot of guys that don't know what to do with a Bessel's function, but that doesn't mean we shouldn't have Bessel's functions.

Fenn: No, but I think that it's one aspect that we have to keep in mind and take care of at the same time that one brings out the model.

McClatchey: Well, the model will probably have to contain that kind of information. The model has to be boiled down ultimately to a number, a limited number of input meteorological parameters that are ordinarily measured at which point the model will determine that if you have a certain relative humidity and a certain visibility and other pieces of information, it will pick out...

Biberman: You will then calculate a not improbable result, that you can expect.

Fenn: The difficulty is that the parameters that seem to be measured are not sufficient to describe the environment sufficiently.

Biberman: You'll never get that result, not except on a research program. Then you can only expect that by correlation. They are not even sufficient to base a decision on thought and to determine what the general condition was.

Walsh: Let me pose a specific question along those lines just to follow up on that point. Do you think that it would be worthwhile to try to decide this question? A model should not be a thing that gives a monotonic or a specific functional relationship between visibility and whatever others you

deem appropriate, and an absorption at 10 micrometers. Rather, it should just let you arrive at a limited set of statistical parameters which would describe a probability distribution of a certain attenuation in the 10 micrometer band. Could we reach some conclusion on that issue?

Biberman: I'm not sure that I understand your question.

Walsh: Well, the question is the following: Suppose that I device a scheme, presumably a functional form, that said when the relative humidity and visibility and temperature and whatever else that seemed to be important was in, there is a calculation that leads to a single specific number for the performance of my FLIR system. An atmospheric attenuation, a single specific number. That's one approach. The oth-r approach would be one that gave me a probability of performance, a range of performance; that range would be narrower than the total range of performance that I could get over all possible parameters of the atmosphere, but never-the-less I would not try to force a single number out of it. Is it worthwhile to try to consider that kind of an approach?

Fenn: I think that it would be worthwhile to consider. The only difficulty is that to develop that probability distribution you have to either solve the first problem that you described or in other words you would have to know what the correlation between the visible visibility and the IR transmission would be (Walsh: You think it's too hard?) to develop the IR transmission probability distribution from the visible probability distribution, or, if you cannot do that, to go out and measure for "um-teen" years the IR transmission to develop the IR distribution from that.

Walsh: You say you prefer the single functional relationship?

Fenn: I think that it would be the faster approach.

McClatchey: I think that the thing is that we have to commit ourselves. I think that there is a reluctance to commit oneself to the scattering problem and to say that, based on the best information that we have, this is the answer. Now certainly, there is some uncertainty in that.

Biberman: Well, it would be very nice if the meteorological people reported not only the meteorological visibility which could be very short but also indicate that it was snowing and when they do, then you put a step function into your model to take account of the fact that it's just not a very, very heavy haze, but it's actually this kind of a problem, and there's one other model that I've heard no one talk about in this connection. We're all talking about normal peace time (so-called) conditions. If these models are going to be of value and we take a look over a hostile area like a battlefield, I think that your conditions are like your volcanic stuff which occurs immediately after the first 3 or 4 shots go off and you're going to have all sorts of crud, and somebody really ought to establish a project crud and look through it. No, seriously.

Benedict: This is exactly the sort of problems...

Woodman: I'd like to make a comment about the models that we've been discussing. How do you start? What kind of project should we have? One of the things, I think, that we should address is - do we collectively feel that there is credibility in the Russian approach to this problem? They've added another variable, another parameter that is measurable but somewhat arbitrary. But I think that we should decide whether we should invent the wheel or perhaps find out what the consensus is about the Soviet approach. They present data and claim that they can characterize and distinguish a summer haze from a stable spring or summer haze. Now, I have difficulty reading the Russian publications, and I'm sure all of you do. But that seems to have some merit. Now, are we going to work around that or perhaps consider that, as a possible way we can go with a new aerosol model. I guess that I would like to see if Dr. Fenn has a comment on that approach because it certainly is an approach.

Fenn: Well, I certainly would agree that it is possible to find a correlation between the optical properties and the general meteorological conditions. Simply, we know that there is a physical relationship. We do not know too well what the physical relations are, but they do exist. Consequently, there has to be a relation between the optical properties and the general

meteorological conditions. Whether the choice of tying the optical properties to the seasons is the best one or not, I would question that. Well, certainly the correlation exists, evidence is in the data, and it's not surprising that one finds that either. We do know on a day with a clear arctic polar air mass moving in, the visibility is going to be much better than on a hazy summer day.

Biberman: That depends on where you live. If you live in South Chicago, and they burn soft coal, and it's clear, and you've got a nice clear arctic air mass moving in, it might be clear at some altitude but it sure isn't on the edge of Michigan Avenue.

Yes...

You've got it on your collar and on your shirt, and everything else.

Fenn: But we have to look at different regimes.

One regime is the type of air mass - the larger scale circulation. Another regime, hidden from that, is the purely local effects or local pollution from a city; if we are east of the city, west winds may deteriorate the conditions. If we're west of the city, an east wind which may mean clear arctic air, however, in that particular situation, it may make things worse because we just now are getting into internal pollution or its local pollution. So this is one reason why a simple relationship like visibility conditions for summer or winter may be meaningful in a certain type of environment, but may not be applicable at all to another type of environment. Then, one has to look at that. For instance, on the first of January, it may be that the large scale circulation regime is the dominating factor whereas, on the third of January, it may be a local phenomenon that determines the local optical conditions, and these are things that one would have to consider. I do not think that we know enough about these things at the present time to describe them for all general conditions. We know that these correlations exist, and we can even today describe them fairly reasonably for certain conditions but not all of them.

Woodman: But this would seem to be a logical starting point to agree that we need more than just the visibility, and that perhaps some type of classification of weather type and air mass could be of value to us. And I look

at what's being done and one of the practices in modeling is to incorporate a combination of a continental and maritime aerosol, and if they model the growth of the particles with the increase of the relative humidity. That's fine, it helps us understand the physics, but the person who is using the model cannot go out and measure the ratio of continental/maritime particles.

Fenn: No, I think that, if one breaks it down into rural, urban and maritime particles, this would be a description that would describe things on the local regime scale. You can come up with another regime in which you relate the optical properties to the seasons or air mass. And certainly this tie in to the air masses is reflected in the data the Russians have because in summer, in winter you have different air masses. That's why they get these consistent differences. But I don't think that you can say well one is a substitute for the other. I think that this is an example of two different regimes that control these optical structures. One is the location thing, the urban vs rural; or continental vs maritime but these are local things. The other regime that may dominate things is the circulation of air masses. Those have to be looked at but separately. In my opinion what one should do is on a given day the model that should be picked should be the summer or say the subtropical air mass type model combined with some parameters which make it fit in an urban environment.

Biberman: Well, lets ask a question. Who's going to use the models and for what purpose? It is clear that nobody is going to plan a mission for the 17th of April, 1975 and sit down and calculate like crazy what the scattering is going to be and what the absorption is goind to be. What he needs to do, however, is to have a background and to know that over some period of time statistically the probability to do such and such arises from two factors - the absorption and the scatter which typically in April is going to give him something like a 90% probability of success and a 10% probability for a failure. And that's all that he really needs for his planning purposes. In the same way in the design of equipment, there's no sense in designing a piece of equipment or a system that's going to see beyond the curvature of the earth if you're going to use it at altitudes below 50 feet. And in

the same manner, there's no point in doing range capability based on clear atmosphere when the probability is less than so much that you're ever going to achieve them. I think that this saves us from over-designing and statistically over-designing equipment and it prevents us from spending fortunes on things that really do us no real good. That does not mean that we do not build some special purpose dedicated equipment which might be used when the opportunity might be required for some very, very high priority mission, but, in general, when we build a hundred something or other aircraft we don't put 100 or so of these aboard each aircraft with capability of seeing 47,000 miles because the probability of seeing 47,000 miles in any real situation is going to be terrible. In fact, we'll probably see four miles, and so I think what we want to do is use our models to make that kind of executive decisions. Administrative decisions on how you're going to distribute your money and your talent and your resources. So we only have to collect data for some typical year and the reason that I used 1970 is because that's where the data is.

Fenn: I think that there are two principal types of problems and applications in this area. One is what you described as the statistical data - what is the probability of occurrence of a certain type of data at certain time of year and under certain type of conditions and at the present time and for the foreseeable future. There is no question in my mind at all that the only way that one can approach that problem is by looking at the statistical data that we have available. And those are visibility from the regular meteorological observations, and surface visibility and eyeball spectral range. Daytime only, no night time with some exceptions. The standard meteorological data, the temperature and humidity which allows us to make an evaluation of the IR transmission, and that's all that we have at the present time.

Biberman: Well, I have records which give me meteorological visibility 24 hours a day.

Fenn: Yes, there are some that give it in day and night time.

Selby: What you don't have though is that subject to visibility, what is the attenuation at 10 micrometers...

Fenn: You're right; there are a lot of things that you don't have. The first thing you don't have is what are the illumination levels. For a lot of systems, specifically night time systems, what is the distribution of the natural illumination level especially at night time?

Biberman: That's fairly easy to go back and reference.

Fenn: Yes, for astronomical data but you have no information on what the atmospheric factors do to them. And the other principal night area of no data at all is the IR transmission. The extrapolation from the visibile to IR transmissions is highly questionable and might be invalid all together.

Biberman: But as far as the distribution of light and its level, if I know the hour of the day and the day of the month and the year so that I can get the ephemeris and I know the cloud cover and a few things like that, I think that I can calculate you the incident illumination and the spectral distribution within quite a reasonable factor.

Fenn: Yes, but another point of view, another area in which one has no data at all is the contrast reduction in the visible. For any kind of system that works on the contrast, it's absolutely inadequate to know what the transmission is. You have to know what the contrast reduction is and there's no measurement of that available. But for 1975 and 1976, and several years after that we're not going to have any additional data of that nature. All we're going to have is the surface visibility, so the only...

Biberman: What about the Dutch effort?

Fenn: Well, that was a one year measurement program.

Biberman: Well, its pretty good, isn't it?

Fenn: Yes.

Biberman: And one year gives you a fair amount of statistics.

Fenn: I wish we had maybe a dozen of these measurements.

Gallagher: Let's go on to the next paper that we had this morning. People keep coming back to this problem, and it looks like one that we're not going

to get rid of the rest of the afternoon. Does anyone have some comments on Wolfhardt's paper on Rocket?

Benedict: I'd like to comment. He certainly raised a very important point that the emission from plumes is different from the continuum and he said what are needed are better data. This also ties in, of course, to the various modeling of things that was made when the emission and absorption were based on calculations using lines from the AFCRL line list. The point that I want to make is that the AFCRL line list was designed solely for use at room temperature.

The actual knowledge of the data that could be made to go into a line list that would give both the emission and the absorption of water vapor, CO_2 and CO at much higher temperature does exist. With regard to CO, there already is such an excellent line list although the frequencies are not the most up to date but those could be easily corrected. That's the one that's due to Birch. As far as CO_2 goes, here the data do not exist to take care of everything up to quite high temperature but I would like to make the point that there are so many vibrational states that are excited with the very low bending frequency of CO_2 that if you're talking about temperature above 1000° the density of lines is almost equal to the Doppler width so that as far as CO_2 goes, you have essentially a continuum source with a certain distribution of course rather than a many line source.

The remaining question of the H_2O is one that the data are not as complete as I would like them to be but they certainly do permit a very considerable extention of the list of lines rather of some of the lines that are in the AFCRL list. As far as all the levels, up to 6000 cm^{-1} of excitation are probably known to an accuracy that will give you the frequency of the line to within 0.1 cm^{-1}, and this should be adequate for taking care of the largest amount of the emission from plumes, in the 2.7 micrometer, the 1.9 micrometer, 6 micrometer and pure rotation regions so its just a matter of getting the data together and making a very much expanded list. Then, the basic data that can be used either in actual line-by-line calculations or model calculations will be there. The quantitative accuracy as far as line strength of H_2O goes may not be terribly good, but, from all the examples

that we have seen this morning, the data in the AFRCL line list are not terribly good for individual lines but when you get to the broadband comparisons of models and data the overall thing is quite good and I believe the same thing can be done for water vapor up to at least a 1000 degrees without too much trouble. To go beyond a 1000 degrees, one needs further effort on high resolution studies on flame sources in the longer wavelength region. Such studies do exist in the region down to short wavelength and up to 4 micrometers. For the record, my name's Benedict from the University of Maryland.

Biberman: Don't we have to take a look at the criticality of the problem from two different points of view. We say that there are plumes that are very hot. And if we take a look at large by-pass engines for instance, the effluence is not extremely hot but if we take a look at LOX-hydrazine or some of the other fuel oxidizer combinations, that can be used in some of our high performance things like some of our larger rockets, then the exhaust temperatures are very high and the problems that we raised this morning are really raised. But are the problems really so bad when we take a look at fairly high by-pass engines?

Long: What's the temperature?

Biberman: A few hundred degrees C.

Long: I don't think that it's really much of a problem in handling that problem.

Benedict: No. There are two types of input data that are needed in the analysis of hot water vapor spectra. What I have been working on have been the hot thin flames and the spectra of the sun spots and these are of course sources of 3000-3800 degrees and once that you know that then going down to low temperatures presents no problem at all.

McClatchey: The other kind of traffic problem that that presents is why you don't want to add stuff unless you really have to because I believe from a computational point of view it could become one hell of a nightmare.

Benedict: Exactly.

McClatchey: Just trying to deal with an order of magnitude more lines or some crazy thing. That could be a real problem so I think that we have to be very careful that we establish that something is really necessary or we have...

Biberman: The adequacy of the model and the adequacy of the data bank concerning the atlas of lines and line strengths. I think that you could use a fairly narrow set of data for many of the studies that we want to do, on aircraft plumes, on some of the modern engines and then move into a completely different and more tough problem when we start moving up drastically.

Burch: But you know in some of the cases I agree with McClatchey in that the computation gets very difficult, but can't you build into your program something that just ignores the lower strength lines for applications where you don't need them.

Long: Oh, yeah, you could put them in and not worry about a horrendous computational problem in those cases where you don't need them.

Biberman: Wait a minute, I don't think that that's really right because the lower strength lines when they predominate in number may be the most important thing that you have to consider.

Benedict: What you have to know is the number of lines in a given intensity range and a given frequency range.

Biberman: You just can't make an arbitrary decision by any means.

Benedict: There are two different types of pieces of information that should be made available; one is the overall one in which you know just how many lines there are and what their range of strength is and approximately where they are. If you're really trying to go into a detailed comparison of a specific region then you ought to know where precisely each line is, each strong line is.

Long: The point that I was trying to make was that it may be a horrendous problem in assemblying this data and on that basis you take care in how many you assemble. Just on the basis of the computation, you can always get the program that allows for that. But if you didn't over compute...

Benedict: As an example of this, there is a paper in the Astrophysical literature by Amat who does essentially this on the question of hot water vapor in stars. It's seven or eight years old, its fairly solid.

Gallagher: How about molecules other than those that are on the list? Can they contribute in this area?

Benedict: In the hot flame region, for instance, there are a number of strong lines that are due to OH for example and those are very valuable in that they can be detected at these temperatures. But [illegible] ordinary type hydrocarbon flames and so on, we are left with the simple type of molecules that we know pretty well.

Long: There are some other things that could be added to this particular data set such as HCl which has shown up in some types of exhaust products and I am sure that there are probably some others too that are still in this category of simple molecules, that I am sure are easy to put together and have the capability...

Benedict: They don't clutter up the list.

Long: Yes, they have a small number of lines.

Benedict: I think for instance adding OH if there is a great deal of importance and interest in the emission problem should be one of our first priorities.

Long: We are trying to find out with respect to the DF laser there are a couple of lines that we see absorption in the most pure nitrogen gas that we can purchase and we're trying to figure out what it is.

Burch: What wavelength is it?

Long: You mean exactly which laser line is it?

...

Long: Yeah, in that general area. Do you want to make a guess?

Burch: Well, I don't have an answer but I would like to look for it when I get home.

Long: I'll call you. I forgot what line it is.

Selby: In addition to the individual lines, you've got a problem with the line shapes still at ordinary temperatures and further complications at higher temperatures. You may need to put into our program... Well, the higher the temperature, the higher the pressure at which the Doppler shape where you have to go to the right regime for the Lorentz width. Also there are, of course, no very accurate measurements of the ...dependence of Lorentz width on temperature, but I think that the few measurements that there are indicate that the higher the temperature the less the effect of anything other than the billiard balls where the collision diameters are of importance. So it's pretty safe to take a constant collision diameter at any temperature above a thousand degrees.

Gallagher: How about the paper that Corcoran gave. Have you comments on that as far as the laser?

Rohde: I have a question to address that Dr. Biberman has already hinted at, and that is when Rudy Buser comes to me and asks me whether or not a laser system is going to work under certain conditions, we also have to consider the battlefield situations and even if I got all the codes to work under the statistics and the weather conditions for all over the world. In a different battlefield situation, do I know if the laser if going to function properly or am I going to wind up with some surprises that I didn't expect? So before I have to go back to him with an answer I would like to get some information as to whether it is possible to make some transmission measurements in a working situation out at Ft. Carson or some place and to really see what the conditions are before they start this game what the visibilities are, what the transmissions are and now make the same measurements while the game is going on so that I could have a feeling for how much these conditions could possibly change and whether because of the new molecules which are coming up or because of the shells exploding or because of the vehicles that are in the area that all the predictions that people are giving me are going right out the window. That's the final number. You know, when I go back to my boss and tell him yes this system will work in a battlefield situation and he can believe it. And that's a problem which I cannot answer.

Silberman: Well, "ive seen a number of Army films which are trying to demonstrate how goodsomething is andone of the typical things that they usually do is show an infrared set looking for something or other, and it's behind a Howitzer or some other kind of gun and some one pulls a lanyard and the thing goes boom. And then there's a television camera, an infrared camera of some sort and you sit and watch as a function of time how long it takes for the horizon to come into view, or the thing down the road or whatever it happens to be. Now there's a fair amount of that stuff that has demonstrated the problem about which you're talking, but which has not been quantified and it seems to me that it is not a terribly difficult job to work in as a companion to some other investigation at the appropriate time and I think that you certainly need to. But there are many sources. One is just the muzzle blast and all that kind of stuff and what it does, it blows the top of the earth off, hurls it into the air and settles down slowly. And then the other thing is that when it gets to the far end, it digs a hole and throws a mine up into the air, and that settles down slowly. And I think if there is a serious engagement you have to make some few measurements and some predictions about the range of difficulties that you get into.

Rohde: Precisely.

Gallagher: How about the questions brought up about linewdith parameters? When one is looking at narrow laser lines, are the linewidth parameters that well known to say that we have a particular transmission at these wavelengths. I think the people up a Cambridge have run into the problems that John has mentioned just looking at SO_2 for instance, for which Clough had trouble with the Lincoln Lab people. On the basis of predicted linewidths, the question came up whether they were getting different linewidths in their experiments.

Benedict: I don't know the situation on SO_2 but it certainly is true in the experiences that I have had that it is never possible to calculate anything as well as it is going to be measured when it can be measured well. When you're doing the kind of measurements like Ron Long is doing, for example, where you have laser lines of known widths and known frequencies then you

see whether the position as calculated for a simple molecule like N_2O, the absorption obeys, he tells me that it obeys very nicely. When it comes to a very difficult molecule like H_2O, the calculations don't agree that well. There are problems remaining in linewidths, particularly in the line shapes on the wings of the H_2O lines which of course leads us into this other mess that we have heard so much about, of the continuum that we heard so much about this morning. But as far as the general order of magnitude thing, 20-30-50% or so of the present calculations are good. For new molecules such as SO_2 where there have not been as far as I know any accurate linewidth measurement, we shouldn't be too surprised that the original ones come out wrong.

McClatchey: Well, it just kind of occurred regarding the data, the measurements of the Lincoln Lab people on water, for example, have not really been introduced empirically into the list. There are, of course, only a limited number of lines that have been measured. But the philosophy of having these narrower lines in high J have been to some degree taken into the calculations.

Benedict: Well, this is a second problem of course. The measurements of the Lincoln Lab people indicate that a limited number of H_2O lines are very much narrower than the ones in our original list. But as Bob has just said, it is not of major importance except to those lasers which happen to operate near these lines.

Long: How do you take that into account now? Is it in the data tabulated or in the program?

McClatchey: What I'm saying is that we haven't taken it into account in detail.

Long: Oh, you said to some limited extent.

McClatchey: Well, in the sense of the calculated linewidths.

Benedict: The current listing, I don't know if its on your lists for general distributions, but Clough put in narrower lines for the pure rotation region, and I heard from Doug Woods who works at SAI up in Ann Arbor that they had checked some of those measurements. Their measurements were indeed narrower than our old tape but they were wider than the guesses that we made on the

basis of the Lincoln Lab extrapolations on the new tapes. So again its got to be measured before you can say anything. But its an awful lot of measuring if you want to know everything. My point is as far as specified transmission for specific laser lines, that's not hard to measure. For overall statistical transmission, current data seem to do a pretty good job.

Gallagher: I believe I just saw Dr. Long flinch.

Long: Well, you said it wasn't hard; I think that it's awful hard.

Benedict: I didn't mean to detract from your actual work. I thought that I was giving you a compliment.

Gallagher: Let's move on to the McClatchey-Selby paper as I think that there will probably be several comments there.

McClatchey: Actually there are two comments that I would like to make that clear up the situation. (1) Regarding the 2.7 micron region, and especially this questionof the modification of the water vapor data, in LOTRAN and its connection with line-by-line calculation, what happens there is that in the first case, the LOTRAN coefficients depend on line-by-line calculations degraded to the appropriate spectral resolution. And what we found was that the result of that calculation did not agree as well as we would like with measurements. So in the iteration which amounts to the input to LOTRAN III, at this point, it was decided to base the coefficients on measurements rather than on the line-by-line calculations. I say this because Charles Randall made some reference to discrepencies in the line-by-line calculations, and some of your other curves. A number of them which... I guess what I'm saying is that when you take all of the lines into account, as they are down on the listing, as individually determined by various measurements, and you then do the calculations for low resolution, that you run into some problems whether these problems have to do with lineshapes or some other things. I don't really know what is all involved. The line-by-line calculations themselves do not seem to work out as well as one would hope.

Long: Which specific region are you talking about?

McClatchey: 2.7 microns.

Benedict: In specific narrow regions, the overall picture seems all right.

Long: The thrust of what I was showing was not to demonstrate that it was bad, but that it was good.

McClatchey: But I'm trying to get at the reason for this modification and what we did to modify it. At least in the context of the LOTRAN code, it appears that we needed to adjust the parameters, the coefficients, more nearly to match the experimental data rather than to match coefficients determined by the line-by-line calculation. There is a lot of interest in this region that's why we might not ordinarily have worried about it, and of course, the discrepancies are not that big you might say, but from the point of view of addressing a specific problem they asked of us regarding the 2.7 micron region, we made these adjustments and we think it gives a better fit for the range of atmospheric conditions that we used.

Long: On a different topic, I would comment on the computation of laser lines transmission, that one of the problems that we have had is that we do not know where the laser lines are well enough and in that regard we are now measuring some things. Rao of Ohio State is measuring the DF lines, he has completed the measurement of the DF line positions, he has completed measuring the HF lines positions. Of course, he did CO sometime ago and we hope to do HCl if the laser works so we'll try that in a little while. And his accuracy is now about 0.002 cm^{-1}. Now there is some other work around, I think at Lincoln Laboratory, frequency heterodyning or what have you, they talk about an order of magnitude better accuracy than this. I think for most of our purposes that this will be good enough. And in some cases we found that this was quite important in getting a proper comparison with the line-by-line tape deck. When we had the right laser frequency, we got a much better comparison than we did before.

McClatchey: OK, I just want to pursue this since I heard someone mention this to me last week, that in your report that you wrote, you showed some substantial discrepancy between calculations based on the tape, especially in the case of HDO lines and the laser measurements. And then I was told

that because of this some shift in frequency that may be this isn't so bad. Is that a correct statement?

Long: I gave the information to Bill here. It improved it slightly with respect to HDO. With N_2O, it brought it into absolutely remarkable agreement between the measured and calculations. But with HDO, there still seems to be a problem there.

Benedict: I suspect that the HDO intensities that we put in are too low. There are measurements going on at SAI that Meredith and Woods are doing, which I hope will clarify this.

Gallagher: Do the results of Rao on CO compare with the heterodyne measurements that are being done at MIT?

Long: In the one case that I know of in which a comparison was made, between Javan's measurement and his, it was really remarkable. It was within the Doppler width of the laser line.

Benedict: As far as CO goes, everything I think frequency wise is in beautiful shape because there are a number of laser frequencies that have been fitted. There are Rao's measurements, there are the Golash and Lee measurements. They used the interferometer and there are the solar spectrum measurements up to very high J. As far as the frequencies of the laser lines, they are certainly known to 10^{-4} wave numbers. I don't think that we can quibble about that.

Selby: Is there a tabulation of the CO laser, Bill? The line positions and intensities that enter this?

Benedict: The new constants for calculating the CO line positions that have been published are the ones of Kildalling and Ross. These aren't quite as good as they should be if you go up to very high J's. If you're only interested in the absorption problem and not going to the emission problem in very hot flames, then this is good enough. The frequencies can then be improved by using the constants of Kildalling and Ross. The intensities that are in Conte's 6 or 7 year old paper I think are just about as good as they

can be. Nothing has come up since then to cause a particular improvement, and this is a very nice table because it has the values at a number of temperatures.

Gallagher: Are there any other comments or questions on the McClatchey-Selby paper? Do they have anything to say about their own work that might concern the problems that bear more looking at?

Harris: I have one question on this thing here... John has mentioned that he inserted spectral aerosol attenuation data. How much detail are you going to put in on that?

Selby: I showed one slide that showed the refractive index of aerosol as a function of wavelength.

Harris: The attenuation coefficient as a function of wavelength?

Selby: Yes, right. So that was digitized and put into LOTRAN III.

Harris: That was for H_2O?

Selby: That was for a composite of dust and water soluable materials.

Harris: Oh, now that was the crux of the whole matter.
Would you like to say what you use in your program. We've had a dialogue on this thing with a couple of the people who are here now. That the atmosphere is so enormously complex that we're hard pressed to specify what the relative parameters are and we need to know and we do not know this yet to be able to predict the things that we want to know for calculations. Now we can measure the thing in a given case, measuring all the things we can probably do it; measure the Mie scattering, measure the things as a function of wavelength, measuring all sorts of things, we can probably do it. But we don't know because the atmosphere is so complex and it is so bad that there is hardly anything left on which, by means of a few things we can predict almost anything, because of the inherent variability. You mentioned two or three times, and about the maritime aerosol and this becomes a variable, the continental is a variable and the earth is a variable and then you get mixtures. Not only the seasonal types of things and the air mass but a lot

of other things that we haven't even considered. Now the simplest thing to do would be to get the information from using visual range or from using an integrating nephelometer which gives you pretty good visual range at a point. But that doesn't do it all because you get various kinds of Mie scattering from all sorts of combinations of things. So the important thing for your model is to take a reasonably good combination of these things which would work in a rather wide variety of circumstances and some sort of mixture of things. But it makes a great deal of difference whether you are going to take horizontal measurements and whether you're over ocean or you're over land. Or if its going to be over a vertical path and then when you get above a certain altitude it is the same as a continental atmosphere anyway.

WORKSHOP ON COMPUTATIONAL ASPECTS OF MODELING THE ATMOSPHERE

G. T. Connell, Moderator

Martin Marietta Corporation
Orlando, Florida

WORKSHOP ON COMPUTATIONAL ASPECTS
OF MODELING THE ATMOSPHERE

G.T. Connell
Martin Marietta Corporation

The computing session was attended by only two members of of the committee, thus the exchange of technical information was limited and the session was ended early to adjourn and go into the experimental session.

Two points were covered, however; one was the experimental work on infra-red laser fusing and the other was the theoretical work on IR transmission calculations being carried out at Avco. The fusing work is being done at NWC, and the program calculates the return of laser energy from clouds and target (which in this case is an airplane). This return energy is used as a designator for a CO_2 homing missile. The program is up and running and some of the results were pointed out. One of the most significant is the problem of backscattered energy off the clouds, the missile at times sees more energy from this source than from the target.

Work on the code was funded by the NWC and the finished program does not make use of LOWTRAN or the Aerospace code.

The second subject discussed was a program written at Avco on atmospheric IR transmission. This program, uses a Goody model for the line strengths and half-widths for a homogeneous path. A procedure to obtain an equivalent homogeneous path in an inhomogeneous atmosphere uses the Curtis-Godson approximation. To use this, tables of line strengths over lines as a function of wavelength and temperature from AFRL were used. An "equivalent homogeneous absorber amount" is then found.

A stratified layer of the atmosphere up to 30 Km. uses 1 Km. increments and takes into account Lorentz boardening. From

30 Km. to 57 Km. doppler effects were taken into account. Refractive effects were not accounted for, but earth curvature effects and atmospheric emission were. Wavelength resolution cells are given by $\lambda/\Delta\lambda$ = 100 (0.1 μ at 10 μ) from 8 to 25 microns from H_2, CO_2, O_3, N_2O, CH_4, CO and HNO_3. The program was made to run on an IBM 360-44 of 20K word capacity. Test runs were made and compared favorably with experimental measurements.

The remainder of the discussion session was concerned heavily with the effects of aerosol. It was pointed out that it is very difficult to make aerosol measurements in which the experimental conditions are well controlled. Combination of aerosols and variations along the path of aerosol concentrations present problems. There is a great need for high precision transmission data to make range predictions. Calculations are needed on different types of aerosols. The models are useful for averages, but a need has been expressed for experimental measurements. The sensitivity of the data is extremely important. Thus, it is indicated that a 2-1 pread of data presents a factor of 10-1 in utility or design of device.

From the discussion of the meeting, it is evident that there is an important need for experimental data in all phases of propagation as inputs to the calculations. Simultaneous precise meterological data is needed for all propagation measurements.

The last part of the recordings of the open discussions was not clear enough to present detailed information.